C. 1

WATER QUALITY MODELLING IN ESTUARIES

by

CHRISTOPHER STEWART JOY

B.Eng., Monash University, 1968
M.App.Sci., Monash University, 1972

A THESIS SUBMITTED IN PARTIAL FULFILMENT OF

THE REQUIREMENTS FOR THE DEGREE OF

DOCTOR OF PHILOSOPHY

in the Department
of
Civil Engineering

We accept this thesis as conforming to the
required standard

THE UNIVERSITY OF BRITISH COLUMBIA

January, 1974

A B S T R A C T

A tidally varying and a tidally averaged mass transport model

are applied to the Fraser River Estuary to investigate the significance

of tidal effects on the concentrations resulting from assumed effluent

discharges. The tidally averaged model is due to Thomann [1963]. The

tidally varying model is developed from first principles. A hydrodynamic

model was used to determine the tidally induced temporal variation in the

longitudinal velocity and cross-sectional area along the estuary. All models

are "mathematical" and one-dimensional.

Finite difference techniques are used to solve the underlying

partial differential equations of all three models. The problems of stabil-

ity and numerical dispersion are examined. Numerical dispersion is seen to

result from the solution of the mass transport equation over a fixed space

grid rather than along the advective characteristics. Advantages of solving

the equation along the characteristics are: no numerical dispersion; the

advective and dispersive transport processes are usefully separated; lateral

dispersion can be partially assessed with a one-dimensional model; and

time dependent behaviour in coefficient of longitudinal dispersion can be

taken into account.

The tidally varying flows along the estuary are seen to cause a

variation in the initial dilution of a discharged effluent. This, together

with the effects of tidal flow reversal produces spikes in the concentration

profile along the estuary. The concentration of these spikes is then re-

duced by the dispersion process, the peak concentration during the first two

ii

tidal cycles being sensitive to the form and magnitude of the coefficient
of longitudinal dispersion. Time dependent variations in this coeffi-
cient are considered. The effect of the lateral dispersion process on
the estimated concentrations is also considered and secondary flows are
tentatively explained in terms of the generation and advection of vor-
ticity. The predicted peak tidally varying concentration was found to
be significantly greater than the tidally averaged value.

TABLE OF CONTENTS

LIST OF TABLES

LIST OF FIGURES

$\bar{a}$: Height of estuary bed above level datum.

A : Cross-sectional area.

$\underset{\sim}{A}$: Matrix of the effects of advection, dispersion and decay on the tidally averaged concentrations (Thomann's Solution).

$A_{i,i+1}$: Average cross-sectional area between segments i and i+1 (Thomann's Solution)

A_j^n : Cross-sectional area at point $j\Delta x$ at time $n\Delta t$ (hydrodynamic equations)

$\bar{c}$: Cross-sectionally averaged concentration

b : Width of estuary

C : Chezy's friction coefficient

c_i : Concentration in segment i (Thomann's Solution)

$\underset{\sim}{C}$: Matrix of segment concentrations (Thomann's Solution)

C_j^n : Cross-sectionally averaged concentration at point $j\Delta x$ at time $n\Delta t$.

e_y : Coefficient of turbulent diffusion

E : Coefficient of longitudinal dispersion

E_f : Coefficient of longitudinal dispersion due to the lateral velocity gradients of the steady velocity component

E_t : Coefficient of longitudinal dispersion due to the lateral velocity gradients of the oscillatory velocity component

E_c : Effective coefficient of longitudinal dispersion over a tidal cycle due to lateral velocity gradients

E_y : Coefficient of longitudinal dispersion due to the vertical velocity gradients

E_p : Coefficient of pseudo dispersion (numerical dispersion)

$E_{i,i+1}$: Tidally averaged coefficient of longitudinal dispersion between segment i and i+1 (Thomann's Solution)

g : Gravitational acceleration

h : Height of water surface above level datum

h_j^n: Height of water surface above level datum at point $j\Delta x$ at time $n\Delta t$

k : Von Karman's constant

K_i : Rate of decay of substance in segment i (Thomann's Solution)

$L_{i,i+1}$: Average length of segments i and i+1 (Thomann's Solution)

n : Manning's "n" (foot-second units)

Q : Freshwater discharge

R : Radius of curvature of a bend

S_i : Rate of production of substance due to the i'th source-sink process

t : Time

$\bar{u}$: Cross-sectionally averaged longitudinal velocity

U_f : Magnitude of the steady component of the longitudinal velocity

U_t : Amplitude of oscillatory component of the longitudinal velocity

U_c : Effective longitudinal velocity over a tidal cycle

u_j^n, U_j^n: Cross-sectionally averaged longitudinal velocity at point $j\Delta x$ at time $n\Delta t$

U_* : Shear velocity

U_*^f : Shear velocity due to U_f

U_*^t : Shear velocity due to U_t

U_*^c : Effective shear velocity over a tidal cycle

V_i : Volume of segment i (Thomann's Solution)

W_s : Cross-channel surface velocity due to secondary flows

W_i : Rate of waste discharge into segment i (Thomann's Solution)

$\underset{\sim}{W}$: Matrix of segment waste discharges (Thomann's Solution)

x : Longitudinal distance along the estuary

y : Vertical distance in the estuary

z : Lateral distance in the estuary

α : Factor given by $\alpha = \ln\{\dfrac{U_* \bar{y}}{11.0\ \nu}\}$

α : Factor relating dispersion coefficients in depth and shear velocity, as in $E = \alpha\ \bar{y}\ U_*$

$\alpha_{i,i+1}$: Tidal exchange coefficient between segments i and i+1 (Thomann's Solution)

γ_{ta} : Standardized concentrations[1] predicted by the tidally averaged model

γ_{tv} : Standardized concentrations[1] predicted by the tidally varying model

Δt : Time increment used in finite difference solutions

Δx : Space increment used in finite difference solutions

ε : Coefficient of lateral dispersion

ε_f : Coefficient of lateral dispersion due to the secondary flows associated with U_f

ε_t : Coefficient of lateral dispersion due to the secondary flows associated with U_t

ε_c : Effective coefficient of lateral dispersion over a tidal cycle

η : Relative depth, given by $\eta = y/\bar{y}$

ξ_z : Vorticity generated in the lateral direction due to the vertical velocity gradients

ξ_x : Longitudinal component of the lateral vorticity

Γ_x : Circulation around a cross-section due to the longitudinal vorticity

[1]The predicted concentrations are standardized by dividing the concentration determined from the mass of effluent and the freshwater flow per tidal cycle.

INTRODUCTION

Throughout history, centers of urban, agricultural and industrial development have commonly been located along rivers and estuaries. The principal uses of these surface water resources in early times were water supply and navigation; the river provided an accessible source of water for domestic and agricultural needs and a relatively cheap and easy means of bulk transport. Modern uses of surface water resources include navigation and water supply and waste disposal for domestic, agricultural and industrial purposes. In addition, rivers and estuaries provide habitat for wildlife, breeding and rearing areas for fish and shellfish and areas for general recreation.

Associated with each use of surface water resources is a set of quantity and quality constraints that determine whether the water is satisfactory for that particular use. The quality constraints consist of the maximum allowable levels of various deleterious substances that may be present in the water. Generally, the constraints for each use are different, and conflicts may arise when water is to be used for multiple purposes. A common example is the conflict between the competing uses of waste disposal, wildlife habitat and recreation. It is recognized that the quantity and quality conflicts are related;[1] however, this thesis only considers quality aspects, and in particular, only those quality aspects that are determined

_____

[1]One obvious way of improving water quality is by low flow augmentation, as has been investigated by Worley *et al.* [1965].

1

by the concentration of a dissolved deleterious substance in the water.

To investigate a situation of existing or potential water quality conflicts it is usual to develop a "water-quality" model, or as it shall be referred to in this thesis, a mass-transport model. Such a model enables the concentration of deleterious substance to be predicted throughout the river or estuary, and is instrumental in assessing the effectiveness of possible control measures to improve water quality.

The simplest type of estuarine mass-transport model is one-dimensional (1-D) and only admits a variation of parameters and variables in the longitudinal direction. In a "tidally averaged" model, parameters and variables are assigned their average values over a tidal cycle, whereas in a "tidally varying" model, they are allowed to vary throughout the tidal cycle. The temporal resolution of the tidally varying model is much finer than its tidally averaged counterpart, but considerably more effort is required in its development than for the latter. Thus, it seems relevant to enquire as to (1) whether the differences between the results of both models are significant; and (2) whether the extra effort involved in developing and applying the tidally varying model is justified by its finer resolution.

In this thesis the significance of these differences is investigated by applying both a tidally averaged and a tidally varying mass transport model to the Fraser River Estuary, a tidal estuary in the Province of British Columbia, Canada. The tidally averaged model was developed by Thomann [1963] and the tidally varying model was developed from first principles. Both mass transport models were developed as part of a larger interdisciplinary study

by the Westwater Research Center of the University of British Columbia
to investigate the effects of possible patterns of future development
on the water quality of the Fraser River Estuary.

This thesis consists of six chapters. The tidally varying
and tidally averaged forms of the one-dimensional mass transport equa-
tion are discussed in Chapter 1. The expected differences between the
results of both models and the applicability of a one-dimensional model
to the Fraser River Estuary are also considered there. In Chapter 2 the
literature is reviewed to investigate the various ways of solving the
one-dimensional mass transport equation. In order to solve the tidally
varying form of the equation, it was necessary to develop a hydrodynamic
model to predict the tidal variations in the longitudinal velocity and
cross-sectional area along the estuary. The hydrodynamic model and the
tidally varying and tidally averaged mass transport models applied to the
Fraser River Estuary are described in Chapter 3. The verification of all
three models is described in Chapter 4 and the results of applying both
mass transport models to the Estuary are described and discussed in Chap-
ter 5. Finally, conclusions about the differences and applicability of
both models are given in Chapter 6.

There are six appendices to this thesis. The one-dimensional
mass transport equation for unsteady non-uniform flow is derived in Appendix
A. The advective and dispersive transport processes are discussed therein,
as are the assumptions in the derivation of the equation. Appendix B con-
sists of a description of the Fraser River Estuary. The various channels of
the estuary, the freshwater flows, the tides and the salinity intrusion are

all described. When finite difference techniques are used to solve the

mass transport equation, there are problems with numerical dispersion

and stability. In Appendix C both of these problems are seen to occur

when a fixed grid is used to solve the equation, rather than a grid along

the more fundamental characteristics of information propagation. Details

of the finite difference schemes used to solve the hydrodynamic equations

and both forms of the mass transport equation are given in Appendix D. In

Appendix E, it is seen that existing estimates of lateral dispersion apparent-

ly underestimate the lateral mixing in the Fraser River Estuary. Secondary

velocities are explained in terms of vorticity, and on the basis of very

limited field data, the predicted secondary flows agree well with those ob-

served in the estuary. Finally, in Appendix F, estimates are made of the

coefficients of longitudinal dispersion. An approximate method is given to

allow for the variable contributions of the effects of vertical and lateral

velocity gradients during the initial period before cross-sectional mixing

is complete.

CHAPTER 1

PRELIMINARY CONSIDERATIONS

The one-dimensional mass transport equation is stated and its
tidally varying and tidally averaged forms are briefly discussed. The
problem of determining the parameters of both forms of the equation is
considered, and expected differences between the results of a tidally
varying and a tidally averaged mass transport model are described. The
ability of a one-dimensional mass transport model to describe the mass
transport processes in the Fraser River Estuary is also considered.

1.1 THE ONE-DIMENSIONAL MASS TRANSPORT EQUATION

The one-dimensional equation for mass transport in unsteady non-
uniform flow in an estuary is obtained by taking a mass balance over an
elemental cross-sectional slice of the estuary. Mass is transported through
the slice by the mass transport processes of advection and dispersion, and
these processes, together with any source-sink reactions that the substance
undergoes, determine the concentration of the substance within the slice.
As it is a one-dimensional equation, the dependent variable and the parameters
are assigned their average cross-sectional values. The equation is derived in
Appendix A and the assumptions in its derivation are discussed there. The one-
dimensional mass transport equation is given by

$$\frac{\partial \bar{c}}{\partial t} = - \bar{u}\frac{\partial \bar{c}}{\partial x} + \frac{1}{A}\frac{\partial}{\partial x}\{AE\frac{\partial \bar{c}}{\partial x}\} + \sum_{i=1}^{n} S_i \qquad (1.1)$$

5

where

$\bar{c}$ is the mean cross-sectional concentration of dissolved substance;

$\bar{u}$ is the mean cross-sectional value of the longitudinal velocity;

A is the cross-sectional area;

E is the mean cross-sectional dispersion coefficient in the longitudinal direction;

S_i is the rate of production per unit volume of water due to the ith source-sink process, it being assumed that there are n source-sink processes;

x is the longitudinal distance;

and

t is the time.

For the sake of brevity, the "mean" value of a parameter or variable is now taken to refer to its "mean cross-sectional" value. The high frequency turbulent fluctuations are assumed to have been averaged out of $\bar{u}$ and $\bar{c}$.

The mean velocity $\bar{u}$, the mean longitudinal dispersion coefficient E and the cross-sectional area A will be referred to as the parameters of Equation (1.1). These quantities are parameters in the sense that they are defined outside the equation by the cross-sectional geometry and hydraulics of the particular estuary. These three parameters can vary with both x and t Thus, Equation (1.1) is seen to be a second-order linear partial differential equation with variable coefficients. The three terms on the right-hand side of the equation will be referred to as the advective, the dispersive and the source-sink terms respectively.

Equation (1.1) was derived for the general case of unsteady non-uniform flow and is the basis of all one-dimensional mass transport models of rivers and estuaries. In an estuary, the rise and fall of the tide causes temporal variations in the parameters $\bar{u}$, A and E. In a tidally varying model, this temporal variation in the parameters is taken into account as Equation (1.1) is solved to determine the mean concentration along the estuary during the tidal cycle. In a tidally averaged model, the parameters are assigned their average values over a tidal cycle, and the mean concentration along the estuary is determined over periods of a tidal cycle. Averaging Equation (1.1) over a tidal cycle does not alter the form of the equation, but merely changes the interpretation of the dependent variable and the parameters. For example, $\bar{u}$ becomes the tidally averaged velocity and is determined by the freshwater discharge through the tidally averaged area A. It should be noted that the concentration predicted by a tidally averaged model is not the "tidally averaged" concentration -- this can only be determined by averaging the results of a tidally varying model over the tidal cycle. The majority of tidally averaged models supposedly predict the mean concentration along the estuary at times of slack-water. The reason for this is the ease of sampling at times of slackwater, and is discussed further in Section 2.1.

1.2 DETERMINATION OF PARAMETERS

The flow field of an estuary consists of an unsteady oscillatory component due to the tide superimposed on a steady component due to freshwater inflow. Before a solution can be obtained to the tidally varying form of Equation (1.1), it is necessary to determine the tidally induced temporal

variation in the parameters $\bar{u}$, A and E. A one-dimensional hydrodynamic model was developed to determine the temporal variation in $\bar{u}$ and A. In this model, the equations of motion and continuity were applied to the water mass of the estuary and solved throughout the tidal cycle. The hydrodynamic model is described in detail in Chapter 3. The temporal variation in E during the tidal cycle was related to the temporal variation in $\bar{u}$, as is discussed in Appendix F.

In a tidally averaged model, the parameters $\bar{u}$, A and E are averaged over a tidal cycle. This reduces the unsteady tidal flow field to a steady freshwater flow field, and consequently $\bar{u}$ can be determined from the equation of continuity alone (the equation of continuity is applied to the freshwater discharge through the tidally averaged area A). The tidally averaged dispersion coefficient includes the effects of upstream advection on the flood tide, as is discussed in Chapter 4.

With a tidally varying model, mean concentrations are determined throughout the tidal cycle, whereas with a tidally averaged model, mean concentrations are determined over periods of a tidal cycle. In effect, the temporal resolution of the tidally varying model is much higher than that of a tidally averaged model. Because of their unsteady nature, the estimation of the tidally varying parameters $\bar{u}$ and A involves significantly more effort than the estimation of their steady tidally averaged counterparts. This is apparent from the discussion of Chapters 3 and 4. Thus the greater temporal accuracy of the tidally varying model is offset by the greater effort required to estimate the tidally varying parameters.

1.3 THE EFFECTS OF THE TIDE ON MASS TRANSPORT PROCESSES

In an estuary, the tidal rise and fall of the water surface
causes temporal variations in the longitudinal flow. Because of this temp-
oral variation of flow, the initial dilution of a discharged effluent also
varies during the tidal cycle. This is illustrated in Figure 1.1 for the
steady discharge of effluent into an estuary during the flood tide. The
effect of the flooding tide is to continuously reduce the seaward flow of
water past the effluent outfall, and thus the slug of water dosed in any
time increment becomes increasingly smaller. However, since the effluent
discharge is steady, the same mass of effluent is added to each of the dosed
slugs and this gives rise to the spatial distribution of cross-sectionally
averaged concentration shown in Figure 1.1. As the tide continues to flood,
flow reversal will occur at the effluent outfall and previously dosed slugs
will move upstream past the outfall and be dosed again, as is illustrated
in Figure 1.2. On the following ebb tide, upstream slugs will move down-
stream past the outfall and be dosed yet again, as is also shown in Figure
1.2. A tidally varying mass transport model can account for the effects of
variation in initial dilution and multiple dosing, whereas a tidally aver-
aged model cannot.

Essentially, the effect of the tidal variation in flow is to in-
troduce "spikes" into the concentration profile along the estuary (as is
apparent from Figures 1.1 and 1.2). The concentration of these spikes is
then reduced by the dispersive transport process. Thus, differences between
the results from a tidally varying and tidally averaged mass transport model
will depend on the magnitude of the tidally varying dispersion process.
Another difference between the results of both models is that a tidally vary-
ing model correctly accounts for the effects of upstream advection on the

Figure 1.1

Effect of Variable Initial Dilution on Concentration

Steady effluent discharge

$t = 4\Delta t$ Rising Tide

| C4 | C3 | C2 | C1 | SEA |

$\bar{u} = 0$

$t = 5\Delta t$ Rising Tide

| C4 C5 | C3 | C2 | C1 | |

$\bar{u} \leftarrow$

$t = 6\Delta t$ Falling Tide

| C4 C5 C6 | C3 | C2 | C1 | |

$\rightarrow \bar{u}$

C4 + C5 + C6

Effect of multiple dosing

$\bar{C}$

C3

Time average concentration

C2

C1

x
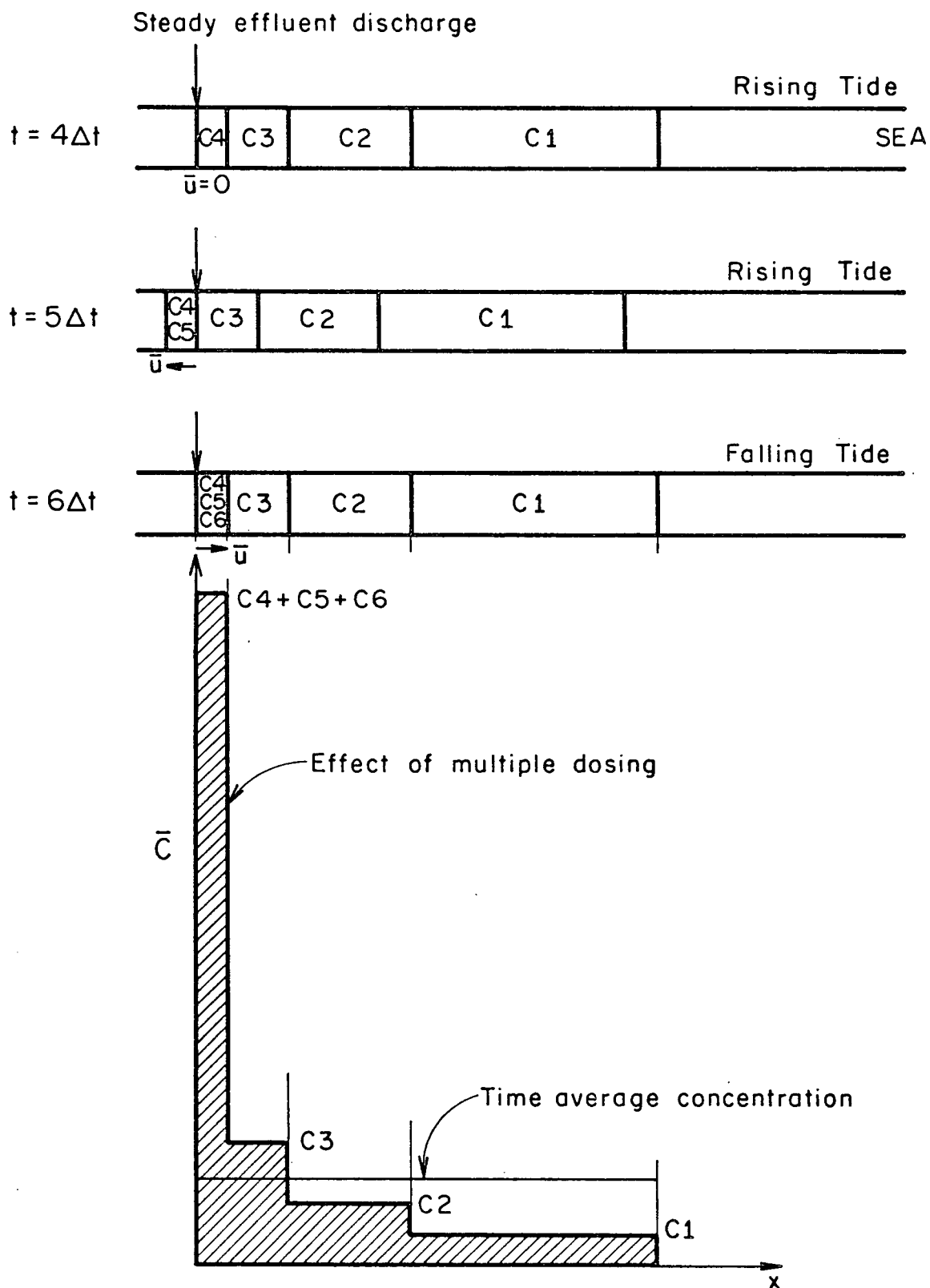
Figure 1.2

Effect of Multiple Dosing
(Due to Flow Reversal) On Concentration

flood tide, whereas a tidally averaged model can only simulate this upstream
transport via the tidally averaged dispersion process.

1.4 ACCURACY OF A ONE-DIMENSIONAL MODEL

Having briefly discussed the tidally varying and tidally averaged
forms of the mass transport equation, the problem of how well a one-dimension-
al model describes the mass transport processes in the Fraser River Estuary
is now considered. When effluent is discharged into a river or estuary, the
time required for complete cross-sectional mixing to occur depends on the
coefficient of lateral dispersion, the width of the river or estuary and the
position of the effluent outfall [Ward, 1973]. In the initial period before
cross-sectional mixing is complete there are significant lateral concentra-
tion gradients across the river or estuary. A one-dimensional mass trans-
port model predicts the cross-sectionally averaged concentrations and does
not "see" these lateral gradients. Thus, in the initial period before cross-
sectional mixing is complete, the predicted concentrations will underestimate
the peak lateral values in the river or estuary. Also, during this initial
period the dispersion of effluent results in a skewed distribution of concen-
tration along the river or estuary rather than the Gaussian distribution pre-
dicted by the tidally varying mass transport model (see Appendix A). When
the cross-sectional mixing is complete, longitudinal gradients dominate the
transport processes, and a one-dimensional model will provide a good descrip-
tion of the actual concentration profile along the river or estuary.

The Fraser River estuary consists of the seven principal channels described in Appendix B. The junctions of these various channels influence how effluent is advected through the estuary. If cross-sectional mixing is not complete at a diverging junction, the bulk of the effluent load may be advected down one of the channels as shown in Figure 1.3. A one-dimensional mass transport model cannot reproduce this behaviour at the junction. The situation shown in Figure 1.3 is further complicated by the effects of tidal flow reversal and the presence of secondary flows at the junction. On the flood tide some effluent is carried back upstream past the junction, and additional cross-sectional mixing occurs before the effluent is advected back through the junction on the ebb tide. If secondary flows are present, the situation may arise where effluent is released from one bank upstream from a diverging junction and is then advected down the opposite channel, as is shown in Figure 1.3. (On the ebb tide, marked secondary flows of this nature are commonly observed at the Main Arm-North Arm junction shown in Figure B.3). Thus, in the period before cross-sectional mixing is complete, the movement of effluent through the various junctions of the Fraser River Estuary is a complex two-dimensional process that also varies during the tidal cycle. To reproduce these effects, a one-dimensional model would have to be modified at the junctions and such modification may require considerable field data. It is noted that the effects of tidal flow reversal and secondary flow will enhance the cross-sectional mixing at junctions.

The ability of a one-dimensional mass transport model to describe the concentration profile along the various channels of the Fraser River Estuary essentially depends on the time required for cross-sectional mixing to occur. In the initial period before cross-sectional mixing is complete,

Limit of Lateral Mixing

Point of Discharge

Flow

Effluent Mass

Secondary Flows (surface)

Flow

Effluent Discharge
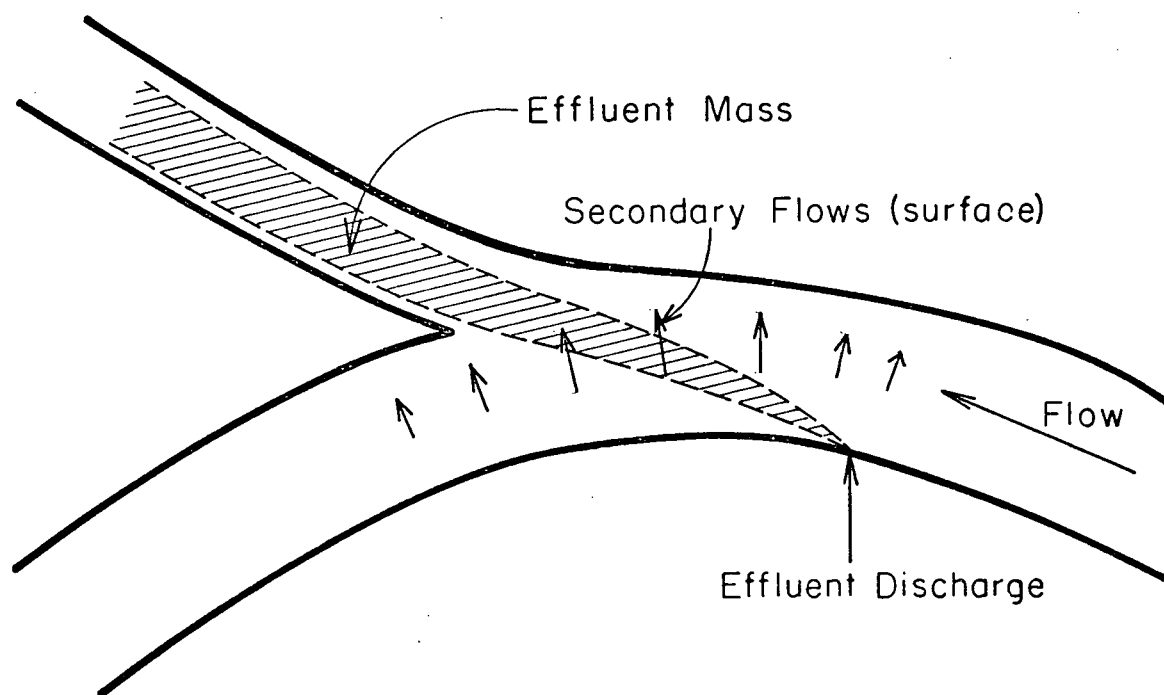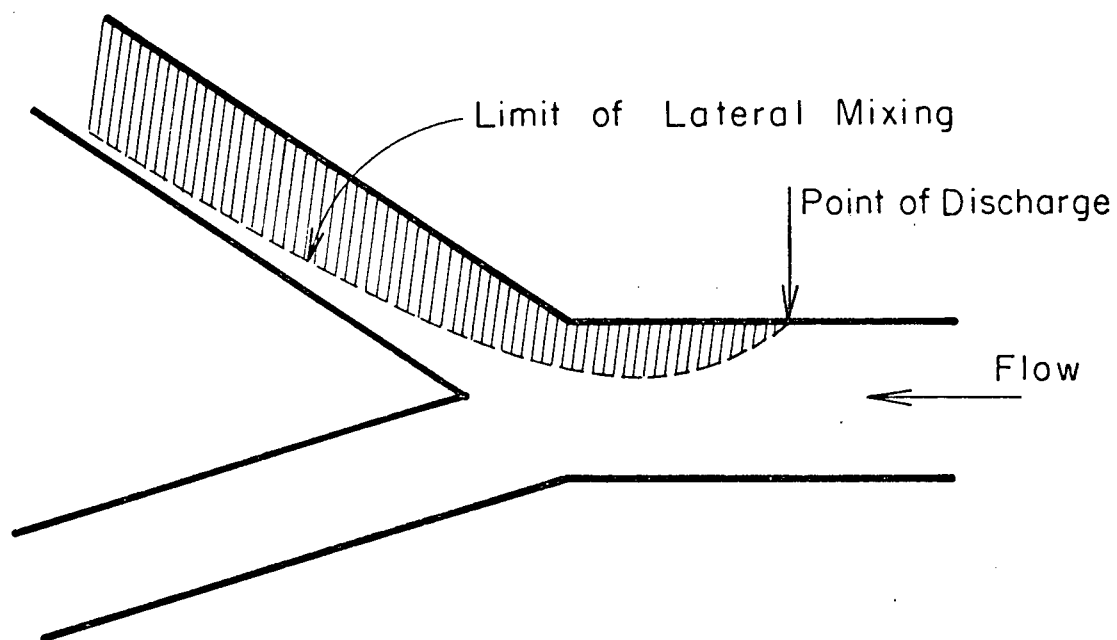
Figure 1.3

Movement of Effluent Through A Diverging Junction

the dispersion process is skewed rather than Gaussian, the peak lateral

concentration is significantly greater than the predicted cross-sectionally

averaged value and the movement of effluent through the junctions may not

be according to the simple mass balance of the one-dimensional equation,

the latter two effects probably being the most important. The time required

for 80 per cent cross-sectional mixing to occur has been estimated in Appen-

dix E. The techniques of Fischer [1969a] and Ward [1972] gave an estimate

of 55 hours, whereas calculations based on vorticity considerations gave an

estimate of five hours, the bulk of the cross-sectional mixing being due to

the influence of secondary flows. It is noted that this last value has not

been confirmed by field experiments. Because of the highly asymmetrical

nature of the tides of the Fraser River Estuary, a more realistic estimate

of the time of cross-sectional mixing in the lower reaches of the estuary

is probably 1-2 tidal cycles. All of these aspects of lateral mixing are

discussed in Appendix E. Unfortunately, time and expense have precluded

using dye studies to measure the actual rate of cross-sectional mixing in

the estuary.

To sum up, in this study it is recognized that lateral mixing

and the complex two and three-dimensional flow characteristics through the

junctions can have a considerable influence on the concentrations along the

various channels of the Estuary. These aspects are considered and their

influence is partially assessed, but the main thrust of the study has been

to obtain accurate solutions to the tidally varying and tidally averaged

forms of the one-dimensional mass transport equation so that the influence

of the tides on the predicted concentrations can be assessed. To some extent,

the two- and three-dimensional effects can be estimated as further modifi-

cations of the one-dimensional results, as is discussed further in Chapter 5.

CHAPTER 2

LITERATURE REVIEW

The literature is reviewed to investigate the various solutions

and applications of one-dimensional mass transport models. Solutions to

the mass transport equation are classified into the categories of analy-

tical solutions, numerical solutions, physical and analogue model solutions

and stochastic solutions. The advantages and disadvantages of each class

of solution are also discussed.

2.1 ANALYTICAL SOLUTIONS

The one-dimensional mass transport equation for unsteady non-

uniform flow in a river or estuary is given by

$$\frac{\partial \bar{c}}{\partial t} = -u\frac{\partial \bar{c}}{\partial x} + \frac{1}{A}\frac{\partial}{\partial x}\{AE\frac{\partial \bar{c}}{\partial x}\} + \sum_{i=1}^{n} S_i, \qquad (2.1)$$

where the terms are as defined in Section 1.2. Equation (2.1) is a second

order linear partial differential equation with variable coefficients (the

source-sink terms are generally linear, and $\bar{u}$, A and E are dependent on x

and t). As such, no completely general analytical solution exists, but

solutions have been obtained under a number of simplifying assumptions.

Before reviewing various solutions, the so-called "slackwater" concentra-

tions predicted by the tidally averaged models are discussed.

The majority of the analytical solutions discussed here are for

the steady-state response ($\partial \bar{c}/\partial t = 0$) of Equation (2.1). This simplification

reduces the partial differential equation to an ordinary differential equation in x alone. In determining this steady state response, the freshwater discharge and effluent inputs are assumed to remain steady or constant for a period of time equal to the residence time of the estuary. Further, any steady-state solution of Equation (2.1) is a tidally averaged solution. (The equation is now independent of time and cannot resolve the within tide temporal fluctuations in $\bar{c}$, $\bar{u}$, A and E). However, the steady state solution to Equation (2.1) does not represent the tidally averaged concentration profile along the real estuary. In fact, it represents the concentration profile along a model estuary that is tideless and has a high degree of longitudinal dispersion. (The tidally averaged E is generally much higher than the tidally varying E, as is discussed in Section 3.3). The tidally averaged concentration profile can only be obtained from the results of a *tidally varying* mass transport model.

In the majority of tidally averaged mass transport models, the steady state solution to Equation (2.1) is assumed to represent the concentration profile along the estuary at times of slackwater. In other words, the tidally averaged mass transport processes are used to determine the concentration profile along the estuary at a particular phase of the tide. The reason for working with slackwater profiles is the relative ease of sampling tracers in the estuary at these times [O'Connor, 1960]. Any correspondence between the steady-state solution of Equation (2.1) and the slackwater concentration profile along the real estuary is because the tidal effects are small, and under these conditions the steady-state solution is an adequate representation of the concentration profile in the real estuary

at any phase of the tide, or because the steady state solution is "forced"
to conform to the slackwater profile by "adjusting" the parameters of
Equation (2.1). It is interesting to note that Preddy and Webber [1963]
developed a tidally averaged model that predicts tidally averaged concentra-
tions rather than slackwater values. This model is described in Section
2.2.2.

In a tidally varying situation, quasi-steady-state conditions
are said to be achieved when the variable of interest (for example, $\bar{c}$)
undergoes a cyclical repetition of the same values from tide cycle to tide
cycle. Thus, in a tidally varying model one speaks of a quasi-steady-state
response, rather than a steady-state response as with a tidally averaged
model.

Essentially, the analytical solutions of Equation (2.1) entail
simplifications in which various terms of the equation are ignored (for
example, the dispersion term) and the parameters of the $\bar{u}$, A and E are repre-
sented as simple functions of x and possibly t. Effluent inputs are treated
as boundary conditions, and solutions have been obtained for both point and
distributed effluent inputs [O'Connor, 1965].

Steady-state solutions to Equation (2.1) have been obtained for
steady effluent discharge into (1) steady uniform flows [O'Connor, 1960, 1962];
(2) steady non-uniform flows where the area is a simple function of x [O'Connor,
1965, 1967]; and (3) steady non-uniform flows where the freshwater discharge
varies exponentially with x due to land run-off [O'Connor, 1967]. Transient
solutions have been obtained for steady effluent discharge into (1) non-steady
freshwater flows during the recession limb of the hydrograph (which was approxi-

mated as negative exponential in time) [O'Connor, 1967]; and (2) steady

flows where the diurnal photosynthetic production of DO is taken into

account (it was approximated as a half sine wave) [O'Connor and Di Toro,

1970]. To obtain these transient solutions, it was necessary to ignore

dispersion.

Kent [1960] used the method of separation of variables to ob-

tain the general solution to Equation (2.1) for a slug input into steady

uniform flows, and the particular solutions for a slug input into steady

non-uniform flows ($\bar{u}$, A and E were assumed to be linear in x). Di Toro

and O'Connor [1968] obtained the transient solution for steady effluent

input into unsteady non-uniform flows where the variation in cross-sectional

area could be separated into independent functions of x and t (dispersion was

ignored).

Li [1962] used the method of characteristics to obtain a solution

for non-steady effluent discharge (sinusoidal variation) into steady uni-

form flow (dispersion was ignored). He later used the method of perturba-

tions to obtain a solution for the same case with dispersion included [Li,

1972].

Holley [1969b] transformed the mass transport equation for BOD

into the elementary diffusion equation. (By travelling with the water

mass, the only transport process an observer "sees" is dispersion -- see

Section A.6). He took the standard solution for a slug input and used the

convolution method to obtain the solution for the continuous (but not neces-

sarily steady) effluent discharge into unsteady uniform flow. Bennet [1971]

used the convolution method to obtain the solution for the complete BOD-DO

system for the same effluent discharge and flow conditions as Holley.

2.2 NUMERICAL SOLUTIONS

2.2.1 <u>Finite Difference Solutions</u>. Finite difference methods for
the solution of partial differential equations can be classified into (1)
fixed mesh methods in which the solution is obtained at fixed predetermined
points in a rectangular mesh of time and distance; (2) *characteristic methods,*
in which the solution is obtained at mesh points along the characteristic
curve(s) in the time-distance plane(s), the position of the mesh points
being determined as the solution progresses; and (3) *combined methods,* in
which the solution is followed along the characteristic curve(s) and then
extrapolated back onto a fixed mesh of uniformly spaced points [Amein, 1966].
In characteristic methods, the mesh points are generally non-uniformly spaced
in time or distance, and consequently the book-keeping of results is somewhat
untidy. Combined methods simplify this bookkeeping by extrapolating the
results back onto a fixed uniformly spaced mesh.

Finite difference methods are discussed in some detail in Section
C.2. The problems of *stability* and *convergence* are considered, and it is
seen that *implicit* finite difference schemes are generally unconditionally
stable, whereas *explicit* schemes are at most conditionally stable. The
stability requirements of explicit schemes are discussed in detail in
Section C.3, and are seen to impose limits on the relative size of Δx and Δt,
the grid spacing.

Generally, fixed mesh finite difference schemes do not simulate
the advective transport process correctly, and result in an additional dis-
persive process being superimposed on the actual advective and dispersive

processes occurring in the river or estuary. This so-called *numerical dispersion* is discussed in detail in Section C.2 and is seen to be eliminated by using characteristic finite difference methods.

Harleman *et al.* [1968] developed a one-dimensional, tidally varying mass transport model of the tidal portion of the Potomac River. A fixed mesh, implicit scheme with central differences was used to solve the mass transport equation. (The various types of space and time differences are described in Section C.2). Tidal velocities were calculated from discharge and tidal records, and the Taylor dispersion equation [Taylor, 1954], modified for the effects of vertical velocity gradients, was used to determine the longitudinal dispersion coefficients. The finite difference solution simulated the results of dye studies in the estuary reasonably well. However, Prych and Chidley [1969] showed that the numerical dispersion in their finite difference scheme was approximately 30 times greater than the modified Taylor dispersion, and was of the order of the same magnitude as the actual dispersion occurring in the estuary. (The modified Taylor equation neglects the effects of transverse velocity gradients and grossly underestimates the dispersion coefficient for streams and estuaries, as Fischer [1966b] has demonstrated). The agreement between the dye results and the finite difference solution was apparently only fortuitous. This example illustrates the significance of numerical dispersion.

Bella and Dobbins [1968] investigated fixed mesh finite difference solutions to the one-dimensional mass transport equation describing the BOD - DO system. They applied a tidally varying finite difference model to a hypothetical estuary and compared the results with an analytical tidally averaged solution.

Dornhelm and Woolhiser [1968] obtained a solution to the one-dimensional, tidally varying mass transport model for conservative substances. They used a fixed mesh implicit scheme with central differences. A hydrodynamic model, solved by the same finite difference scheme, was used to determine the tidally varying parameters. The hydrodynamic model was verified against a steady-state analytical solution, but it exhibited instabilities when applied to the Delaware estuary. (According to a linear stability analysis, their implicit scheme was unconditionally stable. However, the non-linear nature of the hydrodynamic equations may require more stringent stability conditions, as is discussed in Section D.1). The mass transport model was verified for steady uniform flow and was applied in tidally varying form to a hypothetical estuary.

To overcome the problems of numerical dispersion, Gardiner *et al*. [1964] used the method of characteristics to solve the two-dimensional mass transport equation describing the movement of a solvent through sand saturated with oil. A combined finite difference method was used, with a mesh of uniformly distributed moving points superimposed on a fixed two-dimensional space mesh. At the beginning of a time step, the moving points are assigned the concentration of the nearest fixed grid point, and then advected along the characteristics according to the equation analagous to Equation (A.9). After advection, the moving points are assigned to the closest grid point to determine the concentration there. An explicit form of the equation analagous to Equation (A.8) is then used to disperse the concentration over the fixed grid points. The complete process is then repeated for the next time step. Pinder and Cooper [1970] used the same

technique to calculate the transient positions of the salt water front in a coastal aquifier.

Di Toro [1969] recognized that the method of characteristics reduced the mass transport equation for the BOD-DO system into two ordinary differential equations. (He ignored dispersion, and so the equation analagous to Equation (A.8) was a "true" ordinary differential equation). He noted that the numerical solution of ordinary differential equations is more exact than for partial differential equations, and that the accuracy can be controlled by predictor-corrector methods.

2.2.2 "Box Model" Solutions. Another type of mass transport model is the so-called "box model" in which the estuary is divided into finite segments or boxes. Each segment is assumed completely mixed and the concentration of substance in a segment is determined by the discharge of substance into the segment, the advective and mixing processes occuring between adjacent segments, and any source-sink effects that the substance undergoes. Callaway [1971] noted the box models are conceptually very similar to finite difference models, as in effect, the latter segment the estuary into well mixed boxes centred around the grid points. Another similarity is that the box model representation of the estuary results in a set of difference equations relating the concentration in any box to the concentration in neighboring boxes (similar to implicit difference schemes).

Thomann [1963], [1965], developed a tidally averaged box model which was applied to the Delaware estuary. The estuary was segmented into 30 boxes whose length varied from two to four miles. All hydraulic parameters

were assumed steady, but the concentration within each box was allowed to vary with time so that the effect of time varying inputs could be studied. The concentration in each box is determined from a set of simultaneous difference-differential equations. For steady-state inputs, the temporal derivatives are set equal to zero and the system of equations reduces to a set of difference equations similar to those of an implicit finite difference scheme. Thomann's model is described in more detail in Sections 3.3 and D.3. Pence *et al.* [1968] extended the model to account for time varying fresh water inflows(tidal parameters are still averaged over a tidal cycle). Like most tidally averaged models, Thomann's model is a "slack water" model with concentrations being determined at succeeding slack waters.

Preddy and Webber [1963] developed a tidally averaged box model of the Thames estuary to predict the true tidally averaged value of the DO concentration. In their model, the boxes were two miles long and the tidal displacement was six miles to either side of a box. Thus, the tidally averaged concentration within a box depends on the concentrations within the three boxes upstream and downstream of it. This model is one of the few that determine tidally averaged concentrations rather than slack water values.

2.2.3 <u>Finite Element Solutions</u>. Finite element methods have been used to obtain solutions to the one-dimensional mass transport equation. Examples include Price *et al.* [1968], Guymon [1970], Pinder and Friend [1972] and Nalluswami *et al.* [1972]. In finite element solutions, the estuary is segmented and the concentration profile is approximated as a series of functions.

In some respects the method is similar to implicit finite difference methods and box models; in the latter two methods the estuary is also segmented, but the concentration profile is approximated as a point value rather than a function in each segment. Further, the solution of all three methods is given by a set of simultaneous equations governed by a square banded matrix of bandwidth three (see Section D.3 for Thomann's version of this matrix). Price *et al.* [1968] compared finite element, finite difference and method of characteristics solutions for the case of a constant discharge into steady uniform flow. The finite element method was found to be more accurate than the finite difference approximations, but this is only to be expected as this technique can follow variation within a segment, whereas finite difference solutions cannot. The finite element method was faster and more accurate than the method of characteristics of Gardiner *et al.* [1964] However, the accuracy of the latter technique was found to be adequate, and any inaccuracies probably arise from the procedure of extrapolating the moving points back onto the fixed grid points. Apparently, there are no problems with stability and numerical dispersion in finite element methods [Price *et al.*, 1968].

In closing this section, it is mentioned that two-dimensional finite difference finite element and box models have been developed. Fischer [1970], Oster *et al.*[1970] and Leendertse [1971a] are among those who have obtained finite difference solutions for two-dimensional mass transport in the horizontal plane, whereas the box model of Pritchard [1969] was developed to describe two-dimensional mass transport in the vertical plane.

2.3 PHYSICAL AND ANALOGUE MODEL SOLUTIONS

2.3.1 <u>Physical Model Solutions</u>. Physical models of estuaries were origi-
nally developed to investigate sediment erosion and deposition in tidal water-
ways. The use of these models to investigate mass transport processes in the
prototype estuary was a natural development, and examples include O'Connor
[1962], [1965]; Diachishin [1963]; O'Connell and Walter [1963] and Lager and
Tchobanoglous [1968]. In these model investigations of the mass transport
process, a quantity of dye is introduced at the point being investigated and
its distribution throughout the model estuary is recorded over succeeding
tidal cycles.

Physical modelling involves the scaled-down reproduction of the
more important processes that affect the parameter being modelled. For mass
transport in estuaries, these processes are advection, dispersion and source-
sink effects. Physical models can satisfactorily reproduce one-dimensional
advection and the two-dimensional density dependent salinity intrusion pro-
cess [Simmons, 1960; Harleman, 1965]. However, the use of distorted cross-
sectional space scales in the model results in distorted cross-sectional
velocity distributions. From the discussion of Section A.3, it is apparent
that this will result in an incorrect reproduction of the dispersion process.
This has been discussed by Harleman [1965], Harlemen et $al.$ [1968], and Fischer
and Holley [1971]. Even in physical models with undistorted cross-sectional
space scales, the dispersion process may not be reproduced correctly. In this
case, the reproduction of the dispersion process depends on the ratio of the
time of cross-sectional mixing to the tidal period in the prototype estuary
[Fischer and Holley, 1971].

No attempt is made to reproduce any source-sink reactions in model studies, a "conservative" dye being used for the tests. However, the dye does adsorb onto surfaces, and this must be allowed for in interpreting test results. O'Connell and Walter [1963] developed a method to account for a first-order decay reaction.

2.3.2 Analogue Model Solutions. Electrical analogue models have been used to obtain solutions to the mass transport equation [Rennerfelt, 1963 and Leeds, 1967] and the hydrodynamic equations [Harder, 1971]. The estuary is divided into segments, and the space derivatives of the mass transport equation are approximated as finite differences over those segments. This reduces Equation (2.1) to a set of simultaneous difference-differential equations (the time derivative is continuous) similar to those of Thomann [1963]. The electrical analogue of this system of equations can then be constructed in the form of a so-called ladder network [Leeds and Bybee, 1967].

Analogue models can determine the steady-state and transient solutions for either constant or sinusoidally varying effluent discharge into steady non-uniform flows [Leeds, 1967 and Leeds and Bybee, 1967]. As the flow is assumed steady, these models are tidally averaged, but it may be possible to develop an analogue for sinusoidally varying flows.

Depending on the finite difference approximations used for the spatial derivatives, these models may also suffer from numerical dispersion, as was recognized by Bella [1968]. For example, the analogue of Leeds and Bybee [1967] used central differences to approximate the space derivatives of Equation (2.1). From the discussion of Section C.2, it is apparent that this will result in numerical dispersion.

2.4 STOCHASTIC SOLUTIONS

Before reviewing stochastic solutions of the mass transport equation, it is necessary to define several terms. A *process* is any phenomena that undergoes changes with respect to time, an example being daily river flow. If the chance of occurrence is taken into account, a process is said to be *stochastic* or *probabalistic*. A probabalistic process is *time-independent* and the variables are considered pure-random. A stochastic process is *time-dependent* and the variables may be pure-random or non-pure-random. If non-pure-random, the process is composed of a deterministic and a pure-random component. If the probability distribution of the random variable remains constant throughout the process, the process is said to be *stationary*, otherwise it is *non-stationary*. Non-stationary stochastic processes are very complicated mathematically, and in order of increasing simplification they are treated as stationary, probabalistic, and deterministic [Chow, 1964].

Stochastic mass transport models attempt to predict both the mean concentration profile and the variation around the mean. This variation is due to the stochastic nature of the underlying processes that determine the concentration, namely the variations that occur in the freshwater and effluent discharges, effluent concentrations, etc. during the period of analysis. Deterministic models use the mean value of each of these stochastic variables to determine the mean concentration profile.

Diaschishin [1963] assumed tidal mixing to be a pure-random process that can be characterized by a mixing length. On this basis he used a random walk formulation to obtain a tidally averaged solution for waste disposal in purely tidal waters. He allowed for the effect of mixing in the ver-

tical and lateral directions, as well as in the longitudinal direction.

The solution of Equation (2.1) for a slug input into steady uniform flow is a Gaussian distribution. Harris [1962, 1963] assumed this distribution to result from a pure-random dispersion process, and on this basis he obtained maximum likelihood estimates of $\bar{u}$ and E. He used the convolution method to obtain the solution for a continuous release. However, in the initial non-Fickian period, the cross-sectionally averaged concentration profile is skewed and not Gaussian (see Section A.3), as Fischer [1966a] noted.

Loucks and Lynn [1966] obtained the transient and steady state probability distributions of the DO concentrations at the point of minimum DO in a stream (dispersion was ignored). The sequence of daily streamflows was assumed to be a first-order Markov process (a stochastic non-pure-random process), and the sewage flows, ultimate BOD and source-sink parameters were assumed to be dependent on the daily streamflows (via conditional probabilities). Essentially, the technique is as follows. Given a streamflow, the set of sewage flows, source-sink parameters, etc. that result in the minimum DO falling below some prescribed value is determined (by a modified Streeter-Phelps equation). The probability of this set of events occurring is then determined, the process being repeated for each discrete streamflow variate, and the probabilities summed to give the total probability of the minimum DO being less than the prescribed value. Loucks [1967] used a similar technique to investigate the effect of various treatment plant operating policies on the distribution of minimum DO in a stream.

Thayer and Krutchkoff [1967] obtained a stochastic solution for the concentration profiles of BOD and DO in a stream (dispersion was ignored, and

the streamflow was assumed uniform and steady). The basic processes of decay, reaeration, etc. occurring in the modified Streeter-Phelps equation were treated as stochastic, but freshwater and effluent discharges were assumed to be deterministic. Concentration values were divided into discrete units of size Δ, and the probability of a change of Δ occurring in the concentration during a small time interval was assumed to follow a Poisson distribution. This allowed them to lump all of the stochastic variation into the parameter Δ (the sum of a number of independent Poisson processes is itself Poisson), which was determined by fitting the predicted variance in the model estuary to the observed variance in the real estuary. Essentially, they used the same set of results to both estimate and verify the model. Under these conditions, any model will reproduce the observed results, irrespective of whether the underlying processes are correctly modelled. Whereas other stochastic solutions use the explicit variation in the underlying stochastic processes to predict the variation in the concentration profiles, Thayer and Krutchkoff based their solution on the implicit variation in the stochastic processes (the actual variation is not even measured). Their predicted mean concentration value is simply the solution to the (deterministic) modified Streeter-Phelps equation. As such, their technique is no better than any deterministic model that recognizes and incorporates stochastic variation through measurements of field values. Custer and Krutchkoff [1969] used a random walk formulation to extend the technique to include dispersion (the flow was assumed uniform but unsteady), and Schofield and Krutchkoff [1972] further extended the technique to account for variable stochastic parameters along the estuary.

Koivo and Phillips [1971] regarded the measured BOD and DO concentration profiles along a stream to be corrupted by "noise" due to the stochastic nature of the underlying processes. They developed a method based on non-linear regression analysis to determine the values of the stochastic parameters that gave the best overall fit to the observed concentration profiles.

2.5 SUMMARY

Most analytical solutions to the one-dimensional mass transport equation are tidally averaged and may be useful for investigating effluent discharge into estuaries with simple geometries. (When the number of segments with different geometries is greater than four or five, the matching of boundary conditions at their ends becomes cumbersome [O'Connor *et al.*, 1968]). In tidally averaged solutions, upstream transport is by dispersion, and thus a tidally averaged model may not adequately reproduce the interaction of two or more effluent outfalls on the flood tide.

Numerical solutions provide a means of solving the one-dimensional tidally varying mass transport equation, but the problems of stability and numerical dispersion must be considered. Of the various numerical methods, the method of characteristics, methods with higher order approximations and finite element methods are satisfactory with respect to accuracy of solution. The method of characteristics has the additional advantage of directly simulating the advective process.

Undistorted physical models may be useful in resolving complex three-dimensional aspects of the flow-field at important or sensitive sections of the estuary, but because of their inaccurate and inconsistant reproduction

of the dispersion process (in both distorted and undistorted models), at best they are only an adjunct to a mathematical form of solution. As developed, analogue models are tidally averaged and suffer from numerical dispersion, although it may be possible to overcome both these limitations.

It is not clear whether the various stochastic solutions attempt to model "true" stochastic variation, or a combination of stochastic and cross-sectional variation. If the cross-sectional variation is greater than the actual stochastic variation, it may be more meaningful to model the lateral component of the dispersion process with a two-dimensional deterministic model.

CHAPTER 3

A DESCRIPTION OF THE HYDRODYNAMIC AND MASS TRANSPORT MODELS

3.1 THE HYDRODYNAMIC MODEL

To solve the one-dimensional tidally varying mass transport equation, it is necessary to know both the spatial and temporal variation in the parameters $\bar{u}$, A and E of the equation, as is discussed in Section 1.3. A one-dimensional hydrodynamic model was developed to predict the spatial and temporal variation in the parameters $\bar{u}$ and A. (The temporal and spatial variation of the parameter E is discussed in Appendix F. In the hydrodynamic model, the equations of motion and continuity were applied to the water mass of the estuary, and solved throughout the tidal cycle.

3.1.1 The Hydrodynamic Equations. As applied to the Fraser River Estuary, the equations of motion and continuity are given by [Dronkers, 1969]

$$\frac{\partial u}{\partial t} + \bar{u}\frac{\partial \bar{u}}{\partial x} = -g\frac{\partial h}{\partial x} - g\frac{|\bar{u}|\bar{u}}{c^2\bar{y}}$$ (3.1)

$$\frac{\partial}{\partial x}\{A\bar{u}\} = -b\frac{\partial \bar{y}}{\partial t}$$ (3.2)

where

$\bar{u}$ is the mean longitudinal velocity;

h is the height of the water surface above an arbitrary level datum;

$\bar{y}$ is the mean cross-sectional water depth;

34

A is the cross-sectional area;

b is the cross-sectional width;

g is the local gravitational acceleration;

and

C is Chezy's friction factor.

Several of these terms are illustrated in Figure 3.1. Note that in the hydrodynamic equations, x increases in the upstream direction, whereas in the mass transport equation, x increases in the downstream direction.

The two terms on the left-hand side of Equation (3.1) are the local and convective (or Bernoulli) accelerations respectively. The two terms on the right-hand side of the equation are the forces causing these accelerations, the net pressure force due to the slope of the water surface and the friction force respectively. The first term of Equation (3.2) is the net outflow from an elemental cross-sectional slice of the estuary, while the second term represents the accompanying change in storage within the slice.

The assumptions made in deriving equations (3.1) and (3.2) are listed in Dronkers [1964]. The most important assumption is that the storage width is equal to the advective width. The variation of advective and storage widths along the major channels of the estuary is shown in Figures B.6 to B.8. The difference between the advective and storage widths is exaggerated since these values were determined from the cross-sectional areas below local low water. (In the lower reaches of the estuary, the tidally averaged depth is some 10 feet above local low water). Consequently, the assumption of equal advective and storage widths seems reasonable for the Fraser River Estuary. (This is also discussed in Section 4.1 with regard to the verifi-
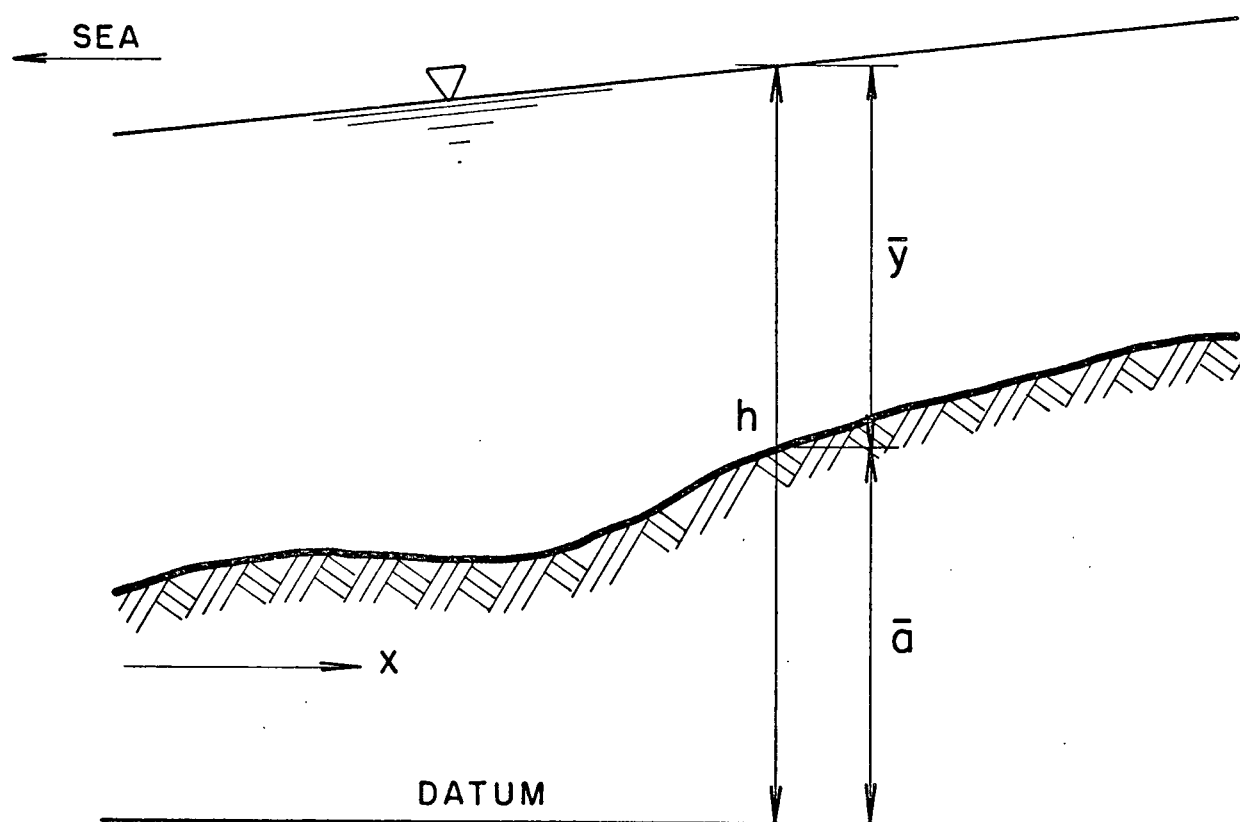
Figure 3.1

The Hydrodynamic Estuary

cation of the hydrodynamic model). The one-dimensional nature of the equations is justified since the various channels of the estuary are much longer than they are wide (see Appendix B). In fact, Callaway [1971] has classified this type of estuary as a "tidal river." In deriving Equations (3.1) and (3.2) the presence of the salt wedge has been ignored because of the complicated nature of its dynamics (see Appendix B). According to Odd [1971], the Chezy formula should adequately represent frictional effects in fast flowing, well mixed estuaries. The Fraser River estuary is fast flowing, but the Chezy formula may not be accurate in the highly stratified lower reaches.

From Figure 3.1, it is seen that

$$h = \bar{a} + \bar{y} \qquad (3.3)$$

where $\bar{a}$ is the height of the river bottom above the same level datum that h is referred to. Thus, Equations (3.1) and (3.2) are seen to be a pair of coupled partial differential equations, the dependent variables being $\bar{u}$ and either $\bar{y}$ or h, and the independent variables being x and t. The width b, Chezy's friction factor C, the area A and the factor $\bar{a}$ all appear in the equations as parameters. In deriving these equations, it has been assumed that the dependent variables and parameters vary in a continuous manner along the estuary. It is noted that both equations contain variable coefficients and that Equation (3.1) contains non-linear terms.

The fixed mesh, explicit finite difference method of Dronkers [1969] was used to obtain a numerical solution to the hydrodynamic equations. Details of the method are given in Appendix D and the fixed mesh of "stations" used in the finite difference solution is shown in Figure B.4. Because the

solution scheme of the hydrodynamic equations is explicit, stability re-
quirements determine the relative size of Δx and Δt. In solving the
hydrodynamic equations, Δx was set equal to 5,000 feet, except in the
deeper waters of Pitt Lake where Δx was increased to 15,000 feet for
stability reasons. It was found that with this space grid, a Δt of 90
seconds was satisfactory as regards stability. The stability requirements
are discussed in detail in Section C.3.

3.1.2 Assumed Quasi-Steady Hydraulic Conditions. For effluent
discharge into an estuary, the quasi-steady state response of an estuary
is usually a condition of interest. Tidally varying mass transport models
usually require many tidal cycles to achieve quasi-steady-state conditions,
whereas hydrodynamic models only require several tidal cycles. The reason
for this is the relative speed of information propagation in both systems.
In the hydrodynamic model, the information consists of small changes in sur-
face elevation that propagate along the estuary as elemental surges with
speeds of $u\pm\sqrt{g\bar{y}}$, whereas in the mass transport model, the information con-
sists of changes in concentration (finite or otherwise) that propagate at
speeds of $\bar{u}$ (if dispersion is ignored). This is discussed further in Sec-
tion C.3. Thus, in applying a mass transport model to determine the quasi-
steady state response of an estuary for some waste loading condition, it
is necessary to run the model for a succession of tidal cycles.

In solving the hydrodynamic and tidally varying mass transport
equations for the Fraser River Estuary, the freshwater discharge and tidal
conditions are assumed to be quasi-steady. Thus, the model estuary "sees"
a constant freshwater inflow and a succession of identical tides. In
actual fact, "slow" variations occur in the freshwater inflow and tidal

conditions, and the estuary may never achieve strict quasi-steady state
conditions. However, as the residence time of the Fraser River Estuary is
only four to six days, it seems reasonable to treat the freshwater and
tidal conditions as constant for this period of time.

3.1.3 <u>The Model Estuary of the Hydrodynamic Equations.</u> The
Fraser River Estuary is described in detail in Appendix B. The model
estuary, as described by the hydrodynamic equations, differs to some ex-
tent from the real estuary because of the assumptions made in deriving
the hydrodynamic equations. The model estuary consists of the same seven
principles as the real estuary, although the Canoe Pass Area has been simpli-
fied into a single channel, as is shown in Figure B.4. The channels of the
model estuary are assumed to be rectangular in cross-section (equal storage
and advective widths), and the salinity is assumed to be everywhere zero.
Because the salt wedge has been ignored, the predicted velocities in the
lower reaches of the estuary are probably somewhat low. The freshwater dis-
charge in the model estuary is constant, and the tidal rise and fall of
the water surface is quasi-steady.

3.2 THE TIDALLY VARYING MASS TRANSPORT MODEL

3.2.1 <u>Method of Solution.</u> The tidally varying mass transport
equation was solved by a characteristic finite difference method. In this
method, the equation is solved along the characteristic curves of the advec-
tive transport process, as is discussed in Appendix C. The accuracy and
directness of solution were instrumental in this choice; there is no numeri-
cal dispersion (see Appendix C) and the advection process is simulated

directly and independently of the dispersive process.

It was not possible to use the usual techniques of dye patch studies or measurement of existing tracers to verify the mass transport models. The large dilutional capacity of the river made extensive dye patch studies too expensive, and as the seven channels of the estuary are essentially unpolluted [Benedict, *et al.*, 1973], there are no suitable existing pollutional tracers. Because of the high degree of stratification and the complicated nature dynamics of the salinity intrusion (see Section B.2.4), salt could not be used as a tracer. Thus, it was not possible to verify the mass transport models by a direct comparison of predicted and observed concentrations. An attempt was made to "verify" the underlying mass transport processes of advection and dispersion independently of each other, as is discussed in Section 4.2. The method of characteristics leads to a natural separation of the advective and dispersive transport processes, and this was one of the reasons for using this method to solve the tidally varying mass transport equation.

The one-dimensional mass transport equation is derived in Appendix A and the assumptions in its derivation are discussed there. The equation was transformed into Lagrangian or characteristic form (see Section A.6) to give

$$\frac{dx}{dt} = \bar{u} \tag{3.4}$$

$$\frac{d\bar{c}}{dt} = \frac{1}{A}\frac{\partial}{\partial x}\{EA\frac{\partial \bar{c}}{\partial x}\} + \sum_{i=1}^{n} S_i \tag{3.5}$$

Equation (3.5) was then separated into its component dispersive and source-sink effects to give

$$\frac{d\bar{c}}{dt} = \frac{1}{A}\frac{\partial}{\partial x}\{EA\frac{\partial\bar{c}}{\partial x}\} \tag{3.6}$$

and

$$\frac{d\bar{c}}{dt} = \sum_{i=1}^{n} S_i \tag{3.7}$$

Initially, a grid of moving points was assigned throughout the estuary. In the advection step, a finite difference form of Equation (3.4) was used to advect the points along the estuary for a time increment, the concentration of the points being adjusted as they passed effluent outfalls or through converging junctions. In the dispersion step, an explicit finite difference form of Equation (3.6) was used to adjust the concentration of the moving points for the effects of dispersion during the time increment. Finally, in the source-sink step, Equation (3.7) was used to adjust the concentration of the moving points for the effects of the source-sink processes during the time increment. (The source-sink step can be done analytically -- for a BOD-DO system, Equation (3.7) is the usual Streeter-Phelps equation). The sequence of these three steps was then repeated for the next time increment, and so the solution progresses through time. At the boundaries of the estuary (the sea, Pitt Lake and Chilliwack), moving particles were added to and removed from the estuary as dictated by the advective boundary conditions. A time increment of one hour was used in solving the tidally varying mass transport equation, and at the end of each hour, the concentrations were extrapolated off the grid of moving points onto the 5,000 foot fixed grid of Figure 3.1. The method of solution is very similar to the combined method of Gardiner *et al.*

[1964], except that whereas Gardiner *et al.* extrapolate the moving points onto the fixed grid, the moving points in the Fraser River Estuary solution always remain on their respective characteristics and only their concentrations are extrapolated onto the fixed grid. Details of the solution of Equations (3.4), (3.6) and (3.7) are given in Appendix D.

An advantage of the characteristic method of solution is that additional moving points can be added to the estuary to more closely define regions of rapid variation in concentration, as occur at times of slackwater at effluent outfalls, and where the variation is slow unnecessary moving points can be removed. Once the moving points are in the estuary, their subsequent positions are determined by the advective transport process, and they are not uniformly spaced along the estuary in the dispersive step. Both an explicit and implicit finite difference scheme were investigated for the dispersive step. The explicit scheme was slightly slower, but was chosen for reasons of simplicity (see Appendix D). The stability requirements of the explicit scheme are discussed in Appendix C, and generally the time increment for stability was less than one hour; the dispersive step then consisted of a number of "internal" iterations within the basic time increment of one hour, as discussed in Appendix D.

3.2.2 <u>The Model Estuary</u>. For the sake of convenience, the model estuary of both the tidally averaged and tidally varying mass transport equations has been simplified to the three major channels of the real estuary, the Main Arm - Main Stem, the North Arm and the Pitt System, as shown in Figure 3.2. The stations along these channels are the same as those of the
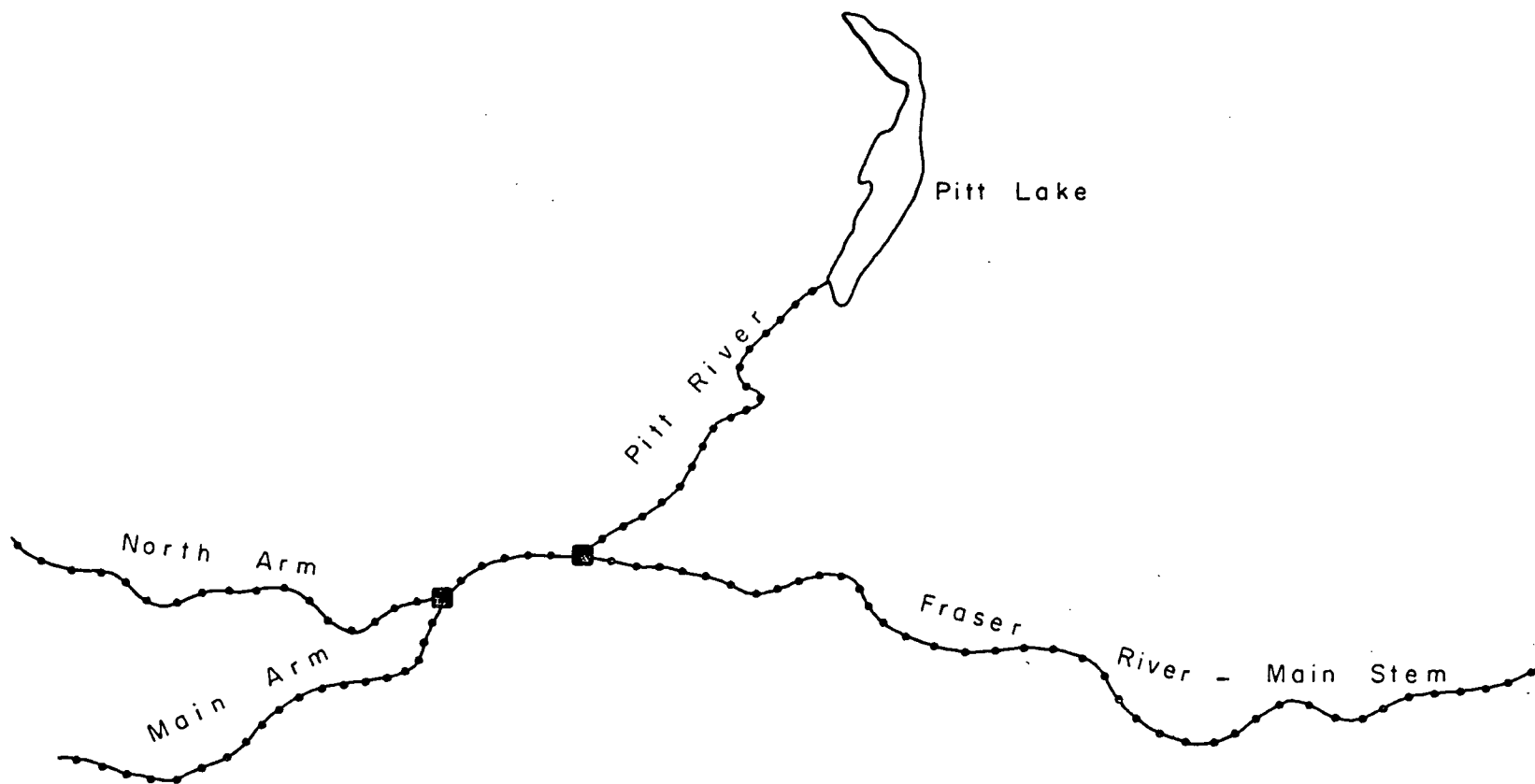
Figure 3.2

Simplified Model Estuary of the Mass Transport Equations

hydrodynamic model. It is possible to include all seven channels of the real estuary, but it would have made the computer programming of the tidally varying mass transport equation considerably longer and more involved. Because of their short length and smaller flows, the concentration profile along the minor channels is essentially determined by the profile along the major channels, and the approximation of ignoring the minor channels seems reasonable.

In the model estuary, the dispersion process is assumed to be Fickian in its entirety and the cross-sectional mixing is assumed to be complete at the junctions. The salinity of the model estuary is zero, but because of the salinity intrusion in the real estuary, the predicted velocity field and advective transport in this region is probably under-estimated. The estuary is highly stratified in the region of the salinity intrusion and little mixing occurs between the fresh and saltwater. This will tend to minimize any chemical or biological effects the saltwater may have on the dissolved substance in question. As in the model estuary of the hydrodynamic equations, the freshwater discharge is constant and the tidal conditions are quasi-steady.

3.3 TIDALLY AVERAGED MASS TRANSPORT MODEL

3.3.1 Method of Solution. The one-dimensional, tidally averaged mass transport model of Thomann [1963] was used to determine the steady state tidally averaged response of the Fraser River Estuary for various waste loading conditions. (As the model is tidally averaged, the response is steady-state rather than quasi-steady state). In this model, the estuary is divided into

a number of longitudinal segments or "boxes", as shown in Figure D.2. Each segment is assumed to be completely mixed, and the tidally averaged advection and dispersion processes transport dissolved substance into and out of each segment. If the tidally averaged transport processes and effluent discharges remain steady, a mass balance about segment i gives

$$a_{i,i-1}c_{i-1} + a_{i,i}c_i + a_{i,i+1}c_{i+1} = W_i \qquad (3.8)$$

where

c_i is the concentration in segment i;

W_i is the mass of effluent discharged into segment i per tidal cycle;

$a_{i,i-1}$ is a coefficient accounting for the tidally averaged transport of substance between segments i and i-1, similarly for $a_{i,i+1}$;

and

$a_{i,i}$ accounts for dispersion out of segment i and any sink effects the substance undergoes.

Details of this equation and its coefficients are given in Appendix D. An equation similar to (3.8) can be written for each of the n segments of the estuary, and in matrix notation the system of equations can be written

$$\underset{\sim}{A} \cdot \underset{\sim}{C} = \underset{\sim}{W} \qquad (3.9)$$

where

$\underset{\sim}{W}$ is a (n x 1) column matrix of the tidally averaged waste loads into each segment per tidal cycle;

$\underset{\sim}{C}$ is a (n x 1) column matrix of the tidally averaged concentration in each segment;

and $\underset{\sim}{A}$ is a (n x n) tri-diagonal matrix containing the tidally
averaged transport terms and any sink effects.

Thus, the steady state tidally averaged response of the estuary is described

by a system of n simultaneous linear equations. Equation (3.9) represents

the concentrations of a conservative substance or a substance undergoing

first order decay, such as BOD. To investigate the steady-state BOD-DO res-

ponse of an estuary, a system of equations similar to (3.9) and coupled to

it are obtained for the DO concentrations (see Thomann [1971] for details).

Thomann's steady-state solution to the one-dimensional tidally

averaged mass transport equation is essentially a fixed grid finite differ-

ence solution similar to that of an implicit difference scheme (see Appendix

D). There is no stability requirement for the steady-state solution (see

Section C.3), but there is a non-negativity requirement that imposes rela-

tive limits on the sizes of the advective and dispersive transport processes.

This is discussed in Section D.3, and if this requirement is violated, the

concentration in a segment becomes negative. Thomann's steady-state solution

does not suffer from numerical dispersion, but for a rather unusual reason.

Because of the fixed grid nature of his finite difference scheme, the advec-

tive process will not be correctly simulated and numerical dispersion should

occur. However, from Section C.2, it is seen that for numerical dispersion

to occur, it is necessary for the concentration at a fixed grid point to

change with time. Thomann's steady-state solution admits no temporal changes,

and thus no numerical dispersion occurs. Numerical dispersion does occur in

his transient solution where the concentration at the fixed grid points does

change with time, as Thomann [1971] recognizes.

3.3.2 <u>The Model Estuary</u>. The model estuary of the tidally aver-
aged equation consists of the same three major channels and stations as the
model estuary of the tidally varying equation and cross-sectional mixing is
assumed to be complete at the junctions. The tidally averaged model estuary
has no tides and has higher dispersion than its tidally varying counterpart.
Thomann [1971] lists typical values of the tidally averaged dispersion coeffi-
cient. They range from 1 - 20 square miles per day with a mean value of
about 10 square miles per day. These values seem high compared to the
tidally varying values of dispersion coefficients, and apparently reflect
the influence of tidal advection in determining the tidally average disper-
sion coefficient. As in the tidally varying solution, the influence of the
salinity intrusion is ignored.

CHAPTER 4

VERIFICATION OF THE HYDRODYNAMIC AND MASS TRANSPORT MODELS

4.1 THE HYDRODYNAMIC MODEL

The verification of the hydrodynamic model is to ensure that
the model estuary, as represented by the hydrodynamic equations, adequate-
ly reproduces the variation in water surface elevations and discharges (or
advective velocities) observed in the real estuary. The "verification"
consists of adjusting the friction factors and the cross-sectional widths
and depths of the model estuary until an adequate fit is obtained between
predicted and observed results. (In deriving the hydrodynamic equations,
the advective flow was assumed to be uniformly distributed over an assumed
rectangular cross-section. In real situations, the cross-section is not
rectangular and the flow is concentrated in the deeper sections. To
compensate for these effects, it is necessary to adjust the cross-sectional
geometry of the model estuary).

4.1.1 Data Available. The network of permanent tide-gauging
stations throughout the estuary is shown in Figure B.11, and provides a
limited but adequate record of the water surface elevations of the estuary
throughout the tidal cycle. Field measurements of velocities and discharges
are sporadic and inadequate for verification purposes. The only existing
data adequate for a complete verification of the hydrodynamic model under
high tide-low flow conditions is due to Baines [1952]. In this study, water
surface elevations were recorded at half-hour intervals at 43 stations

48

throughout the estuary for the high tide-low flow conditions of January 24, 1952. The freshwater discharge at Chilliwack was 36,500 cubic feet per second and the tidal range at Steveston was 11 feet. Baines used the method of cubature to estimate the tidally varying discharges at the 43 stations.

4.1.2 Water Surface Elevations for Low Flows. The high tide-low flow conditions of January 15, 1964 were used in an initial attempt to reproduce the recorded water surface elevations in the real estuary. The freshwater discharge at Chilliwack was 53,500 cubic feet per second and the tidal range at Steveston was 10 feet. The water surface elevations of the model estuary were found to be relatively insensitive to the effects of friction and cross-sectional geometry. In fact, the response of narrow sections with high friction was found to be equivalent to that of broader sections with low friction. This is illustrated in Figure 4.1 which shows the predicted responses for both types of section at Station No. 18 (New Westminster) on the Main Arm - Main Stem. The average values of widths, depths and Manning's "n" along the Main Arm - Main Stem are also shown. Note that while Chezy's formula for friction was used in solving the hydro-dynamic equations, friction coefficients are reported as values of Manning's "n" (the values of n are for feet-second units).

4.1.3 Water Surface Elevations for High Flows. To separate out the independent effects of friction and cross-sectional geometry, an attempt was made to reproduce the water surface elevations of the high tide-high flow conditions of June 16, 1964. The freshwater discharge at Chilliwack was 463,000 cubic feet per second and the tidal range at Steveston was eight feet. It was thought that the greater velocities under high discharge
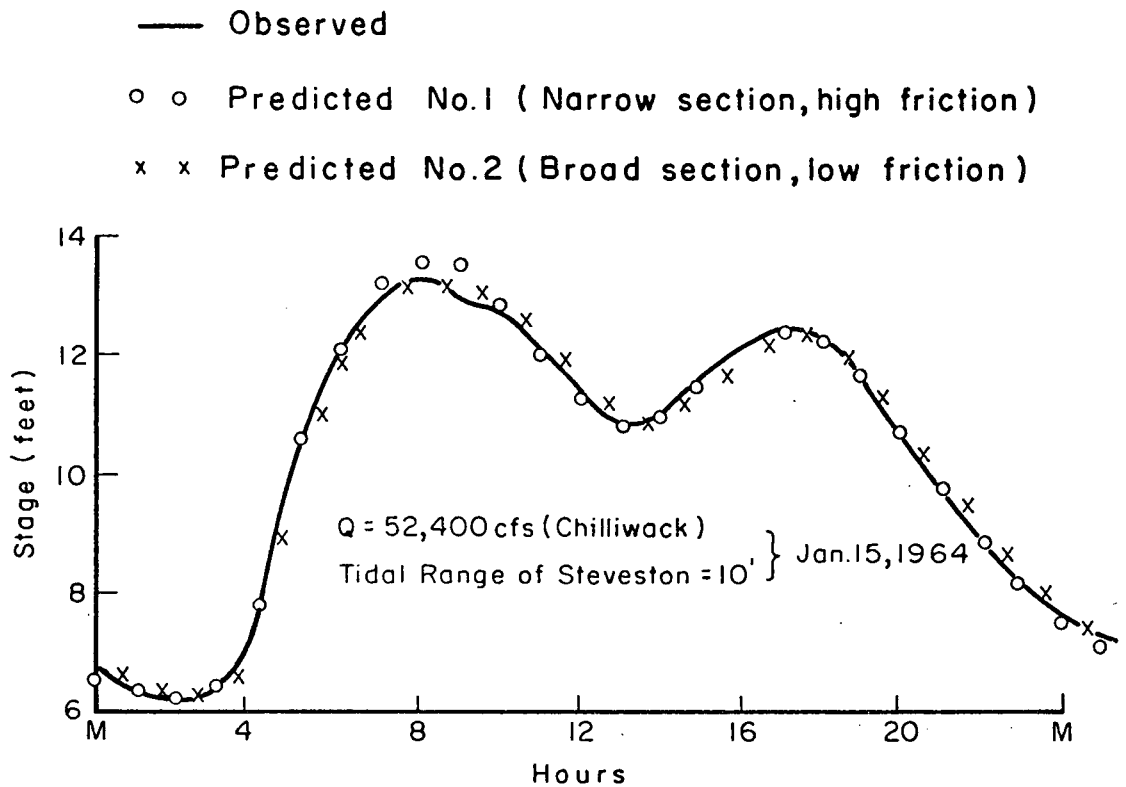
—— Observed

o o Predicted No.1 (Narrow section, high friction)

x x Predicted No.2 (Broad section, low friction)

Q = 52,400 cfs (Chilliwack)
Tidal Range of Steveston = 10' } Jan.15,1964

Average values along Main Arm − Main Stem.

Results	Average Mannings "n"	Average Width (feet)	Average Depth (feet)
Predicted No. 1	0.042	1350	30.6
Predicted No. 2	0.030	1870	22.9

Figure 4.1

Equivalent Stage Response for Two Different Types of Cross-Section

conditions would be more sensitive to frictional effects. This was found

to be the case, the tidally averaged or mean water levels being very sen-

sitive to friction and essentially independent of width. However, the

width was found to govern the range of the water surface fluctuations about

the mean water level. The predicted and observed water surface elevations

are shown in Figures 4.2 and 4.3, and the reproduction of the observed re-

sults is seen to be satisfactory. The gross cross-sectional values of

depths and areas shown in Figures B.6 to B.8 were used in obtaining these

results. The width was determined by dividing the area by the depth, and

was a satisfactory compromise between the narrower advective sections and

the broader sections more representative of the storage width. Manning's

"n" varied from 0.022 in the lower reaches to 0.027 in the upper reaches.

These values are reasonable, and indicate that the Main Arm - Main Stem is

hydraulically smooth [Chow, 1959].

Under these high discharge conditions, the flow in the upper

reaches of the Main Stem is steady, and the predicted water surface slope

can be used to check that the hydrodynamic model satisfactorily reproduces

the frictional effects. The predicted value of Manning's "n", as determined

by the average area, depth and predicted water surface slope between stations

40 and 60 on the Main Stem, was 0.0269. This agrees closely with the actual

value of 0.027 used in the hydrodynamic model over this section of the

estuary.

The "high flow" friction coefficients and cross-sectional geo-

metries were then used in a second attempt to reproduce the water surface

elevations for the low flow conditions of January 15, 1964. To obtain a sat-

isfactory fit between the predicted and observed results it was necessary to

Q = 463,000cfs (Chilliwack)
Tidal range at Steveston = 8' } June 16,1964

Main Arm – Station No.2 (Steveston)

Main Arm – Station No.8 (Deas Island)

—— Observed
o o Predicted

Main Arm – Station No.18 (New Westminster)

Stage – feet (Sandheads datum)

Hours
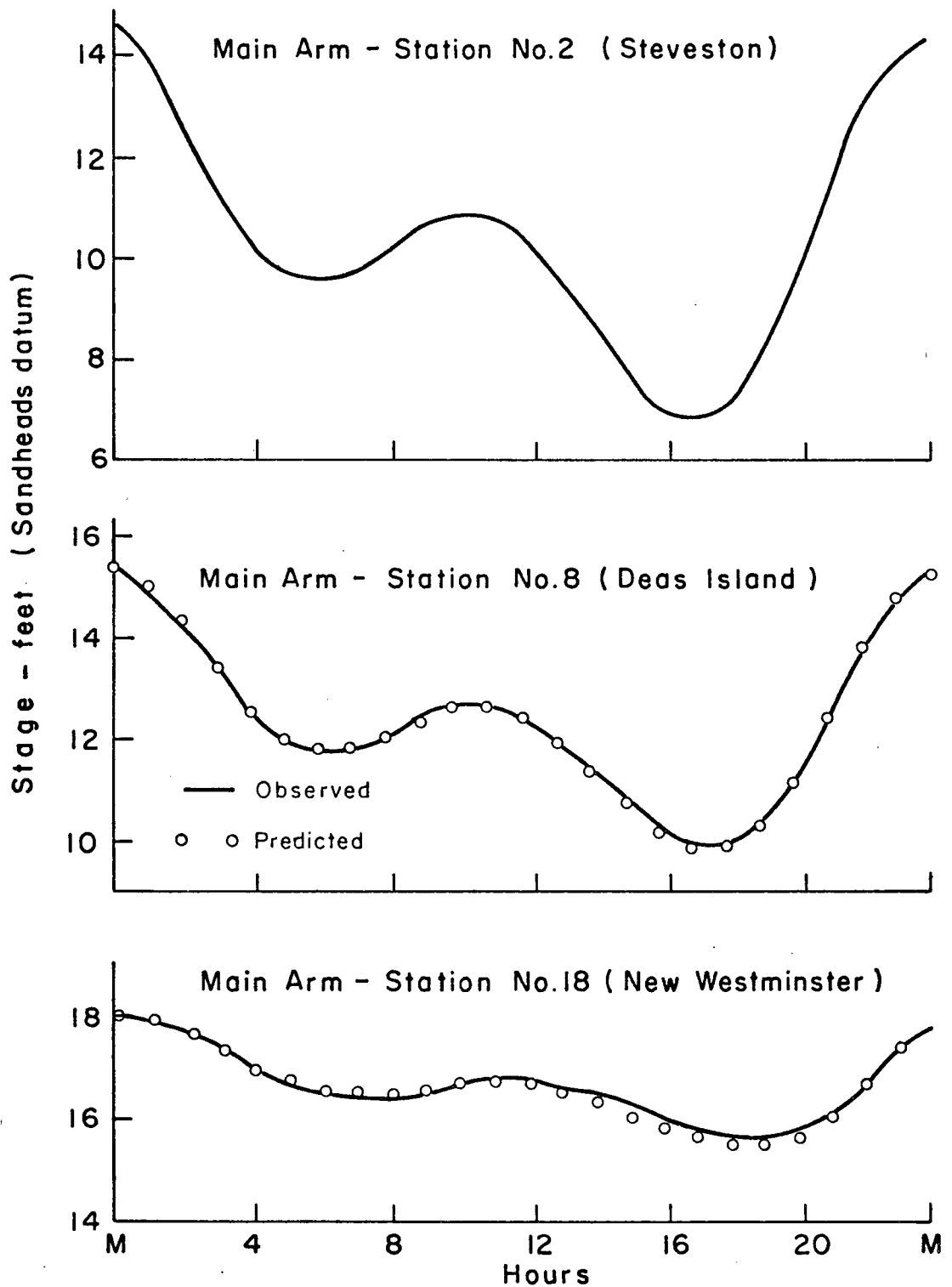
Figure 4.2

Observed and Predicted Stages for June 16, 1964

Q = 463,000 cfs (Chilliwack)
Tidal range at Steveston = 8' ⎫ June 16, 1964

Main Arm — Station No. 22 (Port Mann)

Main Arm — Station No. 32 (Port Hammond)

—————— Observed

o   o   Predicted

Pitt — Station No. 144 (Port Coquitlam)

Pitt — Station No. 162 (Alvin)

Stage – feet (Sandheads datum)

Hours
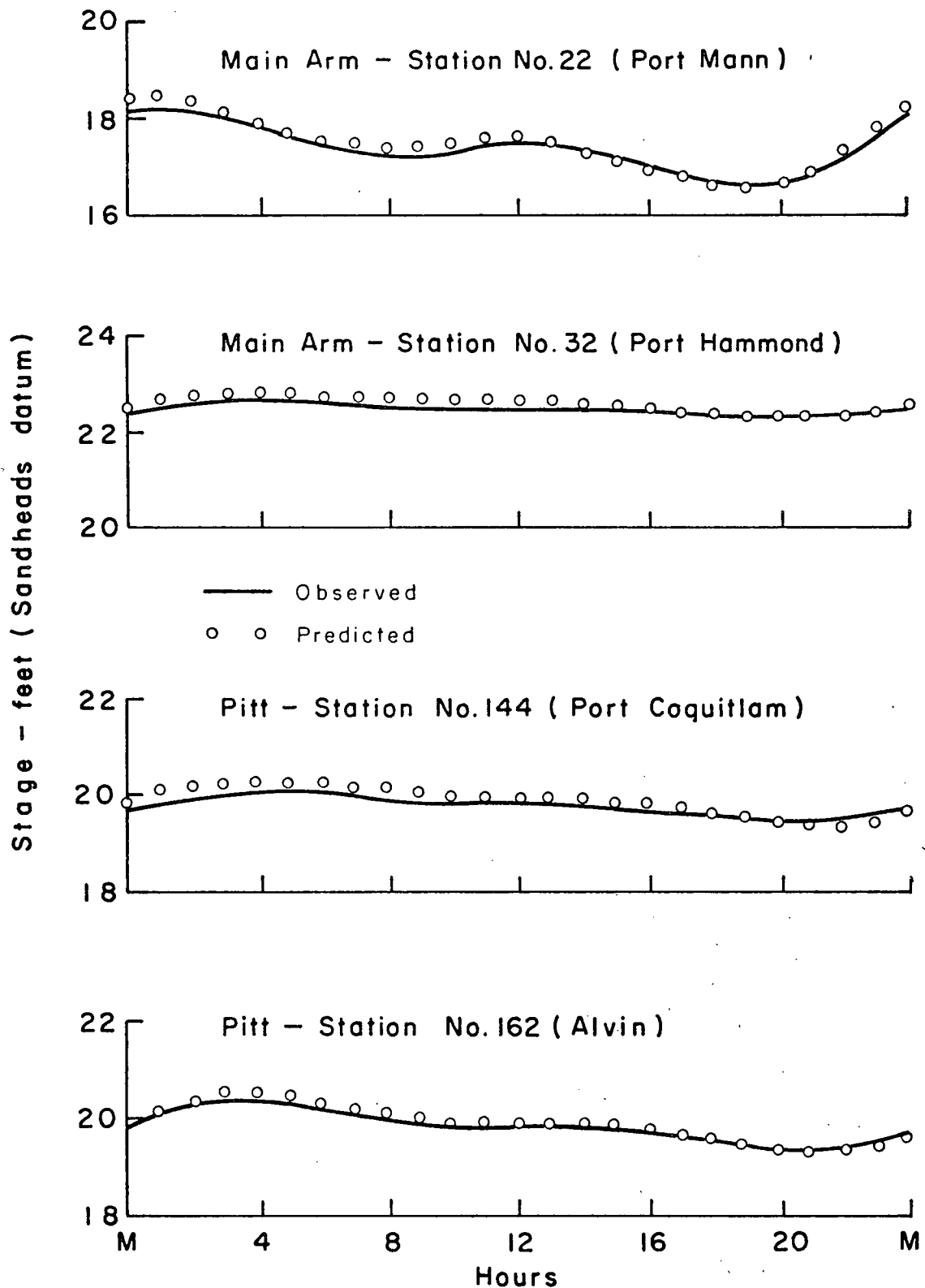
Figure 4.3

Observed and Predicted Stages for June 16, 1964

increase Manning's "n" by approximately 0.005 throughout the estuary.
Under these conditions the value of Manning's "n" along the Main Arm-
Main Stem varied from 0.027 in the lower reaches to 0.032 in the upper
reaches, and once again these values are reasonable. The increase in fric-
tion that low flows experience relative to higher flows also seems reason-
able. During the falling limb of the annual hydrograph sediment is deposited
in the lower channels of the estuary [Pretious, 1972], and thus the low winter
flows experience bed forms defined by the higher summer flows. It is expected
that the relative roughness of these bed forms will be greater for the low
flows -- and hence the greater friction.

4.1.4 Verification for the Conditions of January 24, 1952. Having
made an independent check on the friction coefficients and effective cross-
sectional geometries, an attempt was made to reproduce the recorded water
surface elevations and cubature discharges of Baines [1952]. With minor
adjustments to the friction coefficients, the water surface elevations and
discharges shown in Figures 4.4 to 4.11 were obtained. The predicted dis-
charge curves were found to be insensitive to changes in the cross-sectional
geometries, but relatively sensitive to changes in the friction coefficients.
In certain sections of the estuary, the low-flow friction coefficients of the
section have been slightly lowered to obtain a better fit between the pre-
dicted and observed peak discharges.

Generally, the fit between the predicted and observed water surface
elevations is satisfactory. In the upper reaches of the Main Stem, the range
of predicted water surface elevations is somewhat greater than that observed,
and is probably due to "ending" the model estuary before the tidal rise and

Q = 36,500 cfs (Chilliwack)

Tidal Range at Steveston = 11' } January 24, 1952
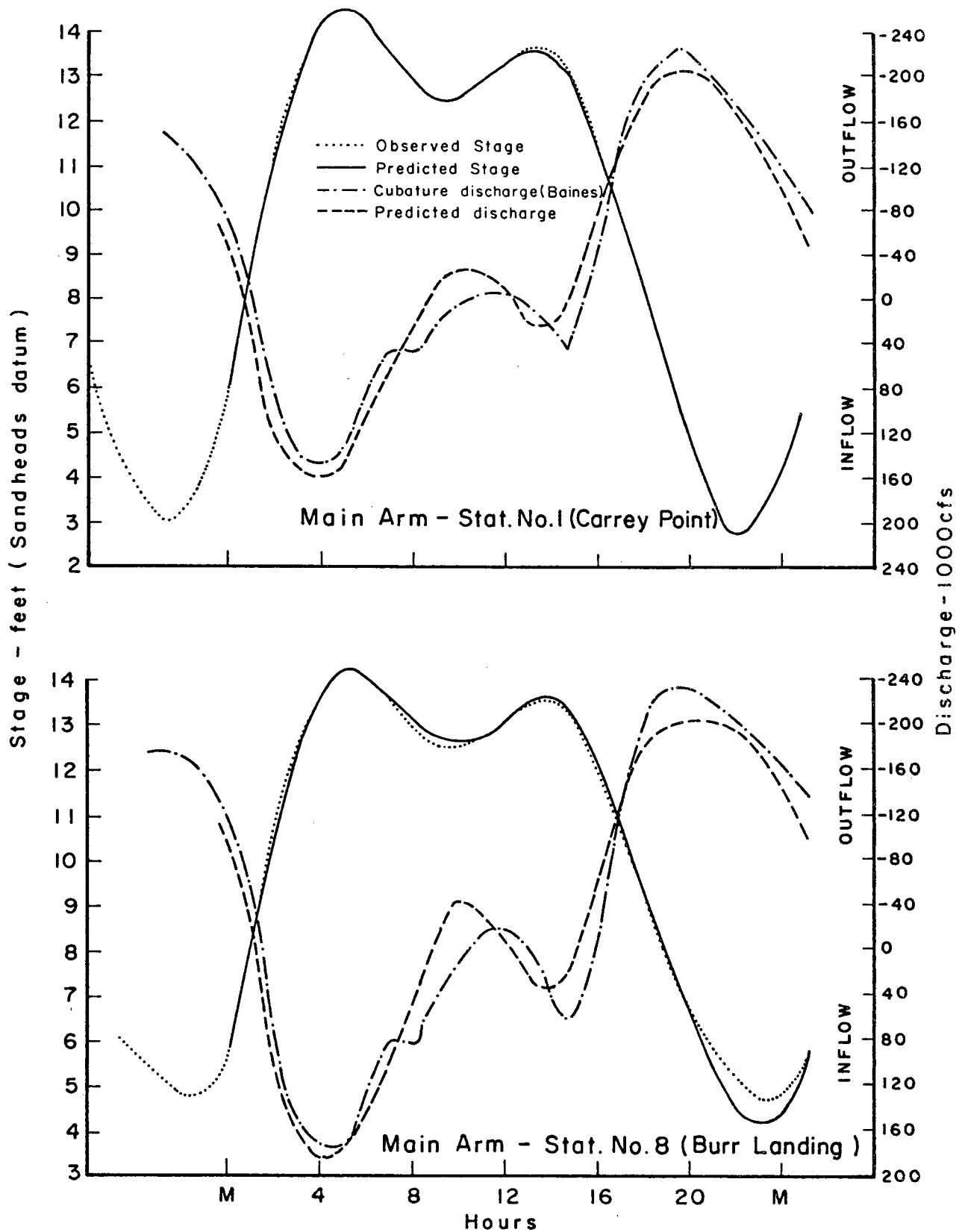
Figure 4.4   Tidally Varying Stage and Discharge - Main Arm

Q = 36,500 cfs (Chilliwack)

Tidal Range at Steveston = 11'$^{\}$ January 24, 1952
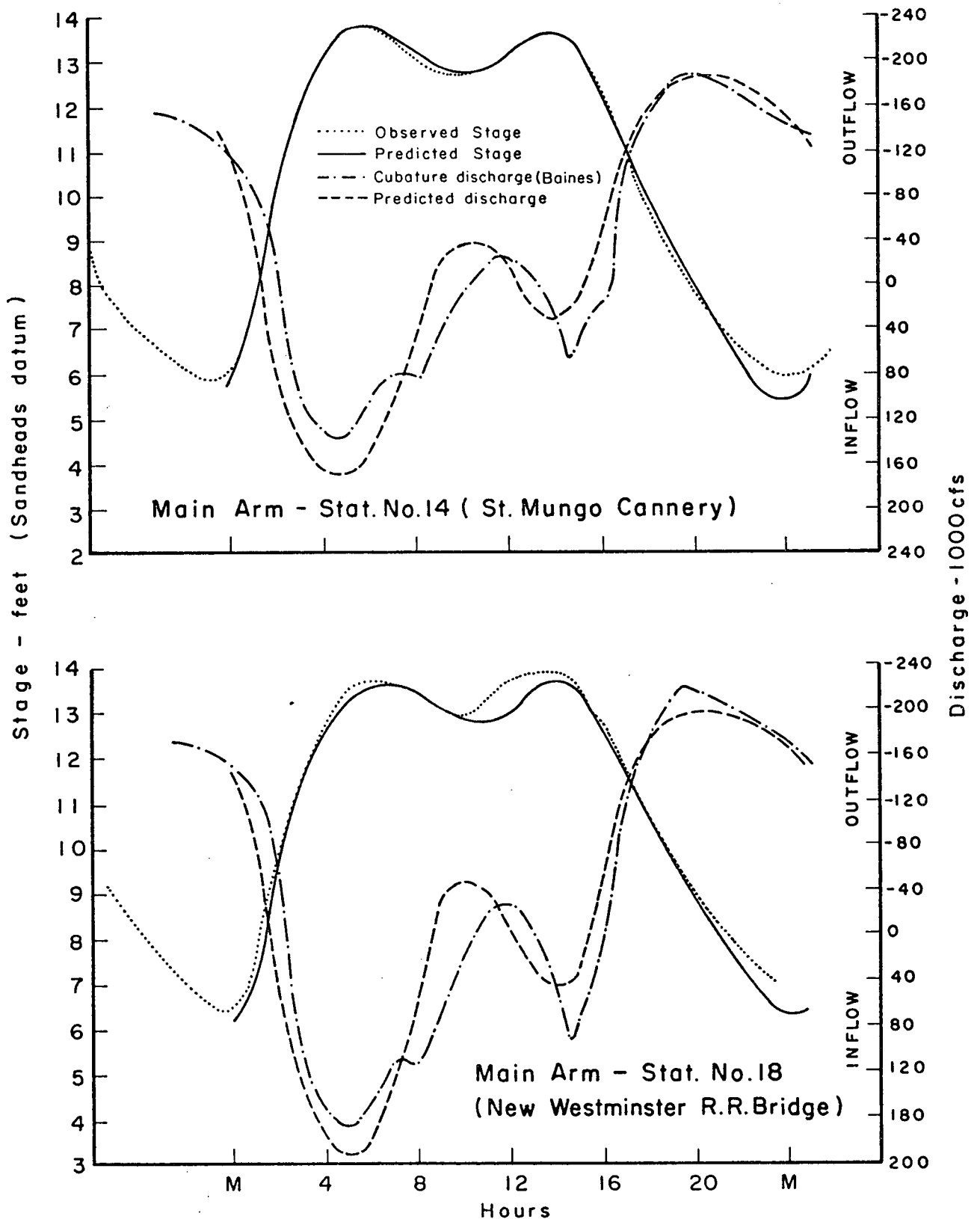
Figure 4.5   Tidally Varying Stage and Discharge - Main Arm

Q = 36,500 cfs (Chilliwack

Tidal Range at Steveston = 11' } January 24, 1952
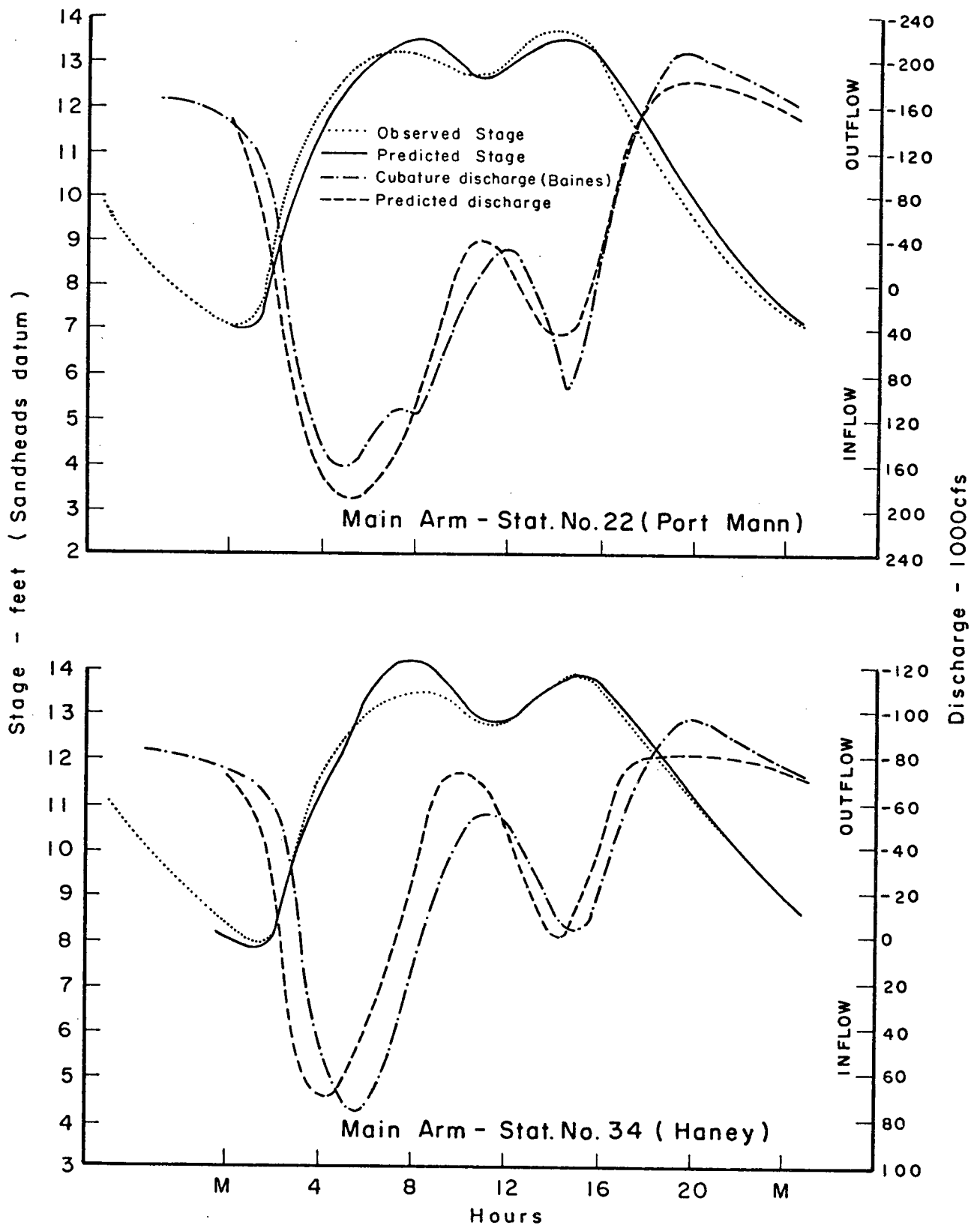
Figure 4.6 Tidally Varying Stage and Discharge - Main Arm

Q = 36,500 cfs (Chilliwack)

Tidal Range at Steveston = 11' } January 24, 1952

.... Observed Stage
————— Predicted Stage
—·—·— Cubature discharge (Baines)
— — — Predicted discharge

Main Arm — Stat. No. 40 (Whonock)

Main Arm — Stat. No. 51 (Mission)
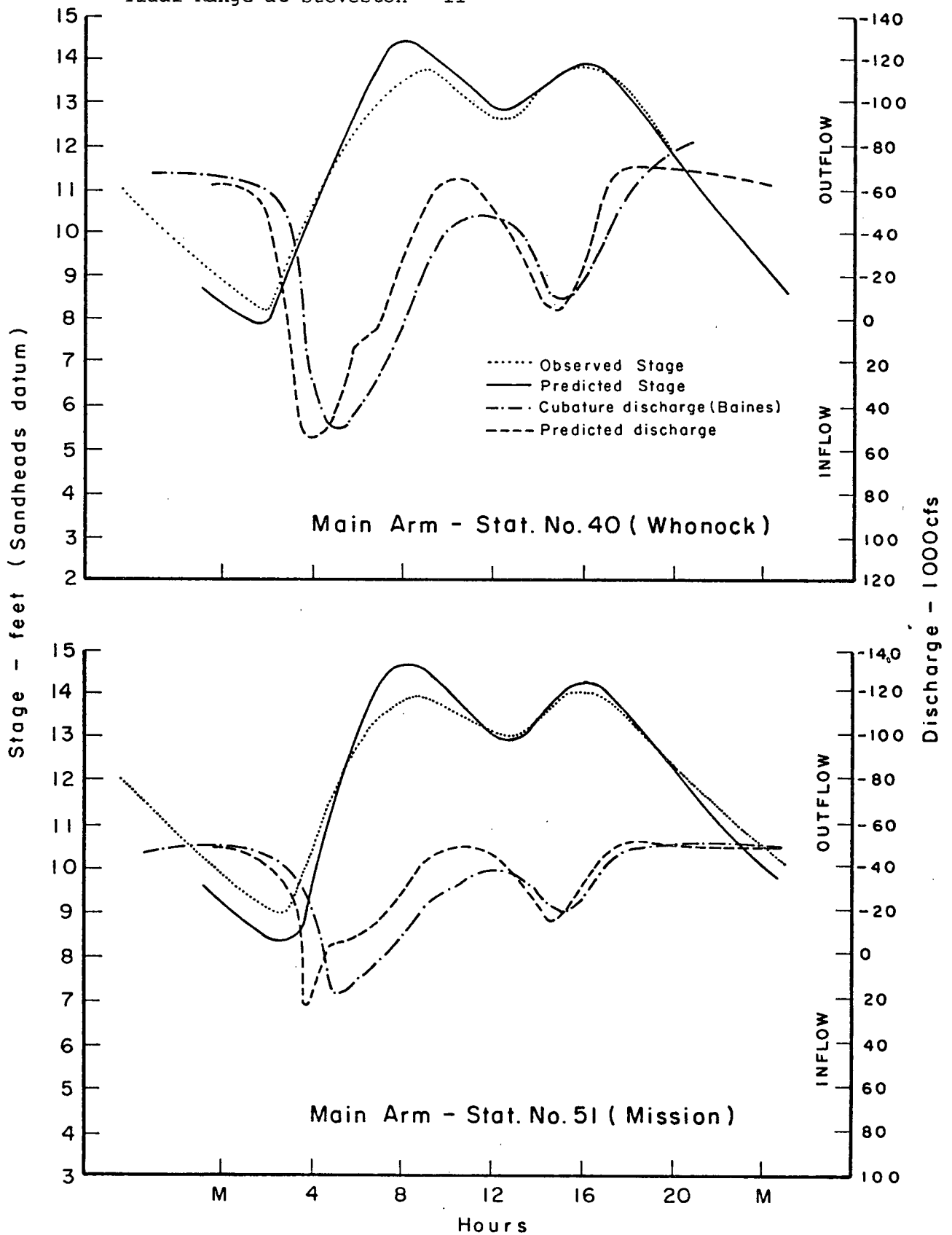
Figure 4.7   Tidally Varying Stage and Discharge — Main Arm

Q = 36,500 cfs (Chilliwack)

Tidal Range at Steveston = 11' } January 24, 1952
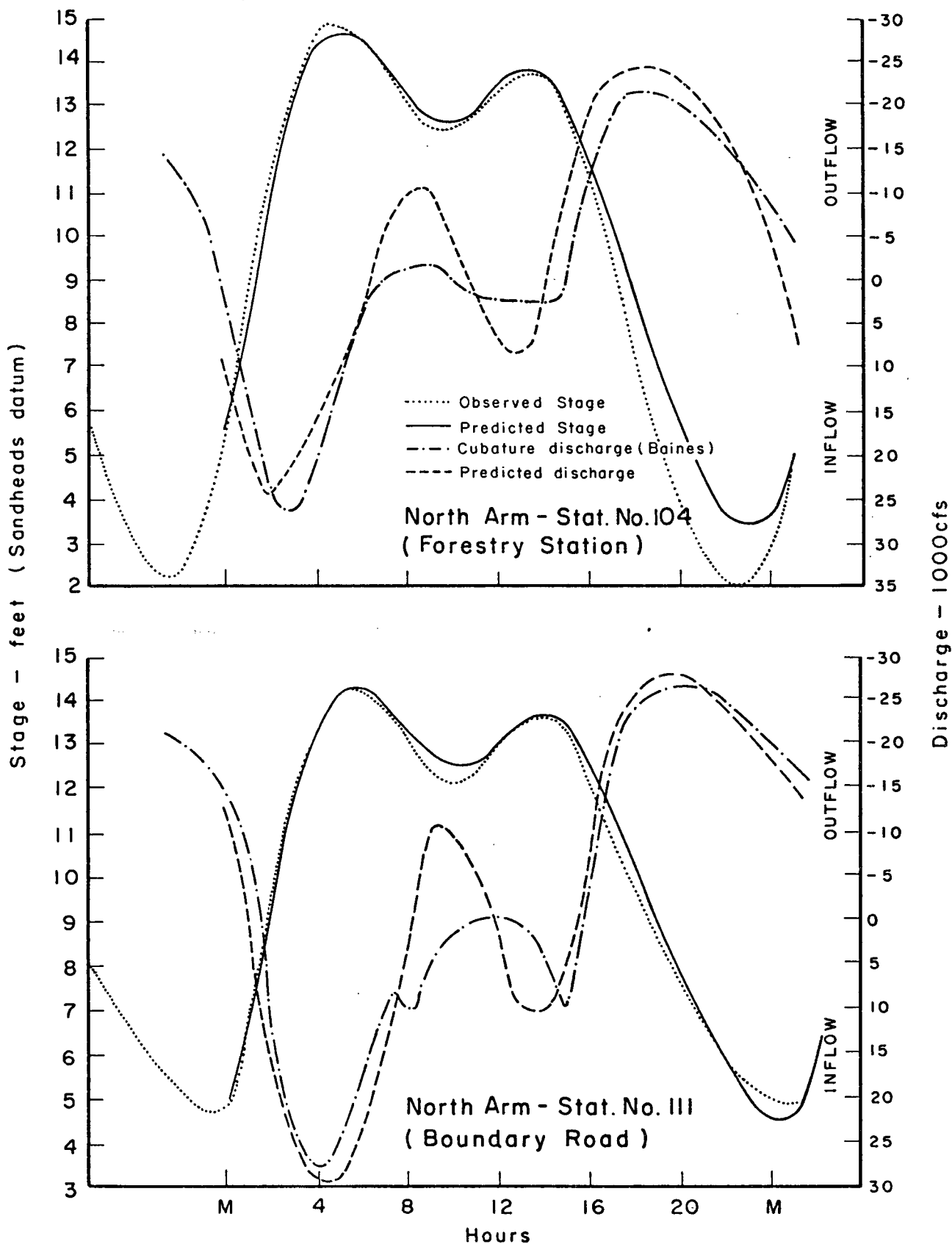
Figure 4.8   Tidally Varying Stage and Discharge - North Arm

Q = 36,500 cfs (Chilliwack)
                                    } January 24, 1952
Tidal Range at Steveston = 11'
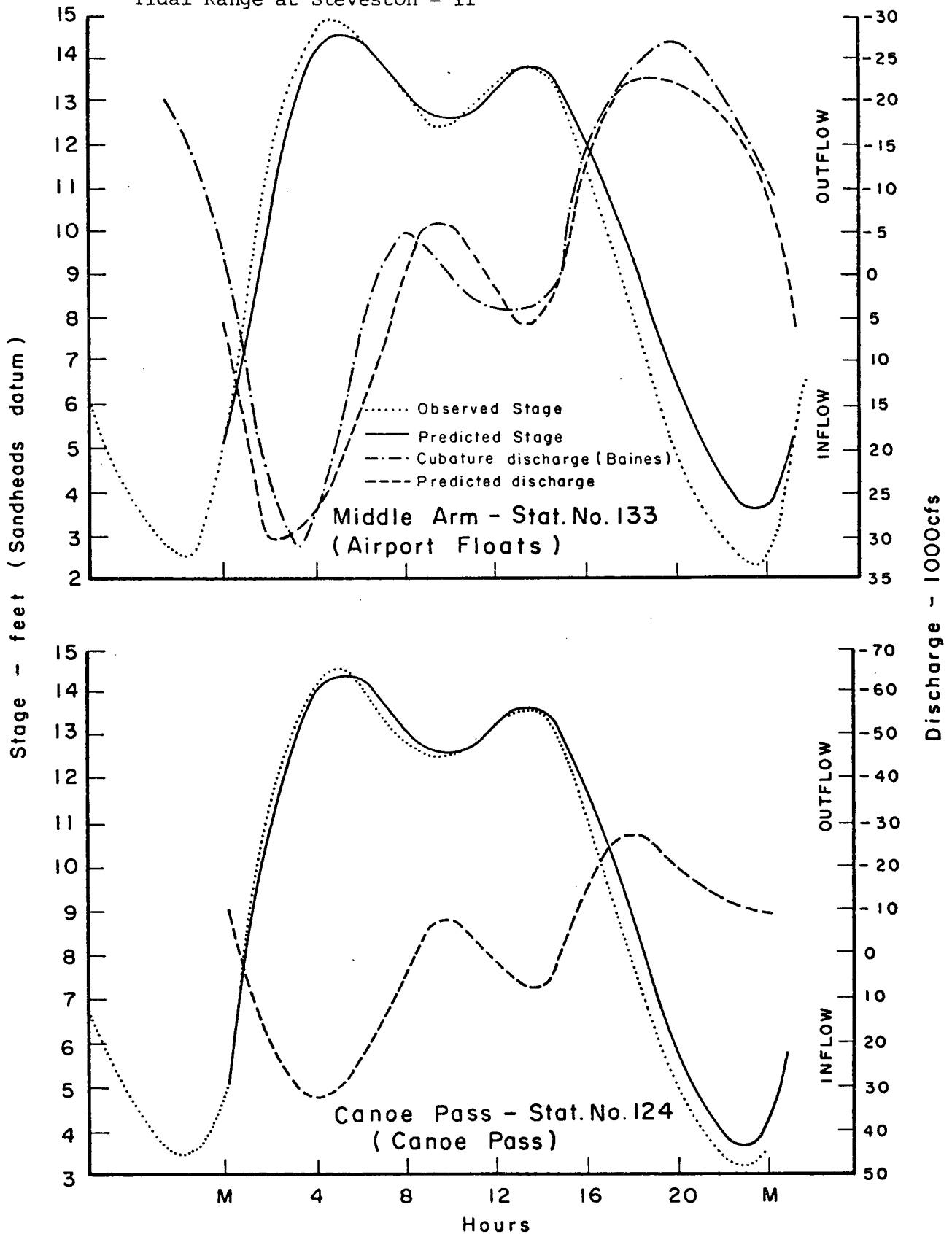
Figure 4.9 Tidally Varying Stage and Discharge - Middle Arm, Canoe Pass

Q = 36,500 cfs (Chilliwack)
} January 24, 1952
Tidal Range at Steveston = 11'
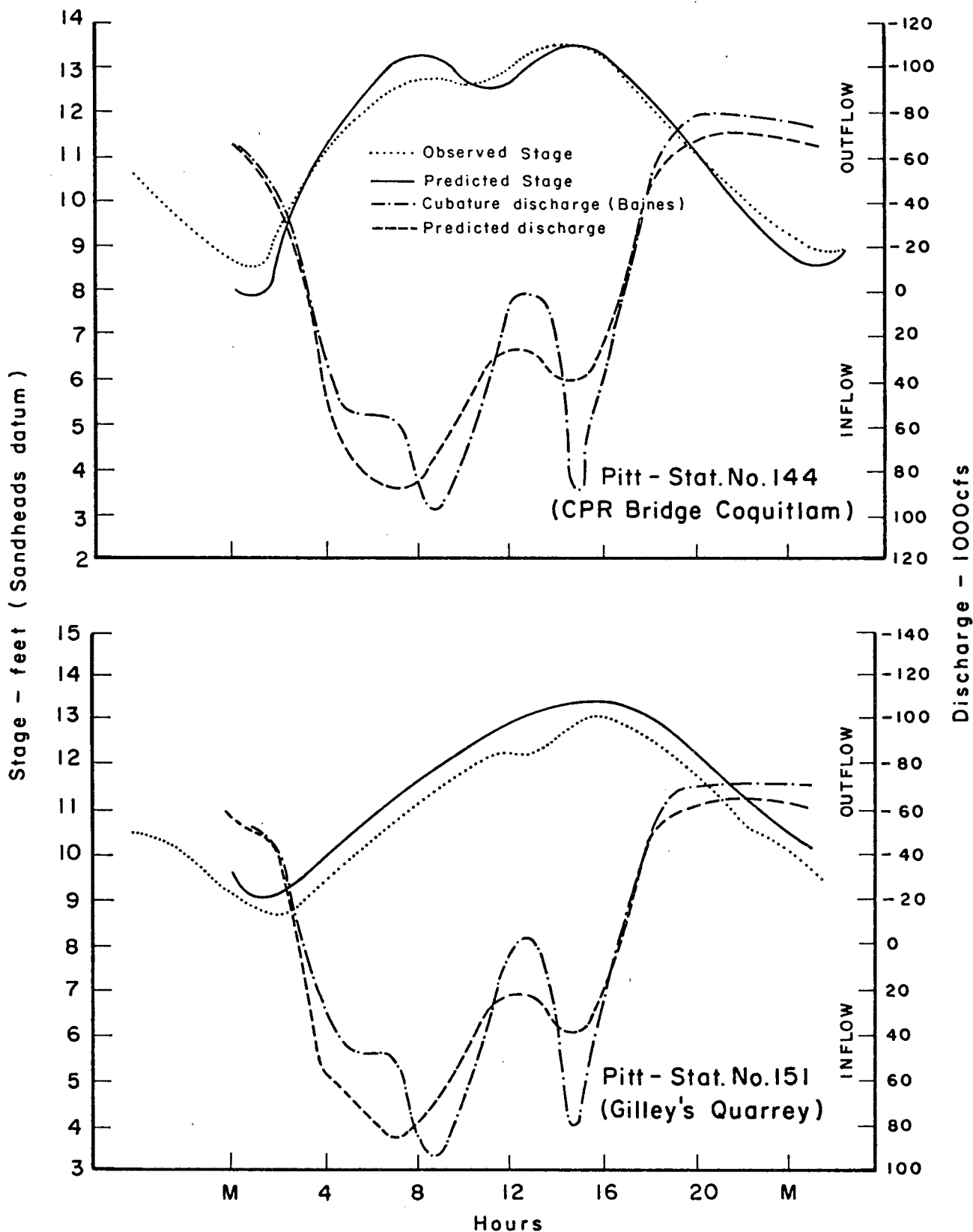
Figure 4.10   Tidally Varying Stage and Discharge - Pitt River
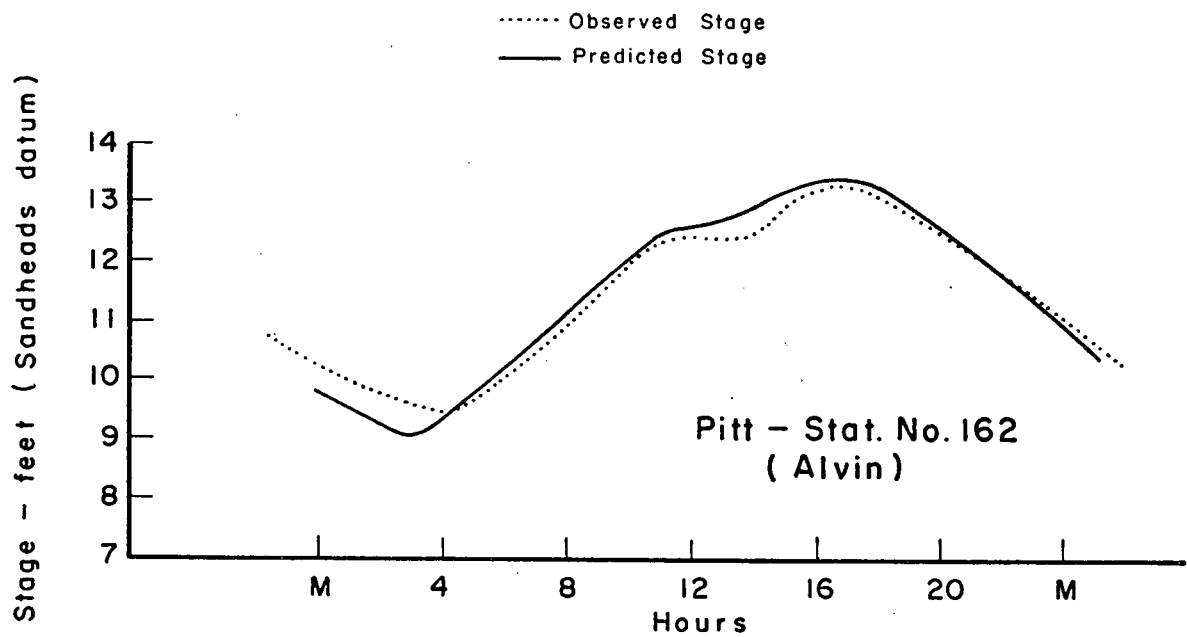
Figure 4.11

Tidally Varying Stage -- Pitt Lake

fall of the water water surface has dissipated. The fit between the pre-
dicted discharges and the cubature discharges of Baines is not as good as
the fit between predicted and observed water surface elevations. There
seems to be a phase difference between the discharges, the predicted dis-
charge tending to occur earlier than the cubature discharge. This phase
difference was insensitive to changes in cross-sectional geometry and fric-
tion coefficients. The cubature discharge curves behave somewhat erratically
between the times of high-high-water and low-high-water. It is not certain
whether this behaviour represents the true discharge response of the estuary,
or is due to inaccuracies in the cubature discharge calculations.

The tidally averaged discharges were found to satisfy continuity
at the Main Arm - North Arm junction, the North Arm - Middle Arm junction
and the Main Arm - Canoe Pass junction. A tidally averaged mass balance
was made over the entire estuary and was found satisfactory. The results
of this mass balance are shown in Table 4.1.

To sum up, the behaviour of an estuary is determined by the inter-
action of the effects of river flow, tides, bed forms and cross-sectional geo-
metry. The freshwater discharge of the Fraser River Estuary undergoes a large
annual fluctuation (see Appendix B) and consequently the bed forms of the var-
ious channels, and possibly their cross-sectional geometries, are in a contin-
ual state of dynamic equilibrium with the freshwater flows and tides. Bearing
this in mind, and the fact that Baines obtained his results some 20 years
ago, and additional dykes, training walls, etc. have been constructed in
the interim, it is impossible for the simple one-dimensional hydrodynamic
model to exactly reproduce the behavior he observed in the estuary. The

TABLE 4.1

TIDALLY AVERAGED MASS BALANCE OF PREDICTED DISCHARGES
FOR JANUARY 24, 1952

	CHANNEL	PREDICTED VALUES
DISCHARGE IN (1000's cfs)	MAIN STEM	36.5
DISCHARGE OUT (1000's cfs)	MAIN ARM NORTH ARM MIDDLE ARM CANOE PASS	27.8 2.9 0.5 1.2
	TOTAL	32.4
INTERNAL STORAGE (1000's cfs)	PITT SYSTEM O T H E R	2.9 ∿0.0
	TOTAL	2.9

results shown in Figures 4.4 to 4.11 represent the "best over-all fit"
between predicted and observed water surface elevations and discharges.
As such, the predicted results are close to the limit of resolution of
the one-dimensional hydrodynamic model, or in other words, the predicted
results are the "best" the model is capable of.

4.2 THE TIDALLY VARYING MASS TRANSPORT MODEL

Because of the lack of field data (see Section 3.2.1), a thorough verification of the tidally varying mass transport model was not possible. However, the model is computationally stable, free from the effects of numerical dispersion and sufficiently flexible to be adjusted to field data when available. It reproduces the advective transport process correctly and demonstrates good agreement with the standard analytical result for the dispersion of a slug load. To obtain preliminary notions of the tidally varying behaviour of the estuary, other peoples' results have been used to estimate the coefficients of longitudinal dispersion.

4.2.1 Advective Transport. In the tidally varying model, the advective transport was simulated by a grid of moving points on the advective characteristics, as described in Chapter 3. This process directly simulates the advective transport occurring in the actual estuary and does not suffer from numerical dispersion (see Appendix C). The hydrodynamic model was used to predict the velocities throughout the estuary at half-hour intervals and these velocities were then used to advect the moving points along. Thus, the tidally varying mass transport model will simulate the advective transport as accurately as the hydrodynamic model simulates the velocities, and the verification of the hydrodynamic model can also be regarded as a partial verification of the advective transport process. The predicted advective transport was found to be relatively insensitive to inaccuracies as in the advective velocities. This is illustrated in Figure 4.12 which shows the advection of a slug load down the Main Arm – Main Stem of two different model estuaries. The freshwater discharge and quasi-steady tidal conditions are the same for both estuaries, but the higher friction of one estuary

January 24, 1952 – Flow at Chilliwack : 36,500 cfs

Stations along Main Arm – Main Stem

····X···· Predicted No.1 (Narrow Section with high friction)

──⊖── Predicted No.2 (Broad Section with low friction)

AVERAGE VALUES ALONG MAIN ARM – MAIN STEM

RESULTS	AVERAGE MANNINGS "N"	AVERAGE WIDTH (feet)	AVERAGE DEPTH (feet)
PREDICTED No.1	0.042	1350	30.6
PREDICTED No.2	0.030	1870	22.9

Hours
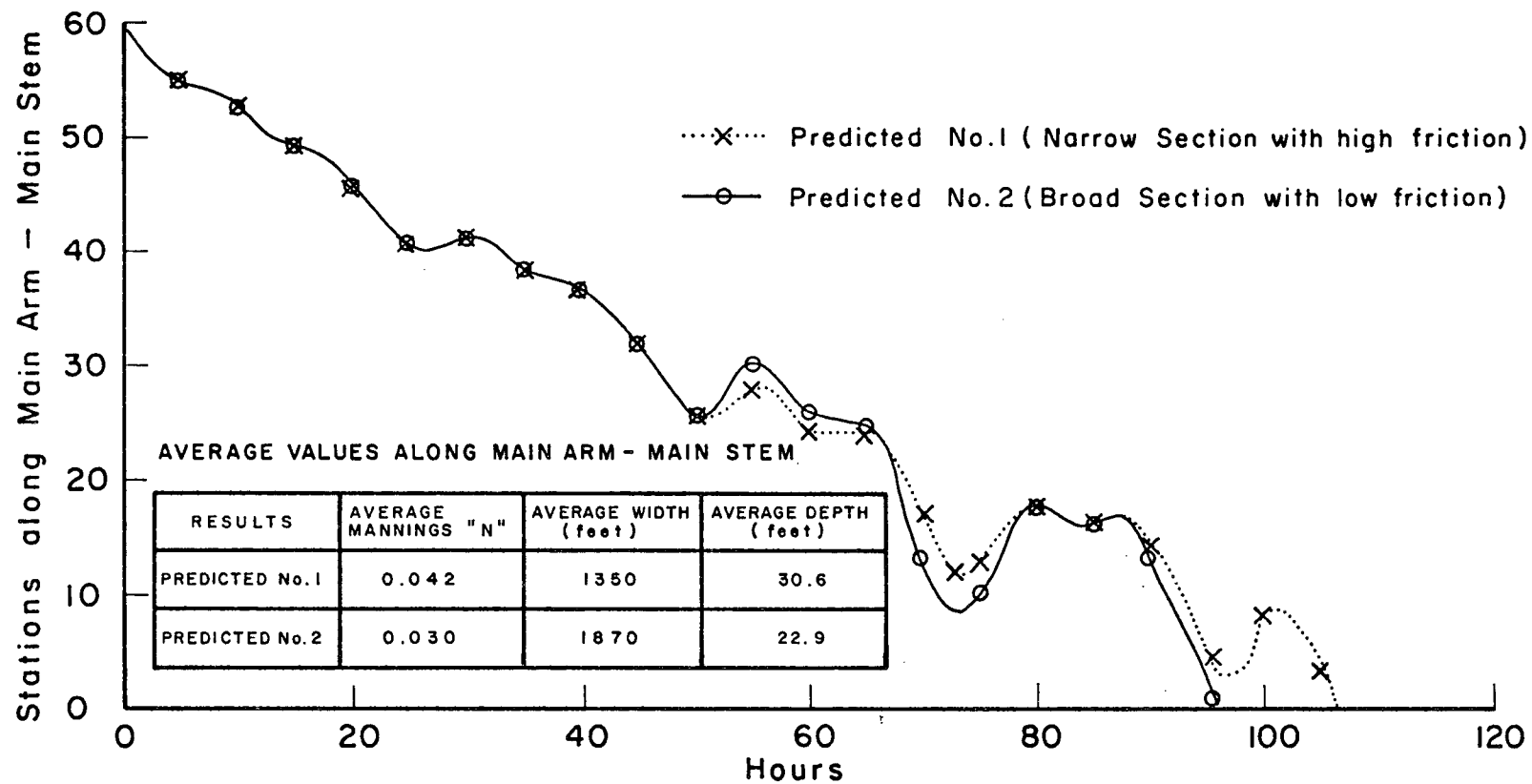
Figure 4.12

Advection Of A Slug Load Down The Main Arm – Main Stem

distorts its velocity field relative to the velocity field of the other.
The only difference between both sets of results is in the tidal excursion
in the lower reaches of the estuaries, and this is not that significant.

When the tidally varying model was run with zero dispersion,
the dilution and advection of effluent through the junctions was found to
be correct (it being recalled that cross-sectional mixing is assumed to be
complete at the junctions). The discrepancy in the mass balances over any
tidal cycle was found to be less than 6% and was due to the discrete spacing
between the moving points.

4.2.2 <u>Dispersive Transport</u>. A slug load was introduced at
Station No. 50 on the Main Stem to verify the capability of the tidally
varying mass transport model to simulate the dispersion process. The fresh-
water discharge at Chilliwack was 36,500 cubic feet per second and the dis-
persion coefficient was set equal to 500 square feet per second and assumed
constant in x and t. The analytical solution for the dispersion of a slug
load is given by [Fischer, 1966a]

$$c = \frac{M}{\sqrt{4 \Pi E t}} \exp\{- \frac{x^2}{4Et}\}$$

where M is the mass per unit area introduced into the flow. For the given
conditions, this reduces to

$$c = \frac{136}{\sqrt{t}} \exp\{- \frac{3.5x^2}{t}\}$$

where

   c is the concentration in milligrams per litre;

t is the elapsed time in hours;

and

x is the distance either side of the mean value in station
co-ordinates (5,000 foot segments).

Figure 4.13 shows the form of the slug inputs for the analytic and tidally
varying solutions. (The effluent discharge in the tidally varying model sim-
ulates continuous discharges, hence the form of the slug input in Figure 4.13).
The predicted and analytic solutions for the dispersion of the slug load are
shown in Figure 4.14 and the agreement between both sets of results is good.
The higher peak concentrations of the analytic solution are due to the higher
initial concentrations of the analytic slug load. It is recalled that the
dispersion process is assumed to be Gaussian in its entirety, and this is
illustrated by the results of Figure 4.14.

The estimation of the coefficients of longitudinal dispersion is
discussed in detail in Appendix F. In obtaining the tidally varying results
of this study, the coefficient of longitudinal dispersion is assumed to be
given by

$$\left.\begin{array}{ll} E = (6 + \dfrac{\alpha t}{T})\bar{y}\, U_* & 0 \le t < T \\ E = \alpha \bar{y}\, U_* & t \ge T \end{array}\right\} \tag{4.1}$$

and

$$U_* = 0.06\bar{u} \tag{4.2}$$

where

E, $\bar{y}$, U_* and $\bar{u}$ are the "instantaneous" values of the respective
parameters during the tidal cycle;

t is the time that has elapsed since a "parcel" of the effluent
was discharged into the estuary;

$T = b^2/\varepsilon_z$ and is the time scale of lateral mixing (an edge dis-
charge is assumed);
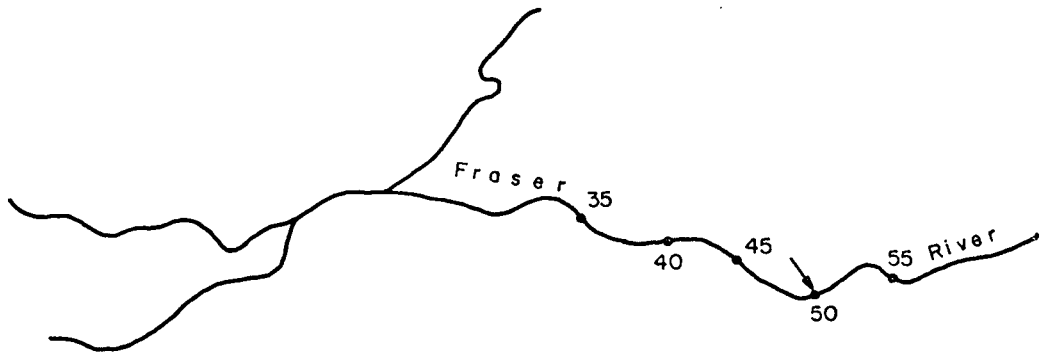
Discharge at Station No. 50

Q = 36,500 cfs (Chilliwack)
Tidal Range at Steveston = 11 feet } Jan. 24, 1952

Mass = 1650×10^3 lbs.
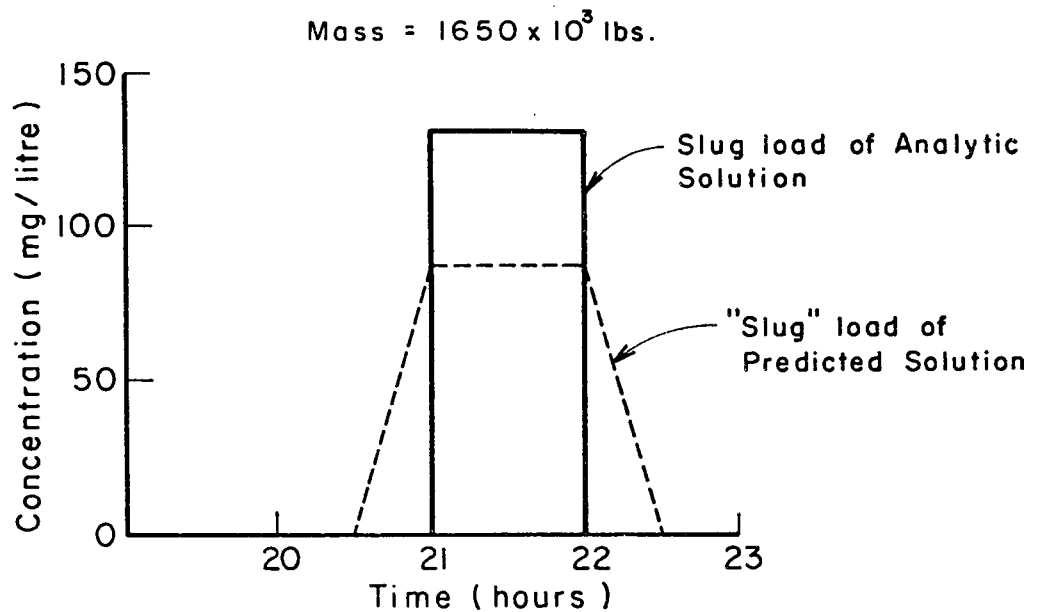
Figure 4.13

Slug Inputs for Analytic and Predicted Dispersion Solutions
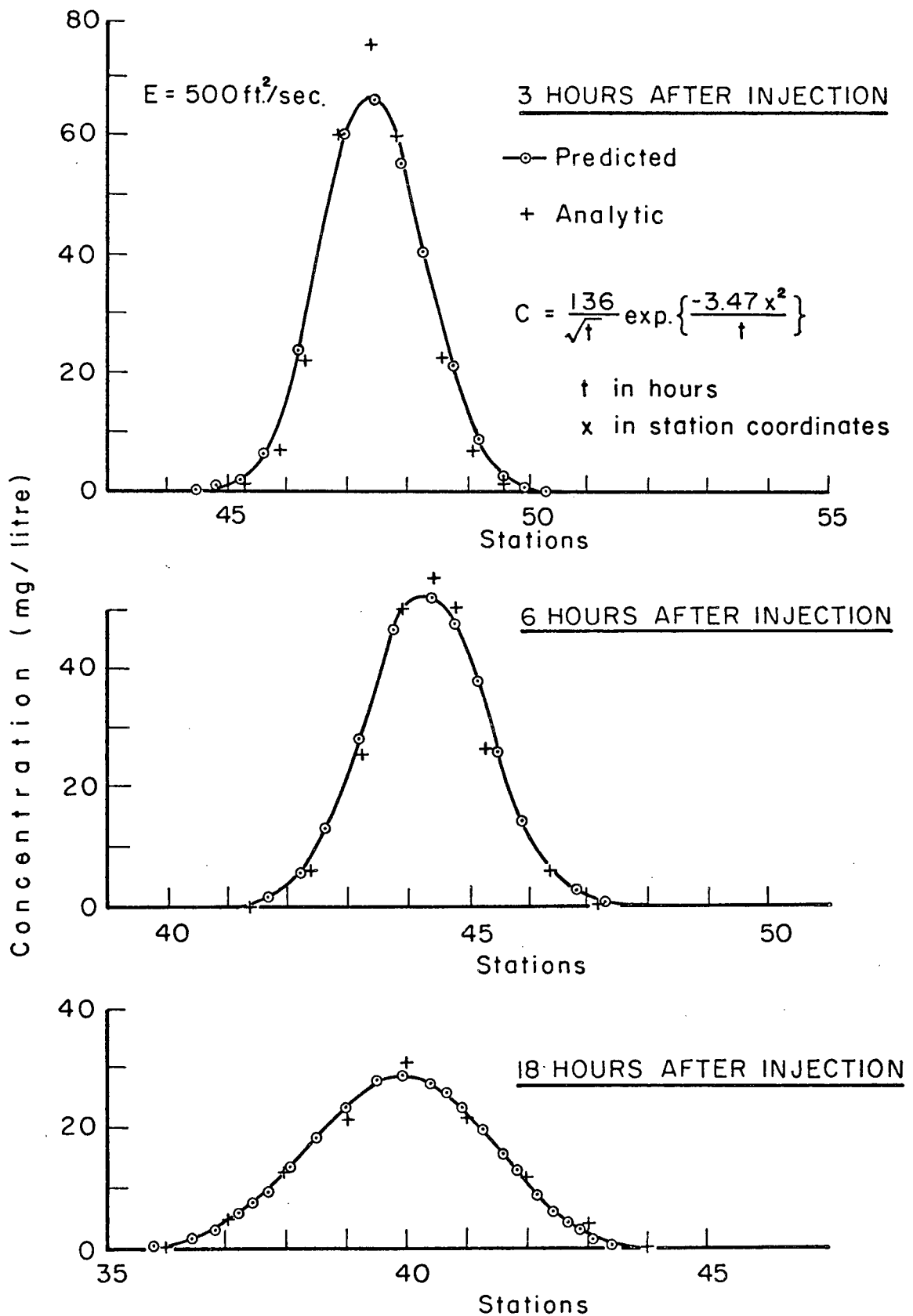
Figure 4.14

Dispersion Of A Slug Load in The Main Stem

and

α is a measure of the effects of lateral velocity gradients
on the dispersion process and is tabulated in Table F.1.

Equations (4.1) allow for the increasing contribution of the lateral velo-
city gradients on the dispersion process as the effluent spreads across the
section and the variation of the coefficient during the tidal cycle. These
aspects are discussed in Appendix F and it is seen that that the peak tidally
varying concentration is quite sensitive to assumptions about the form and
magnitude of dispersion coefficient. Although simplistic, the relationships
of Equations (4.1) are thought to be a reasonable approximation of what
actually occurs in the estuary.

Because the tidally varying mass transport equation has been
solved along the advective characteristics, the position of each effluent
"parcel" and the time that it has spent in the estuary is known. (This in-
formation is "masked" in a fixed grid solution). Consequently, the tidally
varying mass transport model can account for time dependent behaviour of in-
dividual "parcels" of effluent, as is assumed in Equations (4.1).

4.3 THE TIDALLY AVERAGED MASS TRANSPORT MODEL

The tidally averaged dispersion coefficient includes the effects
of advective transport due to tidal flow reversal and longitudinal dispersion.
As such, it has no real physical meaning and the verification of a tidally
averaged mass transport model essentially consists of forcing the model to
fit field data. According to Holley *et al.* [1970] there is no way of making
an *a priori* estimate of this coefficient. Ward and Espey [1971]
suggest using the results of a tidally varying model to estimate the coeffi-

cient. In the absence of field data, this latter approach has been adopted

to obtain estimates of the tidally averaged dispersion coefficients for

the Fraser River Estuary.

Thomann [1971] lists values of the tidally averaged dispersion

coefficient for various estuaries. They range from 1 - 20 square miles per

day with a mean value of around 10 square miles per day. Figure 4.15 shows

the influence of the tidally averaged dispersion coefficient on the predicted

concentrations for a steady, continuous discharge of a conservative effluent

at Station No. 40 on the Main Stem of the Estuary. (The concentrations are

standardized by dividing by the tidally averaged concentration based on the

total mass of effluent discharged during the tidal cycles and the freshwater

flow at Chilliwack. This is plotted as the γ_{ta}, the subscript signifying

that the results have been obtained from the tidally averaged model). The

only significant difference between the results is in the upstream excursion.

The concentration gradients are small downstream of the effluent discharge,

and the dispersion has little effect. It is recalled that the results of

Figure 4.15 have been obtained for a conservative effluent. If the concen-

tration of the effluent decays with time, as with BOD, there will be concentra-

tion gradients downstream of the discharge point, and the downstream concentra-

tions will also depend on the values of the tidally averaged dispersion coeffi-

cient (although the downstream concentrations are not very sensitive to the

values of the dispersion coefficient). The decrease in concentrations around

Stations Nos. 18 and 24 is due to the effects of the junctions and introduces

an error of about 10% into the predicted concentrations. It is not known why

this effect occurs.
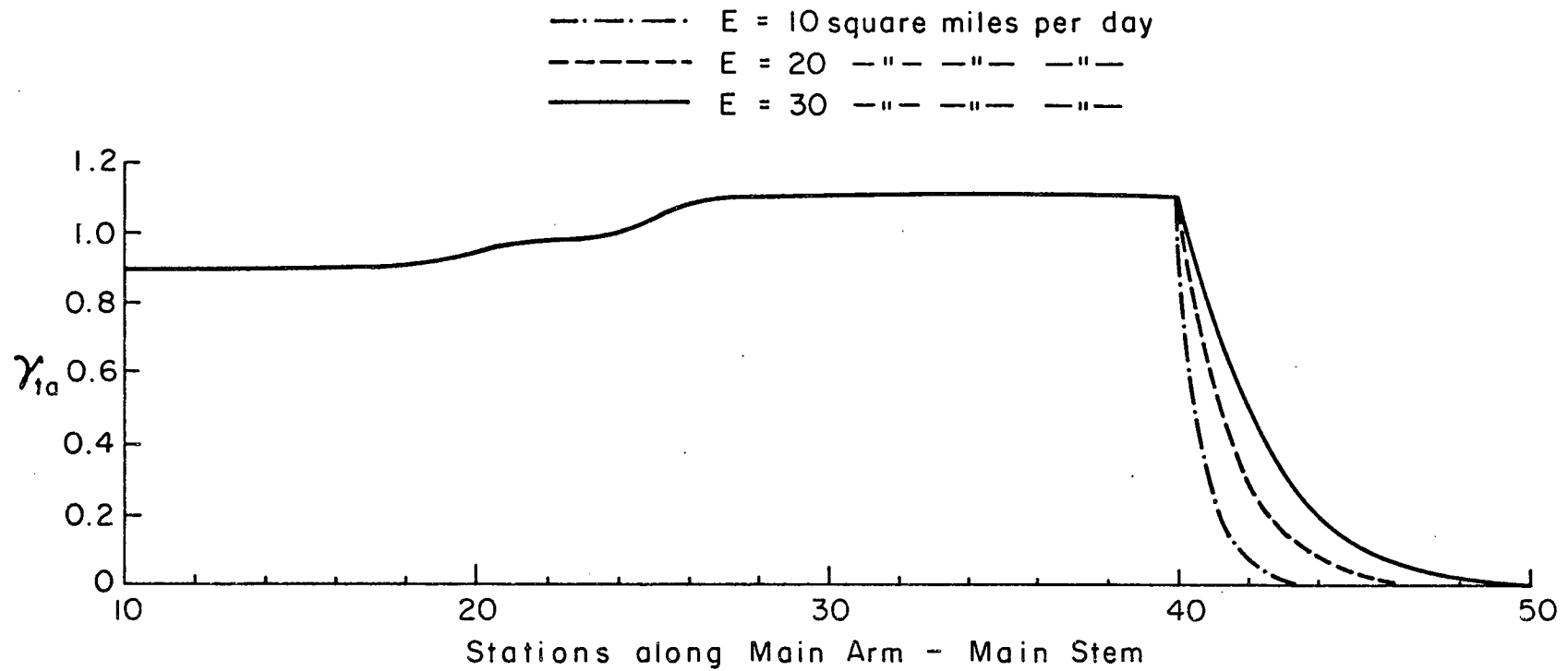
Figure 4.15

Influence Of The Tidally Averaged Dispersion Coefficient On Predicted Tidally Averaged Concentrations

Figures 4.16 and 4.17 show the maximum upstream excursion on the flood flow for effluent released along the various channels. In the lower reaches of the Main Arm it is assumed that the tidally averaged dispersion coefficient is equal to 20 square miles per day, and this value is reduced along the Main Arm - Main Stem according to the results of Figure 4.16. Along the North Arm the tidally averaged dispersion is assumed to equal 10 square miles per day, and along Pitt River it is assumed to equal 30 square miles per day (the rapid decrease in the upstream excursion along the Pitt River, as shown in Figure 4.17, is due to the drastic decrease in advective velocity in Pitt Lake). Although the absolute values of the tidally averaged dispersion may not be correct, and this is discussed in Chapter 5, the relative values along the estuary should be reasonable.

Maximum Upstream Excursion (Stations)

Q = 36,500 cfs (Chilliwack)
Tidal Range at Steveston = 11 feet } Jan. 24, 1952

Position of Effluent discharge along Main Arm — Main Stem
(Station Numbers)
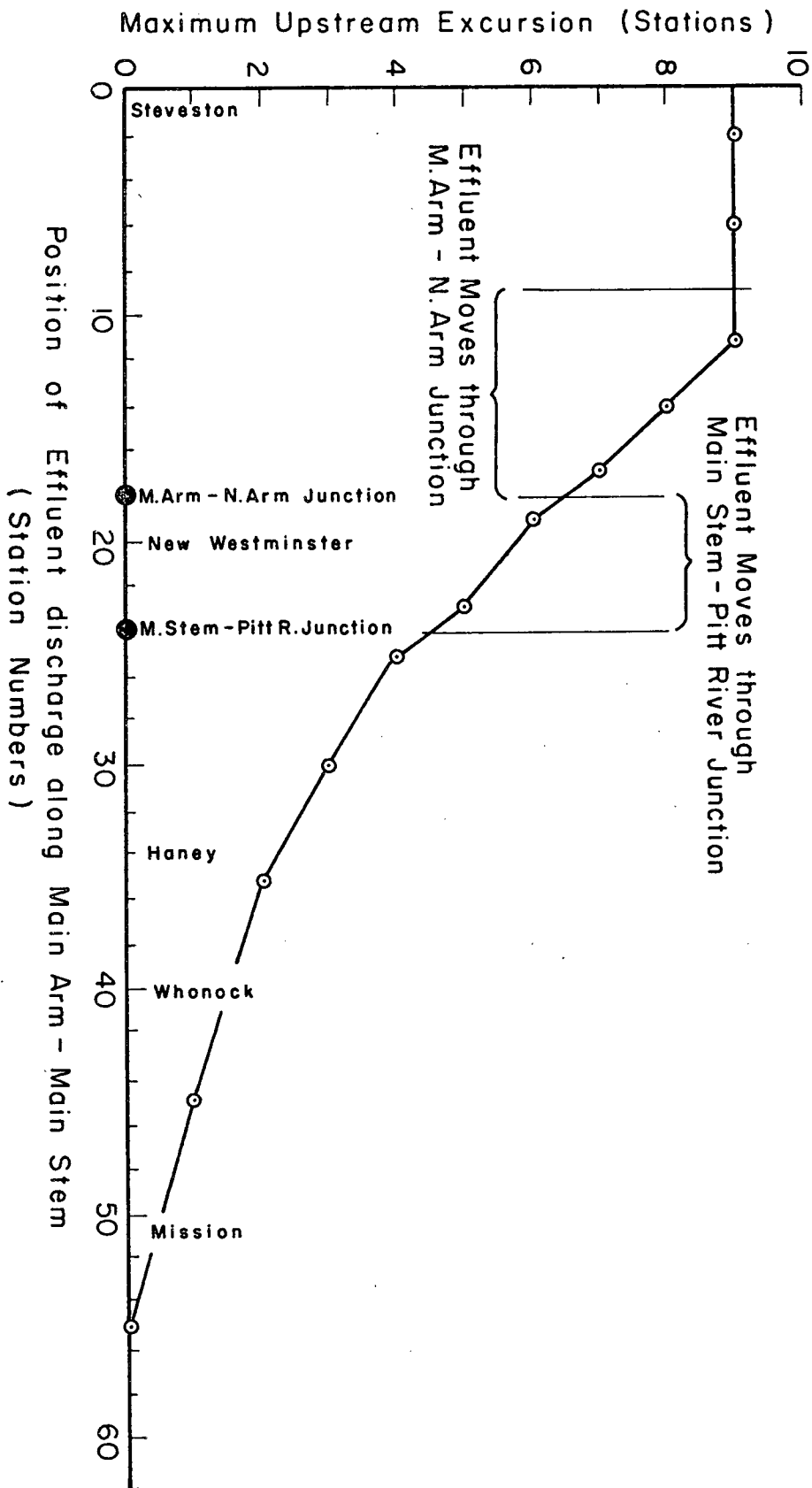
Figure 4.16

Maximum Upstream Excursion During Flow Reversal In Main Arm - Main Stem

Q = 36,500 cfs (Chilliwack)
Tidal Range at Steveston = 11 feet } Jan. 24, 1952
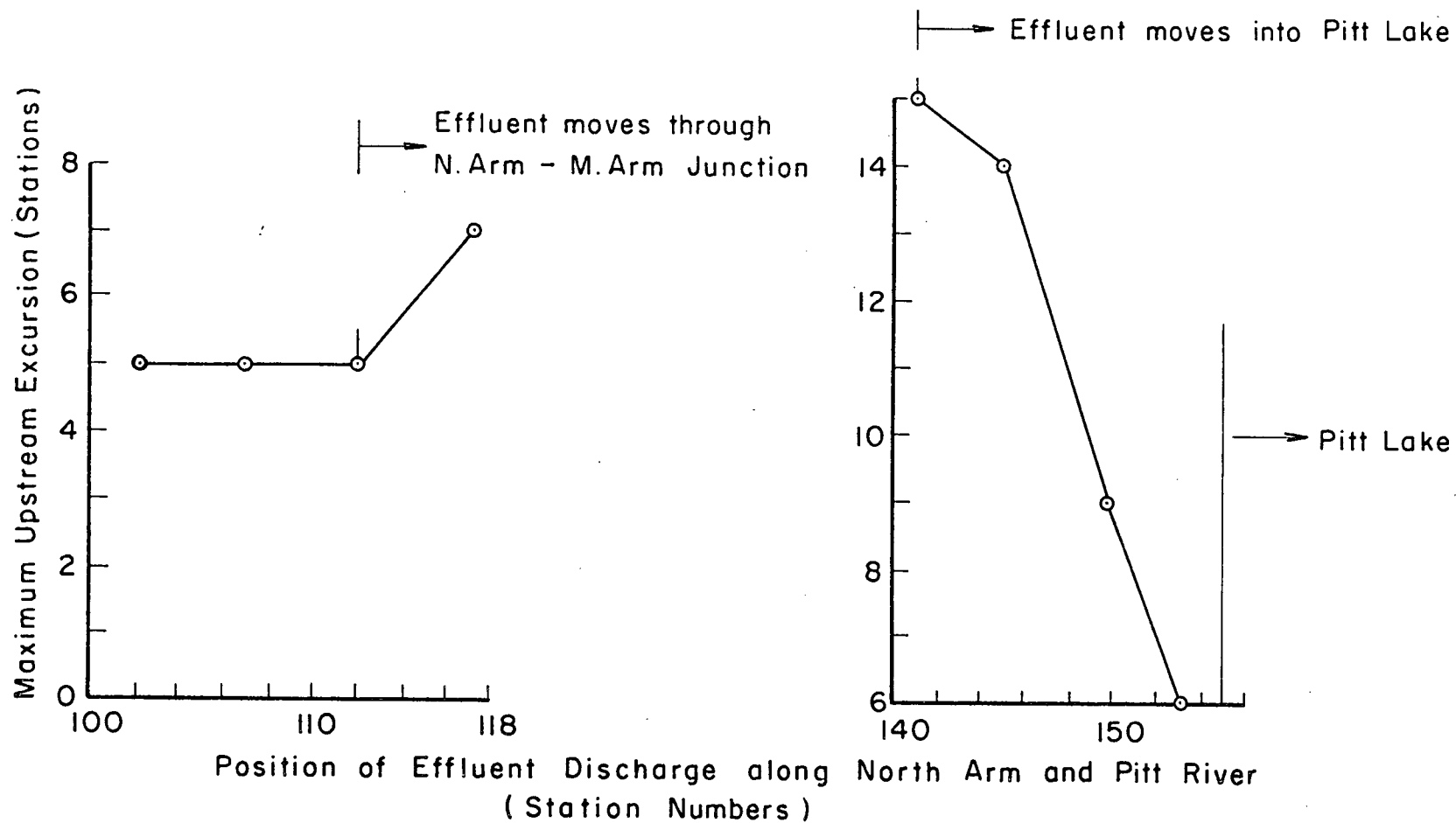
Figure 4.17

Maximum Upstream Excursion During Flow Reversal In The North Arm And Pitt River

CHAPTER 5

COMPARISON AND DISCUSSION OF RESULTS

The three models discussed in the last two chapters are now used

to obtain a preliminary indication of the significance of tidal effects on

predicted concentrations in the Fraser River Estuary. The flow and tidal

conditions of January 24, 1952 were used in this investigation. These are

typical high tide - low flow conditions and were used in the verification

of the hydrodynamic model. The freshwater discharge at Chilliwack was

36,500 cubic feet per second and the tidal range at Steveston 11 feet. A

conservative effluent and an edge discharge were assumed. The hydrodynamic

model was used to obtain the tidally varying velocities and cross-sectional

areas along the various channels of the estuary. These values, together

with estimated dispersion coefficients, were then used to predict the

tidally varying concentrations. The freshwater discharge at Chilliwack, the

tidally averaged areas and estimated dispersion coefficients were used to pre-

dict the tidally averaged concentrations.

Before presenting the results of this investigation, the assumptions

of the mass transport models are briefly recalled: both models are one-

dimensional and predict the cross-sectionally averaged concentrations; the

cross-sectional mixing in both models is assumed to be complete at the junc-

tions; the influence of the saltwedge is ignored in both models; the dispersion

process of the tidally varying model is assumed to be Gaussian in its entirety;

and in the tidally averaged model, all effects of the tides are lumped into the

tidally averaged dispersion coefficient.

5.1 THE EFFECTS OF LATERAL DISPERSION

In the initial period before cross-sectional mixing is complete, there are significant lateral concentration gradients across the estuary, and the peak cross-sectional concentration will be considerably higher than the value predicted by either mass transport model. While this effect has not been quantitatively assessed, it is noted that the tidally varying mass transport model can easily be adapted to give an approximate estimate of this effect. The lateral concentration profile depends on the coefficient of lateral dispersion, the position of the effluent outfall in the estuary cross-section and the period of time that a "parcel" of effluent has spent in the estuary [Ward, 1972]. Because the tidally varying mass transport model has been solved along its advective characteristics, the position of each effluent "parcel" and the time that it has spent in the estuary is known, and the predicted concentrations can be adjusted to account for the effects of lateral dispersion. (This approach was used in allowing for the assumed time dependent variation in the coefficient of longitudinal dispersion).

In the lower reaches of the estuary, there are three distinct periods in each double tidal cycle of 25 hours; a period of strong flood flows; a period of weak ebb and weak flood flows and a period of strong ebb flows. This is apparent in Figures 4.4 to 4.10 and the duration of each of the three periods is seen to be approximately eight hours. The cross-sectional mixing is principally due to the effects of secondary flows, as discussed in Appendix E, and will be greatest during the periods of strong ebb and flood flows. If cross-sectional mixing is not complete at the Main Arm - North Arm junction during the strong ebb flow, or at the Main Stem - Pitt River junction during

the strong flood flow, the effluent will not be advected through these junctions according to the simple flow balance of the one-dimensional mass transport models. The interaction of the time dependent behaviour of the lateral mixing process with the advection of effluent through the junctions is very involved and can only be reliably determined from field studies. If sufficient field data were available, it may be possible to empirically allow for this effect in the tidally varying model.

5.2 THE INITIAL DILUTION OF EFFLUENT

When effluent is discharged into an estuary, the tidally varying flows cause a variation in its initial dilution during the tidal cycle. This process is described in Section 1.3 and is seen to generate concentration spikes at times of slackwater. Figure 5.1 shows typical variations in the initial dilution during the double tidal cycle at four stations along the estuary. During a double tide cycle there are four slackwaters in the lower reaches of the estuary (see Figures 4.4 to 4.10) and the resulting concentration peaks at Stations Nos. 10, 22 and 102 are apparent. At Station No. 50, the tidal flows are significantly smaller in relation to the freshwater flow, and their combined interaction results in only two effective peaks during the double tidal cycle.

Because of the smaller flows along the North Arm, the tidally varying concentrations at Station No. 102 are significantly higher than the values along the Main Arm - Main Stem. The tidally averaged dilution is also shown in Figure 5.1, the higher values at Stations Nos. 10 and 102 reflecting the division of the freshwater discharge between the North Arm and Main Arm.

Q = 36,500 cfs (Chilliwack)
Tidal Range at Steveston = 11 feet } Jan. 24, 1952
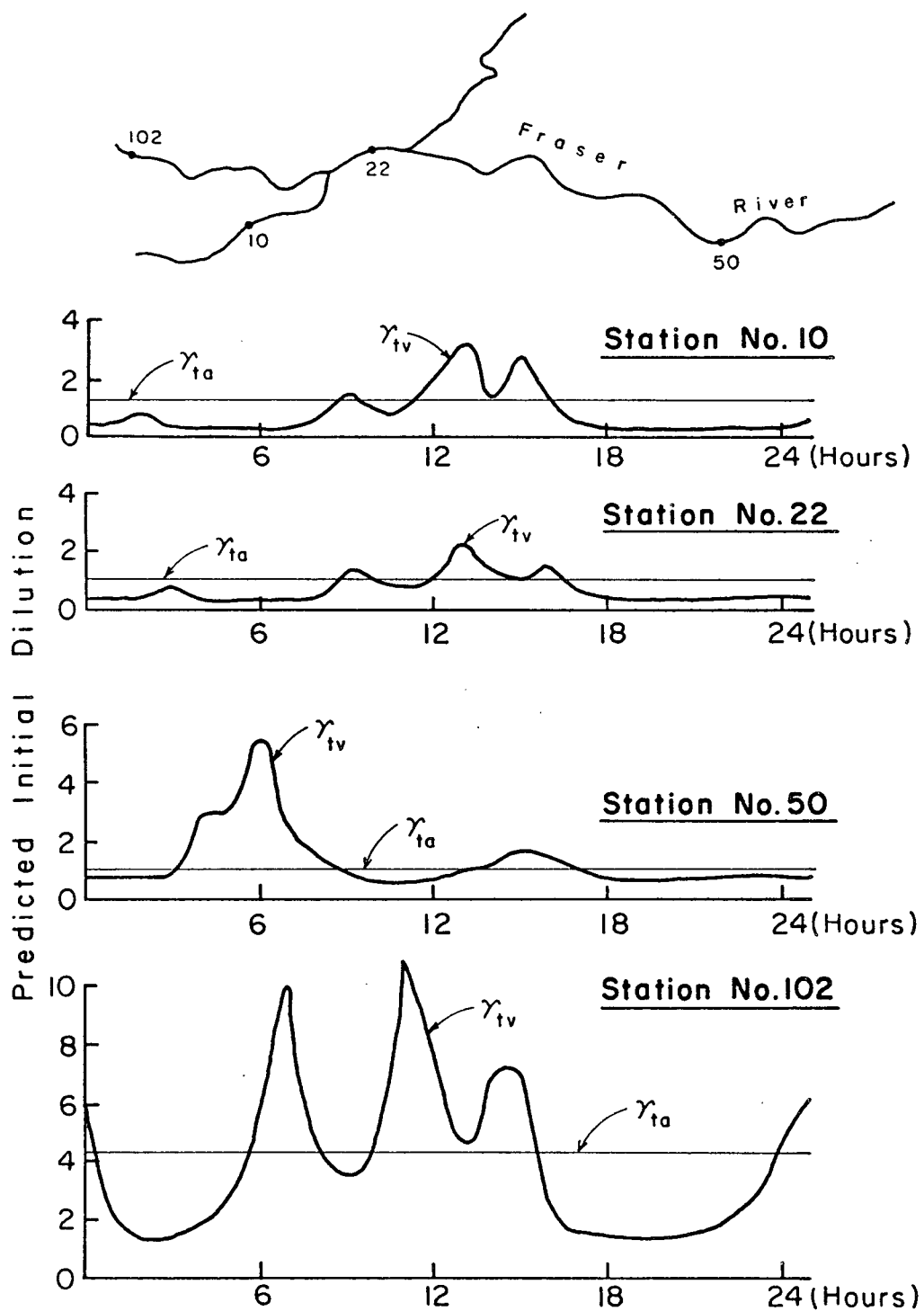
Figure 5.1

Initial Dilution At Station Nos. 10, 22, 50 and 102

The peak tidally varying concentrations in Figure 5.1 are seen to be about twice the tidally averaged values.

The minimum tidally varying concentration occurs during the strong ebb and flood flows, and is reflected as the flat sections of the curves of Figure 5.1. At Stations Nos. 10 and 22, this minimum concentration is approximately half the minimum value at Station No. 50. This is due to the presence of Pitt Lake; discharges downstream from the Main Stem-Pitt River junction are diluted by the combined effects of the tidal prisms of the Pitt system and the Main Stem above the junction, whereas discharges upstream of the junction are diluted only by the latter.

5.3 PEAK EFFLUENT CONCENTRATIONS

As well as the effects of variation in initial dilution, certain slugs of water are dosed with effluent several times due to the effects of tidal flow reversal. This process is described in Section 1.3 and also generates concentration spikes. However, the effects of variation in initial dilution and multiple dosing combine to produce a compound spike whose concentration is higher than that of the individual component spikes. This is well illustrated by an effluent discharge at Station No. 50. The variation of velocity at Station No. 50 is shown in Figure E.2; note the slackwaters at hours 4 and 5 and that the minimal velocity at hour 6. This is the reason for the increased concentration at hours 4 and 5 and the spike at hour 6 in Figure 5.1. Now consider the behaviour of the water mass around Station No. 50 during this time. During hour 4 a slug of water moves downstream past the outfall and is dosed, during hour 5 it moves back upstream and is dosed again

and finally during hour six it moves downstream past the outfall is dosed

yet again. The result of this is that the concentration in this slug of

water is 12 times greater than the tidally averaged value as is shown in

Figure F.2 for the curve with zero longitudinal dispersion. This spike is

composed of the three subspikes generated at hours 4, 5 and 6, their indivi-

dual magnitudes being 3, 3 and 6 as shown in Figure 5.1.

The spikes due to the effects of variation in initial dilution and

multiple dosing combine because both effects occur around the same phase of

the tide. A particularly sensitive portion of the double tidal cycle is the

period of weak ebb and flood flows where there are three slackwaters in the

space of eight hours. The velocities between these times of slackwater are

relatively low (see Figures 4.4 to 4.10).

Once a spike is generated by the effects of variation in initial

dilution, multiple dosing or a combination of both, its peak concentration

begins to be reduced by the longitudinal dispersion process. This is illus-

trated in Figure 5.2 for a steady effluent discharge at Station No. 50. The

compound spike is generated at hour 6 with a peak concentration that is 11

times greater than the tidally averaged value. (The decrease from the pre-

vious value of 12 is due to the effects of dispersion on the subspikes gen-

erated at hours 4 and 5). However, as the spike is advected down the estuary,

the dispersion process reduces the peak concentration as shown. The results

of Figure 5.2 seem to indicate that mass is not conserved since the area under

the spike is not constant. This is only an apparent effect due to extrapolating

the concentrations off the advective characteristics onto the standard 5,000

foot space grid, as described in Section 3.2. In actual fact, the initial

base width of the spike is only 500-800 feet, which is too fine to be resolved

Q = 36,500 cfs at Chilliwack ⎫
Tidal Range at Steveston 11' ⎬ Jan. 24, 1952
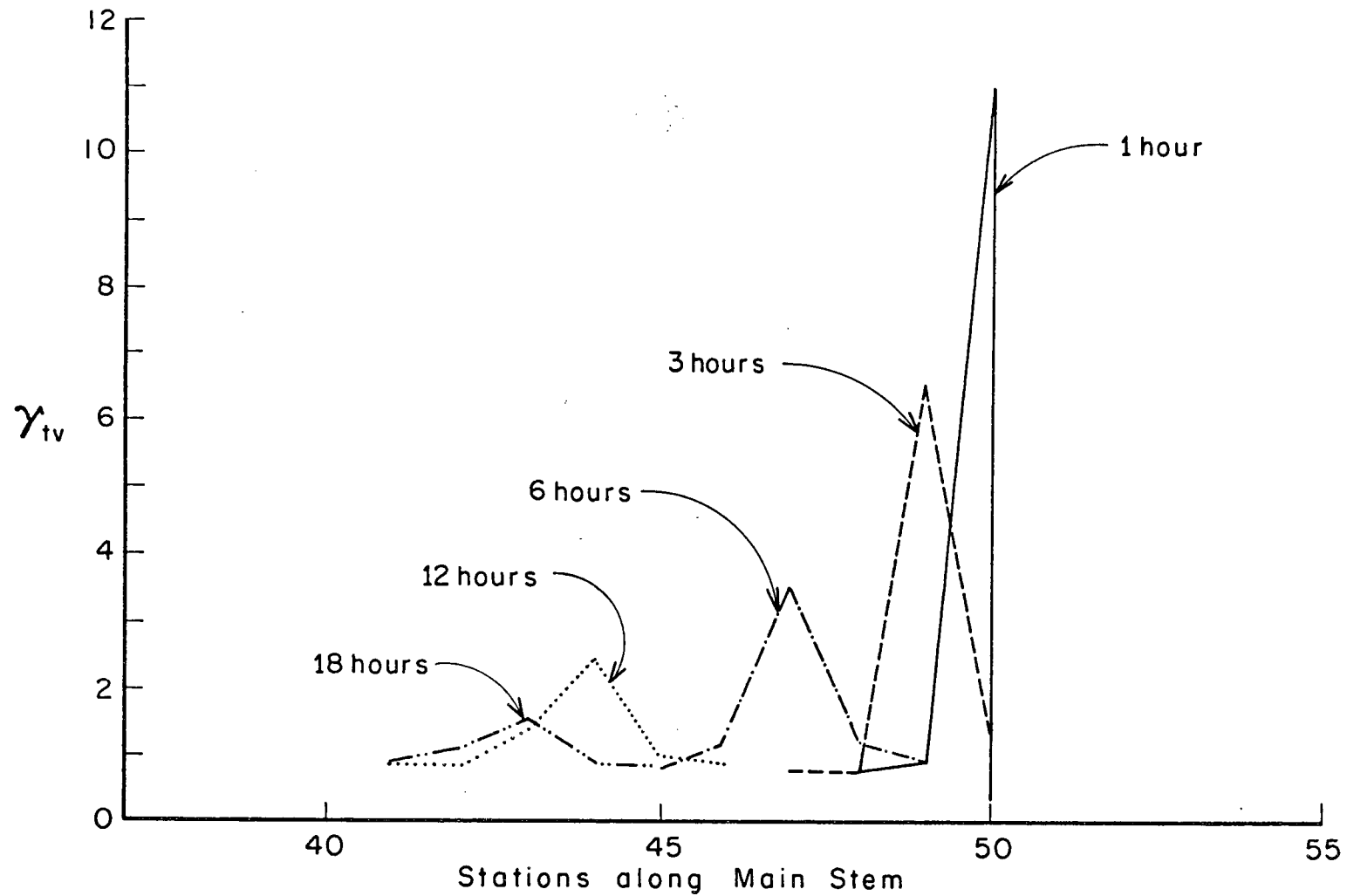
Figure 5.2

Dispersion Of A Concentration Spike

by the fixed grid. (Note that the spike is correctly resolved on the characteristics).

The most significant effects of variation in initial dilution and multiple dosing occur in the first 1-2 tidal cycles after a "parcel" of effluent has been discharged into the estuary. This is due to the high initial concentration gradients of the spike and assumed time-dependent increase in the coefficient of longitudinal dispersion (see Appendix F). These aspects are apparent from Figure 5.2 and are also illustrated in Appendix F.

For the steady discharge of a conservative effluent, the peak tidally varying concentration was found to be from 1 to 10 times greater than the value predicted by the tidally averaged model. These results are summarized in Table 5.1 and were obtained for a single effluent discharge at the designated station. (The peak tidally varying discharge occurs at the discharge point). The results of Table 5.1 are sensitive to the magnitude and assumed temporal variation of the coefficient of longitudinal dispersion, as discussed and illustrated in Appendix F. In obtaining the results of Table F.1, the coefficient of longitudinal dispersion was assumed to be as given in Equation (4.1). The peak cross-sectional concentration will be significantly higher than these values.

5.4 UPSTREAM EFFLUENT TRANSPORT

In a tidally varying mass transport model, effluent is transported upstream by the effects of dispersion and advection during tidal flow reversal. Because of the large tidal flows, advective transport is the more important
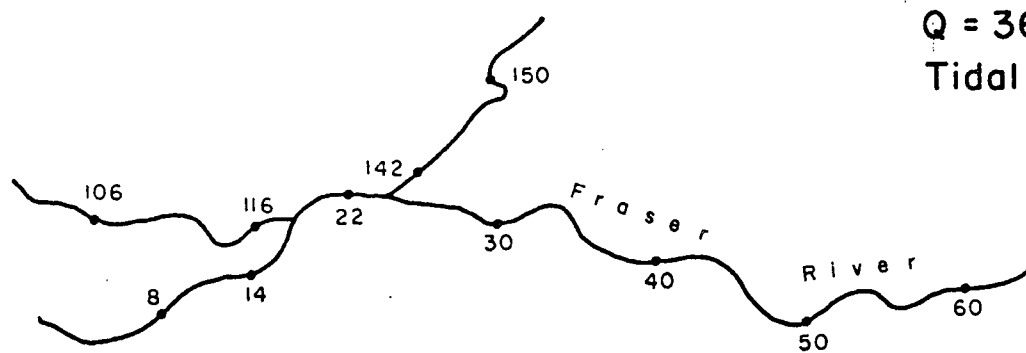
$Q = 36,500\,cfs$ at Chilliwack $\Big\}$ Jan. 24, 1952
Tidal Range at Steveston 11'

CHANNEL	Main Arm - Main Stem							North Arm		Pitt River	
STATION	8	14	22	30	40	50	60	106	116	142	150
$(\gamma_{tv}/\gamma_{ta})_{max.}$	5.4	3.8	3.8	10.7	5.0	10.9	1.0	7.2	8.2	1.2	1.2

Table 5.1

Ratio of Peak Tidally Varying Concentration to Tidally Averaged Value
At Point Of Effluent Discharge

component for the Fraser River Estuary, as is apparent from Figures 4.16 and 4.17. In a tidally averaged model, upstream transport is by the tidally averaged dispersion process. Figures 5.3 and 5.4 show the predicted tidally varying and tidally averaged concentrations at Stations upstream from effluent discharges. In all cases, the tidally averaged value is significantly less than the tidally varying values. A better fit between the results could be obtained by increasing the values of the tidally averaged dispersion coefficient.

The results of Figure 5.4 are for simultaneous effluent discharges at Stations Nos. 10 and 14. Once again, the effects of variation in initial dilution and multiple dosing cause a concentration spike at both discharge points, spike A being generated at Station No. 10 and spike B at Station No. 14. Note that between hours 6 and 17 the tidally varying concentration at Station No. 6 is zero due to uncontaminated seawater moving upstream on the flood tide. The concentration boundary condition at the sea was assumed to be zero, a more realistic boundary condition being possibly as shown. The tidally averaged concentration is not a good indication of the tidally varying response upstream of Station No. 14, between the two stations or downstream of Station No. 10.

5.5 CHANNEL INTERACTIONS

Consider now the effect of an effluent discharge in one channel on the water quality in another channel. The significance of this effect will depend on the proximity of the effluent discharge to the junction. If the discharge point is sufficiently far upstream from a junction, the effluent
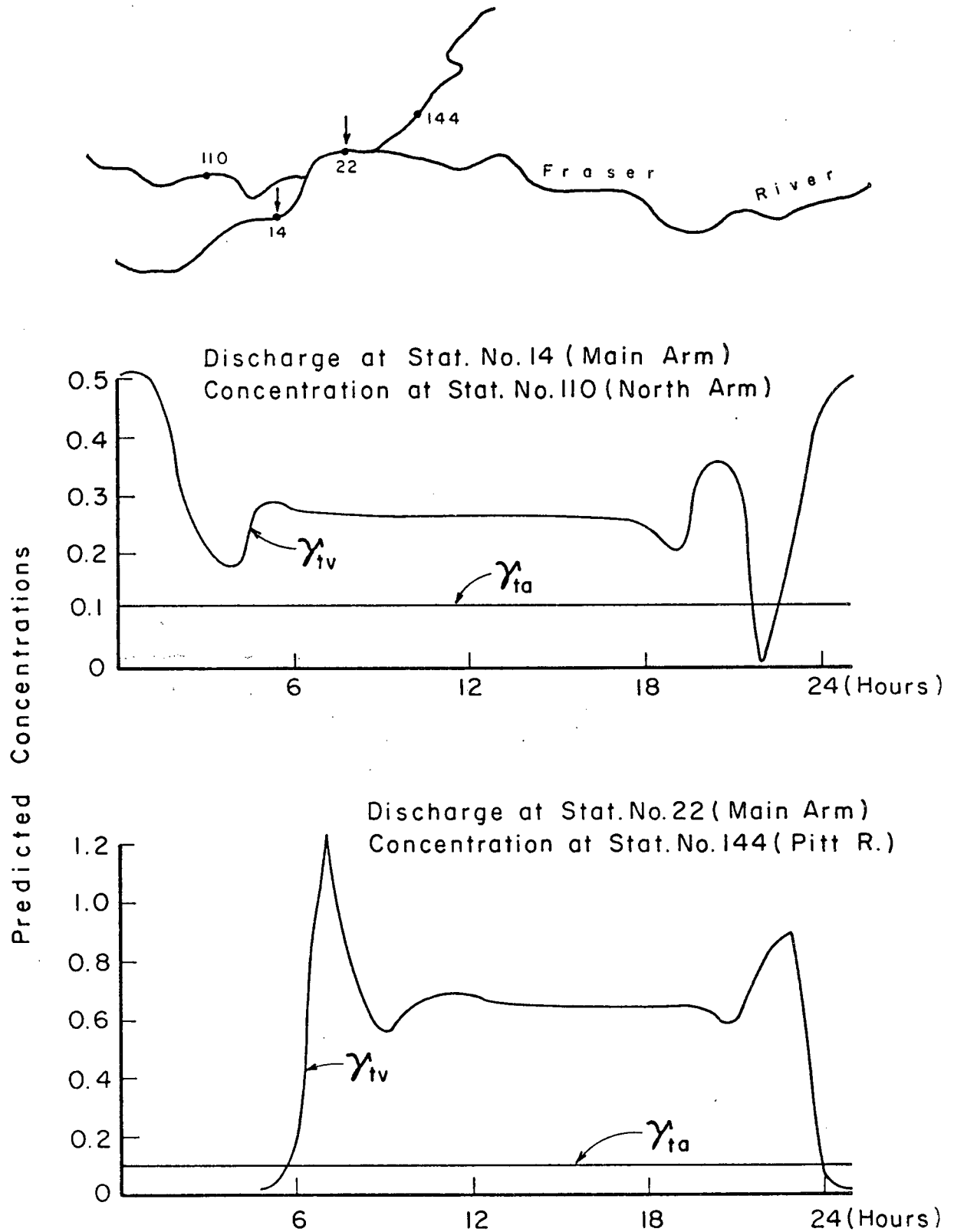
Figure 5.3

Predicted Concentrations in One Channel
Caused By Effluent Discharge In Another Channel

Q = 36,500 cfs (Chilliwack)
Tidal Range at Steveston = 11 feet } Jan. 24, 1952
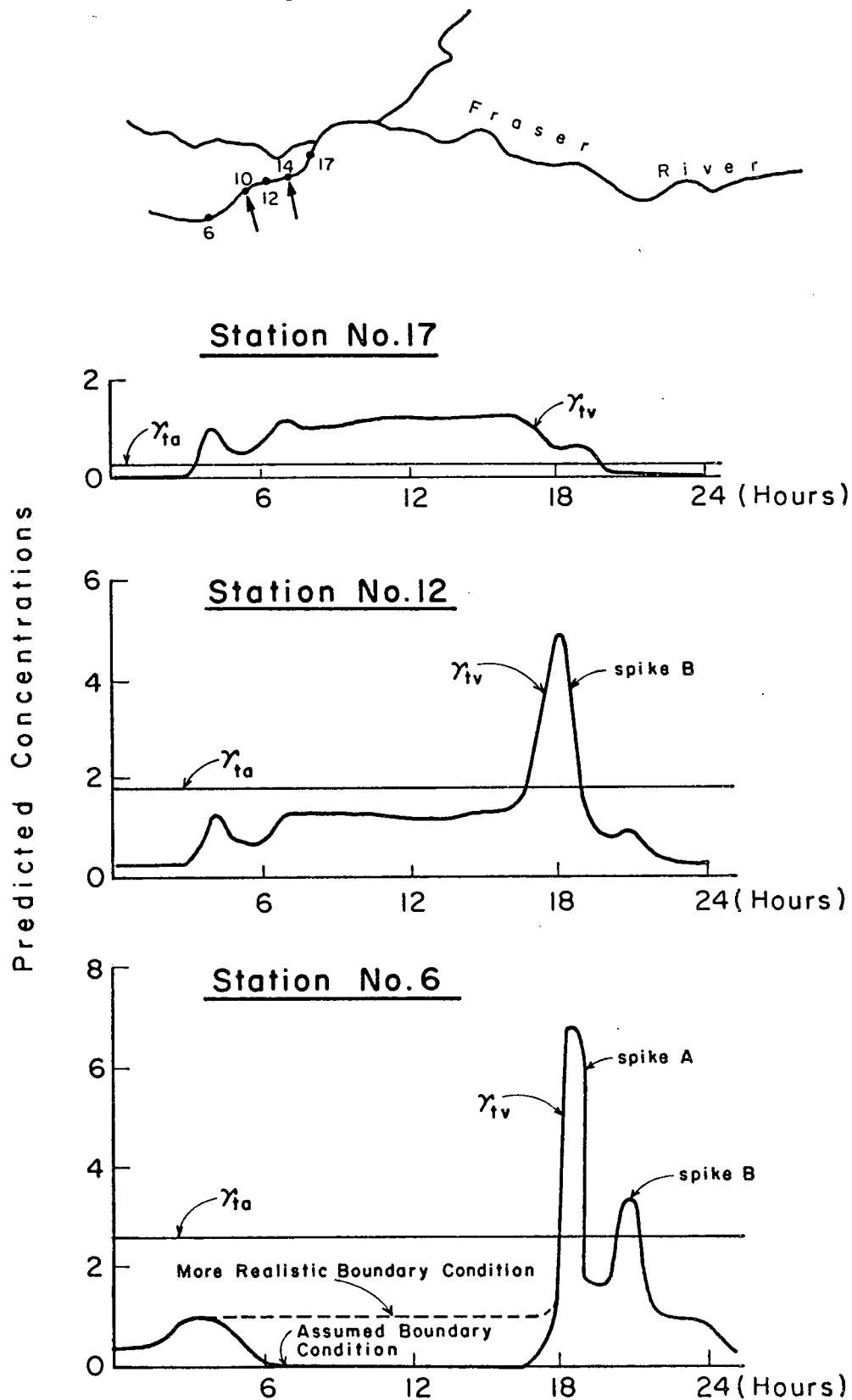
Figure 5.4

Predicted Concentrations Due to Two Effluent Discharges
In The Main Stem

will be dispersed both laterally and longitudinally by the time it reaches

the junction. Under these conditions, the tidally averaged concentration

in both channels downstream of the junction will be a good measure of the

tidally varying values. Of more interest is the case where the effluent

discharge is downstream from a junction. This is illustrated in Figure 5.3

for interactions between the Main Arm and North Arm and between the Main

Stem and Pitt River. Consider the effluent discharged at Station No. 22:

at hour 8 a spike is advected up Pitt River past Station No. 144 on the

strong flood flow and returns past Station No. 144 at hour 23 on the strong

ebb tide, its concentration being reduced by the effects of dispersion dur-

ing its residence in Pitt River. For the two cases of Figure 5.3, upstream

advection causes a slug of contaminated water to be fed into the other

channel during each double tide cycle of 25 hours. The zero concentration

in the North Arm at hour 22 marks the end of one slug and the beginning of

another. In both cases, the tidally averaged concentration is not a good

indication of the tidally varying values, although as remarked in a previous

section, the fit can be improved by increasing the tidally averaged dispersion

coefficient.

5.6 SUMMARY

In this chapter the results from the tidally varying and tidally

averaged mass transport models have been compared to obtain a preliminary

indication of the significance of tidal effects on the predicted concentra-

tions in the Fraser River Estuary.

The tidally varying flows cause a variation in the initial dilution of a discharged effluent. This, and the effects of tidal flow reversal, independently generate concentration spikes. Because both effects occur around the same phase of the tide, the period of weak flood and ebb flows in each double tidal cycle being especially sensitive, the individual spikes combine to generate a spike whose concentration was estimated to be from 1 to 10 times greater than the predicted tidally averaged concentration. Because of incomplete lateral mixing, the peak cross-sectional concentration will be considerably higher than these values. The effects of concentration spikes are most significant in the first 1-2 tidal cycles after their generation. After this period of time, the longitudinal dispersion is due to the effects of lateral concentration gradients and the concentration of the spike is rapidly reduced.

The movement of water through the Fraser River Estuary is a complex process that is influenced by the large tidal effects, the significant freshwater discharge (even at low flows), the various channels and junctions of the estuary and the presence of Pitt Lake. If an effluent discharge is sufficiently far upstream from the junctions, the spikes will be flattened and the effluent dispersed over the cross-section by the time it is advected to the junction. Under these conditions, the predicted tidally averaged behaviour at and downstream of the junction is a good estimate of the tidally varying behaviour, and both should be a reasonable approximation to the actual behaviour in the estuary. Effluent discharges in the Main Stem above Station No. 45 are expected to behave in this manner. Throughout the lower reaches of the estuary, including Pitt River, the predicted tidally averaged behaviour

is not a good indication of the tidally varying behaviour. Because of the effects of incomplete lateral mixing and junctions, as discussed in Section 5.1, the actual response of the estuary may be somewhat different from the predicted tidally varying behaviour.

By adjusting the tidally averaged dispersion coefficients, it is possible to obtain a "best-fit" between the predicted tidally varying and tidally averaged concentrations. However, since the tidally averaged dispersion coefficient has no real physical meaning, there is probably no unique set of values for the estuary. Rather, the best fit dispersion co-efficients will vary with the position and number of effluent discharges.

CHAPTER 6

SUMMARY AND CONCLUSIONS

Mass transport models are commonly used to investigate situations

of existing or potential water quality conflicts in estuaries. Such models

are used to predict the concentration of the offending substance through-

out the estuary and are essentially of two types: those that correctly

allow for tidal effects and those that do not. While tidally varying

models correctly allow for the effects of the tides, their development

and application involves significantly more work than for their tidally

averaged counterparts. In tidally averaged models, all tidal effects are

lumped into the tidally averaged dispersion coefficient, and while such

models are relatively easy to develop and apply, they give no indication

of the significance of tidal effects on the predicted concentrations. In

this study, both a tidally averaged and a tidally varying mass transport

model have been developed and applied to the Fraser River Estuary. The

principal object of this study was to assess the ability of the tidally

averaged model to describe the tidally varying concentrations. This was

investigated by comparing the predicted concentrations from both models for

assumed effluent discharges. The tidally averaged model used in this study

is due to Thomann [1963]. The tidally varying model was developed from

first principles, and during its development it was necessary to consider

the problems of numerical dispersion, stability, the significance of lateral

dispersion and the time dependent behaviour of the coefficient of longi-

tudinal dispersion during the initial period before cross-sectional mixing

is complete.

The principal conclusions to emerge from this study are:

1. Numerical dispersion can be eliminated from
the finite difference solution of mass transport equations
by solving the equations along the advective characteris-
tics.

2. The stability requirements of explicit finite
difference schemes have been shown to be related to the
speed of information propagation. Advective instabili-
ties are eliminated by solving the mass transport equa-
tion along the advective characteristics.

3. Existing theories have been shown to apparent-
ly underestimate the significance of secondary currents on
the lateral mixing process. Secondary currents have been
explained in terms of the generation and advection of vor-
ticity, and estimated values show good agreement with
limited field data. Revised estimates of lateral disper-
sion indicate significantly faster lateral mixing.

4. If the mass transport equation is solved along
the advective characteristics, the time dependent behaviour
of the coefficient of longitudinal dispersion during the
initial period before cross-sectional mixing is complete
can be taken into account. Also, a one-dimensional equa-
tion can be used to estimate lateral concentration profiles.

5. The effect of the tide has been shown to intro-
duce "spikes" into the concentration profile along the estu-
ary. These spikes are caused by variation in the initial
dilution of a discharged effluent and multiple dosing due
to tidal flow reversal.

6. Significantly more work and resources are in-
volved in the development and application of a tidally
varying mass transport model than for a tidally averaged
model. The time required for development, the amount of
field data required for verification and the amount of
computer time required to analyze an identical situation
is estimated to be an order of magnitude greater for the
tidally varying model as compared to the tidally averaged
model.

7. The tidally averaged concentrations were
not found to be a good indication of the tidally vary-
ing response of the Fraser River Estuary. The peak
cross-sectionally averaged concentration predicted
by the tidally varying model was found to be from one
to 10 times greater than the tidally averaged values.

The conclusions are now discussed in detail. In this study

two mass transport models and a hydrodynamic model were developed and

applied to the Fraser River Estuary, the hydrodynamic model being used to

predict the temporal variation in the parameters of the tidally varying

mass transport model. Finite difference methods have been used to solve

the underlying partial differential equations of all three models. Impor-

tant aspects of this type of solution are the problems of numerical dis-

persion and stability. There has been some confusion in the literature

over the origin and means of controlling numerical dispersion. In this

study, numerical dispersion has been shown to result from solving the mass

transport equation over a fixed space grid rather than along the more fund-

amental advective characteristics; if the equation is solved along the ad-

vective characteristics, numerical dispersion is eliminated. As applied,

Thomann's solution is steady state and has no numerical dispersion because

it is independent of time. In addition to the problem of numerical disper-

sion, there is also the problem of stability in explicit finite difference

schemes. In Appendix C this is seen to be related to the speed of infor-

mation propagation along the characteristics of the respective partial dif-

ferential equations. Stability requirements govern the relative size of the

space and time increments in the hydrodynamic equations and in the dispersion

step of the tidally varying mass transport equation. There is no stability

requirement for Thomann's solution as it is independent of time. However,

there is a limit on the relative magnitudes of the tidally averaged advective and dispersive transport processes, and if violated, the concentration in the offending segment will become negative.

There are a number of advantages to solving the tidally varying mass transport equation along the advective characteristics; it results in a direct simulation of the advective transport occurring in the estuary, a useful separation of the advective and dispersive transport processes is achieved, and the position of each separate "effluent parcel" and the time that it has spent in the estuary is known. This last piece of information has been used to account for an assumed time-dependent increase in the coefficient of longitudinal dispersion in the initial period before cross-sectional mixing is complete, and also allows the tidally varying mass transport model to be adapted to predict lateral concentration profiles. A most useful feature of solving the equation along the advective characteristics is that additional moving points can be placed on the characteristics to more accurately define regions of rapid variation in concentration, such as occur at effluent outfalls at times of slackwater, and unnecessary moving points can be removed from regions of slow variation. The concentration spikes generated by the effects of variation in initial dilution and multiple dosing are initially very sharp and only some 500 - 800 feet wide at the base. To achieve adequate resolution of such a spike with a fixed grid solution would require a space grid approximately 10 times finer than the standard 5,000 foot space grid used in this study.

The advantages of solving the mass transport equation along the advective characteristics must be balanced against the somewhat untidy "bookkeeping" of solution results inherent to characteristic methods of solution.

In the tidally varying model of the Fraser River Estuary, this book-keeping is complicated by the multi-channeled nature of the estuary and the inter-actions of these channels at their junctions. But while awkward, the book-keeping of results was not excessively difficult.

Of the three models used in this study, only the hydrodynamic model has been verified with any degree of thoroughness. Because the tidally averaged dispersion coefficients have no real physical meaning, a tidally averaged model is forced to reproduce measured field results rather than being rigorously verified. Lack of field data prevented this, and also prevented the complete verification of the tidally varying mass transport model. However, all three models are sufficiently flexible to simulate the range of flow and tidal conditions of the Fraser River Estuary and can be adjusted to fit field results when available.

Essentially, the effect of the tides is to cause spikes in the concentration profile along the estuary. In a one-dimensional model, the tidally varying flows cause a variation in the initial dilution of a dis-charged effluent, the concentration being greatest at times of slackwater. This generates spikes in the concentration profile along the estuary. The effects of tidal flow reversal result in certain slugs of water being dosed with effluent several times, and this also generates concentration spikes. Because of the asymmetric nature of the tides there is a period of weak flood and ebb flows once in each double tidal cycle. During this time there are three slackwaters and the velocities are low, and the effects of variation in initial dilution and multiple dosing interact to form a compound spike

whose concentration is significantly greater than that of the component spikes.

After a spike has been generated, its concentration is reduced by the effects of lateral and longitudinal dispersion. The initial longitudinal dispersion after a "parcel of effluent" has been discharged into the estuary, is due principally to the effects of vertical velocity gradients. However, when the effluent is mixed over the cross-section, lateral velocity gradients dominate its longitudinal dispersion. To account for this effect, it was assumed that the coefficient of longitudinal dispersion increased between these two extremes as described in Appendix F. Also, the coefficient of longitudinal dispersion was assumed to vary directly as the absolute velocity. While simplistic, these variations are thought to be a reasonable approximation of what occurs in the estuary. The peak tidally varying concentration at the point of effluent discharge was estimated to be from one to 10 times greater than the value predicted from the tidally averaged model. Because the effluent is not uniformly distributed over the cross-section, the peak lateral concentration will be much greater than these values. After a spike has been in the estuary for several tidal cycles, its concentration has been greatly reduced by the longitudinal dispersion process.

In the estuary with relatively short residence times such as the Fraser, lateral mixing will be of considerable importance. For example, in the lower reaches of the estuary, the residence time is only 2-4 tide cycles, and effluent may not be completely mixed over the cross-section even when it leaves the estuary. In the initial period before cross-sectional mixing is complete, the peak lateral concentration is significantly greater

than the cross-sectional averaged value predicted by the tidally varying

model. However, the model can be adapted to predict lateral concentration

profiles as was discussed previously. If cross-sectional mixing is not com-

plete at a diverging junction, the effluent may not be advected through the

junction according to the simple flow balance of the mass transport models.

To account for this effect in a model would require considerable field data.

Because of the influence of secondary currents, cross-sectional mixing is

thought to be relatively rapid in the Fraser River Estuary. Secondary flows

have been tentatively explained in terms of the generation and advection of

vorticity, and on the basis of limited float studies, show good agreement

with values measured in the estuary.

To sum up, the movement of water through the Fraser River Estuary

is a complex phenomenon that is affected by the tides, the freshwater dis-

charge, the various channels and junctions of the estuary and the presence

of Pitt Lake. The advective and dispersive transport processes that distribute

an effluent throughout the water mass of the estuary are similarly complex,

and in particular are significantly affected by the tides. A tidally aver-

aged model, while simpler to develop and apply to the estuary, does not give

a good indication of the tidally varying concentrations. This study does

not pretend to solve the total problem of calculating effluent concentrations

in an estuary as complex as the Fraser. Rather, it has concentrated on deve-

loping stable mathematical models free from numerical dispersion to allow

a preliminary investigation of the significance of tidal effects. In addi-

tion an assessment is made of the importance of lateral dispersion, and it

is seen that with simple modifications, the tidally varying model can at

least partially account for the effects of lateral dispersion.

R E F E R E N C E S

Baines, W. D. [1952]. *Water Surface Elevations and Tidal Discharges in the Fraser River Estuary, January 23 and 24, 1952,* Report No. MH-32, National Research Council of Canada.

Baines, W. D. [1953]. *Survey of Tidal Effects on Flow in the Fraser River Estuary, June 10 and 11, 1952,* Report No. MH-40, National Research Council of Canada.

Bella, D. A. [1968]. "Solution of Estuary Problems and Network Programs," Discussion, Proc. A.S.C.E., *J. Sanit. Eng. Div.,* 94(SA1):180-181.

Bella, D. A. and Grenney [1970]. "Finite-Difference Convection Errors," Proc. A.S.C.E., *J. Sanit. Eng. Div.,* 96(SA6): 1361-1375.

Bella, D. A. and Döbbins, W. E. [1968]. "Difference Modelling of Stream Pollution," Proc. A.S.C.E., *J. Sanit. Eng. Div.,* 94(SA5): 995-1016.

Benedict, A. H., Hall, K. J. and Koch, F. A. [1973]. *A Preliminary Water Quality Survey of the Lower Fraser River System,* Technical Report No. 2, Westwater Research Center, University of British Columbia.

Bennet, J. P. [1971]. "Convolution Approach to the Solution for the Dissolved Oxygen Balance in a Stream," *Water Resources Res.,* 7(3): 580-590.

Bird, R. B., Stewart, W. E., and Lightfoot, E. N. [1960]. *Transport Phenomena* (New York: John Wiley & Sons, 1960).

Callaway, R. J. [1971]. "Application of Some Numerical Models to Pacific Northwest Estuaries," *Proceedings, 1971 Technical Conference on Estuaries of the Pacific Northwest,* Circular No. 42, Engineering Experiment Station, Oregon State University, Corvallis.

Chow, V. T. [1959]. *Open Channel Hydraulics,* (New York: McGraw-Hill, 1959).

Chow, V. T. [1964]. *Handbook of Applied Hydrology,* (Ed.) V. T. Chow. (New York: McGraw-Hill, 1964), Section 8.

Courant, R. and Hilbert, D. [1962]. *Methods of Mathematical Physics* (2 vols; New York: Interscience, 1962), Vol. II.

Custer, S. W. and Krutchkoff, R. G. [1969]. "Stochastic Model for BOD and DO in Estuaries," Proc. A.S.C.E., *J. Sanit. Eng. Div.*, 95(SA5): 865-885.

Diachishin, A. N. [1963]. "Waste Disposal in Tidal Waters," Proc. A.S.C.E., *J. Sanit. Eng. Div.*, 89(SA4): 23-43.

Di Toro, D. M. and O'Connor, D. J. [1968]. "The Distribution of Dissolved Oxygen in a Stream with Time Varying Velocity," *Water Resources Res.*, 4(3): 639-646.

Di Toro, D. M. [1969]. "Stream Equations and The Method of Characteristics," Proc. A.S.C.E., *J. Sanit. Eng. Div.*, 95(SA4): 699-703.

Dornhelm, R. B. and Woolhiser, D. A. [1968]. "Digital Simulation of Estuarine Water Quality," *Water Resources Res.*, 4(6): 1317-1328.

Dronkers, J. J. [1964]. *Tidal Computations in Rivers and Coastal Waters*, (Amsterdam: North-Holland Publishing Co., 1964).

Dronkers, J. J. [1969]. "Tidal Computations for Rivers, Coastal Areas and Seas," Proc. A.S.C.E., *J. Hyd. Div.*, 95(HY1): 29-77.

Einstein, H. A. [1972]. *Sedimentation*, edited and published by Hsieh Wen Shen, Department of Civil Engineering, Colorado State University, Colorado.

Elder, J. W. [1959]. "The Dispersion of Marked Fluid in Turbulent Shear Flow," *J. Fluid Mech.*, 5: 544-560.

Fischer, H. B. [1966a]. "A Note on the One-Dimensional Dispersion Model," *Air Wat. Poll. Int. J.*, 10(6/7): 443-452.

Fischer, H. B. [1966b]. *Longitudinal Dispersion in Laboratory and Natural Streams*, Report No. KH-R-12, Division of Engineering and Applied Science, California Institute of Technology, Pasadena, California.

Fischer, H. B. [1967]. "The Mechanics of Dispersion in Natural Streams," *Proceedings: ASCE Environmental Engineering Conference,* Dallas, Texas, February 6-9, 1967.

Fischer, H. B. [1969a]. "The Effects of Bends on Dispersion in Streams," *Water Resources Res.,* 5(2): 496-506.

Fischer, H. B. [1969b]. "Cross-Sectional Time Scales and Dispersion in Estuaries," Paper C. 19, *Proceedings Volume 3 (Subject C), International Association for Hydraulic Research,* Thirteenth Congress, Kyoto, Japan, 31 August - 5 September, 1969.

Fischer, H. B. [1970]. *A Method for Predicting Pollutant Transport in Tidal Waters,* Water Resources Center Contribution No. 132, Hydraulic Engineering Laboratory, College of Engineering, University of California, Berkeley.

Fischer, H. B. and Holley, E. R. [1971]. "Analysis of the Use of Distorted Hydraulic Models for Dispersion Studies," *Water Resources Res.,* 7(1): 46-51.

Fox, D. G. [1971]. "Finite Difference Convection Errors," Discussion, Proc. A.S.C.E., *J. Sanit. Eng. Div.,* 97(SA5): 766-771.

Gardiner, A. O., Peaceman, D. W. and Pozzi, Jr., A. L. [1964]. "Numerical Calculation of Multi-Dimensional Miscible Displacement by the Method of Characteristics," *J. Soc. Pet. Eng.,* 4(1): 26-36.

Goldie, C. A. [1967]. *Pollution and the Fraser:* Report I Dealing with Preliminary Investigations of Waste Disposal to the Lower Fraser River," prepared for the Pollution Control Board, Victoria, British Columbia.

Guymon, G. L. [1970]. "A Finite Element Solution of the One-Dimensional Diffusion-Advection Equation," *Water Resources Res.,* 6(1): 204-210.

Harder, J. A. [1971]. "Solution Techniques: 1; Analogue and Hybrid Techniques," Chapter 6 of *Estuarine Modelling: An Assessment,* Ed. G. H. Ward and W. H. Espey, Jr. (listed under editors).

Harleman, D. R. F. [1965]. "The Significance of Longitudinal Dispersion in the Analysis of Pollution in Estuaries," *Advances in Water Pollution Research,* Ed. O. Jaag (3 vols; Oxford: Pergamon Press, 1965), I, pp. 279-290.

Harleman, D. R. F., Lee, C. H. and Hall, L. C. [1968]. "Numerical Studies of Unsteady Dispersion in Estuaries," Proc. A.S.C.E., *J. Sanit. Eng. Div.,* 94(SA5): 897-911.

Harris, E. K. [1963]. "A New Statistical Approach to the One-Dimensional Diffusion Model," *Air Wat. Poll. Int. J.,* 7(8): 799-812.

Harris, E. K. [1964]. "Note on the One-Dimensional Diffusion Model and the Log-Normal Distribution," *Air Wat. Poll. Int. J.,* 8(5): 421-423.

Henderson, F. M. [1966]. *Open Channel Flow* (New York: The MacMillan Co., 1966).

Hinze, J. O. [1959]. *Turbulence: An Introduction to its Mechanism and Theory* (New York: McGraw-Hill, 1959).

Holley, E. R. [1969a]. "Unified View of Diffusion and Dispersion," Proc. A.S.C.E., *J. Hyd. Div.,* 95(HY2): 621-631.

Holley, E. R. [1969b]. "Difference Modelling and Stream Pollution," Proc. A.S.C.E., *J. Sanit. Eng. Div.,* 95(SA5): 968-972.

Holley, E. R., Harleman, D. R. F. and Fischer, H. B. [1970]. "Dispersion in Homogenous Estuary Flow," Proc. A.S.C.E., *J. Hyd. Div.,* 96(HY8): 1691-1709.

Kent, R. [1960]. "Diffusion in a Sectionally Homogenous Estuary," Proc. A.S.C.E., *J. Sanit. Eng. Div.,* 86(SA2): 15-47.

Koivo, A. J. and Phillips, G. R. [1971]. "Identification of Mathematical Models for DO and BOD Concentrations in Polluted Streams From Noise Corrupted Measurements," *Water Resources Res.,* 7(4): 853-862.

Lager, J. A. and Tchobanoglous, G. [1968]. "Effluent Disposal in South San Francisco Bay," Proc. A.S.C.E., *J. Sanit. Eng. Div.*, 94(SA2): 213-236.

Leeds, J. V. [1967]. "Accuracy of Discrete Models Used to Predict Estuary Pollution," *Water Resources Res.*, 3(2): 481-490.

Leeds, J. V. and Bybee, H. H. [1967]. "Solution of Estuary Problems and Network Programs," Proc. A.S.C.E., *J. Sanit. Eng. Div.*, 93(SA3): 29-36.

Leendertse, J. J. [1971a]. "Environmental Simulation as a Tool in a Marine Waste Disposal Study of Jamaica Bay," *Advances in Water Pollution Research*, Ed. S. H. Jenkins (2 vols; Great Britain: Pergamon Press, 1971), II, Section III, pp. 4/1-4/7.

Leendertse, J. J. [1971b]. "Solution Techniques: 2; Finite Differences," Chapter 6 of *Estuarine Modelling: An Assessment*, Ed. G. H. Ward and W. H. Espey, Jr. (listed under editors).

Li, W. H. [1962]. "Unsteady Oxygen Sag in a Stream," Proc. A.S.C.E., *J. Sanit. Eng. Div.*, 88(SA3): 75-85.

Li, W. H. [1972]. "Effects of Dispersion on DO Sag in Uniform Flow," Proc. A.S.C.E., *J. Sanit. Eng. Div.*, 98(SA1): 169-182.

Loucks, D. P. [1967]. "Risk Evaluation in Sewage Treatment Plant Design," Proc. A.S.C.E., *J. Sanit. Eng. Div.*, 93(SA1): 25-39.

Loucks, D. P. and Lynn, W. R. [1966]. "Probablistic Models for Predicting Quality," *Water Resources Res.*, 2(3): 593-605.

Nalluswami, M., Longenbaugh, R. A. and Sunada, D. K. [1972]. "Finite Element Method for the Hydrodynamic Dispersion Equation with Mixed Partial Derivatives," *Water Resources Res.*, 8(5): 1247-1250.

O'Connell, R. L. and Walter, C. M. [1963]. "Hydraulic Model Tests of Estuarial Waste Dispersion," Proc. A.S.C.E., *J. Sanit. Eng. Div.*, 89(SA1): 51-65.

O'Connor, D. J. [1960]. "Oxygen Balance of an Estuary," Proc., A.S.C.E., *J. Sanit. Eng. Div.*, 86(SA3): 35-55.

O'Connor, D. J. [1962]. "Organic Pollution of New York Harbour - Theoretical Considerations," *J. Water Poll. Control Fed.*, 34(9): 905-919.

O'Connor, D. J. [1965]. "Estuarine Distribution of Non-Conservative Substances," Proc. A.S.C.E., *J. Sanit. Eng. Div.*, 91(SA1): 23-42.

O'Connor, D. J. [1966]. "An Analysis of the Dissolved Oxygen Distribution in the East River," *J. Water Poll. Control Fed.*, 38(11): 1813-1830.

O'Connor, D. J. [1967]. "The Temporal and Spatial Distributions of Dissolved Oxygen in Streams," *Water Resources Res.*, 3(1): 65-79.

O'Connor, D. J., St. John, J.P. and Di Toro, D. M. [1968]. "Water Quality Analysis of the Delaware Estuary," Proc. A.S.C.E., *J. Sanit. Eng. Div.*, 94(SA6): 1225-1252.

O'Connor, D. J. and Di Toro, D. M. [1970]. "Photosynthesis and Oxygen Balance in Streams," Proc. A.S.C.E., *J. Sanit. Eng. Div.*, 96(SA2): 547-571.

Odd, N. V. M. [1971]. "Practical Application of Mathematical Model Techniques to Predict Effects of Engineering Works on Tidal Flow in Estuaries With A Large Tidal Range," *Proc. Inst. Civ. Engrs.*, 50(December): 507-517.

Oster, C. A., Sannichsen, J. C. and Jaske, R. T. [1970]. "Numerical Solution to the Convective-Diffusion Equation," *Water Resources Res.*, 6(6): 1746-1752.

Pence, G. D. Jr., Jeglic, G. D. and Thomann, R. V. [1968]. "Time Varying Dissolved Oxygen Model," Proc. A.S.C.E., *J. Sanit. Eng. Div.*, 94(SA2): 381-402.

Pinder, G. F. and Cooper, Jr. H. H. [1970]. "A Numerical Technique for Calculating the Transient Position of the Saltwater Front," *Water Resources Res.*, 6(3): 875-882.

Pinder, G. F. and Friend, G. O. [1972]. "Application of Galerkin's Procedure to Aquifier Analysis," *Water Resources Res.*, 8(1): 108-120.

Preddy, W. S. and Webber, B. [1963]. "The Calculation of Pollution of the Thames Estuary by a Theory of Quantized Mixing," *Air Wat. Poll. Int. J.*, 7(8): 829-843.

Pretious, E. S. [1972]. *Downstream Sedimentation Effects of Dams on the Fraser River, B.C.,* Water Resource Series Report No. 6, Department of Civil Engineering, University of British Columbia.

Price, H. S., Cavendish, J. C. and Varga, R. S. [1968]. "Numerical Methods of Higher-Order Accuracy for Diffusion-Convection Equations," *J. Soc. Pet. Eng.,* 8(3): 293-303.

Pritchard, D. W. [1969]. "Dispersion and Flushing of Pollutants in Estuaries," Proc. A.S.C.E., *J. Hyd. Div.,* 95(HY1): 115-124.

Prych, E. A. and Chidley, T. R. E. [1969]. "Numerical Studies of Unsteady Dispersion in Estuaries," Discussion, Proc. A.S.C.E., *J. Sanit. Eng. Div.,* 95(SA5): 959-964.

Quick, M. C. [1973]. "The Mechanics of Streamflow Meandering," paper submitted for publication.

Rennerfelt, J. G. W. [1963]. "An Analogue Computer for Oxygen Sag Calculations," *Air Wat. Poll. Int. J.,* 7(4/5): 367-372.

Richtmyer, R. D. and Morton, K. W. [1967]. *Difference Methods for Initial Value Problems.* 2nd Ed. (New York: Interscience, 1967).

Sawyer, W. W. [1966]. *A Path to Modern Mathematics* (London: Penguin Books Ltd., 1966).

Schofield, W. R. and Krutchkoff, R. G. [1972]. "Stochastic Model for BOD and OD in Segmented Estuary," Proc. A.S.C.E., *J. Sanit. Eng. Div.,* 98 (SA5): 745-762.

Simmons, H. B. [1960]. "Application and Limitation of Estuary Models in Pollution Analyses," *Proceedings: First International Conference on Waste Disposal in the Marine Environment,* Ed. E. A. Pearson (Oxford: Pergamon Press, 1960), pp. 540-546.

Streeter, H. W. and Phelps, E. B. [1925]. *A Study of the Pollution and Natural Purification of the Ohio River,* Public Health Bulletin 146, U.S. Public Health Service, Washington, D.C.

Taylor, G. I. [1954]. "The Dispersion. of Matter in Turbulent Flow Through a Pipe," *Proc. Roy. Soc. London,* 223 (Series A): 446-468.

Thayer, R. P. and Krutchkoff, R. G. [1967]. "Stochastic Model for BOD and DO in Streams," Proc. A.S.C.E., *J. Sanit. Eng. Div.,* 93(SA3): 59-72.

Thomann, R. V. [1963]. "Mathematical Model for Dissolved Oxygen," Proc. A.S.C.E., *J. Sanit. Eng. Div.,* 89(SA5): 1-30.

Thomann, R. V. [1965]. "Recent Results From A Mathematical Model of Water Pollution Control in the Delaware Estuary," *Water Resources Res.,* 1(3): 349-359.

Thomann, R. V. [1971]. *Systems Analysis and Water Quality Management* (New York: Environmental Science Services Division, Environmental Research and Applications, 1971).

Waldichuk, M. Market, J. R., and Meikle, J. H. [1968]. *Fraser River Estuary, Burrard Inlet, HoweSound and Malaspina Strait Physical and Chemical Ocean- ographic Data, 1957-1966: Volume 1, September 1957 to February 1962,* Manuscript Report Series No. 939, Fisheries Research Board of Canada.

Ward, G. H. and Espey, W. H. [1971]. *Estuarine Modelling: An Assessment,* Ed. G. H. Ward and W. H. Espey, Report No. 16070 DZV 02/71, Water Pollution Research Series, Environmental Protection Agency, U.S.A.

Ward, P. R. B. [1972]. *Transverse Dispersion of Pollutants in Oscillatory Open-Channel Flow,* Report No. WHM-2, Department of Civil Engineering, University of California, Berkeley.

Ward, P. R. B. [1973]. "Prediction of Mixing Lengths for River Flow Gauging," Proc. A.S.C.E., *J. Hyd. Div.,* 99(HY7): 1069-1081.

Worley, J. L., Burgess, F. J. and Towne, W. W. [1965]. "Identification of Low-Flow Requirements for Water Quality Control by Computer Techniques," *J. Water Poll. Control Fed.,* 37(5): 659-673.

APPENDICES

APPENDIX A

DERIVATION OF THE ONE-DIMENSIONAL MASS TRANSPORT EQUATION

A.1 GENERAL

The mass transport processes of advection, turbulent diffusion and molecular diffusion transport and distribute any dissolved substance throughout the water mass of a river or estuary. (Advection is also referred to as convection or forced convection in the literature). At the time and space scales of interest, the contribution to mass transport by molecular diffusion is insignificant compared to the other processes, and is not considered further. The inability of the advective or bulk velocity to describe the distribution of velocity over a cross-section of the river or estuary makes it necessary to postulate another transport mechanism, namely dispersion. The mechanisms of advective and dispersive transport are described in Sections A.2 and A.3.

The one-dimensional mass transport equation is derived by taking a mass balance of dissolved substance over an element cross-sectional slice of the estuary. Dissolved substance is transported into and out of this volume by the processes of advection and dispersion, and these processes, together with any source-sink effects that the substance undergoes within the water mass, determine its concentration within the elemental volume.

The only spatial variation that is admitted in the one-dimensional mass transport equation is a longitudinal variation along the estuary. The concentration, longitudinal velocity, depth and dispersion coefficient are

all assigned their average cross-sectional values ($\bar{c}$, $\bar{u}$, $\bar{y}$ and E respec-
tively). For the sake of brevity, the average cross-sectional value of
any parameter will be referred to as its "mean" value. The high fre-
quency turbulent fluctuations are assumed to have been averaged out of
the mean values $\bar{u}$ and $\bar{c}$.

Figure A.1 shows an elemental cross-sectional slice of an
estuary. The direction of the co-ordinate axes x, y and z are as shown,
the positive x axis pointing seawards and the positive y axis vertically
down. Note that the co-ordinate axes are Eulerian, or fixed in space.
The flow is assumed to be both unsteady and non-uniform so that $\bar{c}$, $\bar{u}$, $\bar{y}$, E
and the cross-sectional area A vary both with time (t) and longitudinal
distance (x). The width of estuary b is assumed to vary with x only. It
is assumed that the longitudinal variation in all these parameters is con-
tinuous.

A.2 LONGITUDINAL ADVECTIVE TRANSPORT

The distribution of longitudinal velocity in an estuary is
three-dimensional. Variations in the longitudinal direction occur due
to changes in the cross-sectional area of the estuary, and over any cross-
section, variations in the lateral and vertical directions occur due to
the frictional influence of neighbouring fluid layers with each other and
the solid bed. In a river or estuary, the lateral distribution of longi-
tudinal velocity is modified by the presence of bends, and in an estuary,
the vertical distribution of longitudinal velocity is modified by the
additional influence of salinity.
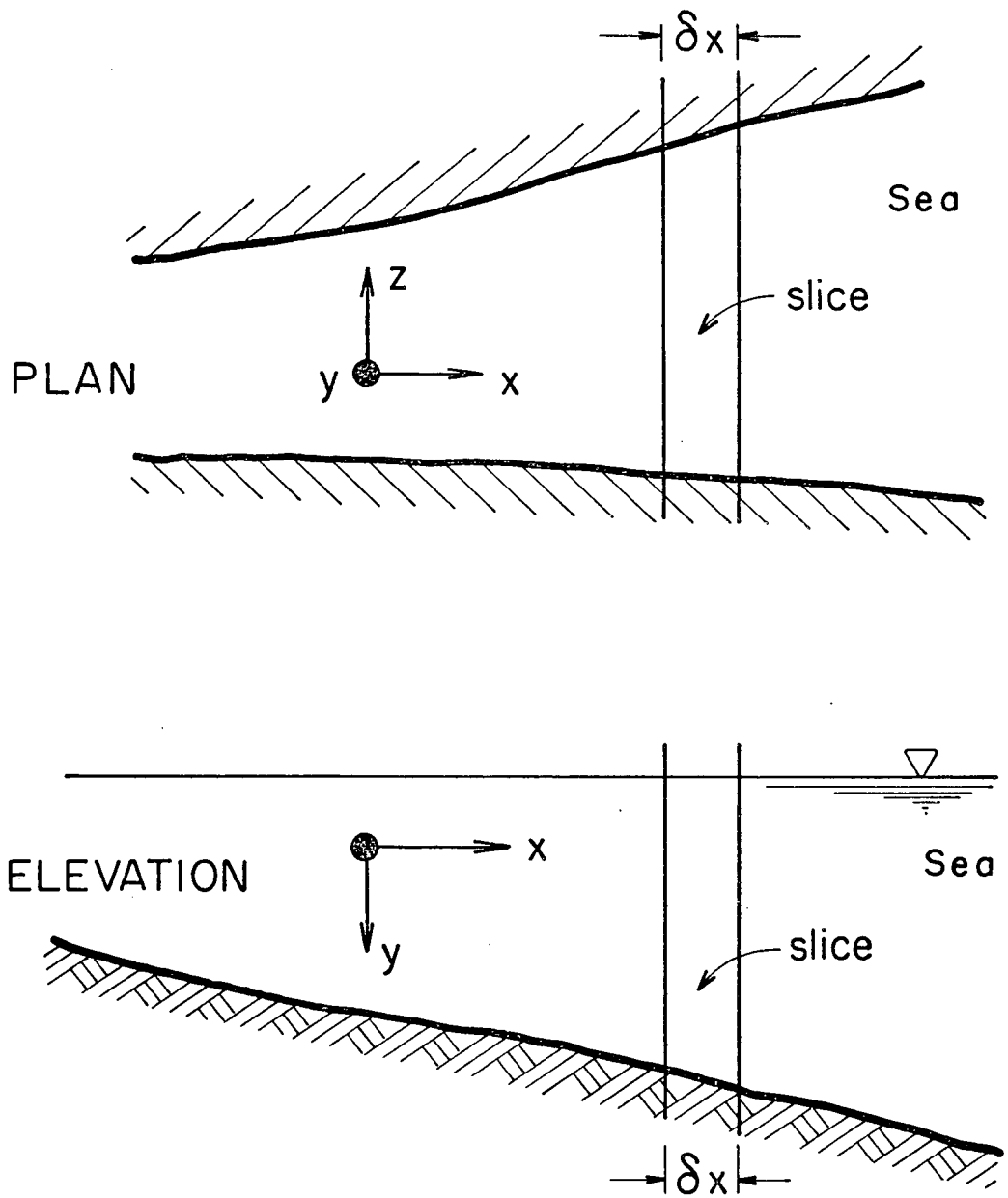
Figure A.1

Elemental Cross-Sectional Slice of A River or Estuary

In one-dimensional mass transport models, it is assumed that a cross-sectional slice or slug of water moves along the river or estuary at the mean cross-sectional velocity $\bar{u}$. The transport of dissolved substance in this slug of water is termed *longitudinal advection*.

The advective transport in a river is always in the downstream direction. In an estuary, the net advective transport over a tidal cycle is in the downstream direction because of the effect of freshwater inflow. However, because of flow reversal due to tidal effects, the advective transport will be in the upstream direction over portion of the tidal cycle.

The mass of dissolved substance (M) advected through any cross-section of a river or estuary in time δt is given by

$$M = \bar{u}A\bar{c}\ \delta t,$$

and thus the net mass (M_{net}) remaining in the elemental volume of Figure A.1 due to advective transport during time δt is

$$M_{net} = -\frac{\partial}{\partial x}\{\bar{u}A\bar{c}\}\delta x \delta t \tag{A.1}$$

A.3 LONGITUDINAL DISPERSIVE TRANSPORT

Advection accounts for the transport of dissolved substance in the longitudinal direction due to the *assumed* uniform distribution of the velocity over the cross-section, $\bar{u}$. The vertical and lateral velocity gradients that exist over any cross-section result in small "parcels" of water preceding and lagging the line of advective advance, as defined by $\bar{u}$. This is illustrated for a vertical velocity profile typical of a river

Vertical Distribution of Velocity

$\bar{u}\Delta t$

Line source position after Time Δt

Effect of Diffusion

Advection Due to Velocity Gradient

Input Concentration

Advection Due to mean Velocity $\bar{u}$

Effect of Velocity Gradient

Longitudinal Distribution of $\bar{c}$

Figure A.2

Dispersive Effects of Vertical Velocity Gradients

in Figure A.2. It is seen that a slug input from a line source is not advected downstream as a slug load, but is spread around the line of mean advance. The effect of this is to reduce the peak concentration and flatten the concentration gradients, as predicted on the basis of advection alone.

Superimposed on the effects of velocity gradients is the process of turbulent diffusion. The mass transport associated with the turbulent velocity fluctuations results in a further flattening of the concentration gradients. The effect of turbulent diffusion over the vertical section "AA" is also illustrated in Figure A.2. The combined effects of velocity gradients and turbulent diffusion in spreading the dissolved substance around the line of advective advance ($\bar{u}$) is termed *longitudinal dispersion*. Unless otherwise qualified, the terms "advection" and "dispersion" will be taken to mean advection and dispersion in the longitudinal direction.

It is necessary to represent the dispersion process mathematically if it is to be included in the mass transport equation. Holley [1969a] discussed the underlying similarity between the mechanisms of molecular diffusion, turbulent diffusion and dispersion. Both molecular diffusion [Bird, *et al.*, 1960] and turbulent diffusion in homogeneous isotropic free turbulence [Hinze, 1959] can be represented mathematically by a Fickian diffusion equation. Taylor [1954] showed that after a suitable time had elapsed, the longitudinal dispersion in flow through a pipe can also be represented by a one-dimensional Fickian diffusion equation. Elder [1959] found a similar result to hold in model experiments of open channel flow. Fischer [1966a] illustrated that in the initial non-Fickian period following the release of tracer, the effects of velocity gradients outweighed the effects of turbulent diffusion, and led to a skewed distribution of mean concentration in

the longitudinal direction, as is illustrated in Figure A.2. According to Fick's Law, the distribution of concentration should be Gaussian, but Fischer [1966a] has shown that this only occurs after cross-sectional mixing has reduced the spatial variation of concentration over the cross-section to a value much smaller than the mean cross-sectional value. In deriving and applying the one-dimensional mass transport equation, the dispersion process in its entirety is assumed to be Fickian.

In actual fact, the longitudinal dispersion of effluent in a river or estuary is a complex phenomenom that is initially controlled by the effects of vertical velocity gradients. As turbulent diffusion and secondary flows distribute the effluent mass over the cross-section, the lateral velocity gradients exert an increasing influence on the longitudinal dispersion process. The lateral mixing due to turbulent diffusion and secondary flows is discussed in Appendix E and an estimate of the coefficients of longitudinal dispersion of the estuary is given in Appendix F. (The effects of vertical and lateral velocity gradients are also discussed in Appendix F). When the cross-sectional mixing is essentially complete (and the dispersion process is Fickian) the effects of lateral velocity gradients dominate the longitudinal dispersion and are of the order of 20 - 100 times greater than the effects of vertical velocity gradients [Fischer, 1966a]. In an estuary, the dispersion process is modified by the additional influence of salinity and tidal effects. The influence of tidal oscillations on the dispersion coefficient has been investigated by Holley *et al*. [1970], and their method has been used in estimating the dispersion coefficients for the Fraser River Estuary in Appendix F.

According to Fick's law of diffusion, the net mass of dissolved substance transported through unit cross-sectional area in time δt is given by [Bird *et al*., 1960]

$$M = -E\frac{\partial \bar{c}}{\partial x}\delta t \qquad\qquad (A.2)$$

the minus sign arising because the net transport is in the direction of decreasing concentration. E is the dispersion coefficient, and as is expected from the previous discussions of the dispersion process, depends on the distribution of velocity over the cross-section and the coefficient of turbulent diffusion (see, for example, Taylor [1954]; Fischer [1966a], [1967] and Holley *et al.* [1970].

According to equation (A.2), the net mass remaining in the elemental volume due to dispersive transport during time δt is

$$M_{net} = \frac{\partial}{\partial x}\{AE\frac{\partial \bar{c}}{\partial x}\}\delta x \delta t \tag{A.3}$$

A.4 SOURCE-SINK EFFECTS

The source-sink terms account for any processes that result in the production or removal of the dissolved substance from the water body. In the BOD-DO system, source processes include reoxygenation by atmospheric oxygen dissolving in the water and the oxygen produced photosynthetically by aquatic plants; the sink processes include oxygen uptake by bacteria breaking down the substances exerting the BOD and oxygen uptake for aquatic plant respiration.

The source-sink processes that a substance undergoes in the aquatic environment are specific to the particular substance, and depend on the physical, chemical and biological processes that the substance undergoes in the particular aquatic environment. Consequently, source-sink effects are included in the mass transport equation in a general manner. Suppose that the particular substance is undergoing n processes that result in its production or removal from the water body. If the rate of production per unit

volume of water due to the ith process is given by S_i, removal processes being regarded as negative production, then the net mass of substance produced in the elemental volume in time δt is

$$M_{net} = A\delta x\delta t \sum_{i=1}^{n} S_i \qquad (A.4)$$

A.5 THE ONE-DIMENSIONAL MASS TRANSPORT EQUATION

The mass of dissolved substance contained in the elemental volume is

$$M = A\delta x \bar{c}$$

As a result of the advection, dispersion and source-sink effects that occur in time δt, the change in mass of dissolved substance in the elemental volume is

$$\delta M = \frac{\partial}{\partial t}\{A\bar{c}\}\delta x\delta t \qquad (A.5)$$

Summing equations (A.1), (A.3) and (A.4) and substituting into equation (A.5) gives

$$\frac{\partial}{\partial t}\{A\bar{c}\} = -\frac{\partial}{\partial x}\{A\bar{u}\bar{c}\} + \frac{\partial}{\partial x}\{AE\frac{\partial\bar{c}}{\partial x}\} + A\sum_{i=1}^{n} S_i \qquad (A.6)$$

Expanding the first two derivatives and using the equation of conservation of fluid mass in the form

$$\frac{\partial}{\partial x}\{A\bar{u}\} + \frac{\partial A}{\partial t} = 0,$$

equation (A.6) reduces to

$$\frac{\partial\bar{c}}{\partial t} = -\bar{u}\frac{\partial\bar{c}}{\partial x} + \frac{1}{A}\frac{\partial}{\partial x}\{AE\frac{\partial\bar{c}}{\partial x}\} + \sum_{i=1}^{n} S_i, \qquad (A.7)$$

the one-dimensional mass transport equation for unsteady non-uniform flow. The terms on the right-hand side of Equation (A.7) shall be referred to respectively as the advective, the dispersive and the source-sink terms.

A.6 THE LAGRANGIAN FORM OF THE ONE-DIMENSIONAL MASS TRANSPORT EQUATION

Equation (A.7) was derived relative to an Eulerian co-ordinate system (xyz) that is fixed in space. To transform the equations relative to a co-ordinate system that is advected along at the mean velocity $\bar{u}$ (a Langrangian co-ordinate system), it is necessary to transform the Eulerian co-ordinates according to

$$\frac{dx}{dt} = \bar{u} \tag{A.8}$$

Relative to the curve (A.8), the time rate of change of concentration is given by (see Section C.1)

$$\frac{dc}{dt} = \frac{\partial \bar{c}}{\partial t} + \bar{u}\frac{\partial \bar{c}}{\partial x}$$

and thus, relative to Langrangian co-ordinates, Equation (A.7) becomes

$$\frac{dc}{dt} = \frac{1}{A}\frac{\partial}{\partial x}\{AE\frac{\partial \bar{c}}{\partial x}\} + \sum_{i=1}^{n} S_i \tag{A.9}$$

Equation (A.8) is the characteristic curve of advective information propagation, and is discussed further with regard to numerical dispersion and stability in Appendix C. Equation (A.7) and Equations (A.8) and (A.9) represent the same situation but from different viewpoints; in Equation (A.7) the "observer" is stationed on the bank of the river or estuary and observes changes

in the concentration as the water flows past him, whereas in the latter two equations, the observer is advected along with the water mass [Equation (A.8)] and observes changes in the water mass around him [Equation (A.9)].

If dispersive transport is ignored, Equation (A.8) reduces to

$$\frac{dc}{dt} = \sum_{i=1}^{n} S_i$$

which is the original one-dimensional mass transport equation developed by Streeter and Phelps [1925] to predict the effect of substances exerting a biological oxygen demand (BOD) on the concentration of dissolved oxygen (DO) in a river. In their model, n was equal to two; the only source of DO was reaeration through the water surface and the only sink was the satisfaction of the BOD.

APPENDIX B

A DESCRIPTION OF THE FRASER RIVER ESTUARY

B.1   GENERAL

The Fraser River is the largest and most important river in

British Columbia.   Its drainage area of 90,000 square miles is shown in

Figure B.1 and occupies almost one-quarter of the Province.   The river

rises in the Rocky Mountains near Jasper and flows north-west for some 330

miles.   North of Prince George the river changes direction and flows south

some 400 miles to Hope.   At Hope the river emerges from the Coast Mountains

and flows westward through the Fraser Valley for almost 100 miles to enter

the Strait of Georgia at Vancouver.   It is this latter section of the river,

from Hope to Vancouver, that is of direct concern to this thesis, and dis-

cussion is now restricted to it.

B.2   THE LOWER FRASER RIVER SYSTEM

The Lower Fraser River from Hope to Vancouver is shown in Figure

B.2.   A convenient way of describing this section of the river is in terms

of the factors that affect the flow.   These factors include: (1) the var-

ious channels of the river system; (2) the tides in the Strait of Georgia;

(3) the river discharge; and (4) saltwater intrusion.

B.2.1   Channels of the River System.   The Fraser River deposits

20 - 25 million tons of sediment into the Strait of Georgia annually [Pretious,

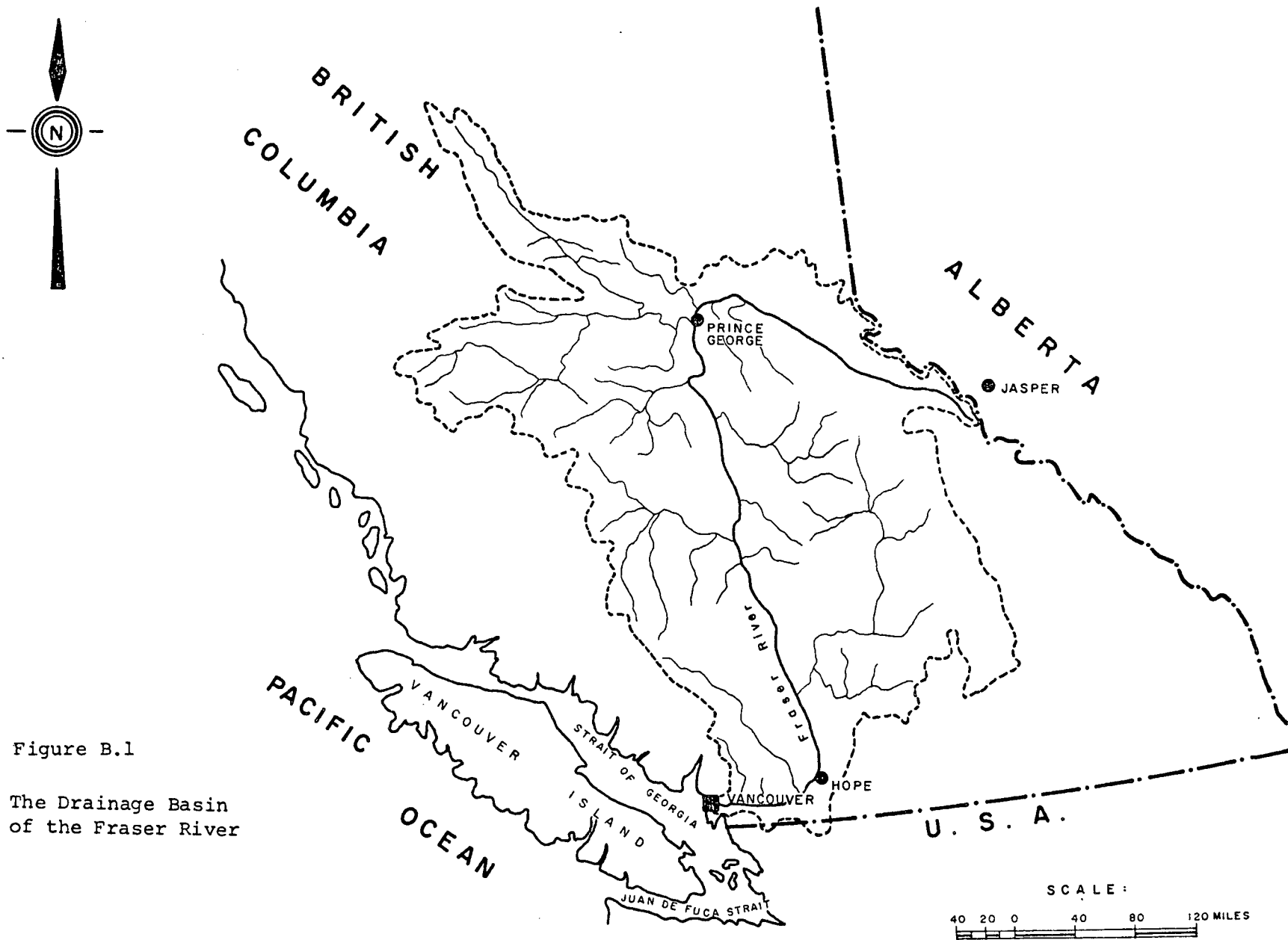1972] and has built a large delta with a seaward perimeter of some 30 miles.

117

Figure B.1
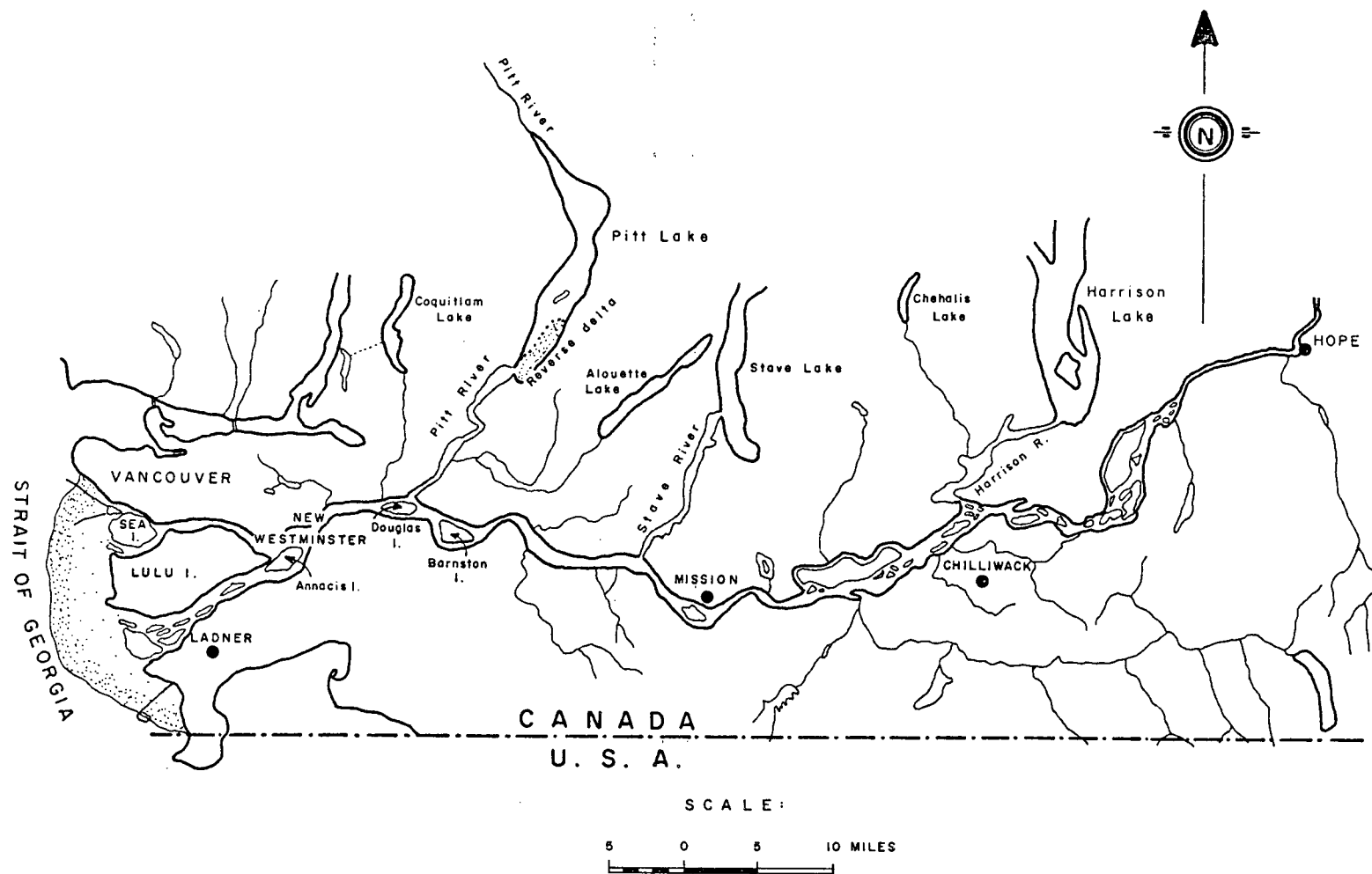
The Drainage Basin
of the Fraser River

Figure B.2

The Fraser River From Hope to Vancouver

The delta is shown in Figure B.3 and it is seen that the river has cut a network of channels through it. At New Westminster the river trifurcates into the *Main Arm,* which enters the Strait off Steveston; *Annacis Channel,* which flows around the back of Annacis Island to reconnect with the Main Arm; and the *North Arm,* which enters the Strait near Point Grey. Annacis Channel is not treated as a separate channel, but as part of the Main Arm. Around Sea Island, the North Arm divides to form the *Middle Arm.* North-west of Ladner, a complex of shallow channels and sloughs (backwater areas) interconnect with each other, the three most important channels being Ladner Reach, Sea Reach and Canoe Pass. This area drains through *Canoe Pass* to provide the Main Arm with another connection to the Strait of Georgia. The percentage of river discharge that enters the Strait through the Main Arm, the North Arm, the Middle Arm and Canoe Pass is approximately 85 per cent, 5 per cent, five per cent and five per cent respectively [Goldie, 1967]. This is only a general indication of the percentage distribution of flows, the summer distribution of flows probably differing from the winter distribution.

The section of river between New Westminster and Hope is referred to as the *Main Stem.* Of the various islands present in the Main Stem (see Figure B.2), only *Douglas* and *Barnston Islands* form significant additional channels. The channels at the "back" of the other islands are treated as part of the Main Stem.

Of the various major lakes that drain into the Main Stem (see Figure B.2), Pitt Lake is of particular significance. The surface elevation of the lake is affected both by the tides in the Strait of Georgia and the fresh-water discharge of the Fraser (the discharge of Pitt River into the north end
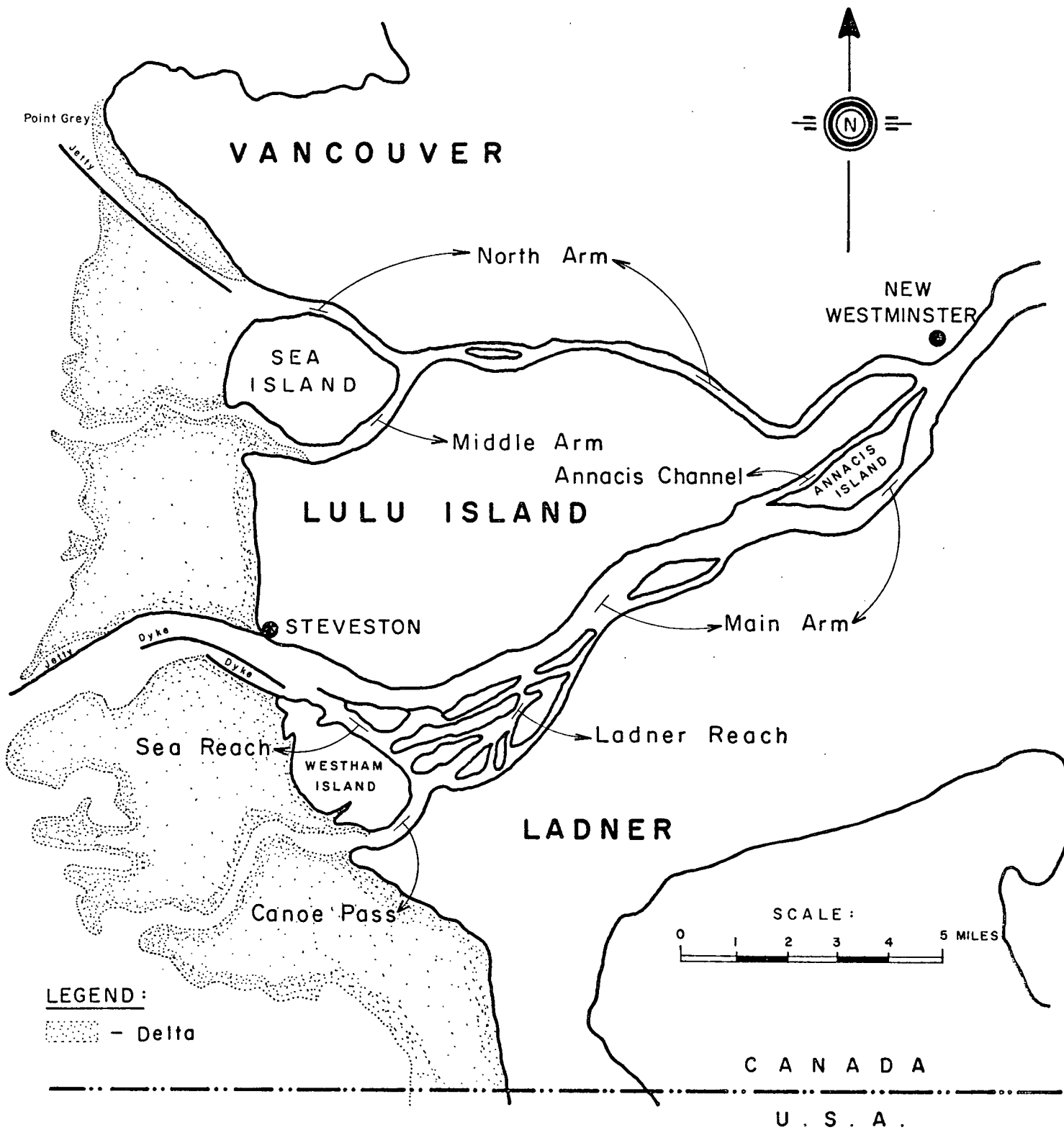
Figure B.3

The Fraser River Delta

of the lake is negligible compared to the Fraser discharge. At low fresh-water flows in the Fraser, the maximum tidal range of the lake is several feet, and as the lake has a surface area of some 25 square miles, the volume of water stored in the lake on the flood tide and released to the Fraser on the ebb tide is very large (see Table B.1). The large reverse delta at the entrance to Pitt Lake (see Figure B.2) is evidence of the large flows that enter the lake. The Pitt River - Pitt Lake system obviously consti-tute an important channel of the lower Fraser system and will be referred to as the *Pitt System*. The other lakes draining into the Main Stem are of sufficient elevation to be independent of tidal influence and freshwater discharge in the Fraser.

Thus, the lower Fraser River system consists of the following seven principal channels:

1. Main Arm - Main Stem

2. North Arm

3. Middle Arm

4. Canoe Pass

5. Pitt System

6. Douglas Channel, and

7. Barnston Channel.

To some extent the channel geometries are determined by the many dykes, jetties and training walls that have been constructed in the lower Fraser system. Each Spring the Fraser Valley is subject to possible flooding during the freshet (time of high runoff due to snowmelt), and an extensive system of dykes has been constructed for flood protection. Ocean-going ships

use the Main Arm to enter and leave New Westminster, an overseas shipping terminal. To maintain the shipping channel, a number of dykes and training walls have been constructed to increase local scour.

Cross-sectional areas, depths and widths were evaluated at the network of stations shown in Figure B.4. The stations are 5,000 feet apart, except in the deeper water of Pitt Lake where the spacing has been increased to 15,000 feet. (This network of stations is used in the finite difference solutions of the hydrodynamic equation and the tidally varying and tidally averaged mass transport equations, as is discussed in Chapter 3). Soundings charts supplied by the Department of Public Works of Canada were used to determine the channel geometries. A typical cross-section of each of the seven channels is shown in Figure B.5. Widths and depths are recorded in feet, and depths are relative to local low water. Figures B.6 to B.8 show the variation in depths, widths and cross-sectional areas along the five major channels. In an attempt to estimate the advective area (effective area of discharge), it was arbitrarily assumed that any depth of section less than 10 feet deep did not contribute to the advective area. This is illustrated for Station No. 35 in Figure B.5, where areas less than 10 feet deep are shown hatched. The storage width of section is AB, but the advective width is only CD. The advective area was used to determine the advective hydraulic radius (which is greater than the hydraulic radius determined from the gross area of section). From Figures B.6 to B.8, it is seen that the advective area is not much smaller than the gross area, but the advective width is often considerably smaller than the storage width. The river sections are essentially wide and shallow and the terms hydraulic radius and mean depth are now used synonymously.

FIRST AND LAST STATIONS :

Main Arm – Main Stem .... 1 – 62

North Arm .... 101 – 118

Canoe Pass .... 119 – 128

Middle Arm .... 129 – 136

Pitt System .... 140 – 163

Douglas Channel..................... 180 – 182

Barnston Channel .... 184 – 190

163

Pitt Lake

159

155

Pitt River

150

■ Junction Stations

○ 5000' spacing

▲ 15,000' spacing

North Arm
101
106
129
136
Middle Arm

118
18

Main Arm

8
128

1

119
Canoe Pass

180
140
Douglas Channel
184
182
190
Barnston Channel

35

Main Stem

40

45

Fraser River 62

55

50
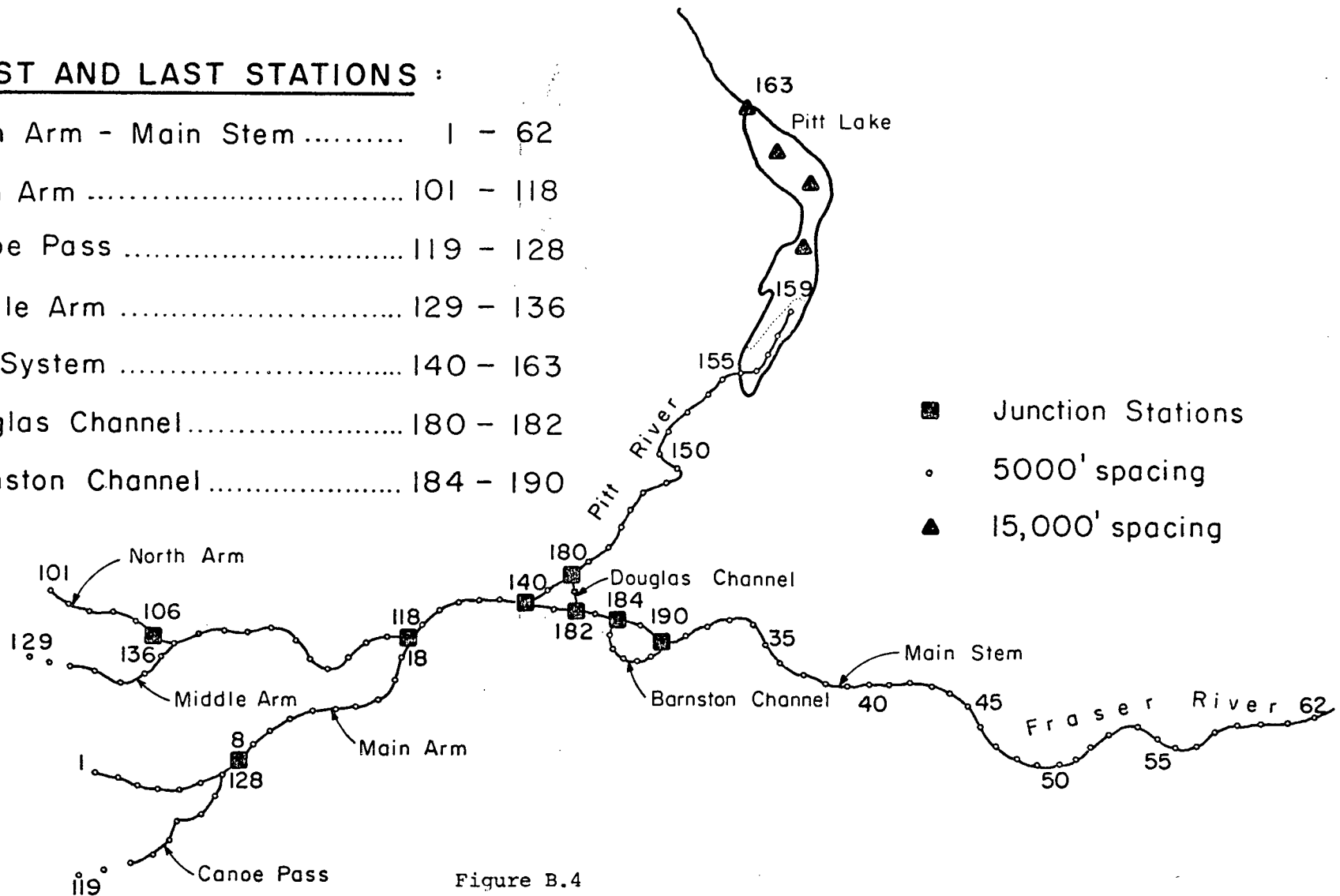
Figure B.4

Network of Stations Used in the Numerical Solution of the Hydrodynamic and Mass Transport Equations
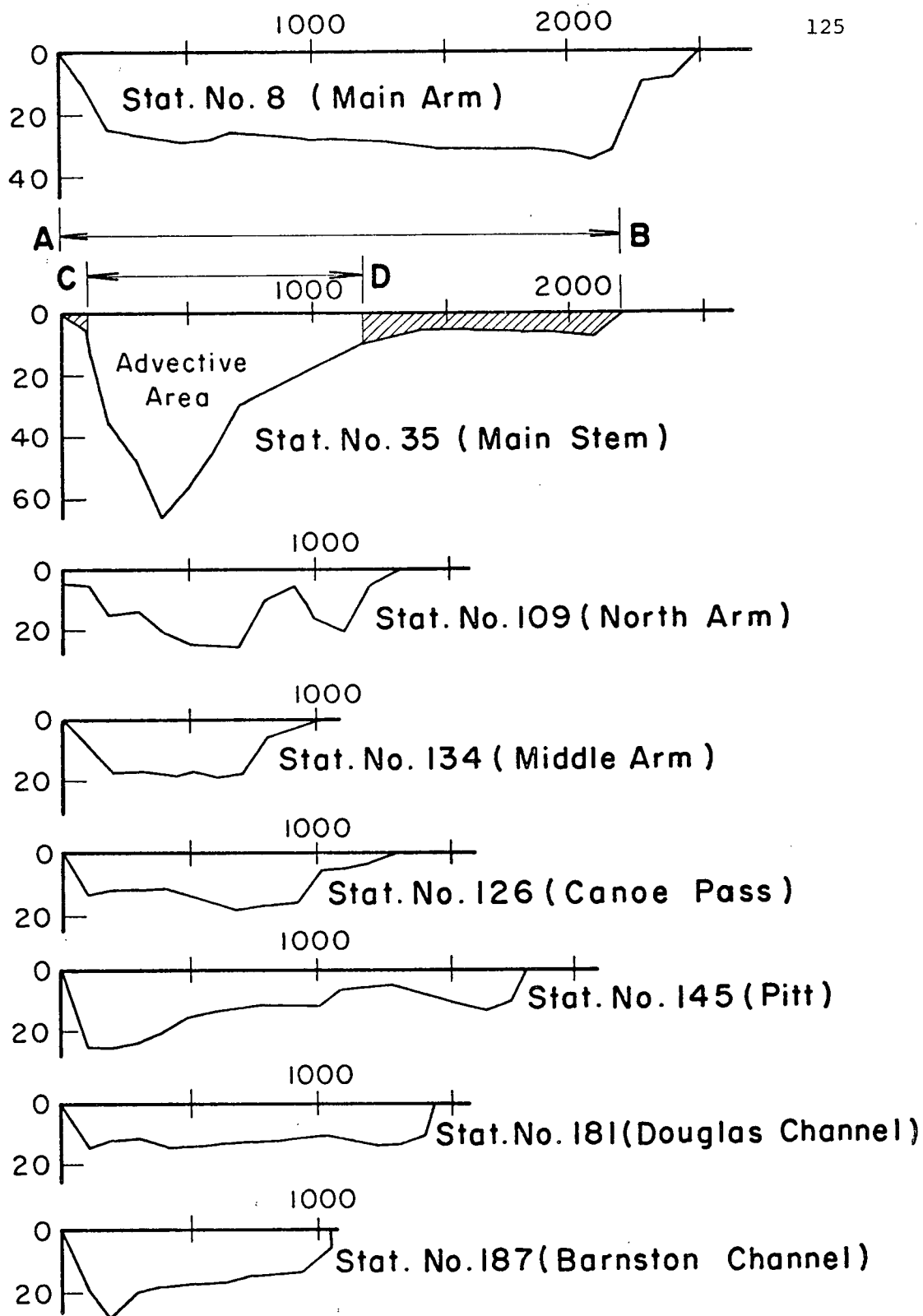
Figure B.5

Typical Channel Cross-Sections (Widths and Depths in Feet,
Depths Relative to Local Low Water)

DEPTHS AND AREAS Relative to local low water.
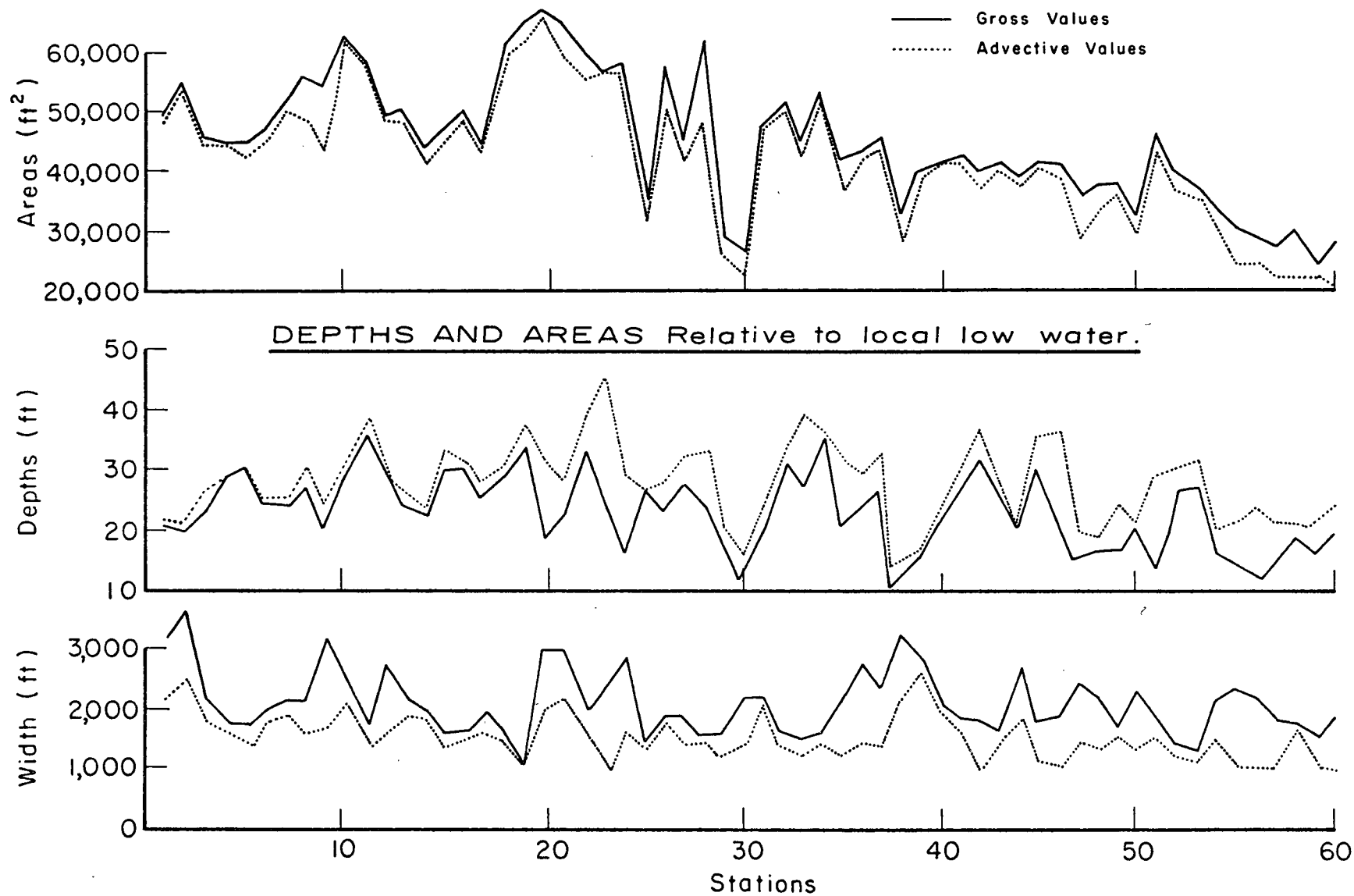
Figure B.6

Cross-Sectional Parameters of Main Arm - Main Stem

Figure B.7   Cross-Sectional Parameters of North Arm, Middle Arm and Canoe Pass

DEPTHS AND AREAS Relative to local low water.

Figure B.8   Cross-Sectional Parameters of Pitt River and Pitt Lake

B.2.2 <u>Tides in the Strait of Georgia</u>. The Strait of Georgia is tidal, being connected to the Pacific Ocean by the Juan de Fuca Strait (see Figure B.1). The tides are of the mixed type characteristic of much of the coast of Northwest America. The tidal range at Steveston for mean and large tides is respectively 10 feet and 15 feet and typical tides at Steveston are shown in Figure B.9.
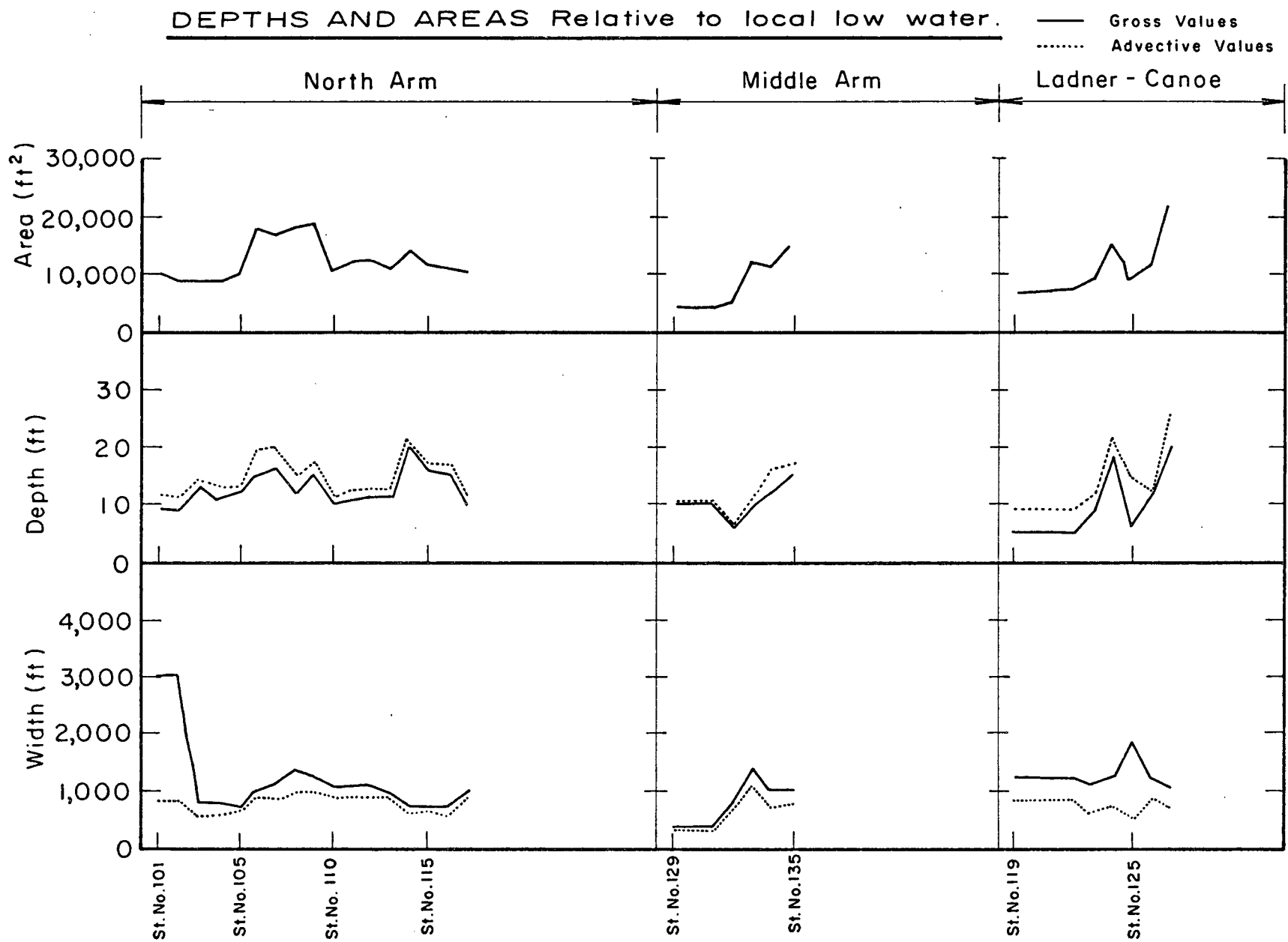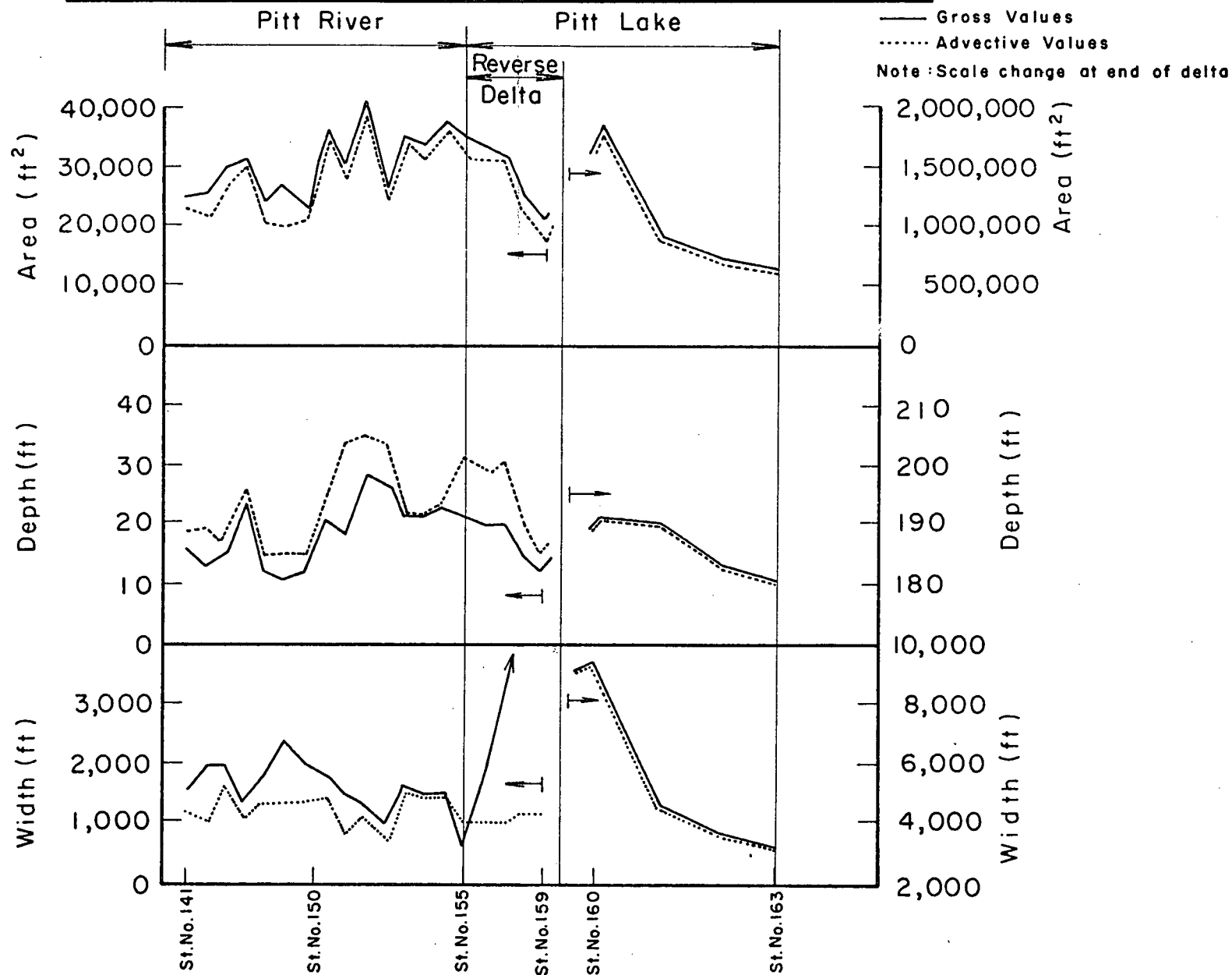
The effects of the tides on the flows in the Fraser system depends both on the tidal range at Steveston and the river discharge. This is illustrated in Figure B.10 [after Baines, 1953] which shows the local low and high tide envelopes of the Main Arm and Main Stem for discharges of 27,000 and 250,000 cubic feet per second at Hope. The greater influence of the tide during low flow conditions is readily apparent, and it is seen that the upstream limit of tidal influence is around Chilliwack, some 60 miles from Steveston. The section of the Fraser system from the Strait of Georgia to Chilliwack will be referred to as the Fraser River Estuary, although it is noted that the Fraser is more properly designated as a tidal river [Callaway, 1971].

During low flow-high tide conditions, flow reversal occurs in the Fraser Estuary. The cubature study of discharges by Baines [1952] predicted flow reversal at Mission, some 50 miles upstream of Steveston.

Downstream of Chilliwack there is a network of tide gauging stations, some equipped with continuous recorders and others only recording the maximum and minimum levels during each 24 hour period. The position and type of gauge at each station is shown in Figure B.11.

B.2.3 <u>River Discharges</u>. The variation of the mean monthly discharge at Hope, as calculated for the period 1912-1970, is shown in Figure B.12. The mean monthly flows vary from a summer maximum of 250,000 cfs during

January 15, 1964
River discharge 53,500 cfs
at Chilliwack
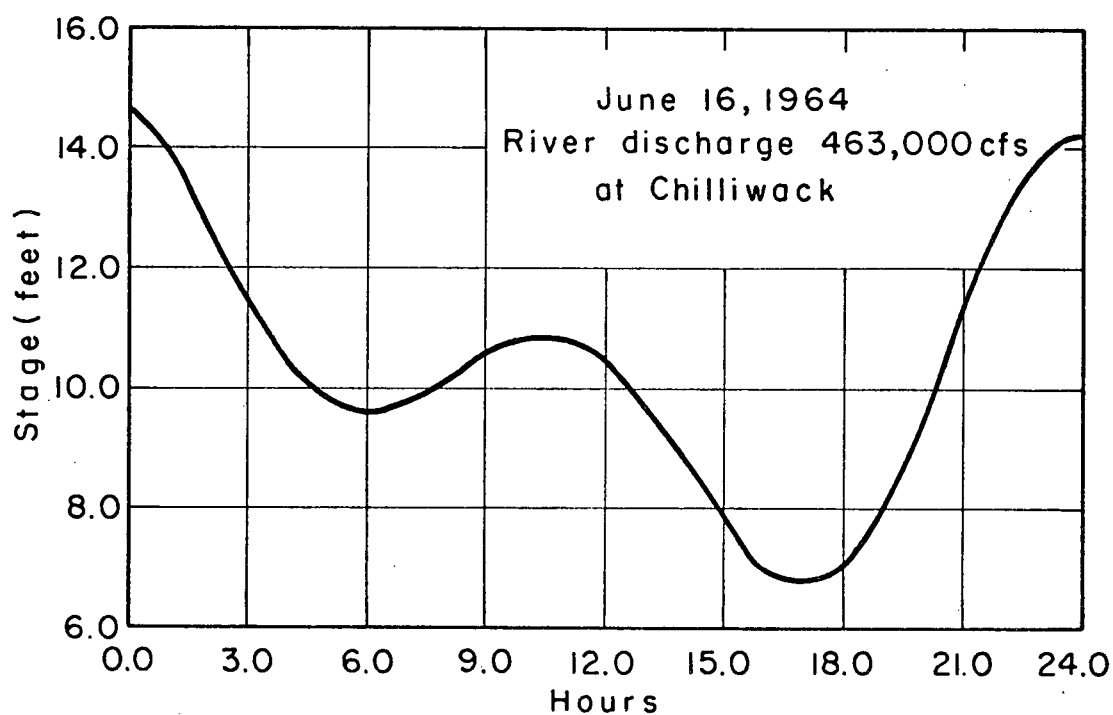
June 16, 1964
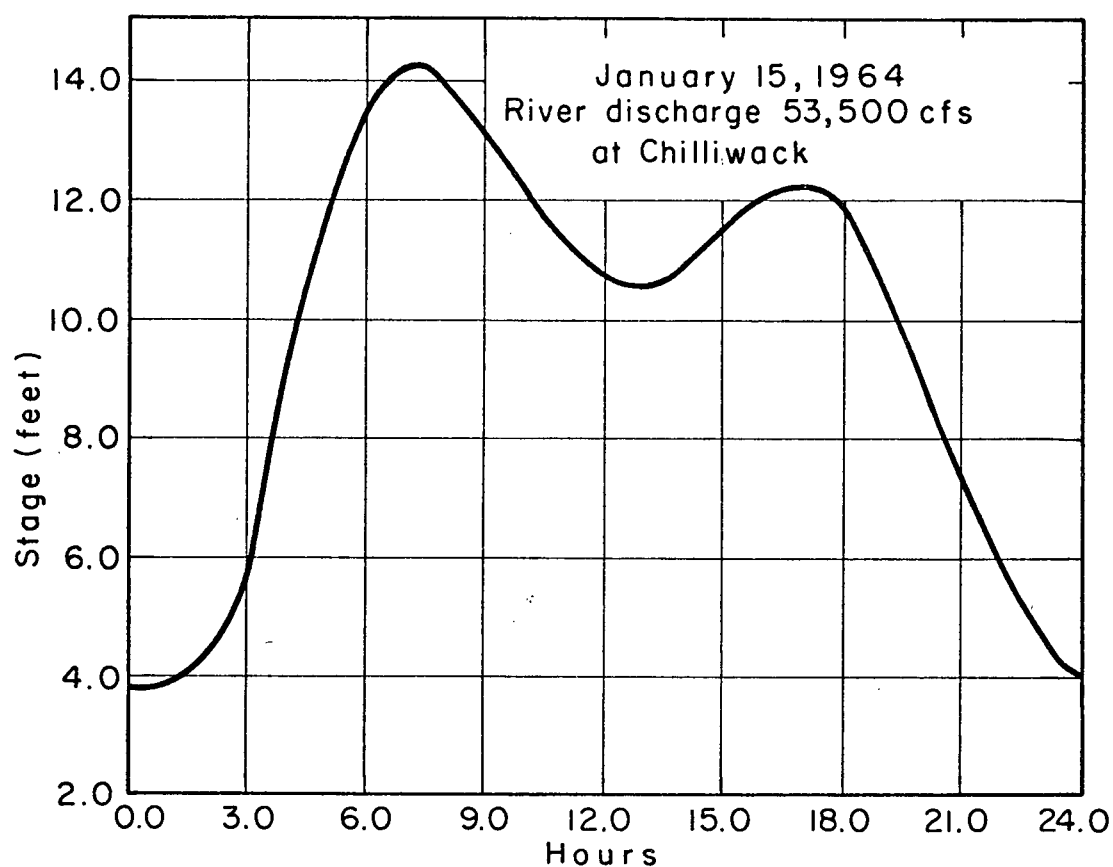River discharge 463,000 cfs
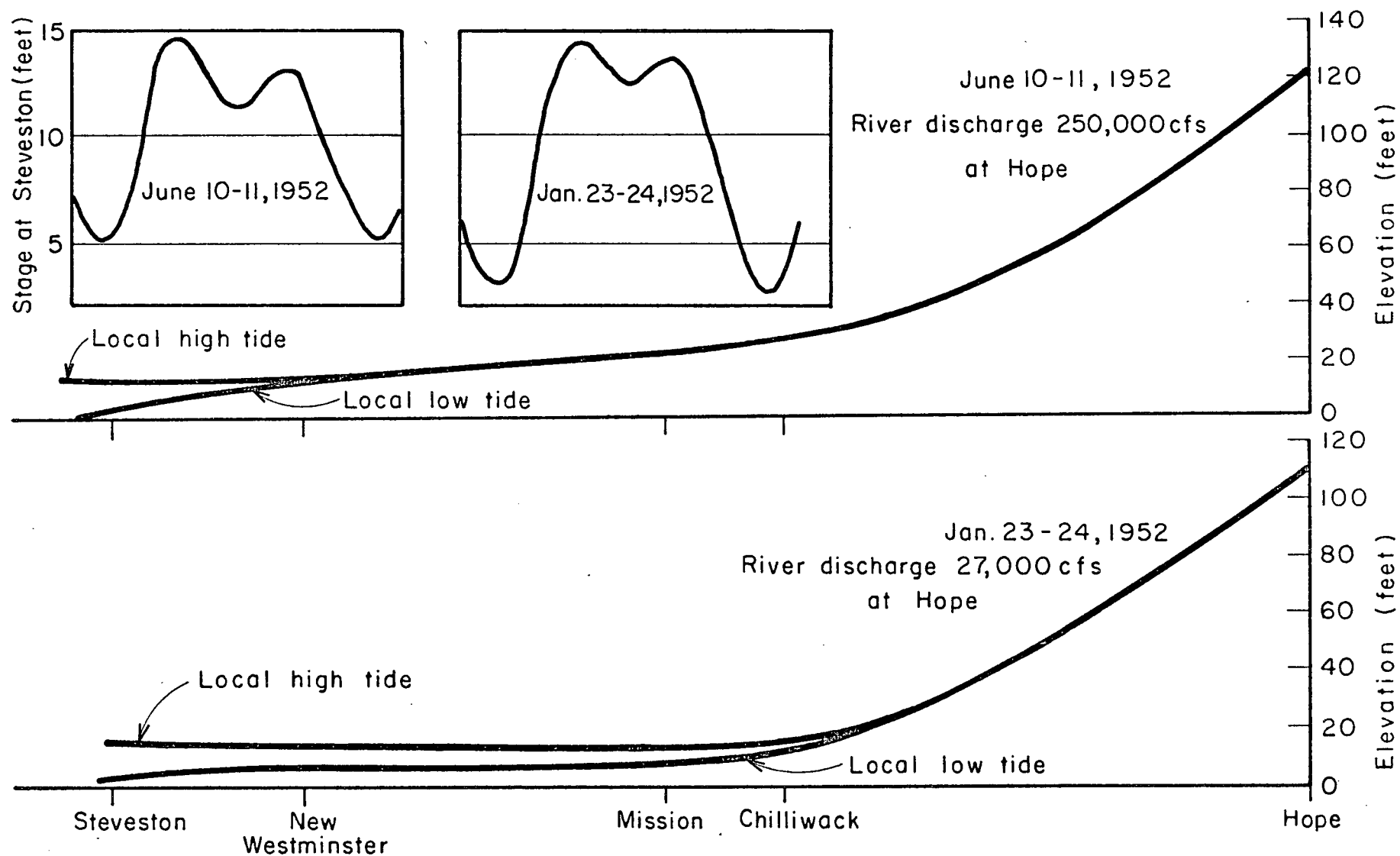at Chilliwack

Figure B.9

Typical Tides at Steveston

Figure B.10

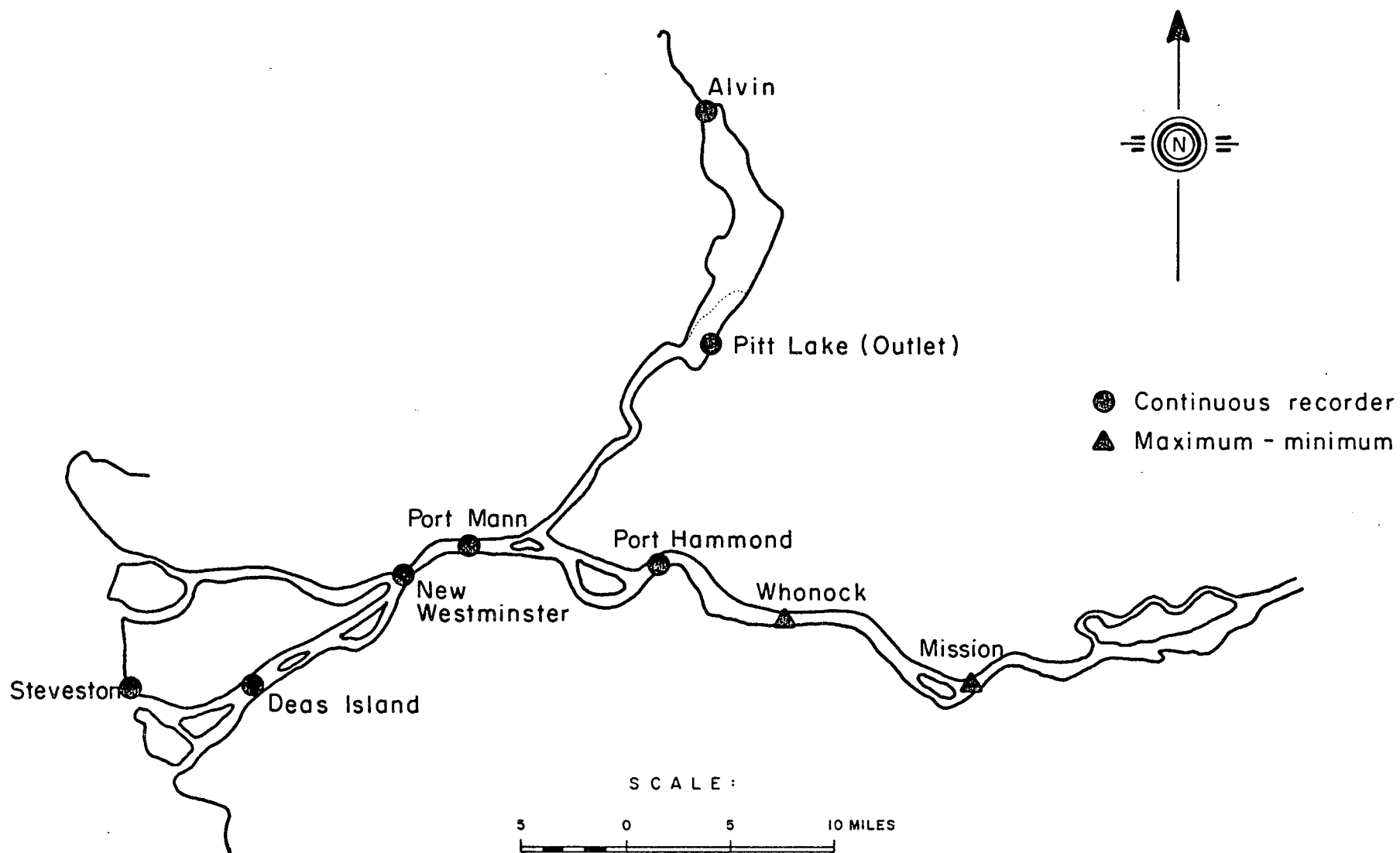Local Low and High Tide Envelopes [After Baines, 1953]

Figure B.11

Tide Gauging Stations in the Fraser River Estuary
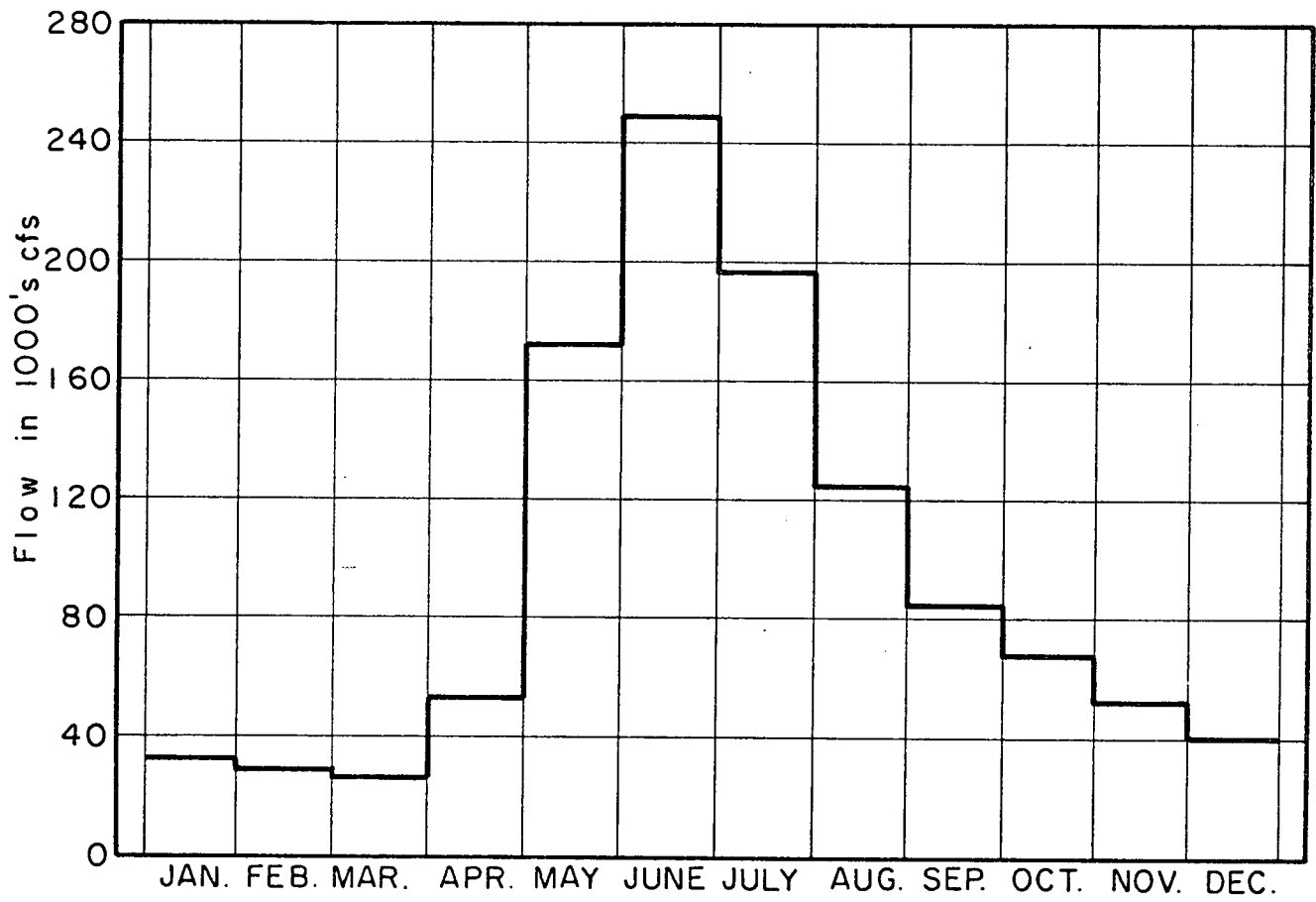
Figure B.12

Mean Monthly Flows at Hope (1912-1970 Inclusive)

freshet to a winter minimum of around 30,000 cfs. Recorded extremes at Hope
are 536,000 cfs on May 31, 1948 and 12,000 cfs on January 8, 1916.

The drainage area of the Fraser River below Hope is some 6,000
square miles, and between Hope and the Strait of Georgia various other rivers
flow into the Fraser system, the most important being the Harrison River
(see Figure B.2). The effect of this additional inflow is to increase the
flow at New Westminster by some 15 per cent over the flows at Hope during
the freshet, and up to 50 per cent during winter.

It should be apparent that the Fraser River Estuary is somewhat
unusual, being characterized by both high river discharges and large tidal
effects. This is illustrated by a calculation of the tidal prism and total
river discharge between the times of low-low-water and high-high-water for the
tidal cycles of January 11 and June 16, 1964. These tidal cycles and the
freshwater discharges are shown in Figure B.9. The volumes of the tidal
prisms and river flows are shown in Table B.1.

B.2.4 Saltwater Intrusion. The salinity of the Strait of Georgia
is essentially some 30 parts per thousand (ppt), and under low river discharge
conditions saltwater intrudes a considerable distance into the four channels
that emerge from the delta. The saltwater intrusion into the Main Arm is
illustrated in Figure B.13 [data from Waldichuk, *et al.*, 1968], which shows
the salinity profile at four stations along the Main Arm. (Note: the station
designation in Figure B.13 is that of Waldichuk, *et al.*, and should not be
confused with the station designation in Figure B.4). The position of the
stations, the tide at Steveston and the time of tide the observations were
taken are also shown. The four observations closely occur around the same
phase of tide and can be regarded as "simultaneous." The freshwater discharge

TABLE B.1

RIVER FLOW VOLUMES AND TIDAL PRISMS ON JANUARY 15 AND JUNE 16, 1964
(Volumes Calculated for Time Between Low-Low-Water and High-High-Water)

DATE	RIVER FLOW (cfs)	TIDAL RANGE (feet)	RIVER FLOW vol. (ft^3)	TIDAL PRISM (ft^3)	$\dfrac{\text{RIVER FLOW}}{\text{TIDAL PRISM}}$
JANUARY 15	53,500	10.4	12×10^8	66×10^8	0.18
JUNE 16	463,000	7.6	104×10^8	25×10^8	4.2
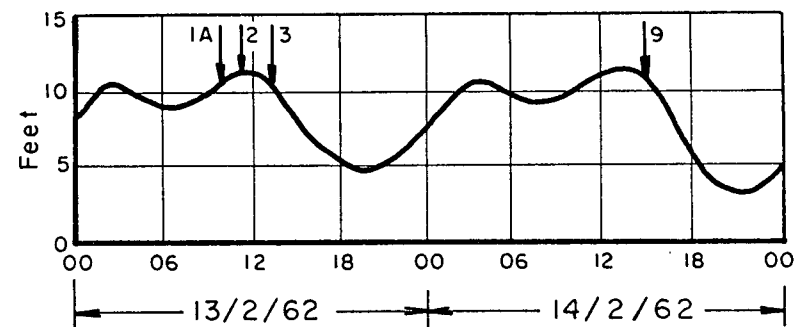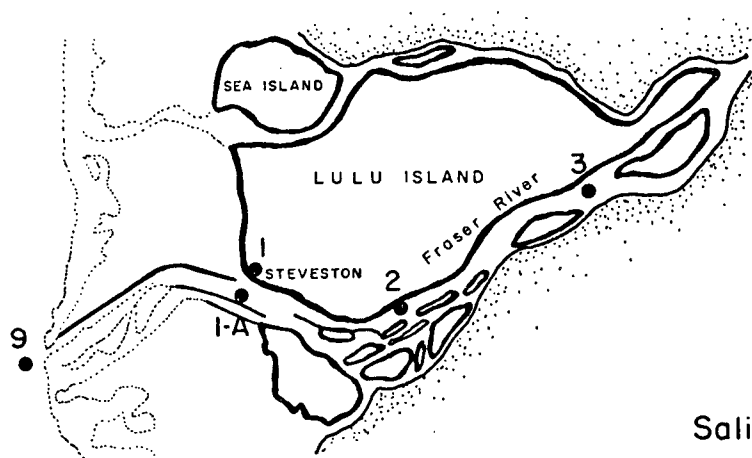
Salinities (parts per thousand)

All depths in feet
River Discharge – 57,600 cfs at Hope.
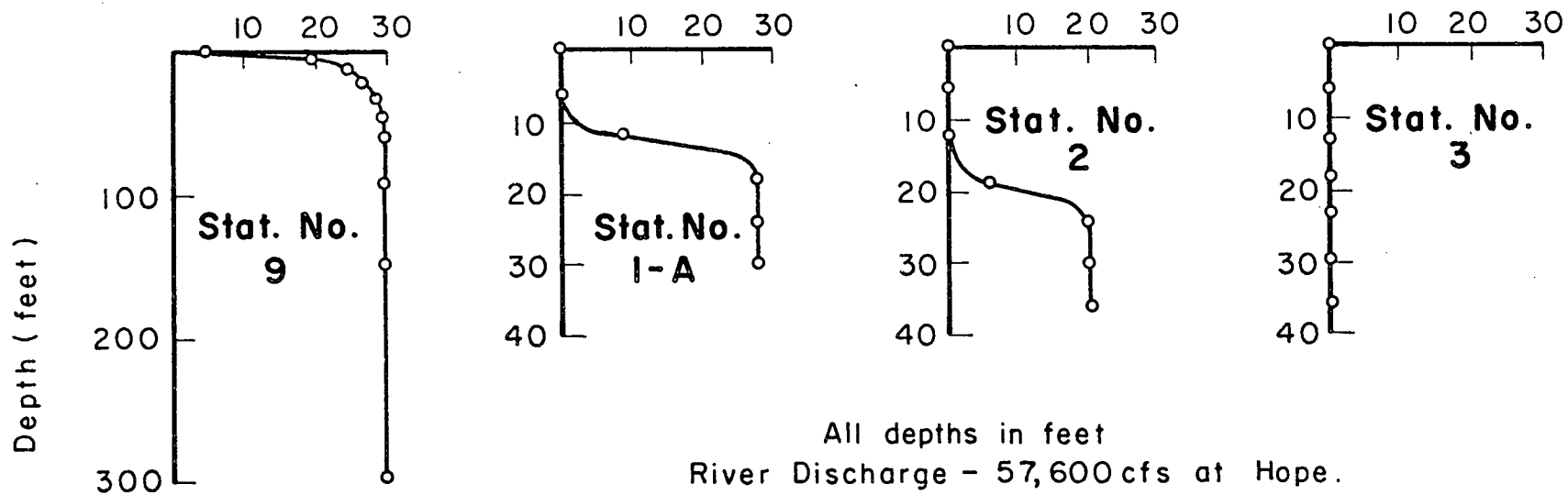
Figure B.13

Salinity Profiles in the Main Arm on February 13-14, 1962

at Hope is 57,000 cfs and it is apparent that under these freshwater dis-

charge and tidal conditions, the Main Arm is highly stratified with the toe

of the salt wedge somewhere between stations 2 and 3.

Recent studies have involved monitoring the salinity profile con-

tinuously at three stations along the Main Arm. This was done for the two

periods February 1 - 16 and March 16 - 30, 1973, during which the average

discharge at Hope was 30,000 cfs and 34,000 cfs respectively. It was found

that the effect of the tides was to move the wedge bodily up and down the

Main Arm [D. O. Hodgins, private communication], the maximum excursion of

the toe of the wedge probably being to somewhere around Annacis Island.

Thus, for low river flows, the Main Arm of the Fraser Estuary is

highly stratified with the salt wedge moving bodily up and down the estuary

under the influence of the tides. During times of flow reversal, the

wedge may move as far upstream as Annacis Island but during seaward discharge

it is washed downstream past Steveston. For high river flows, the wedge prob-

ably does not penetrate past Steveston, if that far. Saltwater intrudes into

the other channels of the delta, and similar situations probably occur there,

although the saltwater movement may be modified by the slower velocities through

these channels. Salinity profiles in these other channels show them to be

typically stratified, but perhaps not quite as stratified as the Main Arm

(probably due to the lower discharge velocities through these channels).

APPENDIX C

NUMERICAL DISPERSION AND STABILITY

The dependent variable of a partial differential equation de-
fines a surface over the plane of the independent variables. In the plane
of the independent variables there are various curves, or "characteristics"
that describe the propagation of information through the system that the
partial differential equation represents. The one-dimensional forms of the
advective transport equation, the dispersive transport equation and the
hydrodynamic equations are of interest to this thesis. The forms of their
respective surfaces are briefly described and the equations of their respec-
tive characteristics are given. In fixed grid finite difference schemes,
the problem of numerical dispersion arises from solving the one-dimensional
advective transport equation (or the one-dimensional mass transport equation)
relative to a fixed space grid, rather than along the advective characteris-
tics. In explicit finite difference schemes, the problem of stability also
arises from solving the above three equations relative to a fixed grid rather
than along their respective characteristics.

C.1 SURFACE GEOMETRY OF PARTIAL DIFFERENTIAL EQUATIONS

The following partial differential equations are of interest

$$\frac{\partial \bar{c}}{\partial t} = -\bar{u}\frac{\partial \bar{c}}{\partial x} \tag{C.1}$$

$$\frac{\partial \bar{c}}{\partial t} = \frac{1}{A}\frac{\partial}{\partial x}\{EA\frac{\partial \bar{c}}{\partial x}\} \tag{C.2}$$

138

$$\frac{\partial \bar{u}}{\partial t} = -\bar{u}\frac{\partial \bar{u}}{\partial x} - g\frac{\partial \bar{y}}{\partial x} - g\frac{\partial \bar{a}}{\partial x} - g\frac{|\bar{u}|\bar{u}}{c^2\,\bar{y}}$$

$$\frac{\partial \bar{y}}{\partial t} = -\bar{y}\frac{\partial \bar{u}}{\partial x} - \bar{u}\frac{\partial \bar{y}}{\partial x} - \frac{\bar{u}\bar{y}}{b}\frac{\partial b}{\partial x} \tag{C.3}$$

Equation (C.1) describes one-dimensional advective transport and Equation (C.2) one-dimensional dispersive transport. These two equations represent the component transport processes of the one-dimensional mass transport equation, and the sum of their effects is the one-dimensional mass transport equation without the source-sink terms. The two coupled equations (C.3) are the hydrodynamic equations and are used to predict the temporal variations in the parameters $\bar{u}$ and A of the tidally varying mass transport equation. [Equations (C.3) are obtained by substituting Equation (3.3) and A = $b\bar{y}$ into Equations (3.1) and (3.2)].

Equations (C.1) and (C.2) define surfaces $\bar{c}(x,t)$ over the (x,t) plane and Equations (C.3) define a pair of coupled surfaces $\bar{u}(x,t)$ and $\bar{y}(x,t)$ over the (x,t) plane. Consider now the form of the surface defined by the advective transport Equation (C.1). Figure C.1 shows the shape of this surface for a slug input into (a) steady uniform flow; (b) steady non-uniform flow along a river of contracting cross-section; and (c) the mixture of steady and oscillatory flow characteristic of an estuary (estuary flow). These surfaces are solutions to Equation (C.1) for a slug input into the various types of flow. It is apparent from Figure C.1 that there are various curves in the (x,t) plane that result in a considerable simplification of Equation (C.1) -- the concentration is constant along each of the curves AB of Figure C.1 while everywhere else in the plane it is zero.

For any continuous, smoothly varying surface $\bar{c}(x,t)$, the time rate of change of $\bar{c}(x,t)$ along the vertical plane defined by the curve
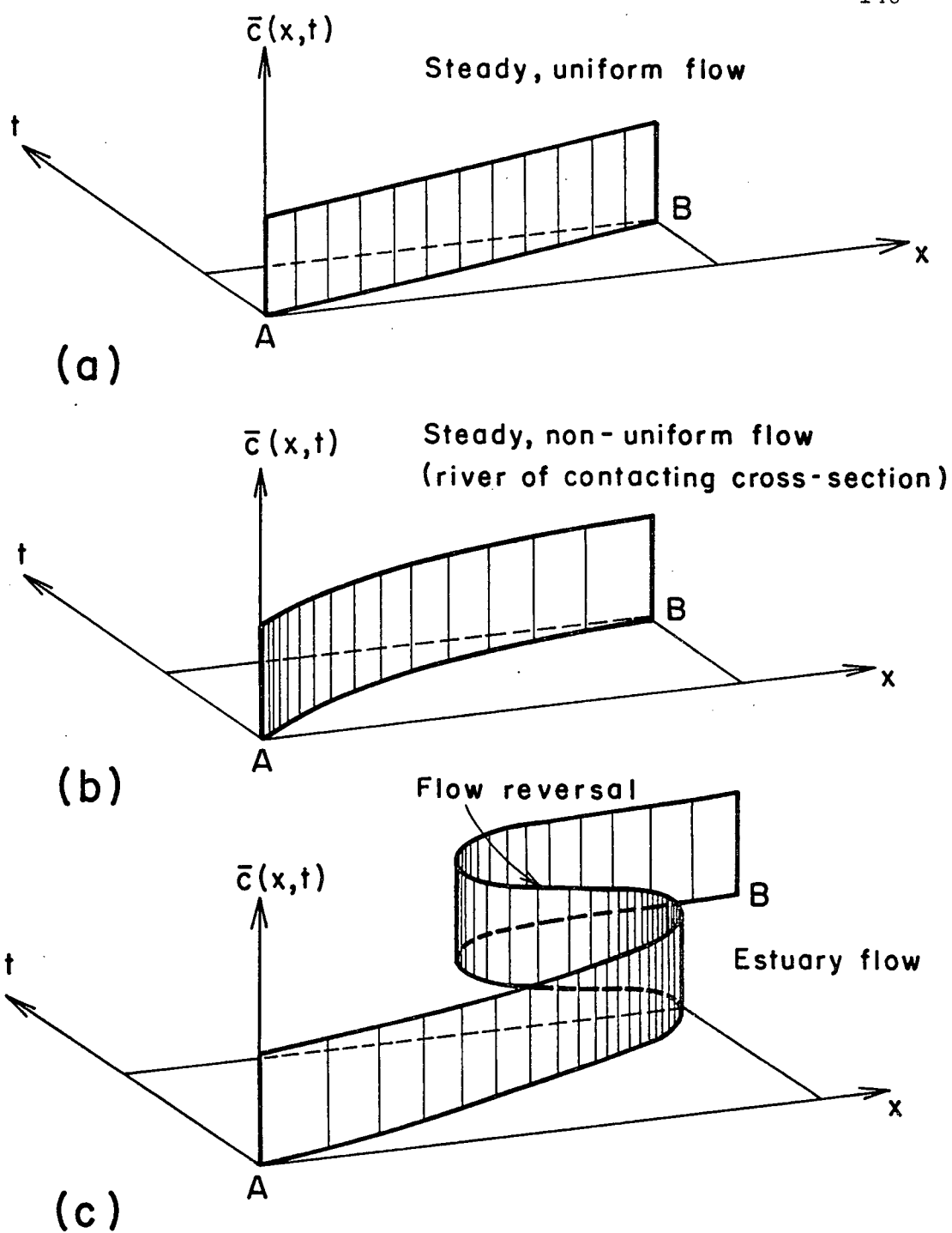
Figure C.1

Concentration Surfaces for the Advection of a Slug Load

$$\frac{dx}{dt} = f(x,t) \tag{C.4}$$

in the (x,t) plane is given by

$$\frac{d\bar{c}}{dt} = \frac{\partial \bar{c}}{\partial t} + \frac{\partial \bar{c}}{\partial x} \frac{dx}{dt} \tag{C.5}$$

The graphical interpretation of this elementary formula of calculus is illustrated in Figure C.2. Substituting Equation (C.1) into (C.5) gives

$$\frac{d\bar{c}}{dt} = \{-\bar{u} + \frac{dx}{dt}\} \frac{\partial \bar{c}}{\partial x} \tag{C.6}$$

and along the curve defined by

$$\frac{dx}{dt} = \bar{u} \tag{C.7}$$

the time rate of change of concentration is given by

$$\frac{d\bar{c}}{dt} = 0 \tag{C.8}$$

Equations (C.7) and (C.8) are the well-known Langrangian form of the advective transport equation and curve (C.7) obviously defines the three curves AB of Figure C.1. In deriving Equation (C.1) it is assumed that the variation of $\bar{c}$ and $\bar{u}$ with x and t is continuous. For the cases shown in Figure C.1, the variation of c is discontinuous and the partial derivatives $\partial \bar{c}/\partial t$ and $\partial \bar{c}/\partial x$ are not defined everywhere in the (x,t) plane. Thus, Equation (C.1) does not correctly represent the advection of a slug load (this is the fundamental reason for numerical dispersion). It is only when the solution to Equation (C.1) is examined along the curve (C.7) that the problem of the non-definition of the partial derivatives is avoided. [See Equation (C.6)].
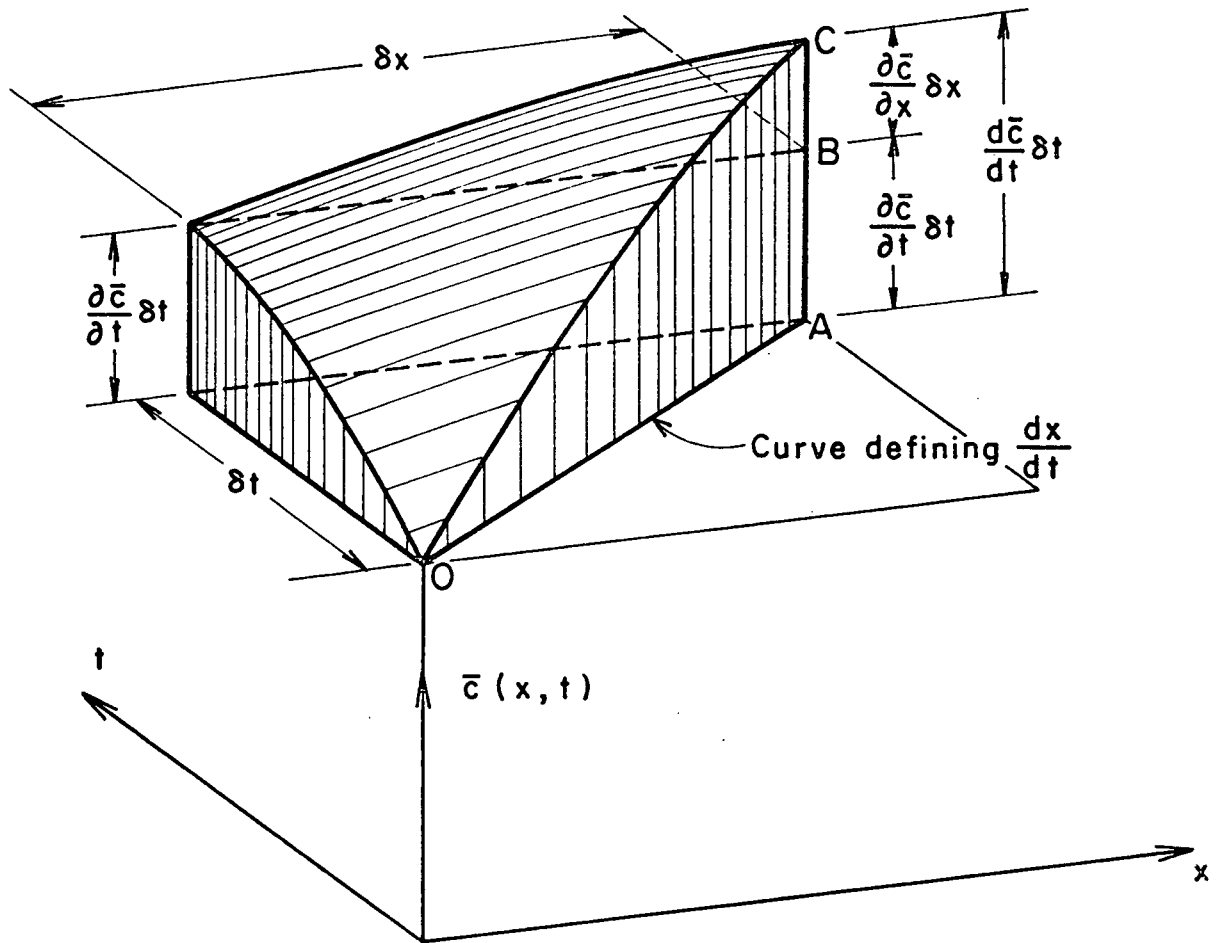
$$AC = AB + BC$$

$$\therefore \frac{d\bar{c}}{dt}\,\delta t = \frac{\partial \bar{c}}{\partial t}\,\delta t + \frac{\partial \bar{c}}{\partial x}\,\delta x$$

$$\therefore \frac{d\bar{c}}{dt} = \frac{\partial \bar{c}}{\partial t} + \frac{\partial \bar{c}}{\partial x}\,\frac{dx}{dt}$$

Figure C.2

Time Rate of Change of Concentration
Along A Curve in the (x,t) Plane

Consider disturbing the system represented by Equation (C.1) by introducing an elemental slug load of $\Delta \bar{c}$. This disturbance, or "information," will propagate through the system according to Equation (C.7). Thus, Equation (C.7) is of direct physical significance, and along this curve the solution to the advective transport equation reduces to the simple form of Equation (C.8). The fixed (Eulerian) space grid used to derive Equation (C.1) "masks" the underlying physics of the transport process and the simplicity of the solution.

Now consider the equation of dispersive transport (C.2). If both E and A are constant in x and t, Equation (C.2) reduces to

$$\frac{\partial \bar{c}}{\partial t} = E \frac{\partial^2 \bar{c}}{\partial x^2} \tag{C.9}$$

The surface defined by Equation (C.9) for the dispersion of a slug load is shown in Figure C.3. The equation of this surface is [Fischer, 1966a]

$$\bar{c}(x,t) = \frac{M}{4\Pi E_t} \exp\{-\frac{x^2}{4E_t}\} \tag{C.10}$$

where M is the mass per unit area of tracer released. At any time t' the shape of the surface is a Gaussian distribution and $\bar{c}(x,t')$ is uniquely defined by the location of the point of standard deviation. This is illustrated in Figure C.3. Thus, the locus of the standard deviation in the (x,t) plane directly describes the underlying mass transport process. From Equation (C.10) the locus of the standard deviation is the parabola

$$x^2 = 2E_t \tag{C.11}$$

or in the form of Equation (C.4)

$$\frac{dx}{dt} = \frac{E}{x} \tag{C.12}$$
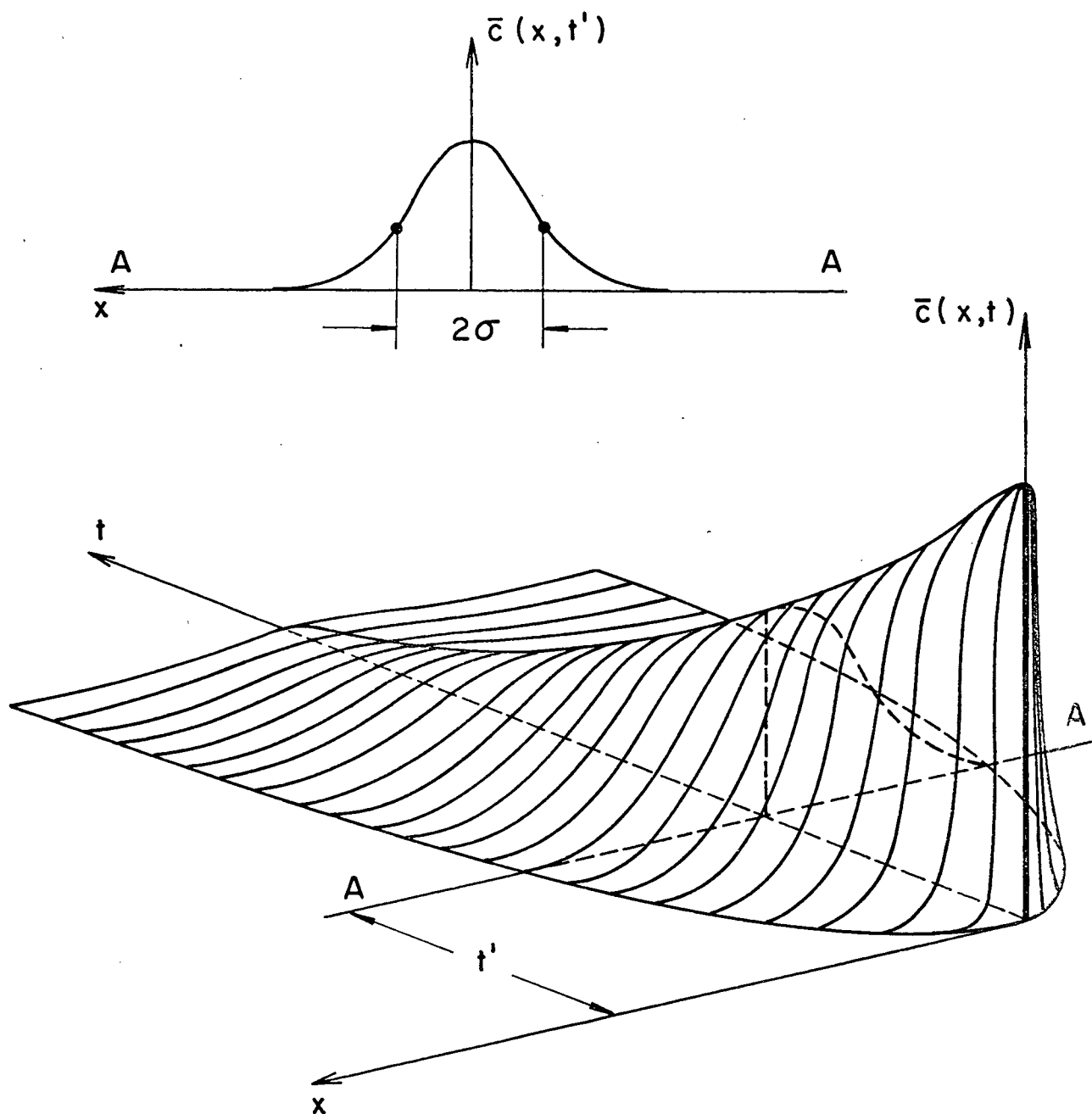
Figure C.3

Dispersion of A Slug Load

If this system is disturbed by introducing an elemental slug load of $\Delta\bar{c}$, the effect of this slug load, or its "information", will propagate through the system according to Equation (C.11) or (C.12). Once again, the curve (C.12) is of fundamental significance and along this curve the concentration is given by

$$\bar{c}(x,t) = \frac{M}{\sqrt{2\Pi e}} \left|\frac{1}{x}\right| \qquad (C.13)$$

Finally, consider the hydrodynamic Equations (C.3). The well-known characteristics of this system are given by [Courant and Hilbert, 1962]

$$\frac{dx}{dt} = u \pm \sqrt{gy} \qquad (C.14)$$

If this system is disturbed by introducing a small change in the water surface elevation $\Delta\bar{y}$, this "information" will propagate through the system according to Equation (C.14) and along this curve Equations (C.3) reduce to [Henderson, 1966]

$$\frac{d}{dt}\{\bar{u} \pm 2\sqrt{gy}\} = -g\frac{\partial h}{\partial x} + \frac{|\bar{u}|\bar{u}}{c^2\bar{y}} \qquad (C.15)$$

In summary, there are certain curves in the (x,t) plane that directly describe the propagation of information through the systems that Equations (C.1), (C.2) and (C.3) represent. These curves can be called *characteristics of information propagation*, and along these curves the solutions to the respective equations are greatly simplified. This underlying simplicity is masked by the Eulerian nature of the derivation of the equations. The problems of numerical

dispersion and stability arise directly from viewing the numerical solutions to Equations (C.1) to (C.3) from a fixed Eulerian space grid, rather than from a space grid along the characteristics.

C.2 NUMERICAL DISPERSION

Before discussing numerical dispersion in detail, it is necessary to briefly consider a few fundamentals of finite difference solutions to partial differential equations. In using finite difference methods to solve differential equations, derivatives are approximated by finite difference expressions and the differential equation is reduced to a difference equation. The justification of replacing the derivatives by difference expressions can be illustrated by the Taylor's Series expansion of the variable $U(x,t)$ with respect to t in the neighborhood of the point $(x = j\Delta x, \ t = n\Delta t)$. This can be written as

$$\frac{U_j^{n+1} - U_j^n}{\Delta t} - \left(\frac{\partial U}{\partial t}\right)_j^n = \tfrac{1}{2}\Delta t \left(\frac{\partial^2 U}{\partial t^2}\right)_j^{n+\theta} \tag{C.16}$$

where the partial derivatives are assumed continuous and $0 < \theta < 1$ [Richtmyer and Morton, 1967, p. 19]. By making Δt small enough, the difference expression of Equation (C.16) can be made to approximate the derivative to any desired degree of accuracy. The term on the right-hand side of Equation (C.16) is the *truncation error* that results when the derivative $\partial U/\partial t$ is replaced by the difference expression of Equation (C.16).

When a partial differential equation in x and t is approximated by a partial difference equation, the truncation error consists of terms containing

Δx and Δt raised to various powers. The conditions under which the truncation error tends to zero is the problem of *convergence*. That is, as the mesh is refined (Δx, $\Delta t \rightarrow 0$), does the numerical solution converge to the true solution of the partial differential equation? The behaviour of the truncation error as the solution progresses through time is the problem of *stability*. If the difference scheme is unstable, errors generated during the solution (for example, round-off errors) may become so magnified during the calculations as to make the final results meaningless.

There are many fixed mesh difference schemes for approximating the derivatives of partial differential equations, but essentially they can be classified into explicit and implicit schemes. An *explicit* scheme uses forward time differences (see Figure C.4), and each difference equation contains only one unknown variable which can be solved for explicitly. *Implicit* schemes use backward time differences (see Figure C.4) and each difference equation contains several unknown variables. To obtain a solution at any time step, the resulting system of simultaneous equations must be solved over the entire space grid. Generally, implicit schemes are unconditionally stable, whereas explicit schemes are at most conditionally stable. This is discussed further in Section C.3.

Consider now the numerical solution of the one-dimensional mass transport equation (C.1). This equation is a component of the one-dimensional mass transport equation. Fixed mesh finite difference schemes generally do not simulate the advective transport process correctly, and result in an additional dispersive process being superimposed on the actual advective and dispersive processes occurring in the river or estuary. This so-called *numerical dispersion* can be illustrated by considering the truncation error associated with

Forward Time Differences :

$$U_j^{n+1} = \text{function} \left\{ U_{j-1}^n, U_j^n, U_{j+1}^n \right\}$$

time = $(n+1)\Delta t$

time = $n\Delta t$

$(j-1)\Delta x$ $j\Delta x$ $(j+1)\Delta x$
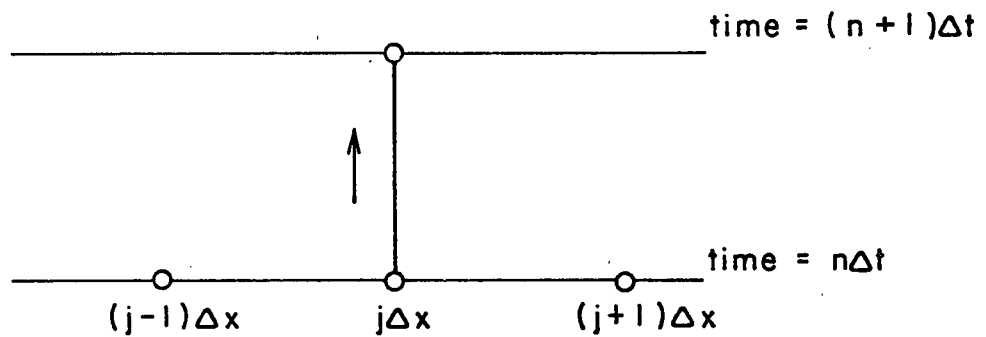
Backward Time Differences :

$$U_j^{n+1} = \text{function} \left\{ U_j^n, U_{j+1}^{n+1}, U_{j-1}^{n+1} \right\}$$

$(j-1)\Delta x$ $j\Delta x$ $(j+1)\Delta x$ time = $(n+1)\Delta t$

time = $n\Delta t$
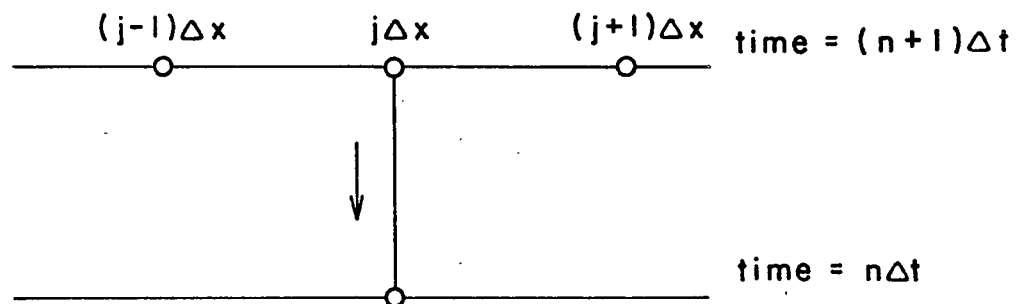
Figure C.4

Forward and Backward Time Differences

replacing the partial differential equation of advective transport (C.1) with its corresponding explicit difference equation

$$\frac{C_j^{n+1} - C_j^n}{\Delta t} + U[\frac{(1-\alpha)(C_j^n - C_{j-1}^n) + \alpha(C_{j+1}^n - C_j^n)}{\Delta x}] = 0 \qquad (C.17)$$

where the flow is assumed to be uniform and steady, $x = j\Delta x$, $t = n\Delta t$ and α is a weighting factor such that $\alpha = 0$ for upstream differences, $\alpha = 1/2$ for central differences and $\alpha = 1$ for downstream differences. These various differences are illustrated in Figure C.5. Equation (C.17) is an example of an explicit difference scheme that uses forward time differences (the concentrations at time step n are used to determine the concentrations at time step n+1). A Taylor's Series expansion of the derivatives of Equation (C.1) shows that the difference equation (C.17) approximates the differential equation

$$(\frac{\partial C}{\partial t})_j^n + U(\frac{\partial C}{\partial x})_j^n = \tfrac{1}{2}U\Delta x(1-2\alpha)(\frac{\partial^2 C}{\partial x^2})_j^n - \tfrac{1}{2}\Delta t(\frac{\partial^2 C}{\partial t^2})_j^n + O(\Delta x)^2 + O(\Delta t)^2 + \ldots \qquad (C.18)$$

the terms on the right-hand side being the truncation error. As C is a solution of Equation (C.1) it also satisfies

$$\frac{\partial^2 C}{\partial t^2} - U^2 \frac{\partial^2 C}{\partial x^2} = 0 \qquad (C.19)$$

Substituting Equation (C.19) into (C.18) and neglecting terms of order $(\Delta x)^2$. $(\Delta t)^2$ and higher, it is found that the difference equation approximates the differential equation

$$\frac{\partial C}{\partial t} = -U\frac{\partial C}{\partial x} + E_p \frac{\partial^2 C}{\partial x^2} \qquad (C.20)$$

Upstream Differences :

$$\frac{\partial c}{\partial t}\Big]_{j\Delta x} \approx \frac{c_j - c_{j-1}}{\Delta x}$$

Central Differences :

$$\frac{\partial c}{\partial t}\Big]_{j\Delta x} \approx \frac{1}{2}\left\{\frac{c_j - c_{j-1}}{\Delta x} + \frac{c_{j+1} - c_j}{\Delta x}\right\}$$

Downstream Differences :

$$\frac{\partial c}{\partial t}\Big]_{j\Delta x} \approx \frac{c_{j+1} - c_j}{\Delta x}$$
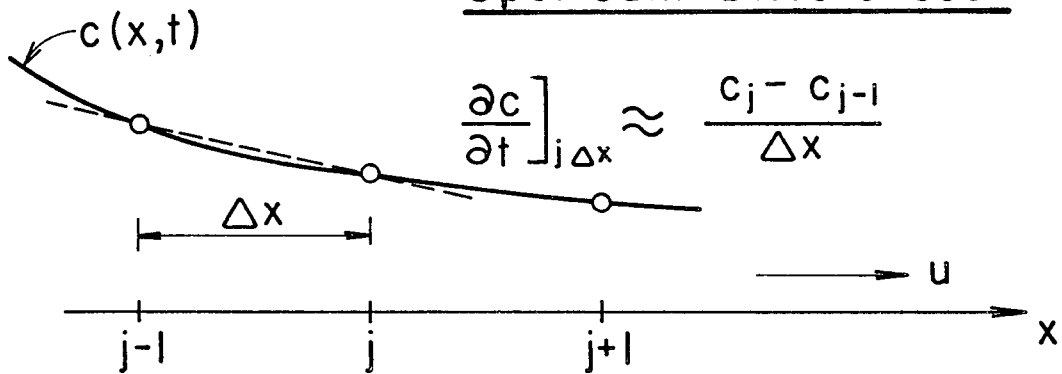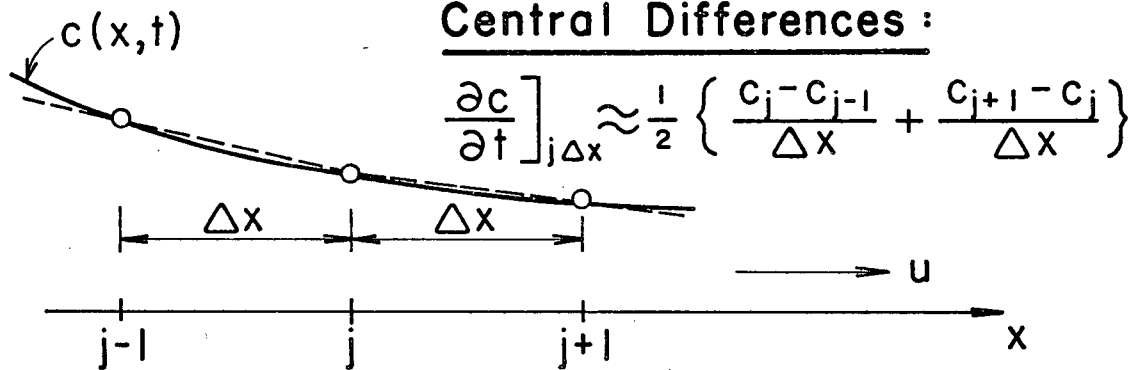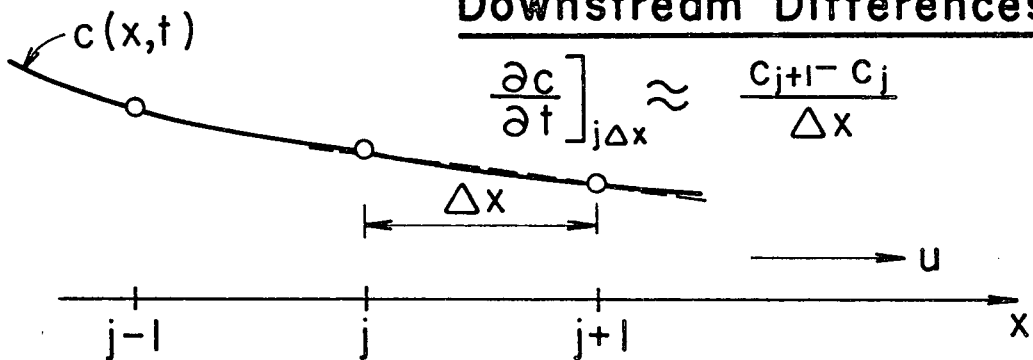
Figure C.5

Upstream, Central and Downstream Space Differences

where E_p can be considered to be a coefficient of pseudo or numerical dispersion, and is given by

$$E_p = \tfrac{1}{2}U\Delta x\{(1-2\alpha) - \frac{U\Delta t}{\Delta x}\}$$ (C.21)

Thus, the solution to the difference equation (C.17) approximates the solution to an advective-dispersive equation rather than the correct advective equation. As $\Delta x \rightarrow 0$, $E_p \rightarrow 0$ and the mass transport associated with the numerical dispersion becomes increasingly smaller. However, in difference schemes Δx is always finite, and while the solution to difference equation converges to the solution of the correct advective equation in the limit ($\Delta x = 0$), it converges to the solution of an advective-dispersive equation at the level of application ($\Delta x \neq 0$).

It is apparent from Equations (C.20) and (C.21) that numerical dispersion will always occur unless either

$$U \cdot \frac{\Delta t}{\Delta x} = 1 - 2\alpha$$ (C.22)

or

$$\frac{\partial^2 C}{\partial x^2} = 0$$

Ignoring the trivial latter case (the mass transport associated with any real dispersion is also zero), it is seen that numerical dispersion does not occur when upstream differences are used ($\alpha = 0$) and Δx and Δt are defined by

$$\frac{\Delta x}{\Delta t} = U$$ (C.23)

as was recognized by Bella and Dobbins [1968]. Under these conditions Equation (C.17) reduces to

$$C_j^{n+1} = C_{j-1}^n = \text{constant} \tag{C.24}$$

Equations (C.23) and (C.24) are simply the finite difference versions of Equations (C.7) and (C.8). Thus, the use of upstream differences with the grid spacing defined by Equation (C.23) is equivalent to solving Equation (C.17) along the characteristic curve in the (x,t) plane. Under these conditions the underlying advective mass transport process is correctly simulated and there is no numerical dispersion.

Consider now using central differences ($\alpha = 1/2$) to solve Equation (C.17). From Equation (C.22) it is seen that numerical dispersion will always occur except in the trivial case of $U = 0$. According to Leendertse [1971b] there is no numerical dispersion when central differences are used. He apparently assumes that central differences correctly describe the advection process, and then uses this incorrect assumption to demonstrate that numerical dispersion will occur when upstream or downstream differences are used.

The use of downstream differences ($\alpha = 1$) will always result in numerical dispersion except when

$$\frac{\Delta x}{\Delta t} = -U \tag{C.25}$$

The use of downstream differences with Equation (C.25) defining the grid spacing can be interpreted as an attempt to determine upstream conditions from those downstream by working backwards through time (hence the negative sign) along the characteristic curve in the (x,t) plane. Although this procedure is impractical, it would correctly determine the preceeding concentration distributions

with no numerical dispersion if the final concentration distribution was known.

Bella and Grenney [1970] investigated the numerical dispersion resulting from the advection of a slug load by various fixed mesh finite differences schemes. They found that the coefficient of numerical dispersion was as given by Equation (C.21) and that no numerical dispersion occurred when upstream differences were used with Equation (C.23) defining the grid spacing. Numerical dispersion always occurred with central or downstream differences. Fox [1971] made a Fourier series analysis of the difference schemes of Bella and Grenney and showed that the effect of discretization was to introduce amplitude and phase errors into the solution of the difference equations. His results demonstrate that neither amplitude nor phase errors occur when upstream differences are used with a grid spacing according to Equation (C.23).

In conclusion, numerical dispersion occurs because fixed mesh finite difference schemes do not correctly simulate the advective transport process. (Although numerical dispersion has only been demonstrated for explicit difference schemes, it also occurs in implicit difference schemes). The truncation error of the simple difference schemes discussed here corresponds to an actual physical mode of mass transport and will modify the advective transport and any dispersive transport that is occurring in a river or estuary. To correctly simulate the advective transport process, it is necessary to solve the advective mass transport equation along the characteristic curve in the (x,t) plane. The magnitude of the numerical dispersion depends directly on the magnitude of $\partial^2 c/\partial x^2$, and so is greatest for a slug load and less for a continuous release. A continuous release can be treated as a succession of

slug loads, and apparently the numerical dispersion due to any particular slug is compensated by the numerical dispersion of neighbouring slugs, as has been noted by Bella and Grenney [1970]. In deriving Equation (C.1) and writing the difference equation (C.17), it is implicitly assumed that $c(x,t)$ varies in a continuous manner with x and t. This is certainly not the case for a slug load, as is seen in Figure C.1. It is only along the characteristic curve that $c(x,t)$ varies continuously, as is also apparent from Figure C.1. Thus, in using Equation (C.17) to advect a slug load, there is the added problem that the partial derivatives $\partial c/\partial t$ and $\partial c/\partial x$ are not defined, and the numerical dispersion can be interpreted as an attempt to define them.

Numerical dispersion can be eliminated by solving the equation advective-dispersive mass transport along the characteristics of advective information propagation. Such a numerical solution is referred to as a characteristic method in Section 2.2, where the problem of the bookkeeping of solution results is discussed. Numerical dispersion can be controlled by the use of more sophisticated differencing schemes [see Fox, 1970], or by reducing the actual dispersion coefficients by E_p according to Equation (C.21). Numerical dispersion is apparently reduced in finite element solutions [Price *et al.*, 1968; Fox, 1970], but because of the fixed grid nature of finite element solutions, the numerical dispersion is probably not totally eliminated.

C.3 STABILITY

If a fixed grid difference equation is used to approximate a linear partial differential equation with constant coefficients, the von Neumann stability condition requires that the eigenvalues of the amplification matrix

should not exceed unity in absolute value for physically stable systems [Richtmyer and Morton, 1967]. To illustrate these ideas, consider the explicit finite difference scheme of Equation (C.17) that was used to approximate the advective transport equation. This difference scheme can be written

$$c_j^{n+1} - c_j^n = - \frac{U\Delta t}{\Delta x} \{ (1-\alpha)(c_j^n - c_{j-1}^n) + \alpha(c_{j+1}^n - c_j^n) \} \qquad (C.26)$$

where $\alpha = 0$ for upstream differences, $\alpha = 1/2$ for central differences and $\alpha = 1$ for downstream differences. The von Neumann stability condition is based on a Fourier Series analysis of the difference equation. At any time, the concentration profile along the river or estuary can be considered to be composed of a number of Fourier components. The contribution of the k'th component to the concentration at point $j\Delta x$ at time $n\Delta t$ is given by

$$c_j^{n+1} = c_j^n \exp\{ikj\Delta x\}$$

where $i = \sqrt{-1}$. Substituting into Equation (C.26) for the k'th Fourier component and simplifying gives

$$c^{n+1} = G c^n$$

where

$$G = 1 - \beta(1-2\alpha)(1-\cos\theta) + i\beta\sin\theta \qquad (C.27)$$

$$\beta = \frac{U\Delta t}{\Delta x}$$

and

$$\theta = ik\Delta x$$

G is the amplification matrix of the difference equation (C.26). As c^{n+1} only depends on c^n, the eigenvalue of the amplification matrix is given by the value of G from Equation (C.27). Thus, the von Neumann stability condition

requires

$$\{1-\beta(1-2\alpha)(1-\cos\theta)\}^2 + \{\beta\sin\theta^2\} \leq 1$$

Evaluating this for the three cases of upstream, central and downstream differences, the stability criterion in each case is given by

$$\frac{U\Delta t}{\Delta x} \leq 1$$

or

$$\frac{\Delta x}{\Delta t} \geq U \qquad\qquad\qquad (C.28)$$

If the stability condition is violated, certain Fourier components will be unacceptably amplified, and the value of the concentration, as determined by Equation (C.26) will oscillate with ever-increasing amplitude. Richtmyer and Morton [1967] give a very clear example of this oscillation for the simple dispersion equation (C.9). In the hydrodynamic equations, the instability manifests itself as an oscillation of the water depths and velocities (the water depths eventually becoming negative). Note that the von Neumann stability condition has been derived for linear equations with constant coefficients. This implies that the U of Equation (C.26) is constant, or that the flow is uniform and steady. In a situation where U varies with x and t, the stability condition is assumed to be determined by the worst case of Equation (C.28) along the estuary.

Consider the simple dispersion equation (C.9). This can be approximated by the explicit finite difference scheme

$$c_j^{n+1} - c_j^n = \frac{E\Delta t}{(\Delta x)^2} \{c_{j+1}^n - 2c_j^n + c_{j-1}^n\}$$

and if E is constant, the stability condition is given by [Richtmyer and Morton, 1967]

$$\frac{2E\Delta t}{(\Delta x)^2} \leq 1$$

or

$$\frac{(\Delta x)^2}{\Delta t} \geq 2E \qquad\qquad (C.29)$$

The hydrodynamic equations (C.3) are non-linear and have non-constant coefficients. Richtmyer and Morton [1967] linearize the equations and obtain the following stability condition

$$\frac{\Delta x}{\Delta t} \geq U \pm \sqrt{gy} \qquad\qquad (C.30)$$

It is apparent that Equations (C.28), (C.29) and (C.30) are the finite difference equivalents of Equations (C.7), (C.11) and (C.14), which describe the characteristic curve of information propagation in the (x,t) plane (see Section C.1). The physical reason for this can be seen from a consideration of Equation (C.26), the explicit finite difference approximation to the advective transport equation. This equation states that the value of C at the point $j\Delta x$ at time $(n+1)\Delta t$ depends on the value of C at points $(j-1)\Delta x$, $j\Delta x$ and $(j+1)\Delta x$ at time $n\Delta t$. If this advective system is disturbed at point $j\Delta x$ at time $n\Delta t$, as shown in Figure C.6, the disturbance propagates through the system according to Equation (C.7). If the stability condition of Equation (C.28) is violated, the disturbance will reach the point $(j+1)\Delta x$,

Stable Explicit Scheme u∆t < ∆x :
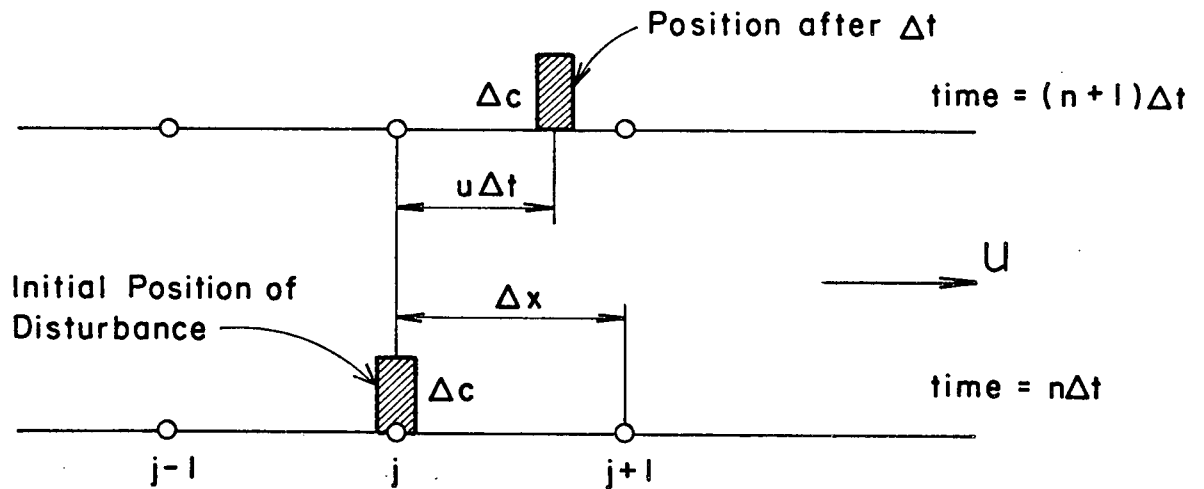
Unstable Explicit Scheme u∆t > ∆x :

Figure C.6

Stable and Unstable Explicit Advective Schemes

and alter the concentration there, before the concentration at point $j\Delta x$ has been updated according to Equation (C.26). In other words, the concentration at point $j\Delta x$ at time $(n+1)\Delta t$ 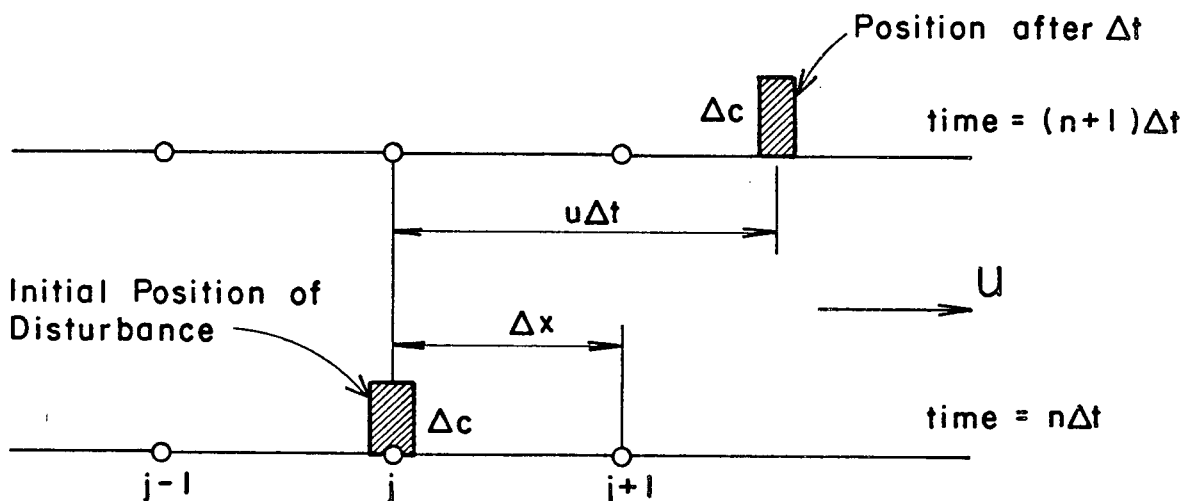now depends on what is occurring at a distance greater than Δx from $j\Delta x$ (see Figure C.6). Obviously, under these conditions the difference equation (C.26) is no longer physically meaningful, and it is only to be expected that it behaves in some strange manner. Similar reasoning holds for the relationship of Equation (C.29) to (C.11) for the dispersive equation, and Equations (C.30) to (C.14) for the hydrodynamic equation.

The problem of stability only arises with explicit differencing schemes, where the time differencing is forward. In implicit differencing schemes, where the time differencing is backward, the values are simultaneously determined at each grid point along the estuary. This technique automatically adjusts for the effect of the information propagating distances greater than Δx in the time increment. A difference scheme is simply a means of determining the value c^{n+1} from the value c^n. In effect, the difference equation maps c^n into c^{n+1}, and the eigenvalues of this mapping (in other words, the eigenvalues of the amplification matrix) define the characteristic directions along which c^{n+1} is determined from c^n [see Sawyer, 1966]. It is only to be expected that these eigenvalues should reflect the underlying physics of the problem.

C.4 SUMMARY

For any one-dimensional physical system, there are characteristic curves in the (x,t) plane that directly reflect the physical behaviour of the

system. These curves are often hidden or masked when a differential equation is derived relative to a fixed grid in the (x,t) plane. The problem of numerical dispersion occurs because the equation of advective transport is solved relative to a fixed grid, rather than along its appropriate characteristic. In an explicit difference scheme, the problem of stability arises for exactly the same reasons. If the equations are solved along their characteristic curves (or by an implicit method) there are no stability requirements, and the relative size of Δx and Δt are determined by the variation in the dependent variable.

DETAILS OF THE SOLUTION SCHEMES
OF THE HYDRODYNAMIC AND MASS TRANSPORT EQUATIONS

D.1 NUMERICAL SOLUTION OF THE HYDRODYNAMIC EQUATIONS

The fixed mesh, explicit finite difference method of Dronkers [1969] was used to obtain a numerical solution to the hydrodynamic equations. The finite difference forms of Equations (3.1) and (3.2) are respectively

$$u_{2m}^{2n+1} = u_{2m}^{2n-1} - \left(\frac{\Delta t}{2\Delta x}\right) u_{2m}^{2n+1} (u_{2m+2}^{2n-1} - u_{2m-2}^{2n-1}) - g\frac{\Delta t}{\Delta x}(h_{2m+1}^{2n} - h_{2m-1}^{2n})$$

$$- \frac{2g\Delta t\, u_{2m}^{2n-1}}{c^2 y_{2m}^{2n}} \tag{D.1}$$

and

$$h_{2m+1}^{2n+2} = h_{2m+1}^{2n} - \frac{\Delta t}{\Delta x b_{2m+1}^{2n}} (u_{2m+2}^{2n+1} A_{2m+2}^{2n} - u_{2m}^{2n+1} A_{2m}^{2n}) \tag{D.2}$$

where u_m^n and h_m^n are respectively the mean velocity and surface elevation at the grid point given by $x = m\Delta x$ at time $t = n\Delta t$. Note that the difference scheme employs central differences and that the "bar" sign has been dropped from the cross-sectionally averaged variables and parameters to avoid confusion with the subscripts and superscripts. (This convention will be followed when presenting finite difference quantities).

Because an explicit finite difference scheme was used to solve the hydrodynamic equations, the relative size of Δx and Δt is governed by the

stability criterion

$$\frac{\Delta x}{\Delta t} \geq \bar{u} \pm \sqrt{g\bar{y}}$$

This stability criterion is discussed in detail in Appendix C. Because

of the friction term, the hydrodynamic equations are naturally dissipative,

and this helps maintain stability. In fact, stability was found to be de-

pendent on a minimum value of friction. For the cross-sectional gemoetries

and flow and tidal conditions of Section 4.1.4, the hydrodynamic equations

became unstable when Manning's "n" was less than 0.012. (Manning's "n" was

constant throughout the estuary for this investigation). The stability cri-

terion of Appendix C is independent of the effects of friction. However,

it was derived from a linear stability analysis on the non-linear hydrodyna-

mic equations. The true non-linear stability criterion may be more strict

than the derived linear criterion, and this is reflected by the necessity

of a minimum level of friction to preserve stability.

The solution points for the finite difference scheme are shown

in Figure D.1. It is seen that the velocity and elevation points are stag-

gered in both time and space. In effect, the values of velocity and water

surface elevations are marched forward through time in a "leap-frog" manner.

From Equation D.1, the velocities at any time step 2n+1 are determined by the

surface elevations at time step 2n and the velocities at time step 2n-1.

The surface elevations at time step 2n+2 are then determined from the velo-

cities at time step 2n+1 by using Equation (D.2).

The fixed mesh of space points or "stations" used in solving the

hydrodynamic equations is shown in Figure B.4. Velocities are evaluated at

odd -numbered stations and water surface elevations are evaluated at even-
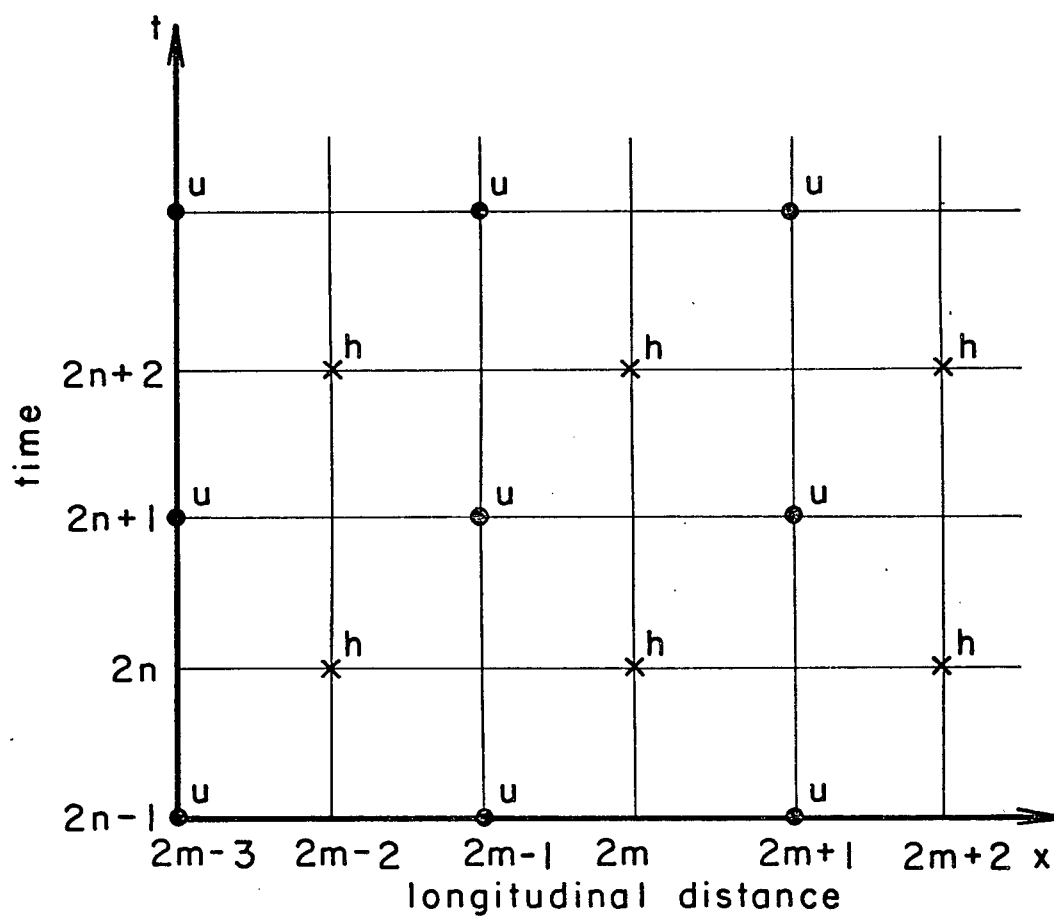
Figure D.1

Explicit Finite Difference Grid
of the Hydrodynamic Equations [After Dronkers, 1969]

numbered stations. At channel junctions, it is necessary that the junction station be a water surface elevation station, and this accounts for the non-coincidence of the junctions of the model estuary and real estuary in several cases (see Figure B.4).

In applying the hydrodynamic model, a design tidal cycle of selected flow and tidal conditions is chosen. The freshwater inflow forms a boundary condition at Chilliwack and the tidal rise and fall of the water surface forms boundary conditions at the seaward ends of the four channels that emerge from the delta. The velocity and water surface elevations throughout the estuary are set to initial values, and Equations (D.1) and (D.2) are then used to march the velocities and water surface elevations through time. The initial values of velocity and water surface elevations do not have to be exact as the model will converge to the true initial values after several tidal cycles.

The hydrodynamic model was programmed in high speed FORTRAN (FORTRANH) for solution by digital computer. The program consisted of 670 active statements and required approximately 40 seconds to analyse two complete tidal cycles. (The first tidal cycle was required for the estuary to converge to the true initial values of velocity and water surface elevation). The values of velocity and cross-sectional area were recorded at half-hourly intervals and later used in solving the tidally varying mass transport equation.

D.2 NUMERICAL SOLUTION OF THE TIDALLY VARYING MASS TRANSPORT EQUATION

From Section 3.2 it is seen that the solution of the tidally varying mass transport equation over any time increment involves an advection step, a dispersion step and a source-sink step. The finite difference form

of Equation (3.4) used to advect the moving points along the characteristics during the advection step was

$$x_j^{n+1} = x_j^n + u^n \Delta t \qquad (D.3)$$

where

x_j^{n+1} is the position of moving point j at the end of time increment n;

x_j^n is the position of moving point j at the start of time increment n;

and

u^n is the average velocity between positions x_j^n and x_j^{n+1} during time increment n.

The hydrodynamic model was used to obtain the longitudinal velocities and cross-sectional areas throughout the estuary at half-hourly intervals during the tidal cycle. The value of u^n can be obtained from these velocities.

In the dispersion step, the concentration of the moving points is adjusted for the effects of dispersion during the time increment. Both an explicit and an implicit finite difference scheme were investigated for the dispersive step. The implicit scheme was the Crank-Nicholson scheme described in Richtmyer and Morton [1967]. Irrespective of whether an implicit or explicit scheme is used, the "information" propagates through a dispersive system according to

$$x^2 = 2Et \qquad (D.4)$$

as is discussed in Appendix C. The finite difference form of Equation (D.4), namely

$$\Delta t \leq \frac{(\Delta x)^2}{2E} \qquad (D.5)$$

defines the stability criterion of an explicit scheme, as is also discussed

in Appendix C. Equation (D.5) also determines the response of an implicit

system, and although the implicit system is unconditionally stable, the con-

vergence criterion is related to Equation (D.5). In other words, if Δt is

significantly larger than the Δt of Equation (D.5) an implicit scheme may

converge to the wrong solution. Of the two schemes, the implicit scheme

was slightly faster, but because of the large somewhat ill-conditioned

matrices involved (of order 150) there were uncertainties in the signifi-

cance of round-off errors. Consequently, the simpler explicit scheme was

used. (The ill-conditioned nature of these matrices was due to the variable

spacing of the moving points. This variable spacing is discussed in Chapter

3).

The following explicit central difference equation was used to

Equation (3.6)

$$c_j^{n+1} = c_j^n + \frac{2\Delta t}{A_j^n (\Delta x)_{j+1,j-1}^{n+1}} \{ (\frac{EA}{\Delta x})_{j,j-1}^n (c_{j+1}^n - c_j^n) - (\frac{EA}{\Delta x})_{j,j-1}^n (c_j^n - c_{j-1}^n) \}$$

(D.6)

where

c_j^n is the concentration of moving point j at the start of time increment n;

$\Delta x_{j,j-1}^n = x_j^n - x_{j-1}^n$

x_j^n is the position of moving point j at the start of time increment n;

$(EA)_{j,j-1}^n$ is the average value of EA between moving points j and j-1 during time increment n;

and

A_j^n is the average cross-sectional area at moving point j during time increment n.

Equation (D.6) is the usual explicit central difference approximation except that it is applied over a grid where Δx is not constant. The stability requirement of Equation (D.5) generally results in a Δt smaller than the basic time increment of one hour. When this occurred, Equation (D.6) was solved repeatedly within the hour for as many iterations required by Equation (D.5). (This assumes that the relative spacing of the particles and the values of E and A remain constant during the hour -- which is a reasonable assumption).

Finally, in the source-sink step, the concentrations of the moving points are adjusted for the effects of any source-sink processes occurring. The following finite difference equation can be used to approximate the source-sink equation (3.7)

$$c_j^{n+1} = c_j^n + \Delta t \sum_{i=1}^{n} S_i \qquad \text{(D.7)}$$

although it is noted that Equation (3.7) can be solved analytically during the time increment.

The tidally varying mass transport model was programmed in high speed FORTRAN (FORTRANH) for solution by digital computer. The program consisted of some 1,300 active statements and required approximately 100 seconds to analyse six tidal cycles.

D.3 NUMERICAL SOLUTION OF THE TIDALLY AVERAGED MASS TRANSPORT EQUATION

The one-dimensional, tidally averaged mass transport was solved by the method of Thomann [1963]. In this solution, the estuary is divided into a number of segments or boxes, as shown in Figure D.2, and each segment is assumed to be completely mixed. If the tidally averaged transport processes
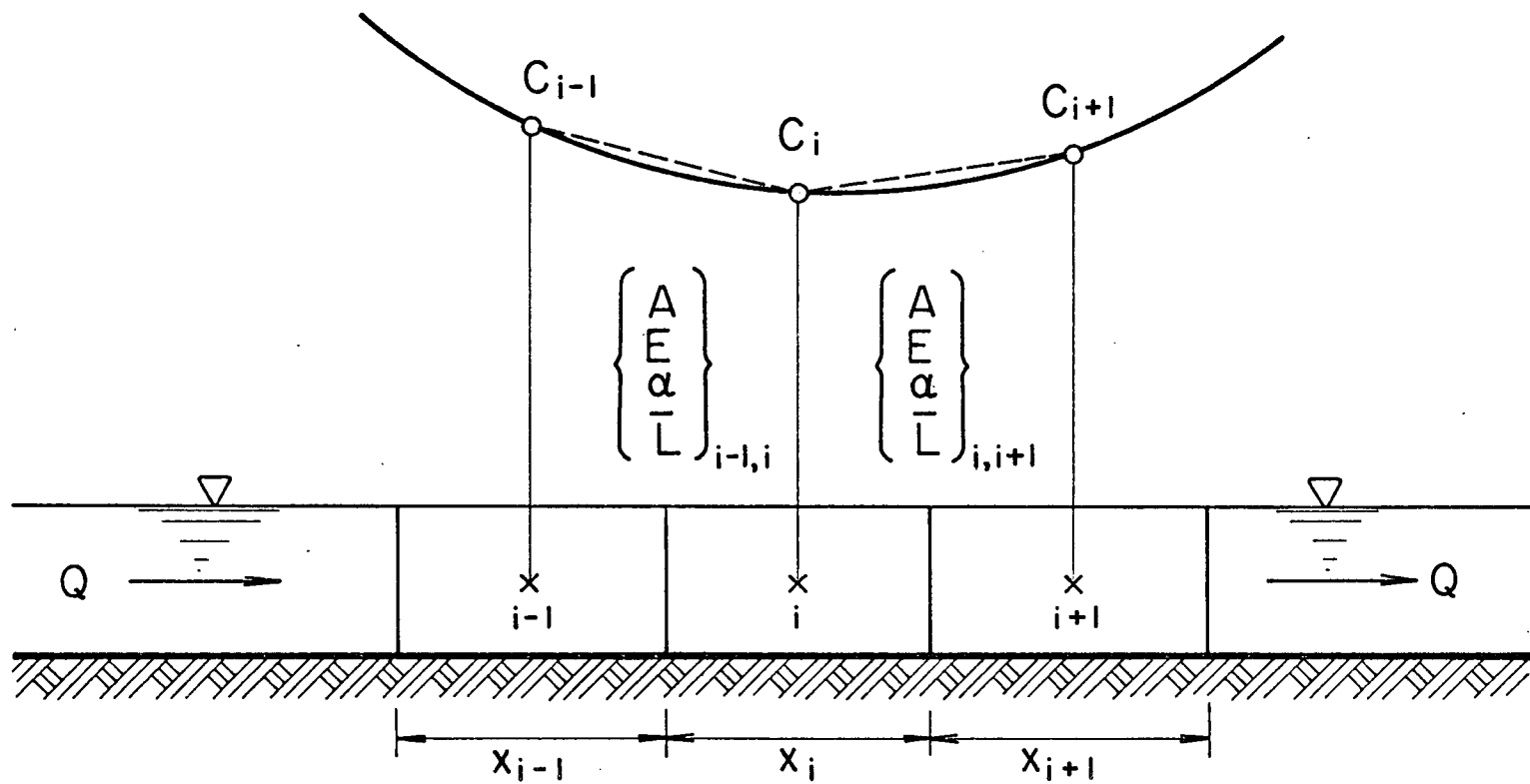
Figure D.2

Segments of Thomann's Tidally Averaged Model

and waste discharges are steady in time, a mass balance over segment i for a substance undergoing first-order decay gives (see Thomann [1971] for details)

$$Q\{\alpha_{i-1,i}c_{i-1} + (1-\alpha_{i-1,i})c_i\} - Q\{\alpha_{i,i+1}c_i + (1-\alpha_{i,i+1})c_{i+1}\}$$

$$+ E'_{i-1,i}(c_{i-1}-c_i) + E'_{i,i+1}(c_{i+1}-c_i) - K_i c_i V_i + W_i = 0 \qquad (D.8)$$

where

c_i is the concentration in segment i;

V_i is the volume of segment i;

W_i is the mass of waste substance discharged into segment i per tidal cycle;

K_i is the decay coefficient for segment i;

Q is the tidally averaged discharge through the estuary (the freshwater discharge);

$\alpha_{i,i+1}$ is the tidal exchange coefficient between segments i and (i+1);

and

$E'_{i,i+1}$ is the "effective dispersive" transport between segments i and (i+1).

The subscript notation of the various terms is illustrated in Figure D.2.

The first two terms on the right-hand side of Equation (D.8) are the tidally averaged advective transport into and out of segment i. The factor α is a weighting factor used to determine the concentration at the interface of two segments from the concentration at within each segment. In purely tidal flows α is set equal to 0.5 to allow for the effects of flow reversal, whereas in a river flow situation α is set equal to 1.0 as the flow is always downstream. The next two terms on the right-hand side of the equation

represent the net dispersive transport of mass into segment i from the

neighbouring segments. E' is given by

$$E'_{i,i+1} = \frac{E_{i,i+1} \, A_{i,i+1}}{\bar{L}_{i,i+1}}$$

where

$E_{i,i+1}$ is the effective coefficient of dispersion over a tidal period at the interface of segments i and (i+1);

$A_{i,i+1}$ is the cross-sectional area (tidally averaged) of the interface between segments i and (i+1);

and

$\bar{L}_{i,i+1}$ is the average of the lengths of segments i and (i+1).

The final two terms on the right-hand side of Equation (D.8) represent the

effects of decay and waste discharge.

An equation similar to (D.8) can be written for each of the

n segments of the estuary to give a system of n simultaneous, linear,

difference equations. Equation (D.8) can be written

$$a_{i,i-1}c_{i-1} + a_{ii}c_i + a_{i,i+1}c_{i+1} = W_i \qquad (D.9)$$

where

$$a_{i,i-1} = -\alpha_{i-1,i}Q - E'_{i-1,i};$$

$$a_{ii} = Q\{\alpha_{i,i+1} - (1 - c_{i-1,i}\} + E'_{i-1,i} + E'_{i,i+1} + V_iK_i;$$

$$a_{i,i+1} = (1-\alpha_{i,i+1})Q - E'_{i,i+1}.$$

In matrix notation, the system of Equations (D.9) can be written

$$\underset{\sim}{A} \; \underset{\sim}{C} = \underset{\sim}{W} \qquad (D.10)$$

where $\underset{\sim}{A}$ is a (nxn) tri-diagonal matrix and $\underset{\sim}{C}$ and $\underset{\sim}{W}$ are (nx1) column matrices.

Thomann [1971] gives details of the complete BOD-DO system of equations.

Thomann's model is essentially a finite fixed grid finite dif-
ference model that uses central differences for the dispersive transport,
and central differences for the advective transport when $\alpha = 0.5$ and up-
stream differences for the advective transport when $\alpha = 1.0$. (Upstream and
central differences are described in Appendix C). Thomann's model is simi-
lar to an implicit finite difference scheme. In both schemes the concentra-
tion at a gridpoint or in a segment depends on the concentrations at neigh-
bouring gridpoints or segments, and consequently the response of the
estuary is determined by a square tri-diagonal matrix in both equations.
Finite element solutions are also governed by a square tri-diagonal matrix,
as is discussed in Section 2.2.3.

Thomann's difference equations are unconditionally stable and do
not suffer from numerical dispersion, as is discussed in Chapter 3. How-
ever, there is a non-negativity requirement for each segment given by

$$\alpha_i, i+1 > 1 - \frac{E_{i,i+1}}{Q} \qquad (D.11)$$

If this criterion is violated the discharge of a waste substance into seg-
ment i results in a negative concentration in the segment. The physical
reason for this is that more substance is being transported out of the
segment per tide cycle than is being added. The substance is transported
upstream by dispersion and downstream by advection and dispersion. Rearrang-
ing Equation (D.11) gives

$$E_{i,i+1} > (1-\alpha_{i,i+1})Q$$

which imposes limits on the relative size of the dispersive and advective
transport processes.

Finally, the ease with which Thomann's approach handles the separate channels of the estuary should be mentioned. Figure D.3 shows the matrix A of Equation (D.10). Note that the three channels of the estuary are contained in the one matrix. In effect, the matrix is partitioned into three separate blocks, each of which represents a single channel. Note that each block or channel is uncoupled from the others except at the junction stations, where an additional term, which is not tri-diagonal, appears in the rows and columns of the matrix. These additional terms reflect the extra boundary through which mass transport occurs at the junctions.

The tidally averaged mass transport model was programmed in FORTRAN for solution by digital computer. The program consisted of some 250 active statements and required approximately 10 seconds to determine the steady state response of the estuary.
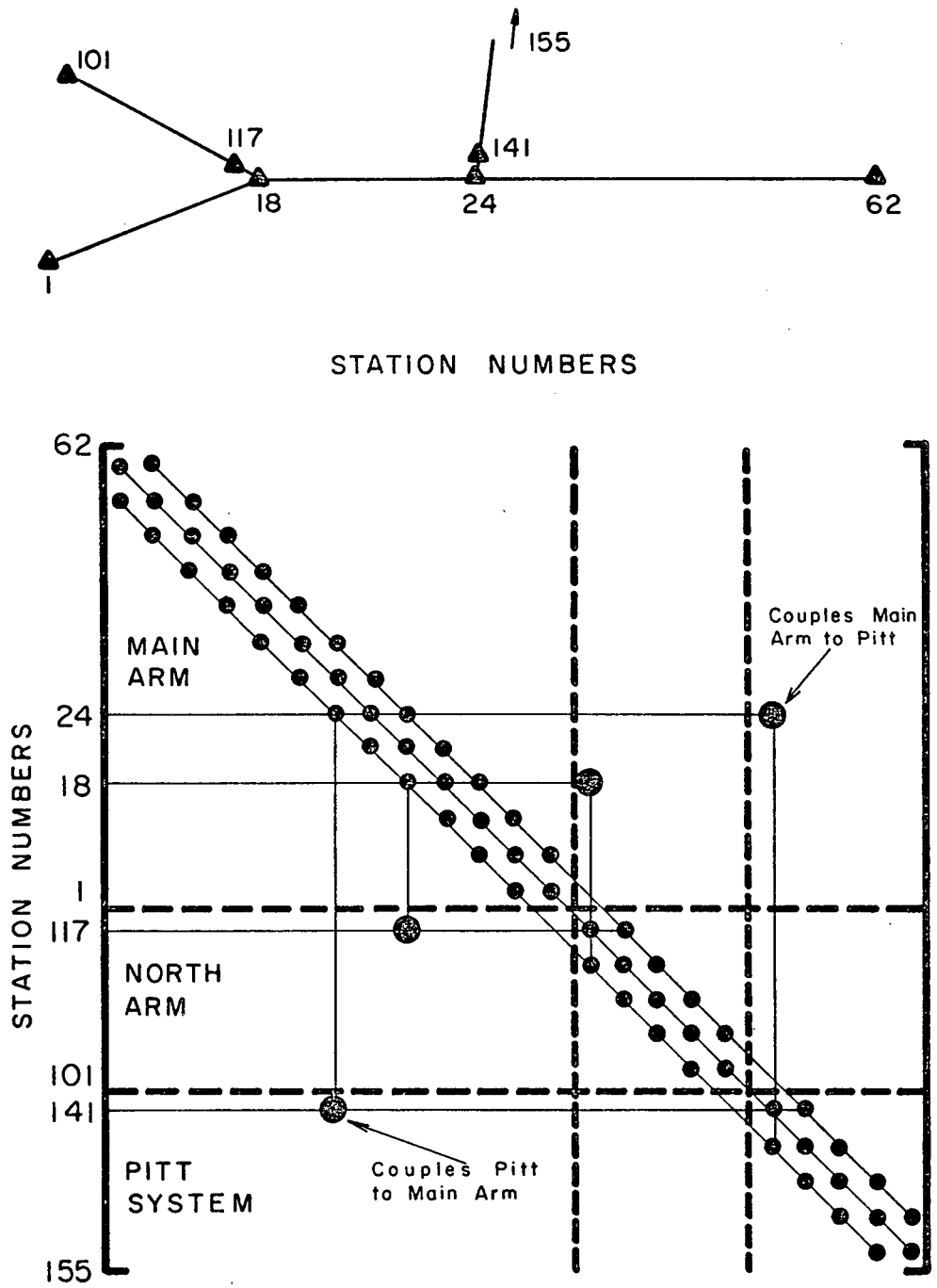
STATION NUMBERS

Figure D.3

The Matrix A of Equation (D.8) For The Fraser River Estuary

APPENDIX E

ESTIMATION OF LATERAL DISPERSION

Existing theories of lateral dispersion were used to estimate the
time of cross-sectional mixing in the Main Arm - Main Stem of the Fraser
River Estuary. The predicted time of cross-sectional mixing appears high
for the conditions of this study. More recent work on secondary currents
in rivers was used to develop revised estimates of the cross-sectional
mixing time. These revised estimates indicate much faster mixing over the
cross-section.

E.1 EXISTING ESTIMATES OF LATERAL MIXING

For steady uniform flow in straight channels, the coefficient of
lateral dispersion is given by [Fischer, 1969a].

$$\epsilon_z = 0.23 \bar{y} U_* \qquad (E.1)$$

where

$\bar{y}$ is the mean depth of cross-section;

and

U_* is the shear velocity.

The presence of bends in the channel of a river or estuary induces spiral
secondary currents that increase the rate of lateral mixing. For steady
flow around a bend, the increase in the coefficient of lateral dispersion
due to these secondary currents has been estimated as [Fischer, 1969a]

$$\delta \epsilon_z = - \frac{\bar{u}^2 \bar{y}^3}{k^5 R^2 U_*} \cdot I \qquad (E.2)$$

where

u̅ is the mean longitudinal velocity;

k is Von Karman's constant;

R is the radius of curvature of the bend;

and

I is a factor (negative) that depends on channel friction and

k, and is evaluated by Fischer. (A typical value of I is -0.3).

Ward [1972] measured the coefficient of lateral dispersion from

laboratory experiments of oscillatory flow (purely tidal) in a channel con-

sisting of a series of bends. His results are of the form

$$\varepsilon_z' = \alpha \bar{y} U_*^t \tag{E.3}$$

where

ε_z' is the tidally averaged coefficient of lateral
dispersion due to oscillatory flow;

U_*^t is the tidally averaged shear velocity due to
oscillatory flow;

and

α is a factor depending on the ratios of the depth
and width of the channels to the radius of curvature
of the bends. (For straight channels $\alpha = 0.5$, and
for wide shallow channels with a small radius of
curvature $\alpha \sim 2.0$).

In a tidally varying situation where there is both a steady velocity compo-

nent and a sinusoidally varying component, the tidally averaged shear velocity

can be estimated from

$$U_*^c = \frac{3.8n}{\bar{y}^{1/6}} [U_f^2 + 0.5 U_t^2]^{\frac{1}{2}} \tag{E.4}$$

where

n is Manning's "n";

U_f is the steady velocity component;

and

U_t is the amplitude of the oscillatory velocity component. Equation (E.4) is obtained from the Manning formula relating steady velocity to frictional effects. According to Odd [1971], the Manning or Chezy formulation should be an adequate description of frictional effects in fast flowing, well-mixed estuaries.

The following estimation of dispersion coefficients is limited to the Main Arm - Main Stem of the Fraser River Estuary. This is the widest channel and carries the bulk of the flow through the delta. Along this channel, there are 12 significant bends whose radii of curvature range from 7,000 feet to 35,000 feet, as illustrated in Figure E.1. The variation of longitudinal velocity throughout the tidal cycle at three stations along the Main Arm - Main Stem is shown in Figure E.2. The predominance of the tidal component in the lower reaches and the steady component in the upper reaches is apparent.

The following procedure was used to estimate the coefficients of lateral dispersion. The velocity at each bend was divided into a steady component U_f, which is given by the freshwater discharge through the tidally averaged area, and an approximating sinusoidal component of amplitude U_t. Equations (E.1) and (E.2) were used to estimate the coefficient of lateral dispersion due to the steady component of velocity (ε_f), and Equation [E.3] was used to estimate the coefficient of lateral dispersion due to the sinusoidal or oscillatory component (ε_t). Equation (E.4) was used to estimate the shear velocities due to the steady (U_*^f) and oscillatory (U_*^t) velocity components. The total lateral dispersion was assumed to be the sum of these two separate effects. The results of the calculations are shown in
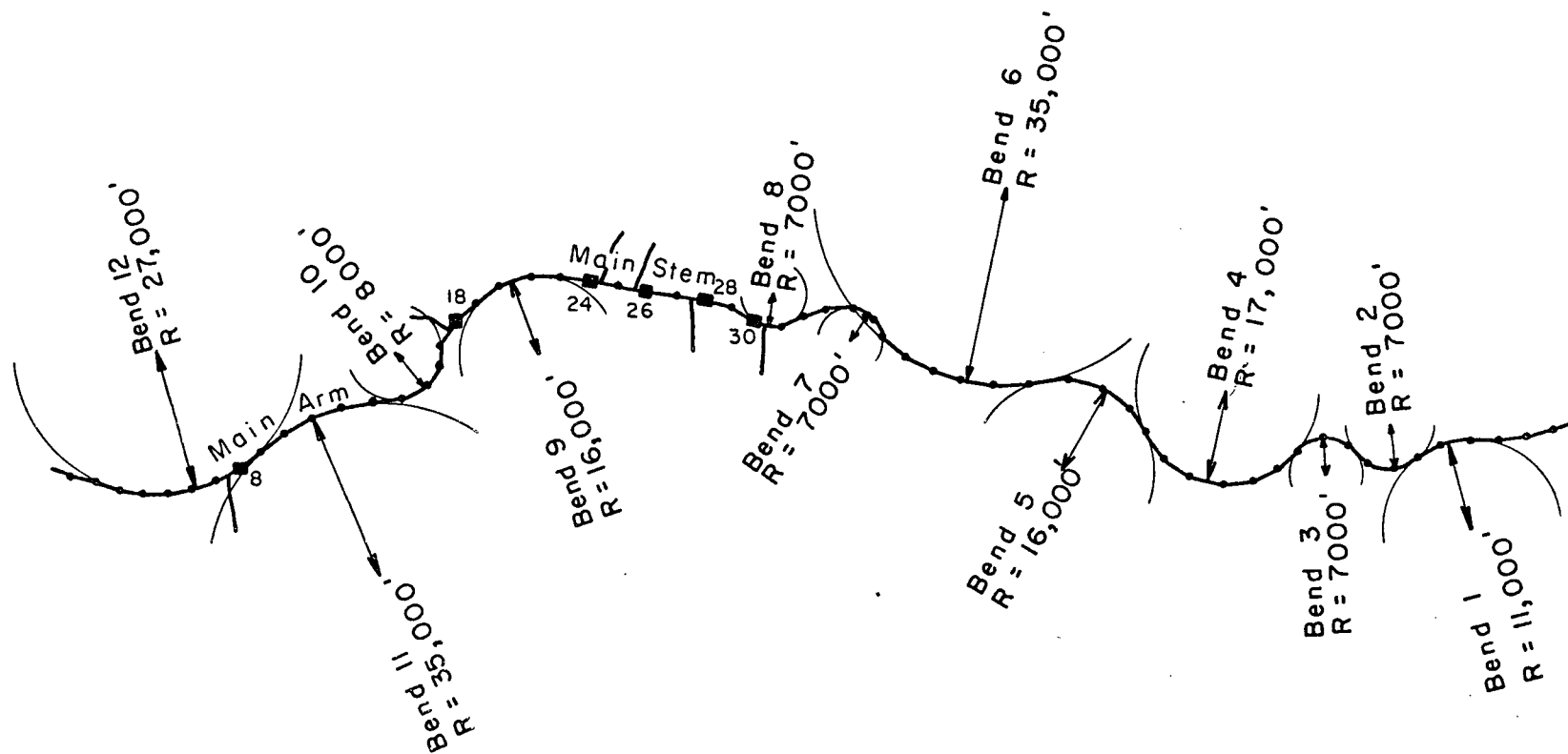
Figure E.1

Bends Along The Main Arm - Main Stem

Q = 36,500 cfs at Chilliwack
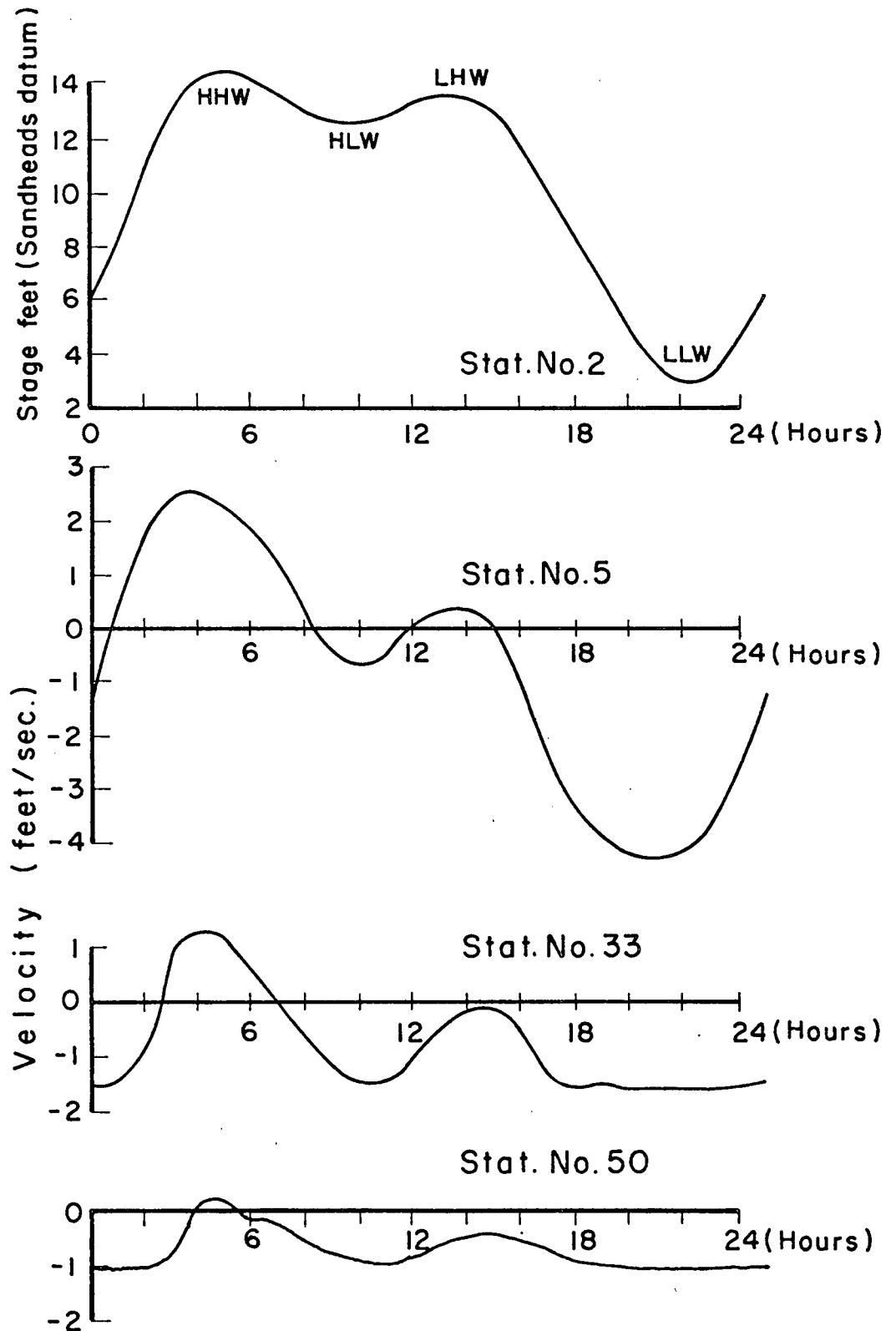Tidal Range at Steveston = 11' } Jan. 24, 1952

Figure E.2

Tidally Varying Velocities

TABLE E.1

ESTIMATION OF COEFFICIENTS OF LATERAL DISPERSION

BEND NO.	STAT. NUMBERS	R (Feet)	$\bar{y}$ (Feet)	U_f (Ft./Sec.)	U_t (Ft./Sec.)	"n"	U_*^f (Ft./Sec.)	U_*^t (Ft./Sec.)	U_*^c (Ft./Sec.)	b/R	$\bar{y}/R$ (x10^2)	$\dfrac{\epsilon_t}{\bar{y}\,U_*^t}$	$\dfrac{\epsilon_f}{\bar{y}\,U_*^f}$	ϵ_c (Ft.^{2}/Sec.)
1	57–60	17,000	24	1.2	0.1	0.032	0.088	0.005	0.088	0.12	0.14	1.0	0.24	0.6
2	55–57	7,000	24	1.2	0.8	0.032	0.088	0.037	0.097	0.29	0.34	1.9	0.29	2.3
3	52–55	7,000	35	0.9	0.7	0.032	0.062	0.031	0.070	0.29	0.40	1.8	0.37	2.8
4	46–52	17,000	31	0.9	1.2	0.032	0.063	0.054	0.087	0.13	0.18	1.0	0.24	2.2
5	41–46	16,000	37	0.8	1.3	0.032	0.055	0.057	0.083	0.13	0.23	1.0	0.26	2.7
6	36–41	35,000	32	0.7	1.3	0.032	0.049	0.058	0.081	0.06	0.09	0.6	0.23	1.5
7	32–35	7,000	43	0.7	1.5	0.025	0.036	0.050	0.066	0.29	0.62	1.8	0.62	4.8
8	29–31	7,000	38	0.7	2.2	0.025	0.037	0.074	0.091	0.29	0.54	1.8	0.52	5.8
9	19–23	16,000	38	0.6	2.5	0.025	0.033	0.088	0.10	0.13	0.24	1.0	0.28	4.7
10	14–17	8,000	38	0.7	3.3	0.025	0.037	0.11	0.12	0.25	0.48	1.6	0.45	7.3
11	8–14	33,000	34	0.6	3.0	0.025	0.032	0.10	0.11	0.06	0.10	0.6	0.24	2.3
12	2–8	27,000	34	0.6	3.5	0.025	0.032	0.12	0.13	0.07	0.13	0.6	0.24	2.7

Table E.1, the combined coefficient of lateral dispersion being designated ε_c.

From the results of Table E.1, the average value of the coefficient of lateral dispersion along the Main Arm - Main Stem is approximately 3.3 square feet per second. Assuming an average width and depth of channel of 1800 feet and 30 feet respectively, and an effluent discharge at the channel edge, the time required for 80 per cent mixing in the lateral direction is 55 hours [Ward, 1973]. (The percentage lateral mixing is defined as the ratio of the lateral root-mean-square concentration deviation to the average lateral concentration).

This estimate of 55 hours for the time of 80 per cent cross-sectional mixing seems very high. Strong secondary currents around bends 9, 10 and 11 are observable in the estuary during ebb flow conditions. In fact, if the fishermen lose a net in the Main Stem, it is often washed ashore on the north bank of bend 11 by these secondary currents. In a surface float study during ebb tide conditions, the floats were also washed ashore on the north bank of bend 11. It seems that the results of Table E.1 underestimate the effects of the secondary currents on the lateral mixing process. In view of this, an attempt was made to estimate the velocities of the secondary currents and the influence of the secondary currents on lateral mixing.

E.2 VORTICITY ESTIMATE OF SECONDARY CURRENTS

First consider the lateral mixing due to secondary currents. For the sake of simplicity, the vertical distribution of the secondary velocities is assumed to be linear, as shown in Figure E.3. This velocity distribution should be a satisfactory approximation for wide, shallow cross-sections.
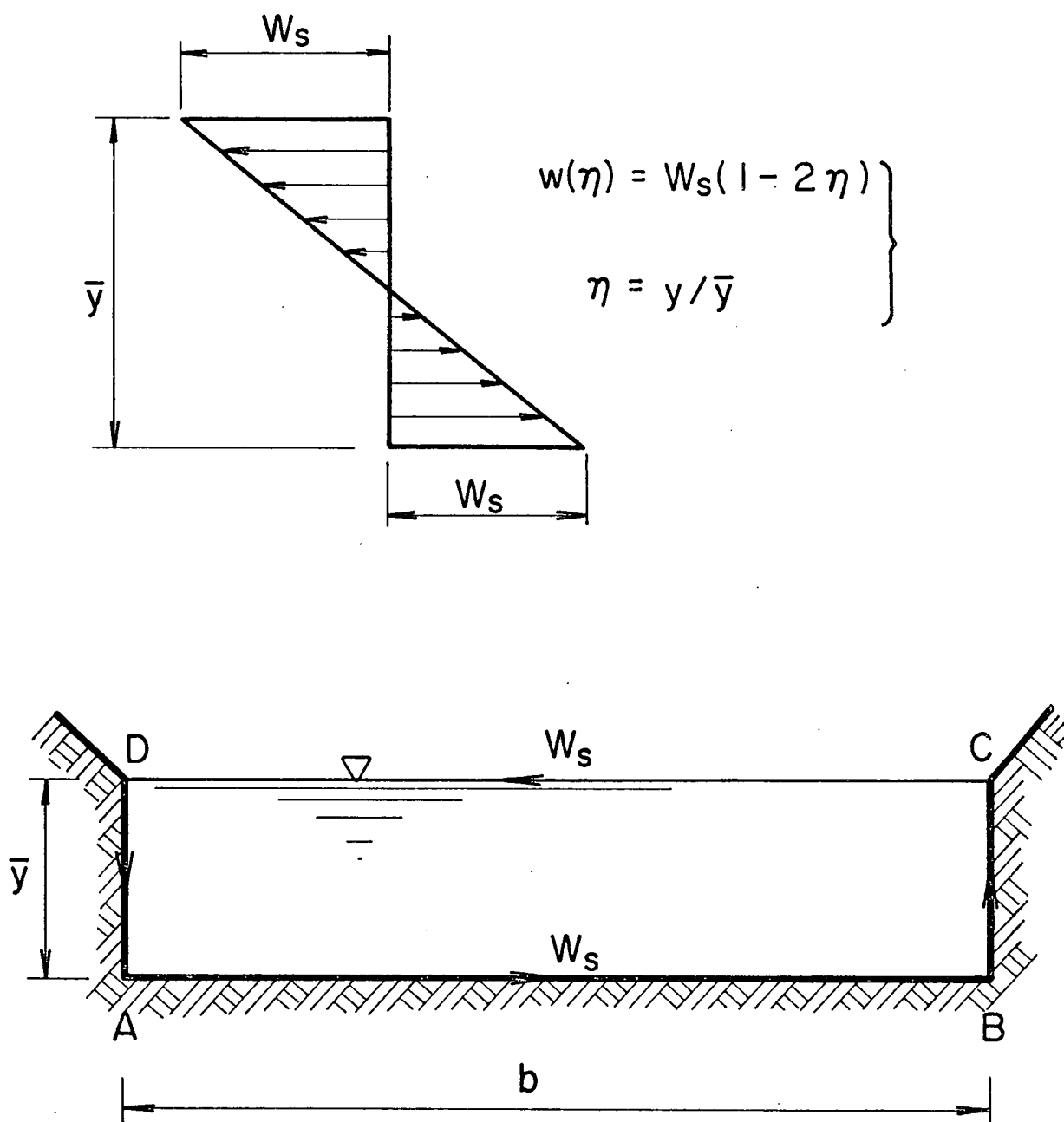
$$w(\eta) = W_s(1 - 2\eta)$$

$$\eta = y/\bar{y}$$

Figure E.3

Assumed Linear Distribution of Secondary Velocities

The variation of velocity with depth is given by

$$\dot{w}(\eta) = W_s (1 - 2\eta) \tag{E.5}$$

$$\eta = y/\bar{y}$$

where W_s is the surface velocity of the secondary current. In the manner of Elder [1959] and Fischer [1969a] the coefficient of lateral dispersion can be estimated from

$$\varepsilon_z = -\bar{y}^2 \int_0^1 w(\eta) \{ \int_0^\eta w(\eta) [\int_0^\eta \frac{1}{e_y} d\eta] d\eta \} d\eta \tag{E.6}$$

where e_y is the coefficient of vertical mixing. If we assume the flow to be steady and uniform, the vertical profile of the longitudinal velocity $\bar{u}$ is logarithmic, and is given by [Einstein, 1972]

$$\bar{u}(y) = \frac{U_*}{k} \ln\{\frac{9.05yU_*}{\nu}\} \tag{E.7}$$

where

   y is measured vertically upwards from the bend;

and

   ν is the kinematic viscosity.

For this logarithmic profile, the value of ε_y is given by [Fischer, 1969a]

$$e_y = k (1-\eta)\eta\bar{y}U_* \tag{E.8}$$

where k is von Karman's constant. Using the relations of Equations (E.5) and (E.8), the integration of Equation (E.6) gives

$$\frac{\varepsilon_z}{\bar{y} U_*} = 0.42\{\frac{W_s}{U_*}\}^2 \tag{E.9}$$

This result closely agrees with the value of

$$\frac{\varepsilon_z}{\bar{y} \, U_*} = 0.5 \{\frac{W_s}{U_*}\}^2$$

that Ward [1972] gives for the same distribution of secondary velocities. Thus, it only remains to estimate or measure the secondary velocity W_s to determine the coefficient of lateral mixing.

Quick [1973] has developed a theory of river meanders that nicely predicts the types of meanders that are observed in nature. The existance of secondary flows when bends or meanders are present in a river is well known, and Quick's theory has been used to obtain an estimate of the secondary velocity W_s. The basis of this theory is the generation of vorticity by the gradient of the vertical distribution of longitudinal velocity $\bar{u}$, and the subsequent advection of this vorticity by $\bar{u}$. This is illustrated in Figure E.4, the sense of the vorticity being given by the right-hand-screw rule. Because of the large velocity gradients of $\bar{u}$ close to the bed, the vorticity is generated in this region as intense, small-scale, highly anisotropic vortices. The vorticity then diffuses vertically into the flow and is advected along by $\bar{u}$. During this diffusion and advection, the vorticity degenerates into increasingly isotropic turbulence and is ultimately dissipated by frictional effects. However, in any steady flow situation there must be a balance between the generation and dissipation of vorticity. The vertical logarithmic profile of $\bar{u}$ reflects the energy balance of a steady flow situation, and presumably the vorticity balance also. Because of the velocity gradients of this profile, the flow at any section has a "bulk" vorticity given by

$$\xi_z = \left. \frac{\partial \bar{u}(y)}{\partial y} \right]_{average} \tag{E.10}$$

$$\bar{u}(y)$$

log profile

Region of Intense
Vorticity Generation

$\bar{y}$

y

ELEVATION

ξ_{sz}

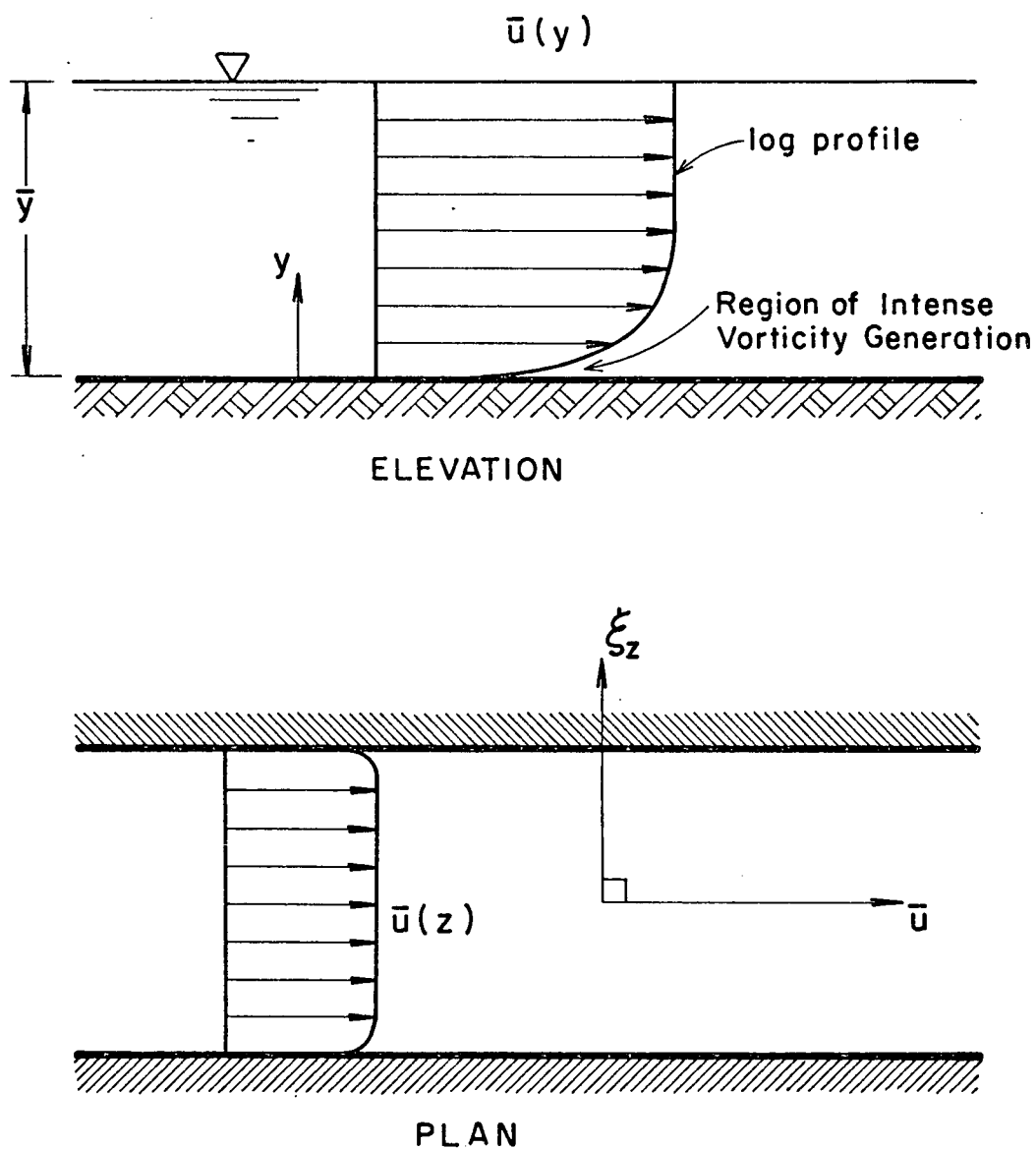$\bar{u}(z)$

$\bar{u}$

PLAN

Figure E.4

Interaction of $\bar{u}$ and ξ_z In A Straight River

where the velocity gradient is averaged over the depth of flow. If this
argument is correct, there is an intermediate stage between the generation
and dissipation of the vorticity, in which the vorticity retains an organized,
anisotropic state. This state is reflected by the velocity gradients of the
logarithmic velocity profile.

In a straight river, the velocity vector $\underset{\sim}{\bar{u}}$ and the vorticity vec-
tor $\underset{\sim}{\xi_z}$ are perpendicular to each other and do not interact. This is illus-
trated in Figure E.4. However, the situation is different when the flow
moves around a bend. Initially, the water on the inside of the bend flows
faster than the water on the outside of the bend, but in the bend proper, the
faster filaments of flow move to the outside of the bend, and the outside
water moves faster than the water on the inside of the bend. This is illus-
trated in Figure E.5. At A the faster filament is on the inside of the bend
while at B it is on the outside of the bend. Because of the lateral velocity
gradient of $\bar{u}$ as the flow moves around the bend, the vorticity is being gener-
ated and advected at an angle Θ to $\bar{u}$, as illustrated in Figure E.5. Note
that Θ varies as the flow moves around the bend and this variation of Θ will
depend on the radius of the curvature of the bend. Quick's theory predicts
this angle Θ between $\underset{\sim}{\bar{u}}$ and $\underset{\sim}{\xi_z}$. Thus, there is a streamwise component of
vorticity given by

$$\xi_x = \left|\xi_z\right| \cos\Theta \tag{E.11}$$

and it is this streamwise component that gives rise to the secondary current
as the flow moves around the bend.

Substituting the logarithmic profile (E.7) into (E.10) and aver-
aging over the depth between the limits $y = 11.0\nu/U_*$ and $y = \bar{y}$, the lower
limit being an estimate of the depth of the laminar sublayer, gives
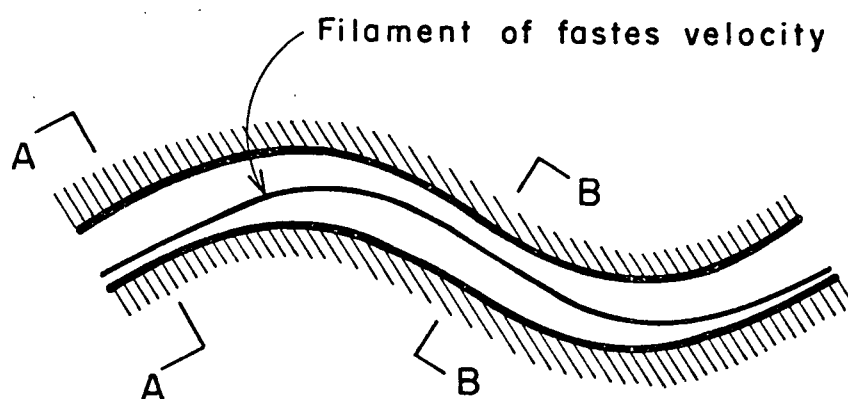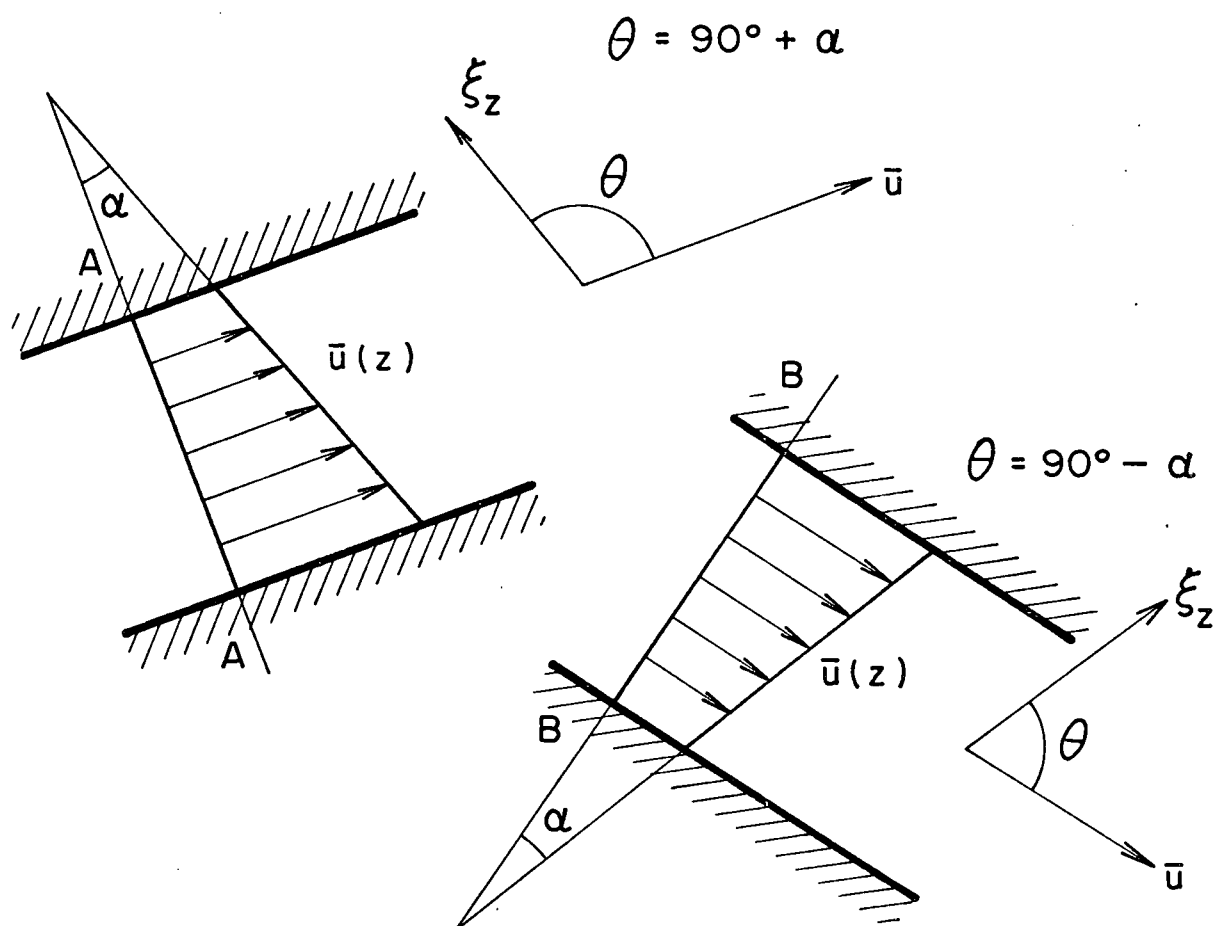
Figure E.5

Interaction of $\bar{u}$ and ξ_z Around A Bend

$$\xi_z = \frac{\alpha U_*}{k \bar{y}} \tag{E.12}$$

where $\qquad \alpha = \ln\{\frac{U_* \bar{y}}{11.0\nu}\} \tag{E.13}$

and thus from Equation (E.11)

$$\xi_x = \frac{\alpha U_* \cos\Theta}{k \bar{y}} \tag{E.14}$$

Now, consider the circulation around the section ABCD of Figure E.3 due to this streamwise vorticity. This circulation is given by

$$\Gamma_x = \oint_{ABCD} \xi_x \cdot dA$$

$$= \frac{1}{k} \alpha U_* b \cos\Theta \tag{E.15}$$

where b is the width of the river. Now, the circulation around the cross-section ABCD is also given by

$$\Gamma_x = \oint_{ABCD} U \cdot dl \tag{E.16}$$

Assuming there is sufficient time for the streamwise vorticity to "arrange" itself into the linear distribution of secondary velocities of Figure E.3, Equation (E.16) can be evaluated as

$$\Gamma_x \approx 2W_s b \tag{E.17}$$

where the contributions over BC and DA have been ignored (the section is assumed to be wide and shallow). Finally, putting k = 0.4 and substituting Equation (E.15) into (E.17), the following expression for W_s is obtained

$$W_s = 1.25\alpha U_* \cos\Theta \tag{E.18}$$

The results of a surface float study indicate a cross-channel surface velocity of approximately 0.6 feet per second around bend No. 11 of Figure E.1. The study was made on March 20, 1973 when the freshwater discharge at Hope was 31,000 cubic feet per second. The floats had drogues to minimize the effects of wind and were released during the initial period of the strong ebb phase of the tide. The following velocity values were obtained:

$$\bar{u} = 3.1 \text{ feet per second (from floats)};$$

and

$$U_* = 0.15 \text{ feet per second (Manning's equation)}$$

In his study of stable meanders, Quick found that for geometrically similar meanders to bend No. 11, the value of Θ varied from about 50 to 70 degrees. Taking U_* as above and

$$\bar{y} = 34 \text{ feet (Table E.1)}$$

$$\nu = 1.6 \times 10^{-5} \text{ square feet per second};$$

and

$$\Theta = 60 \text{ degrees}$$

we obtain from Equations (E.13) and (E.18)

$$W_s \doteq 0.7 \text{ feet per second}$$

which agrees well with the value obtained from the float studies.

Assuming a linear variation of secondary flow with depth (as in Figure E.3) and using a value of W_s of 0.6 feet per second, the coefficient of lateral dispersion from Equation (E.9) is given by

$$\frac{\varepsilon_z}{\bar{y}\,U_*} = 6 \qquad\qquad\qquad (E.19)$$

or $\varepsilon_z = 30$ square feet per second.

The value of Equation (E.19) is considerably larger than other values that have been reported (for example, the values in Table 1 of Ward [1972]), and it should be emphasized that the estimated value has not been confirmed experimentally. A possible reason for this high value is that the Fraser is essentially a "tidal river" with both high freshwater and tidal flows. The Fraser is relatively wide when compared to other rivers where values of $\varepsilon_z/\bar{y}\,U_*$ have been measured, but relatively narrow when compared to estuaries (see Table 1 of Ward). It is noted that the dispersion equation (E.9) for determining the lateral dispersion coefficient in secondary flows is very sensitive to the value of (W_s/U_*).

Using a value of $\varepsilon_z = 30$ square feet per second, the previous estimate of 55 hours for 80 per cent cross-sectional mixing is reduced to five hours. This will underestimate the time of cross-sectional mixing as the flow is not steady during the tidal cycle. Because of the highly assymetrical nature of the tides, there is only one strong ebb and flood tide in each double tidal cycle of 25 hours to generate secondary currents (see Appendix B for typical tides). Thus, within any tidal cycle, the lateral mixing will vary from a maximum during the strong flood or ebb to a minimum at times of slackwater. Consequently, an estimate of the effect of cross-sectional mixing is probably one tidal cycle (12.5 hours) for the lower reaches of the estuary and Pitt River and 1-2 tidal cycles for the upper

reaches where the tidal effects are smaller. On this basis, the effective or tidally averaged coefficient of lateral dispersion would be about 15 square feet per second in the lower reaches and seven square feet per second in the upper reaches of the Main Arm - Main Stem. On the basis of the relative magnitudes of the tidally averaged values of $\bar{y}$ and U_*, the lateral dispersion in the North Arm is estimated to be five square feet per second and 10 square feet per second in Pitt River.

At this stage, the theory relating vorticity and secondary currents is neither fully developed theoretically nor confirmed experimentally, but future work is planned in both directions. In concluding, it is noted that some values quoted for lateral dispersion coefficients are based on the results of laboratory experiments. Cross-sectional mixing in the presence of secondary currents is a complex three-dimensional phenomena, and it may be that some components of this process are not being scaled properly in model experiments.

APPENDIX F

ESTIMATION OF LONGITUDINAL DISPERSION

The coefficients of longitudinal dispersion due to the effects
of vertical and lateral velocity gradients are estimated for the Fraser
River Estuary. Simple approximations are given for the time-dependent
behaviour of the longitudinal dispersion coefficient during the initial
period before cross-sectional mixing is complete and during the tidal
cycle. The predicted tidally varying concentrations during the first
double tidal cycle were found to be very sensitive to assumptions about
the time-dependent behaviour of the dispersion coefficient. Neither the
magnitude nor time-dependent behaviour of the dispersion coefficients has
been verified by field measurements, and it is recognized that they may be
in error.

F.1 GENERAL

When effluent is discharged into a river or estuary it is dispersed
in the longitudinal direction by the effects of both vertical and lateral
velocity gradients, as described in Appendix A. The effluent must disperse
over a reasonable depth and width of the estuary before these velocity grad-
ients can exert a significant effect on the longitudinal dispersion process.
Most rivers and estuaries are much wider than they are deep and consequently
mixing in the vertical direction is much more rapid than in mixing in the
lateral direction. Thus, when a "parcel" of effluent is initially discharged,

the longitudinal dispersion is essentially due to the effects of vertical velocity gradients. However, as the effluent spreads across the cross-section, the lateral velocity gradients exert an increasing influence on the longitudinal dispersion process. In an estuary, the longitudinal dispersion is complicated by the effects of tidal flow reversal. If the cross-sectional mixing is not essentially complete within a tidal cycle, some of the longitudinal dispersion due to the oscillatory flow will be "undone" by the effects of flow reversal [Holley et al., 1970].

The Fraser River Estuary falls into a class that Holley et al. [1970] describe as "sinuous, multi-channeled or island-studded estuaries." Because of the complicating effects of the bends, islands and junctions of the estuary, the coefficients of longitudinal dispersion can only be reliably determined by field dye studies. Time and expense precluded such studies, and in the absence of adequate field data, the work of Fischer [1966b, 1969b] and Holley et al. [1970] has been used to obtain preliminary estimates of the longitudinal dispersion.

F.2 TIDALLY AVERAGED COEFFICIENTS OF LONGITUDINAL DISPERSION

For steady flow the longitudinal dispersion due to the effects of vertical and lateral velocity gradients can be respectively estimated as

$$\frac{E_y}{\bar{y} \, U_*} = 6 \tag{F.1}$$

and

$$\frac{E_z}{\bar{y} \, U_*} = 0.075 \left(\frac{\overline{u'^2}}{U_*^2}\right) \left(\frac{b}{\bar{y}}\right)^2 \tag{F.2}$$

where u'^2 is the square of the velocity deviation and is given by

$$u'^2 = (u(y,z) - \bar{u})^2$$

the over-bar in Equation (F.2) signifying the average cross-sectional value. Equation (F.1) was obtained by Elder [1959] for the logarithmic velocity profile. In obtaining Equation (F.2), Fischer [1966b] assumed the lateral mixing to be due to turbulent diffusion alone. According to the triple integral of Equation (E.6), the longitudinal dispersion due to lateral velocity gradients will vary inversely as the coefficient of lateral dispersion. This is because mixing over the cross-section tends to "undo" the effects of dispersion in the longitudinal direction. The lateral dispersion in the Fraser River estuary is thought to be quite high because of the effects of secondary flows (see Appendix E), and Equation (F.2) is subsequently adjusted for this effect.

To apply Equation (F.2) it is necessary to have some estimate of $\overline{u'^2}$ and U_*. Two velocity profiles were made in the Main Arm at Stations Nos. 14 and 15 on April 4, 1973. The freshwater flow at Hope was 34,700 cubic feet per second, the tidal range at Steveston was 11 feet and the measurements were taken during the strong ebb phase of the tide. The depth-averaged velocity profiles across the sections are shown in Figure F.1, and for these conditions, the various velocities are estimated to be

$$\bar{u} = 3.6 \text{ feet per second (measured)};$$

$$U_* = 0.18 \text{ feet per second (Manning's equation)};$$

$$U_f = 0.9 \text{ feet per second;}$$

and

$$U_t = 3.3 \text{ feet per second}$$

Q = 31,000 cfs (Hope)
April 4, 1973

STATION No. 15
10 A.M. — 11 A.M.

$\bar{u}$ = 3.6 ft./sec.
$\overline{u'^2}$ = 0.25 ft.^{2}/sec.^{2}

STATION No. 14
11:15 A.M. — 12 Noon

$\bar{u}$ = 3.6 ft./sec.
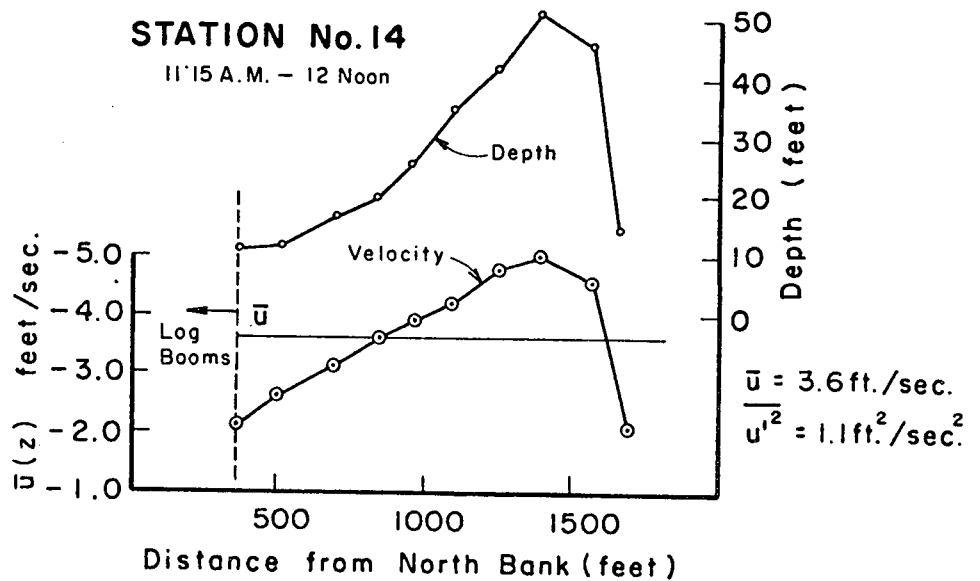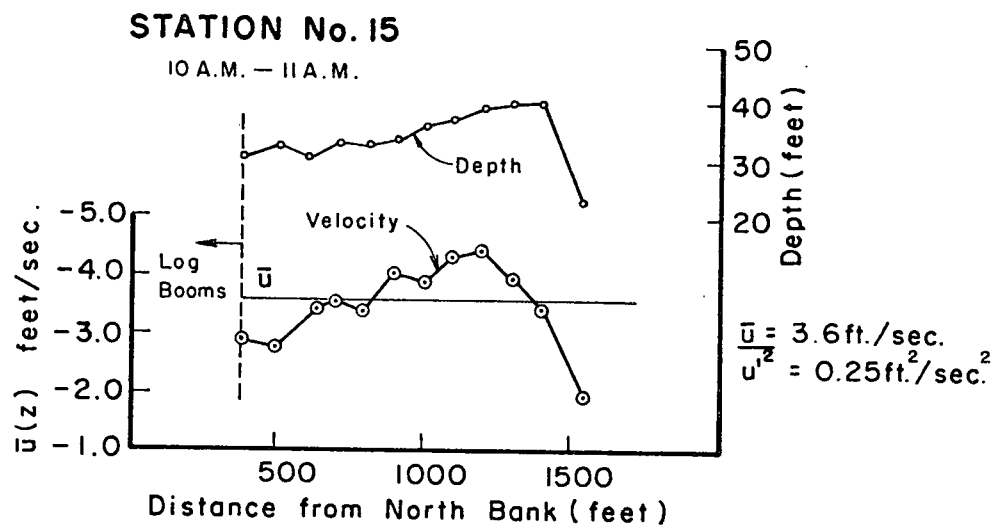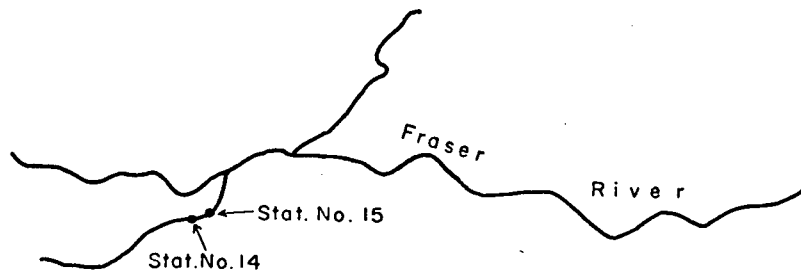$\overline{u'^2}$ = 1.1 ft.^{2}/sec.^{2}

Figure F.1

Lateral Velocity Profiles At Stations No. 14 and 15, Main Arm

where it is assumed that the total velocity $\bar{u}$ consists of a steady compo-
nent (freshwater) of magnitude U_f and a sinusoidally varying oscillatory
component (tidal) of amplitude U_t.

Stations Nos. 14 and 15 are located in bend No. 10 of Figure
E.1, a region of strong secondary flows. Using the average of the measured
values of $\overline{u'^2}$ at both stations, Equation (F.2) can be evaluated as

$$\frac{E_z}{\bar{y}\, U_*} = 3600 \qquad\qquad (F.3)$$

which is much higher than recorded values in other rivers [Fischer, 1966b,
Table 1]. However, the value of Equation (F.3) has to be reduced to account
for the greater cross-sectional mixing in the Fraser. The relative magnitude
of lateral mixing due to turbulent diffusion is 0.23, as in Equation (E.1),
whereas the relative magnitude for the effects of secondary currents in the
region of the estuary has been estimated to be 6.0 (see Appendix E). Thus
the adjusted value of Equation (F.3) is

$$\frac{E_z}{\bar{y}\, U_*} = 140 \qquad\qquad (F.4)$$

which is much more reasonable when compared to the values that Fischer
lists.

Equation (F.4) is an estimate of the "instantaneous" longitudinal
dispersion due to the lateral velocity gradients existing at one particular
time during the tidal cycle. According to Fischer [1969a], the effects of
the steady and oscillatory components on the longitudinal dispersion are

separate and additive, and thus Equation (F.4) can be separated into the following steady and oscillatory components

$$\frac{E_f}{\bar{y}\, U_*^f} = 140 \qquad\qquad (F.5)$$

and

$$\frac{E_t}{\bar{y}\, U_*^t} = 140 \qquad\qquad (F.6)$$

where

$$U_* = U_*^f + U_*^t$$

For the sake of simplicity, the subscript z has been dropped. Note that Equations (F.5) and (F.6) sum to give the correct combined dispersion of Equation (F.4). To apply the analysis of Holley *et al.* [1970], the oscillatory component has to be corrected back to a tidally averaged value. In the manner of Equation (E.4), this is estimated to be

$$\frac{E_t}{\bar{y}\, U_*^t} = 120 \qquad\qquad (F.7)$$

In the absence of other field data, Equations (F.5) and (F.7) have been used to estimate the longitudinal dispersion due to lateral velocity gradients throughout the estuary. The equations are applied as is for the Main Arm – Main Stem of the estuary, but have been corrected for the different depths and widths of the other channels to give

$$\left.\begin{array}{l} \dfrac{E_f}{\bar{y}\, U_*^f} = 75 \\[2em] \dfrac{E_t}{\bar{y}\, U_*^t} = .65 \end{array}\right\}\ \text{North Arm} \qquad\qquad (F.8)$$

$$\frac{E_t}{\overline{y} \, U_*^t} = 120 \qquad\qquad \text{Pitt River} \qquad\qquad (F.9)$$

Note that there is no steady dispersion component in Pitt River, the flow is purely oscillatory. The estimates of the various velocity components and the steady and oscillatory dispersion components are given in Table F.1.

If the cross-sectional mixing is not essentially complete within a tidal cycle, some of the oscillatory dispersion is undone by the effects of tidal flow reversal. To account for this effect, the values of E_t have been reduced to their effective values E_t' according to the procedure in Holley *et al.* These results are also shown in Table F.1, the effective period of flow oscillation is designated T and the ratio of this value to the time scale of lateral mixing is designated T'. Finally, the steady and effective oscillatory dispersion components are summed to give a combined tidally averaged coefficient of longitudinal dispersion due to the effects of lateral velocity gradients (E_c).

It is recognized that the values of the dispersion coefficients given in Table F.1 have been obtained from very limited field data and depend heavily on the unverified estimate of lateral dispersion from Appendix E. Consequently, the estimates may be considerably in error. However, the ratio $E_f/\overline{y} \, U_*^f$ and the absolute value E_f are reasonable when compared to values measured in other rivers [Fischer, 1966b, Table 1] and the maximum value of the effective oscillatory component E_t' of 450 square feet per second agrees well with the upper limit of approximately 500 square feet per second that Fischer [1969b] suggests. The combined dispersion coefficient E_c shows an

ESTIMATED COEFFICIENTS OF LONGITUDINAL DISPERSION DUE TO LATERAL VELOCITY GRADIENTS
(January 24, 1952: Freshwater Discharge at Chilliwack 36,500 cfs; Tidal Range at Steveston 11 feet)

CHANNEL	STATS.	U_f (Ft./Sec.)	U_t (Ft./Sec.)	U_*^f (Ft./Sec.)	U_*^t (Ft./Sec.)	U_*^c (Ft./Sec.)	E_f (Ft.²/Sec.)	E_t (Ft.²/Sec.)	ε_z (Ft.²/Sec.)	T (Hours)	T'	$\bar{E_t}$ (Ft.²/Sec.)	E_c (Ft.²/Sec.)	$E_c/\bar{y} U_*^c$
MAIN ARM	1-10	0.6	3.5	0.025	0.11	0.12	120	450	15	25	1.7	450	570	140
	11-18	0.6	3.3	0.025	0.10	0.11	130	430	15	25	1.7	430	560	140
	19-24	0.6	2.5	0.033	0.088	0.10	180	400	15	25	1.7	400	580	140
	25-30	0.7	2.2	0.037	0.074	0.091	190	340	15	12.5	0.8	200	390	110
MAIN STEM	31-40	0.7	1.4	0.042	0.055	0.074	220	240	7	12.5	0.4	70	350	130
	41-50	0.9	1.2	0.059	0.055	0.085	280	220	7	12.5	0.4	60	320	110
	51-60	1.1	0.7	0.079	0.035	0.082	310	120	7	12.5	0.4	40	350	120
NORTH ARM	101-118	0.2	1.6	0.011	0.063	0.064	20	100	5	25	2.8	100	120	70
PITT RIVER	140-154	----	2.8	------	0.11	0.11	--	400	10	25	1.8	400	400	120

increase down the Main Stem - Main Arm due to increasing effects of tidal flows in the lower reaches, and this also seems reasonable. The sensitivity of the predicted concentrations to errors in the coefficient of longitudinal dispersion is investigated in Section F.4.

F.3 TIME DEPENDENT LONGITUDINAL DISPERSION COEFFICIENTS

The tidally averaged values of the combined dispersion coefficient E_c listed in Table F.1 represent the effects of the lateral velocity gradients on the longitudinal dispersion process when the cross-sectional mixing is essentially complete. In the initial period following the discharge of a "parcel" of effluent, the longitudinal dispersion is principally due to the effects of vertical velocity gradients alone, as discussed in Section F.1. (The time scale of vertical mixing is a half-hour). According to Fischer [1969a], the effects of vertical and lateral velocity gradients on the longitudinal dispersion are separate and additive. To allow for the variable contribution of both components, it is assumed that

$$E = E_y + E_c \frac{t}{T} \qquad 0 \le t < T$$

and
$$\left. \vphantom{\begin{array}{c} a \\ a \end{array}} \right\} \qquad (F.10)$$

$$E = E_c \qquad t \ge T$$

where

t is the time that has elapsed since a "parcel" of effluent was discharged into the estuary;

T is the time scale of lateral mixing based on the width of section b (an edge discharge is assumed); and

E_y, E_c are the coefficients of longitudinal dispersion due to the effects of vertical and lateral velocity gradients respectively.

Equations (F.10) are a simplistic representation of a complex three-dimensional phenomenom, but they should adequately reproduce both the short- and long-term dispersion effects. It is only possible to account for the effects of such temporal variations in E because the tidally varying mass transport equation has been solved along its advective characteristics. Consequently, the position of each effluent "parcel" and the time that it has spent in the estuary is known, information that is masked by a fixed grid solution to the mass transport equation.

As well as increasing with time due to the influence of lateral velocity gradients as the effluent spreads over the cross-section, the coefficient of longitudinal dispersion will also vary during the tidal cycle. It will be minimal during times of slackwater and greatest during the times of strong ebb and flood flow. To investigate this effect, it was assumed that the coefficient of longitudinal dispersion given by Equations (F.9) also varied directly as the absolute velocity

$$E = (t + \frac{\alpha t}{T}) \, y \, \bar{U}_* \qquad\qquad 0 \leq t < T$$

$$\text{(F.11)}$$

$$E = \alpha \bar{y} \, U_* \qquad\qquad t \geq T$$

and

$$U_* = 0.06 \, \bar{u} \qquad\qquad \text{(F.12)}$$

where E, $\bar{y}$, U_* and $\bar{u}$ are the instantaneous values of the respective parameters during the tidal cycle and α is assumed equal to the tabulated values of $E_c / \bar{y} \, U_*^c$ in Table F.1. The relation (F.12) is obtained from Manning's equation and represents a "best over-all fit" for the entire estuary. The average of Equation (F.11) over a tidal cycle was found to be a satisfactory estimate of Equation (F.10).

F.4 SENSITIVITY OF PREDICTED CONCENTRATIONS

The sensitivity of the predicted concentrations to assumptions about the coefficient of longitudinal dispersion was investigated for a steady discharge of a conservative effluent at Station No. 50 on the Main Stem. Figure F.2 shows the variation in concentration at Station No. 50 during a double tidal cycle and the concentration profiles along the Main Stem 50 hours after the initial discharge. The predicted concentrations have been standardized by dividing by the tidally averaged concentration obtained from the mass of effluent discharged per tidal cycle and the freshwater discharge at Chilliwack. This is plotted as the parameter γ_{tv}, signifying that the results have been obtained from the tidally varying model. The effects of variation in initial dilution and multiple dosing due to flow reversal, as discussed in Section 1.3, result in spikes in the concentration profile along the channel. It should be noted that the base of these spikes is initially only some 500 - 800 feet wide, and is much "thinner" than it appears in Figure F.2. The reason the base appears wide is that the predicted concentrations are extrapolated of the advective characteristics onto the standard 5,000 foot space grid (see Section 3.2). This grid is too coarse to accurately resolve the initial forms of the spikes. It is noted that the spikes are correctly resolved on the advective characteristics (where necessary, additional moving points were added to define regions of rapid variation, as discussed in Section 3.3). Note that the concentration of the most seaward spike (E = 0) has been halved by dilution from the Pitt River in passing through the Main Stem - Pitt River junction.

Q = 36,500 cfs (Chilliwack)
Tidal Range at Steveston = 11 feet } Jan. 24, 1952

Variation in Concentration at Station No. 50

Concentration Profile along Main Arm – Main Stem (50 hours after initial discharge)

(i) E = 0
(ii) E = E_y (20 ft.^{2}/sec.)
(iii) E = E_c (350 ft.^{2}/sec.)
(iv) E = $E_y + E_c \frac{t}{T}$
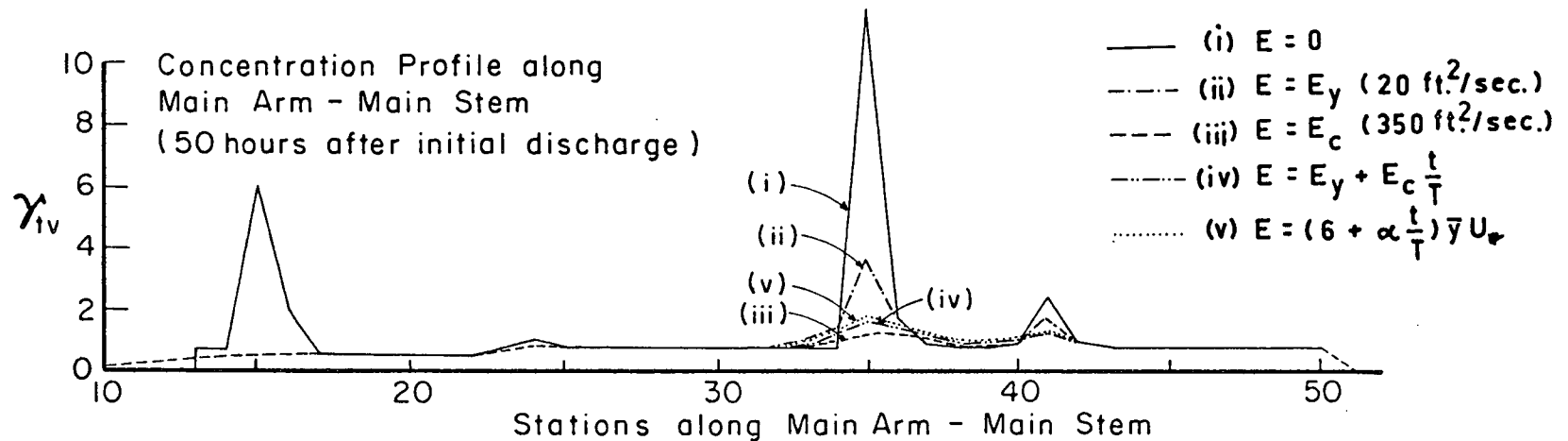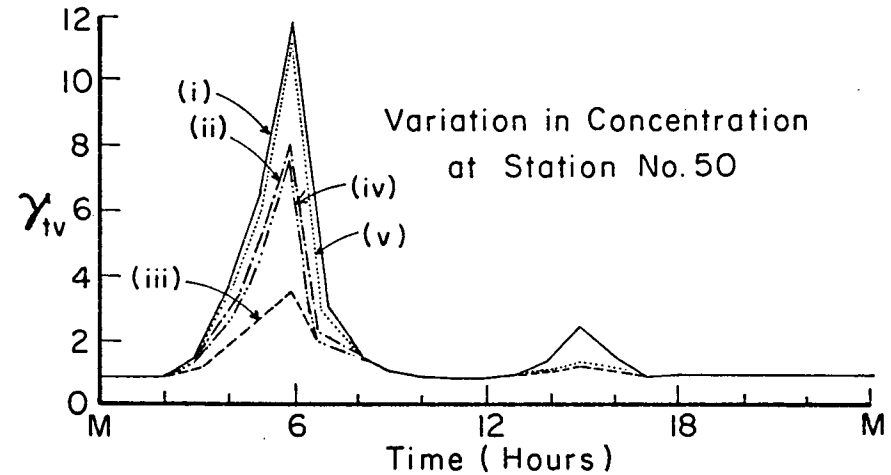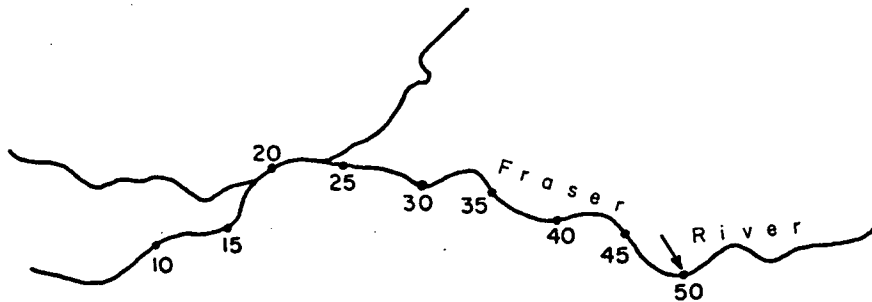(v) E = $(6 + \alpha \frac{t}{T}) \bar{y} U_*$

Figure F.2   Sensitivity of Tidally Varying Concentrations to the Coefficient of Longitudinal Dispersion

The results of assuming E to be constant and independent of
time are shown as curves (i), (ii) and (iii) in Figure F.2. The
corresponding values of E are:

Case (i)   E   =   0

Case (ii) E   = E_y (20 square feet per second);

and

Case (iii) E   = E_c (350 square feet per second).

The peak concentration at Station No. 50 is seen to be quite sensitive to
the magnitude of E. Eighteen hours after its generation, the spike has
been advected downstream to Station No. 35 and its concentration is seen
to be significantly reduced irrespective of whether E equals E_y or E_c.

When E is allowed to vary with time according to Equations (F.10)
and (F.11), the predicted concentrations are given by curves (iv) and (v)
respectively. Once again, the greatest effect is on the peak concentrations
at Station No. 50, the differences between both curves being negligible
after 18 hours when the spike is at Station No. 35. Note the significant
increase in the peak predicted concentration at Station No. 50 when E is
allowed to vary with $\bar{u}$. The reason for this is apparent from the velocity
variation at Station No. 50 during the tidal cycle. This is shown in Figure
E.2, the spike being due to the low velocities and flow reversals around
hours 4, 5 and 6. Because of the low values of $\bar{u}$, the value of U_* is very
low and the effective dispersion is very small compared to other times dur-
ing the tide cycle.

Because of the assymetric nature of the tides, the velocities in
the lower reaches of the estuary are quite low during the period of time

between high-high-water and low-high-water. This is illustrated by the velocity variation at Station No. 5 in Figure E.2, and the dispersion will certainly be less during this phase of the tide than during the strong ebb and flood flow that are seen to occur once each double tide cycle. The effects of variation in initial dilution and multiple dosing are most significant during the slackwaters around the time between high-high-water and low-high-water, and this can be identified as a sensitive period of the tide cycle.

In conclusion, the peak concentrations at the point of effluent discharge are very sensitive to assumptions about the form and magnitude of the coefficient of longitudinal dispersion. However, after a spike has been in the estuary several tidal cycles, its peak concentration is reasonably insensitive to the form and magnitude of the coefficient. Until adequate field data is available, the assumed temporal variations of E in Equation (F.11) are thought to be a reasonable approximation of what occurs in the estuary.

F.5 SUMMARY

The dispersion of effluent in an estuary is a complex, time-dependent three-dimensional phenomenom due to an intimate combination of the effects of turbulent diffusion, vertical and lateral velocity gradients and secondary flows. Limited field data and the results of other peoples' work have been used to obtain estimates of the coefficients of longitudinal dispersion. Due to the lack of field data, these estimated values may be substantially in error. However, they provide a basis for obtaining preliminary notions of the tidally varying response of the estuary to waste discharges. For the assumed time-dependent behaviour of the coefficient of longitudinal dispersion

the predicted concentrations were found to be relatively insensitive to
the value of E_c. The predicted peak concentrations at this point of efflu-
ent discharge were found to be very sensitive to the assumed time-dependent
behaviour of the coefficient of longitudinal dispersion. It is thought
that the assumed time dependent behaviour is a reasonable approximation
of what happens in the estuary.